Dehydroepiandrosterone and Dehydroepiandrosterone Sulphotransferase Activity and Expression in Human Disease

By

Joanne Christine McNelis

A thesis submitted to The University of Birmingham for the degree of

Doctor of Philosophy

School of Clinical and experimental medicine

College of Medical and Dental Sciences

The University of Birmingham

August 2009

Abstract

The adrenal steroid dehydroepiandrosterone (DHEA) and its sulphate ester, DHEAS are the most abundant circulating steroid hormones in humans. Uncongugated DHEA predominately exerts its effects via its downstream conversion to active sex steroids in peripheral target tissues. In contrast the conversion of DHEAS to androgens first requires cleavage of the sulfate group, catalysed by the microsomal enzyme steroid sulfatase (STS). Conversely, DHEA is converted to inactive DHEAS by the activity of the cytosolic enzyme DHEA sulphotransferase (SULT2A1). However, in addition, evidence is growing that DHEA and DHEAS can have specific, direct effects.

In this thesis, I have demonstrated that abrogation of DHEA metabolism can result in the manifestation of pathophysiological conditions. SULT2A1 requires 3'-phosphoadenosine-5'-phosphosulfate (PAPS) for catalytic activity. I have identified compound heterozygous mutations in the gene encoding human PAPS synthase 2 (PAPSS2) in a girl with androgen excess and confirmed the inactivating nature of the mutations via in vitro activity analysis. These observations indicate that PAPSS2 deficiency is a novel monogenic adrenocortical cause of androgen excess.

In addition, I have demonstrated that DHEA can have specific direct effects, attenuates human adipogenesis, while enhancing glucose uptake in mature adipocytes. These findings highlight DHEA metabolism, particularly by SULT2A1, as important mechanisms regulating DHEA activity.

Acknowledgements

First and foremost I would like to thank my supervisor, Professor Wiebke Arlt for all her support, encouragement and confidence in me over the last three years. I am also grateful to the entire Arlt group, notably Dr Vivek Dhir for his help with protein work and writing this thesis, and Hannah Ivison and Ian Rose for being great lab tech's and making everything in the lab a little easier.

I also express my gratitude to Professor Paul Stewart and the 'fat' group, Dr Jeremy Tomlinson, Dr Laura Gathercole, Stuart Morgan and Dr Iwona Bujalska, for their helpful discussion, technical support and guidance with writing papers. I am grateful to the past and present colleagues of the 2nd floor IBR for making my PhD such an enjoyable experience.

Last, but not least, I would like to thank my parents, my brother and Neil for all their support, both financially and emotionally. I am very grateful.

This work was supported by an MRC studentship, a British council RXP award, funding from the Endocrine Society and the School of Clinical and Experimental Medicine.

Abbreviations

6P	6-phosphogluconolactonate
11β-HSD1	11β hydroxysteroid dehydrogenase type 1
11β-HSD2	11β hydroxysteroid dehydrogenase type 2
18S	18S ribosomal subunit
ACC	acetyl coenzyme A carboxylase
ACRD	apparent cortisone reductase deficiency
ACTH	adrenocorticotrophic hormone
AI	adrenal insufficiency
AME	apparent mineralocorticoid excess
aP2	adipocyte fatty acid binding protein
ApoE	apolipoprotein E
APS	ammonium persulphate
AR	androgen receptor
ArKO	aromatase knock out
ARKO	androgen receptor knock out
ASC	adipose stromal cell
ATP	adenosine triphosphate
BAT	brown adipose tissue
BMD	bone mineral density
BMI	body mass index
C/EBP	CCAAT/enhancer-binding protein
cAMP	cyclic adenosine mono psphate
CAH	congenital adrenal hyperplasia
cDNA	complementary deoxyribose nucleic acid
Dex	dexamethasone
DHEA	dehydroepiandrosterone
DHEAS	dehydroepiandrosterone sulphate
DHT	dihydrotestosterone
DMEM	Dulbecco's modified eagles medium
DNA	deoxyribose nucleic acid
dNTP	deoxynucleotide triphosphate
E	cortisone
ER	oestrogen receptor
F	cortisol
FCS	foetal calf serum
FFA	free fatty acids
FSH	follicle stimulating hormone
G3PDH	glycerol-3-phosphate dehydrogenase
G6P	glucose-6-phosphate
G6Pase	glucose-6-phosphatase
GnRH	gonadatrophin releasing hormone
GR	glucocorticoid receptor
GRE	glucocorticoid response element
HAIR-AN	hyperandrogenic-insulin resistant–acanthosis nigricans
H6PDH	hexose-6-phosphate dehydrogenase
HPA	hypothalamic-pituitary-adrenal
HPG	hypothalamic-pituitary-gonadal
Hrs	hours
HSL	hormone sensitive lipase

HSP90	heat shock protein 90
IGF-1	insulin growth factor 1
IR	insulin receptor
Kb	kilo base
LB	Luria Bertani broth
LH	leutinising hormone
LPL	lipoprotein lipase
Min	minute
MR	mineralocorticoid receptor
mRNA	messenger ribonucleic acid
NaCl	sodium chloride
NAD	nicotinamide adenine dinucleotide
NADH	dihydonicotinamide adenine dinucleotide
NCAH	non-classical congenital adrenal hyperplasia
OD	optical density
Om	omental
P	p value
PAPS	3'-phosphoadenosine 5'-phosphosulphate
PAPSS	3'-phosphoadenosine 5'-phosphosulphate synthase
PBS	phosphate buffered saline
PCOS	polycystic ovary syndrome
PCR	polymerase chain reaction
PEPCK	phosphoenolpyruvate carboxylase
POMC	pro-opiomelanocortin
PPARα	peroxisome proliferator activated receptor alpha
PPARγ	peroxisome proliferator activated receptor gamma
PPP	pentose phosphate pathway
Pref-1	pre-adipocyte factor 1
RNA	ribonucleic acid
rpm	revolutions per minute
RT-PCR	reverse-transcriptase PCR
Sc	subcutaneous
SD	standard deviation of the mean
SDR	short chain dehydrogenase/reductase
SDS	sodium dodecyl sulphate
SE	standard error of the mean
Sec	second
SH2	src homology domain
SHBG	sex hormone binding globulin
SNP	single nucleotide polymorphism
SREBP-1	sterol regulatory element binding protein-1
StAR	steroidogenic acute regulatory protein
T2D	type 2 diabetes
TC	tissue culture
TAG	triacylglycerol
THE	tetrahydrocortisone
THF	tetrahydrocortisol
UV	ultra violet
WAT	white adipose tissue
WT	wild type

Table of Contents

List of Figures

List of Tables

1 Chapter 1: Introduction

1.1 Adrenal steroidogenesis

1.1.1 The anatomy and structure of the adrenal gland

The adrenal glands are located above the kidneys. Each gland weighs approximately 4g (McNicol, 2008) in the human adult and is encapsulated in a layer of thick connective tissue which serves to maintain its structure. The adrenal can be morphologically and functionally divided into two zones of different embryological origin (Ehrhart-Bornstein and Bornstein, 2008); the outer cortex which comprises the largest volume of the gland, and the inner medulla, which contributes approximately 10% of the adrenal gland (McNicol, 2008).

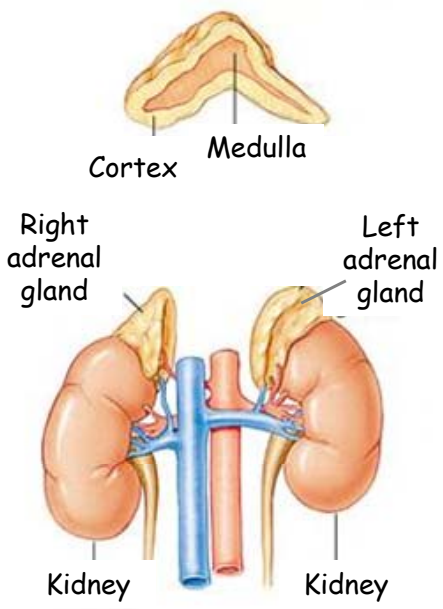

Figure 1-1 Diagram of the adrenal gland *The adrenal glands are positioned above the kidneys. They can be divided into two distinct zones based on their morphology and function; the cortex and medulla. Taken from jcsurgery.com/lap%20adrenal.htm*

The adrenal cortex can be further sub-divided into three histologically and enzymatically distinct concentric zones; the outer zona glomerulosa, the site of mineralocorticoid synthesis; the intermediate zona fasiculata, the site of glucocorticoid production; and the inner zona reticularis, which synthesises androgens including DHEA (**Figure 1-2**). In general each of the zones of the cortex possesses a distinct enzyme profile allowing the synthesis of a particular set of steroid hormones (**Figure 1-4**).

The adrenal medulla is developmentally, physiologically, and functionally distinct from the adrenal cortex (Fung et al., 2008). In the medulla catecholamines, notably adrenaline and to some extent noradrenaline, are synthesised from the amino acid tyrosine and secreted upon stimulation by a groups of specialised cells, termed chromaffin cells (Ehrhart-Bornstein and Bornstein, 2008). The medulla is highly innervated by preganglionic sympathetic neurones in the splanchnic nerves, which upon stimulation, in response to environmental stress, causes acetylcholine (ACH) to be released from nerve endings (Fung et al., 2008). ACH induces an increase in permeability of the chromaffin cells to Ca^{2+}, stimulating the release of catacholamines by exocytosis. In addition, due to its location within the adrenal, the medulla is exposed to relatively high levels of glucocorticoids (which are elevated in response to stress) inducing the activity of N-methyltransferase resulting in the stimulation of the biosynthesis of adrenaline (Ehrhart-Bornstein and Bornstein, 2008). Catecholamine release induces physiological changes that prepare the body for physical activity, termed the fight-or-flight response. Physiologically this manifests as increases in blood vessel constriction, heart rate, circulating glucose concentrations, and bronchiole dilation.

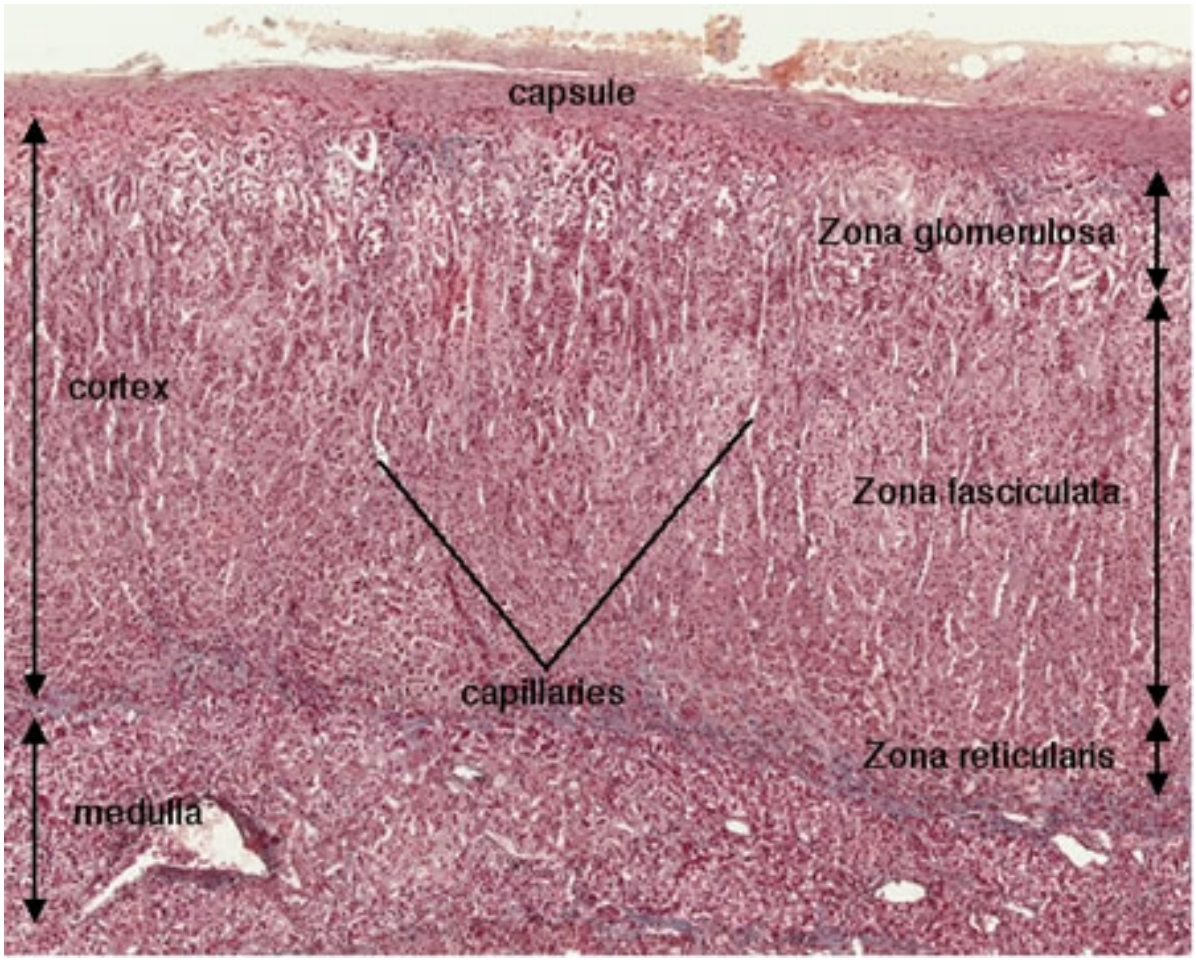

Figure 1-2 Histology of the human adrenal cortex. *The adrenal cortex can be sub-divided into three histologically distinct zones; the glomerulosa, the fasiculata and the reticularis which are clearly distinguishable following Mallory-Azan staining. Taken from missinglink.ucsf.edu/.../Assets/Endo_histo.htm*

1.1.2 Principles of steroid hormone synthesis

1.1.2.1 Steroid hormone structure

Steroid hormones are synthesised from the precursor cholesterol in the adrenal glands, gonads and placenta. All steroid hormones share a basic cyclopentanoperhydrophenanthrene ring structure, which comprises three cyclohexane rings; A, B and C, and a cyclopentane ring, D. The differential properties of steroids are conveyed by the number of carbon atoms and side chain groups. The conventional numerical nomenclature for steroid hormones is shown in **Figure 1-3**. Based on the number of carbon atoms, five groups of steroids can be identified: progestagens, glucocorticoids and mineralalocorticoids with 21, androgens with 19 and oestrogens with 18 carbon atoms.

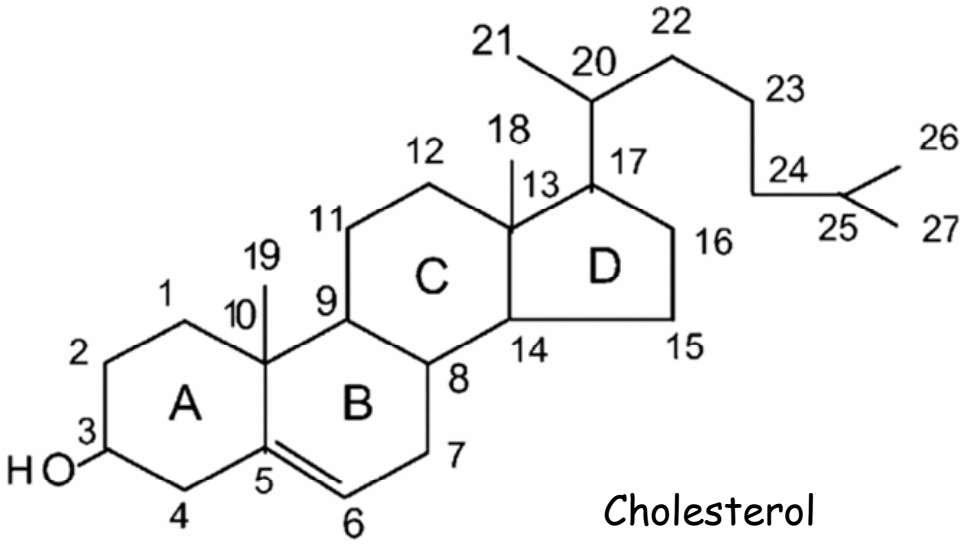

Figure 1-3 The conventional nomenclature used for steroid hormone structures. *The structure of cholesterol, the precursor for the synthesis of all steroid hormones, is shown. Letters identify the cyclohexane rings; A, B and C, and the cyclopentane ring D. Numbers identify the carbon atoms.*

1.1.2.2 Steroid precursor synthesis

Cholesterol, the common precursor for all adrenal steroidogenesis, can be acquired by three mechanisms. In the human, the principle source is in the form of low-density lipoprotein (LDL) from the diet. LDL cholesterol esters are internalised into cortical cells from the circulation by endocytosis via specific LDL receptors present on the cell surface (Miller, 2007). Subsequently free cholesterol is produced following hydrolysis.

Secondly, cholesterol can be synthesised *de novo* within the adrenal cortex from acetyl coenzyme A. The rate-limiting step in this pathway is the conversion of ß-hydroxy-ß-methylglutaryl-CoA to mevalonic acid by the enzyme hydroxymethylglutaryl coenzyme A (HMG CoA) reductase. Cholesterol itself exerts negative feedback on HMG CoA reductase activity, thus the rate at which LDL enters the cell by receptor-mediated endocytosis tightly regulates the rate of *de novo* synthesis (Miller, 2002). In contrast, ACTH stimulates the expression of HMG CoA reductase and LDL receptors, resulting in enhanced uptake of LDL cholesterol (Miller, 2009). Finally, high-density lipoprotein (HDL) cholesterol can be internalised into the adrenal via a putative HDL receptor, scavenger receptor class B type 1 (SR-B1), which is thought to be the principle mechanism of cholesterol synthesis in rodent adrenals. However this pathway appears to play a minor role in human steroidogenesis (Ikonen, 2006).

Prior to conversion to steroid hormones, hydrophobic cholesterol is required to translocate the aqueous space to the mitochondria, a process regulated by a group of proteins termed StarD4, 5 and 6 (Miller, 2007). In turn, cholesterol is transported across the aqueous space from the outer mitochondrial membrane to the inner

membrane (Kraemer, 2007), which is the rate-limiting step in adrenal steroidogenesis. This process is performed by the steroidogenic acute regulatory protein (StAR), a 30Kd protein whose expression is confined to the adrenal and the gonad (Miller, 2007). The mechanism of action of StAR is not fully understood. However, it is known that StAR acts exclusively on the outer mitochondrial membrane (Bose et al., 2002), causes structural changes of the membrane, and requires the binding of cholesterol for its activity (Miller, 2007). Once inside the cholesterol deprived inner mitochondrial membrane the C18 side chain of cholesterol is cleaved by the cytochrome P450 side chain cleavage enzyme (P450scc, encoded by *CYP11A1*) involving sequential hydroxylations to produce Δ5-pregnenolone. Subsequently, pregnenolone is translocated from the mitochondrion to the cytosol or smooth endoplasmic reticulum and is converted to progesterone by the type II isozyme of the enzyme 3ß-hydroxysteroid dehydrogenase (3ß-HSD2, encoded by *HSD3B2*) (Arlt and Stewart, 2005). Further steroidogenic conversion is specific for the distinct enzyme profile of the respective zones (**Figure 1-4**).

.

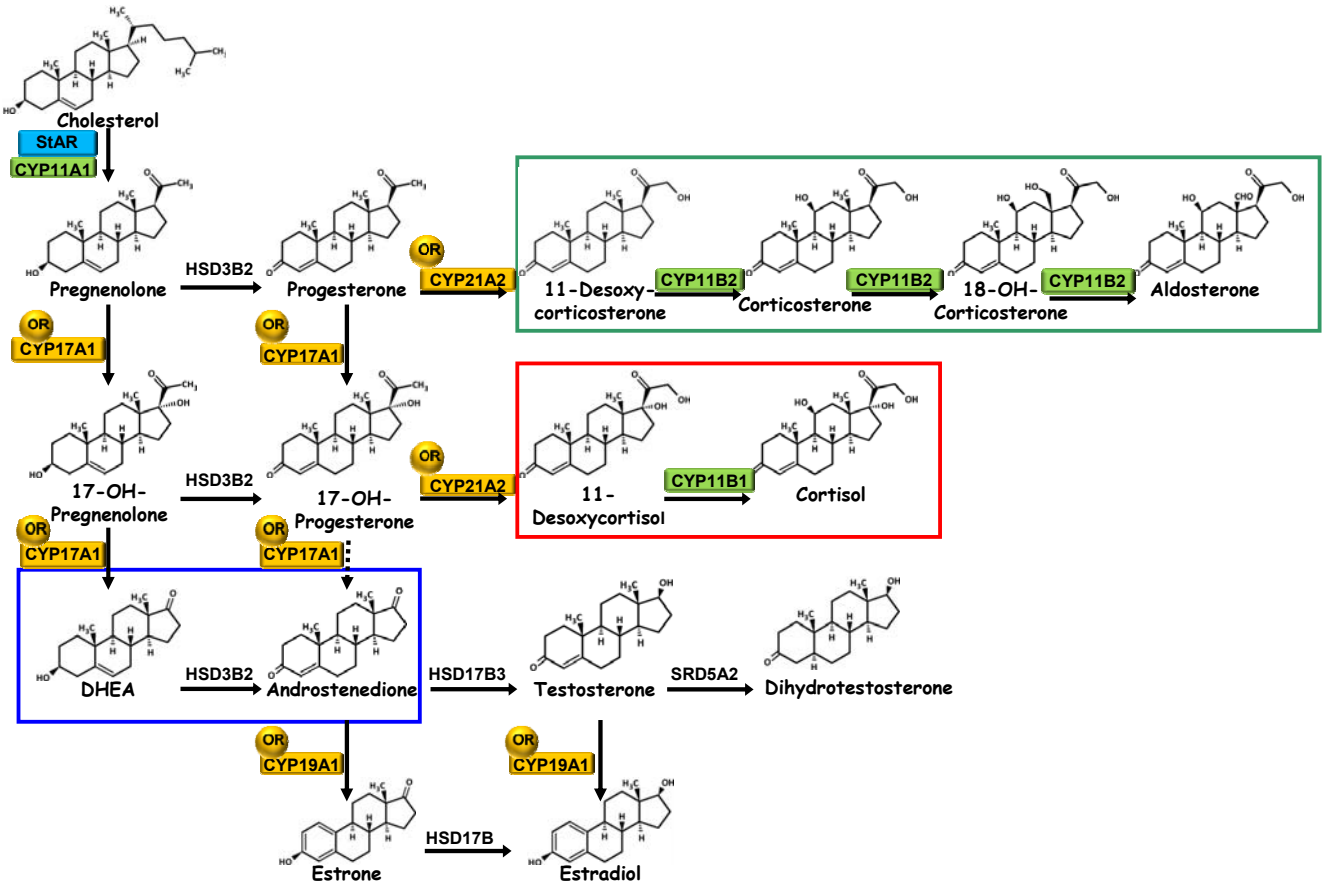

Figure 1-4 The steroid pathways and regulatory enzymes of adrenal steroid biosynthesis. *Mineralocorticoids, which regulate the homeostasis of minerals, predominately sodium, are synthesised in the adrenal zona glomerulosa (green outline). Glucocorticoids which regulate circulating glucose concentrations are synthesised in the adrenal zona fasiculata (red outline). Adrenal androgens (DHEA and DHEAS) are synthesised in the zona reticularis (blue outline). DHEA is metabolised to active androgens and oestrogens in peripheral target tissues.*

1.1.3 Mineralocorticoids

1.1.3.1 Synthesis of mineralocorticoids

The enzyme system responsible for the synthesis of the most potent mineralocorticoid, aldosterone, is expressed uniquely in the zona glomerolosa, the outer layer of the adrenal cortex. Since adrenal circulation is centripetal, only minimal amounts of corticosterone produced by the zona fasiculata reach the zona glomerolosa cells to be converted to aldosterone (Muller, 1995). Therefore the daily cortisol output of the adrenal cortex (15-40 mg) is 300 times higher than that of aldosterone (50-150 µg) (Muller, 1995). In the glomerolosa, following the conversion of pregnenolone to progesterone by *HSD3B2*, progesterone is 21-hydroxylated by the enzyme *CYP21A2* to form 11-deoxycorticosterone (DOC) (Shinzawa et al., 1988). Subsequently, DOC is converted to aldosterone via corticosterone and 18-hydroxycorticosterone, catalysed by *CYP11B2* in the mitochondria (Lisurek and Bernhardt, 2004).

1.1.3.2 Regulation of synthesis and secretion of mineralocorticoids

Aldosterone levels have to be continually adapted in response to changes in the body sodium and potassium concentrations. This is achieved via the regulation of aldosterone synthesis being under control of the renin-angiotensin system (RAS) (Quinn and Williams, 1988) and in contrast to the synthesis of glucocorticoids and androgens is largely independent of pituitary ACTH secretion (Bureik et al., 2002). In the RAS angiotensinogen is first converted into the inactive deca-peptide angiotensin

I, by an aspartyl protease, renin, in specialised juxtaglomerular cells (Lumbers, 1999). Angiotensin converting enzyme (ACE) subsequently catalyses the conversion of angiotensin I into the active octa-peptide angiotensin II. Angiotensin II and potassium positively regulate the synthesis of aldosterone by the zona glomerulosa by inducing the expression of *CYP11B2 (Bureik et al., 2002)*. Aldosterone synthesis is also negatively regulated by inhibitory factors such as sodium status and the atrial natriuretic peptide (ANP) (Lisurek and Bernhardt, 2004; Quinn and Williams, 1988).

1.1.3.3 Mechanism of action

The main function of aldosterone is the maintenance of mineral concentrations, in particular that of sodium and potassium in extracellular fluids. Aldosterone principally performs this role by acting on the distal tubule of the kidney, increasing the transport of sodium into the nephron in exchange for potassium and hydrogen ions. This results in a reduction in sodium loss and a reabsorbtion of water by osmosis, thus elevating the volume of extra cellular fluid and consequentially blood pressure. Indeed it is well characterised that hyperaldosteronism may be accompanied by hypertension and heart disease (Marney and Brown, 2007; Nagata, 2008).

The principle effector of the cellular response to mineralocorticoids is the mineralocorticoid receptor, a member of the nuclear receptor superfamily. Upon binding of aldosterone to the MR, the activated complex translocates to the nucleus of the target cell and initiates transcription of mineralocorticoid specific genes, including the gene encoding the sodium-potassium adenosine triphosphatease (Na+/K+-ATPase). The MR is regulated in part, at least in epithelial tissue, by pre-receptor regulation via co-expression with 11β-Hydroxysteroid dehydrogenase 2

(11β-HSD 2) (Stewart et al., 1995b), described in detail in section 1.1.4.5.2. In non-epithelial tissues, predominantly in the cardiovascular system, aldosterone and angiotensinogen II can additionally synergistically activate inflammatory cascades which provoke the cardiac hypertrophy and fibrosis (Nagata, 2008).

1.1.4 Glucocorticoids

1.1.4.1 Synthesis of glucocorticoids

The zona fasiculata, located between the zona glomerulosa and the zona reticularis, expresses the enzymes necessary for glucocorticoid production. In this zone pregnenolone is released from the mitochondria and converted by microsomal enzymes to 17-OH-progesterone by one of two pathways. In the principle pathway pregnenolone is first dehydrogenated at the 3-hydroxyl group and isomeration of the double bond at C5, catalysed by 3β-HSD2, encoded by *HSD3B2*, to form progesterone (Arlt and Stewart, 2005). Subsequently progesterone is hydroxylated at the C17 position to 17-OH-progesterone by the 17α-hydroxylase activity of P450c17, a product of the *CYP17A1* gene. In the alternative pathway pregnenolone is first converted to 17-OH-pregnenolone by the 17α-hydroxylase activity of P450c17, which is subsequently converted to 17-OH-progesterone by 3β-HSD2 (Arlt and Stewart, 2005). Subsequently P450c21, encoded by the *CYP21A2* gene, catalyses the hydroxylation at the C21 position of 17-OH-progesterone to produce 11-deoxycortisol. Finally, 11-deoxycortisol is hydroxylated at C11, by the mitochondrial enzyme P450c11, encoded by the *CYP11B1* gene, to produce cortisol (Arlt and Stewart, 2005).

1.1.4.2 Regulation of synthesis and secretion

Glucocorticoid secretion is under control of prototypic neuroendocrine feedback system, the hypothalamic-pituitary-adrenal (HPA) axis (**Figure 1-5**). In response to neural stimuli, induced by both psychological and physical stressors, a rapid induction of the transcription factor c-fos in the parvocellular of the paraventricular cells of the hypothalamus ensues. This induces the activation of numerous genes, including corticotrophin releasing hormone (CRH) and arginine vasopressin (AVP), which are transported by the hypophyseal portal vein to the anterior pituitary, where they synergistically stimulate the synthesis and release of adrenocorticotrophin (ACTH) from the corticotroph cells (Buckingham, 2006). ACTH acts on the adrenal cortex to stimulate the synthesis and release of cortisol by increasing intracellular cAMP levels, the activation of the cholesterol transporter and StAR and the induction of *CYP11B1* expression (Bureik et al., 2002). The coding sequences of the *CYP11B2* (involved in aldosterone synthesis) and *CYP11B1* genes are highly homologous. However, their promoter regions are significantly different, allowing for distinct mechanisms of induction by the RAS or ACTH respectively. As with numerous endocrine systems, cortisol induces negative feedback of the HPA axis via its specific receptor the glucocorticoid receptor (GR), at the hypothalamus and pituitary level.

In addition to stress the HPA axis is also regulated by 'the clock' and exerts a circadian pattern of cortisol secretion; an early morning peak of after awakening to a serum concentration of approximately 800nM, followed by a rapid decline over the course of the day to very low levels, approximately 200nM at midnight

(Nieuwenhuizen and Rutters, 2008). In contrast, the circulating cortisone level is significantly lower and shows no circadian rhythm (Walker et al., 1992).

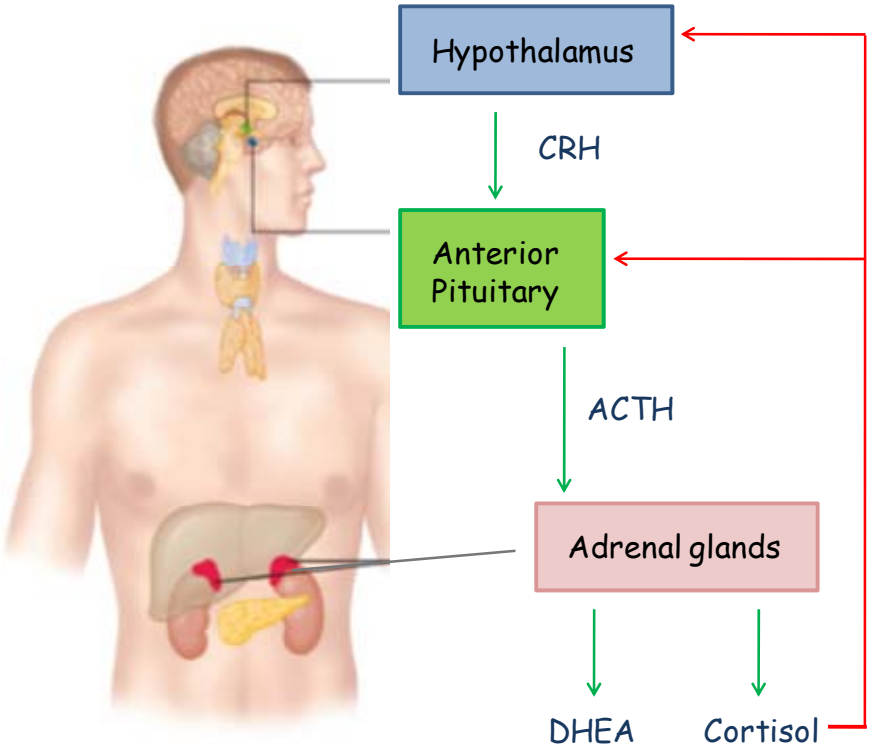

Figure 1-5 The Hypothalamo-Pituitary-Adrenal axis. *The synthesis of cortisol and DHEA is under control of the HPA axis. The hypothalamus produces corticotrophin releasing hormone (CRH) which stimulates the anterior pituitary to synthesise and release adrenocorticotrophic hormone (ACTH). ACTH in turn stimulates the synthesis and release of DHEA and cortisol from the adrenal gland. Glucocorticoids regulate their own circulating levels via the inhibition of CRH and ACTH synthesis and secretion from the hypothalamus and pituitary, respectively. Adapted from www.vitalifenetworks.com/VL_Cortisol.php*

1.1.4.3 Mechanism of action of glucocorticoids

While circulating plasma cortisone is largely unbound, approximately 90% of cortisol is bound to corticosteroid binding globulin (CBG) and a further 6% is bound to albumin (Meulenberg and Hofman, 1990a). In principle, only free cortisol is able to diffuse into target cells and exert its effects. At a cellular level GCs elicit diverse effects, modulating approximately 10% of our genes, by an array of mechanisms including the rapid modulation of signalling pathways, to post translational modifications that occur well after gene transcription. However, GCs predominantly mediate their effects via their specific receptor, the glucocorticoid receptor (GR), a member of the nuclear receptor (NR) superfamily. Activation of the GR can result in both the positive or negative regulation of gene transcription.

As with other NRs the GR consists of five distinct domains (**Figure 1-6**). The N terminal A/B domains include activational functional domain 1 (AF-1), which facilitates transcriptional activity. The C domain contains two cystine rich Zn2+ fingers and is responsible for receptor dimerisation and DNA binding. The D-domain or hinge region aids nuclear translocation as does the C-terminal E domain. The E domain is also responsible for ligand binding and includes a second activational functional domain (AF-2) (Warnmark et al., 2003).

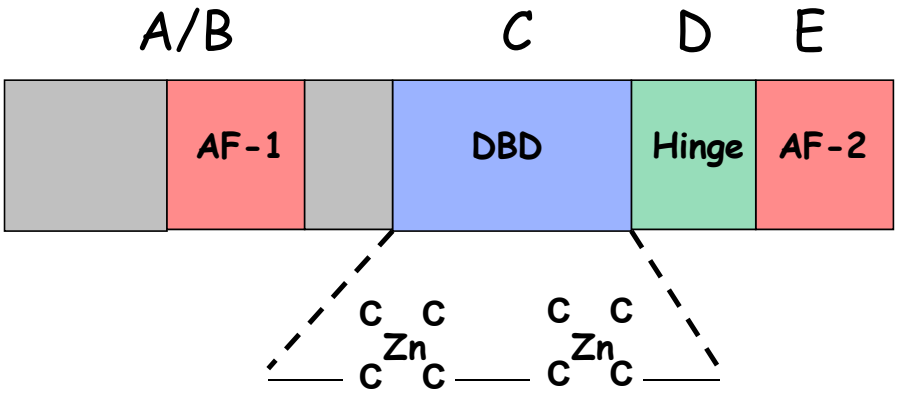

Figure 1-6 Schematic of the domain structure of the glucocorticoid receptor. *The five main domains of the GR, with some detail of the C-domain. The N-terminal A/B-domains include activational function domain 1 (AF-1), which facilitates transcriptional activity. The C-domain includes two cysteine-rich Zn2β fingers and is responsible for receptor dimerisation and DNA binding (DBD). The D-domain or hinge region aids nuclear translocation as also does the C-terminal E-domain. The E-domain is also responsible for ligand binding, includes a second activational function domain 2 (AF-2). Adapted from (Buckingham, 2006).*

In the unbound state the GR is part of a large heteromeric complex in the cytoplasm, containing various heat shock proteins including heat-shock protein 90 (HSP-90). Upon GC binding in the cytosol, a conformational change is induced, and the GR is released from the inactivating complex. The GR is then sequentially phosphorylated, homodimerised and translocated into the nucleus where it binds to a specific cis regulatory region in the promoter of target genes termed a glucocorticoid response element (GRE), via the DNA binding domain, and induce gene transcription (Chandler et al., 1983). Alternatively, in rare instances the GR can bind to negative GRE (nGRE), and inhibit gene transcription (Malkoski and Dorin, 1999). Additionally,

co-activators and co-repressors, expressed in a tissue or cell specific manner, are recruited to the activated ligand bound GR complex and act to facilitate or inhibit transcription.

The ligand activated GR can also modulate gene transcription, independent of GREs via protein-protein or 'tethering' interactions (Reichardt and Schutz, 1998). In this situation the GR is recruited to DNA bound transcription factors in a regulatory complex, thus itself acting as a co-repressor or co-activator (Garside et al., 2004; Nissen and Yamamoto, 2000). Examples of protein-protein interactions include suppression of transcription evoked by the transcription factor NF-κB (Nissen and Yamamoto, 2000) (Auphan et al., 1995; Barnes and Adcock, 2003; Reichardt and Schutz, 1998) and stimulation of transcription induced by AP-1, c-fos/c-jun (Reichardt and Schutz, 1998).

More recently, it is becoming recognised that GC's can also effect gene transcription via modulating the mRNA stability and translation of target genes. Sequences have been identified in the untranslated region of inflammatory genes which mediate GC induced acceleration or inhibition of mRNA decay (Stellato, 2004).

In addition to their genomic actions, which require hours to be fully operative, GC's also exert effects characterised as non-genomic, which occur within minutes or even seconds of drug administration (Matthews et al., 2008). Non genomic effects of GC involve the production of second messenger molecules and activation of signal transduction pathways, either by the nuclear glucocorticoid receptor or by a membrane glucocorticoid receptor that has net yet been fully characterised.

Two isoforms of the GR have been identified, α and β, which are formed by alternative splicing. The α isoform has a greater affinity for GC, while the β isoform, when co-expressed with GRα, acts as a negative regulator of GC signalling.

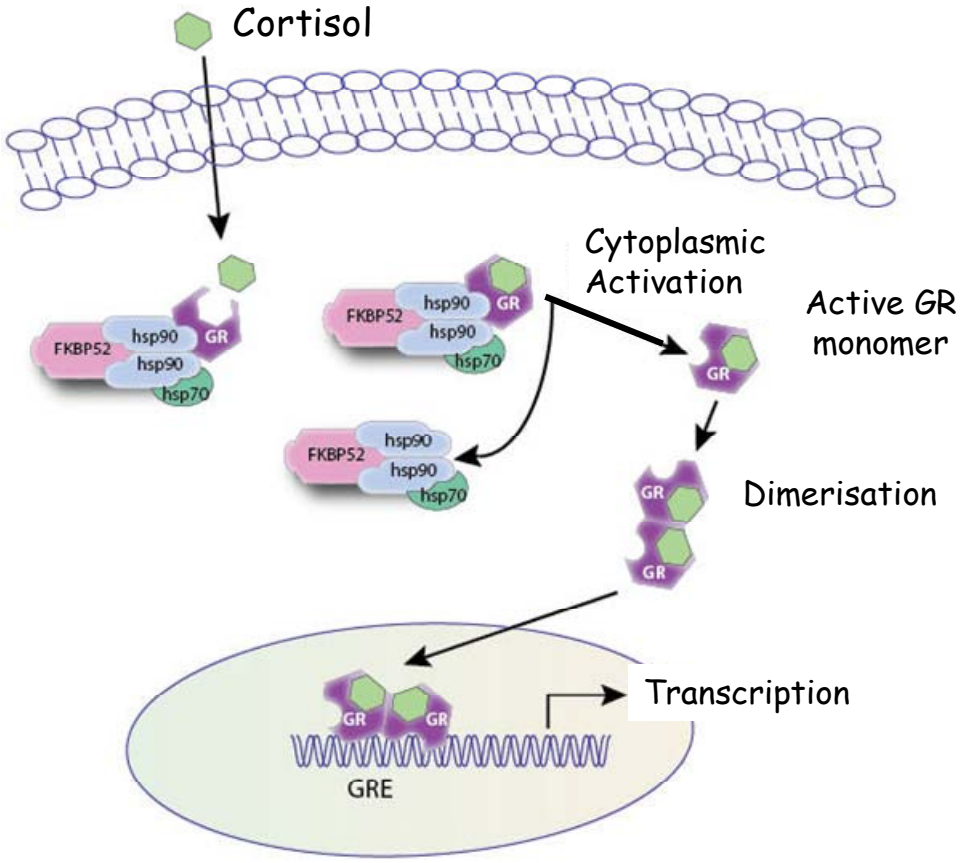

Figure 1-7 Glucocorticoid receptor activation. *In the unbound state the GR is complexed with various inactivating heat shock proteins including heat-shock protein 90 (HSP-90). Upon cortisol binding in the cytosol, a conformational change is induced, and the GR is released from the inactivating complex. The GR is then sequentially phosphorylated, homodimerised and translocated into the nucleus where it binds to a glucocorticoid response element (GRE) in the promoter of target genes, via the DNA binding domain, inducing gene transcription. Additionally, co-activators and co-repressors, expressed in a tissue or cell specific manner, are recruited to the activated ligand bound GR complex and act to facilitate or inhibit transcription. Adapted from www.panomics.com*

1.1.4.4 Cortisol metabolism

Cortisol has a half life in the circulation of approximately 70-120 minutes (Tomlinson et al., 2004). The major site of cortisol clearance is the liver, where cortisol is reduced or oxidized, and hydroxylated prior to conjugation of the resultant metabolites to sulfate or glucuronic acid in preparation for their excretion in urine (Tomlinson et al., 2004). Briefly, the principle steps in cortisol metabolism, as shown in (**Figure 1-8)**, are the conversion to 5α-tetrahydrocortisol (5α- THF/ allo-THF) and 5β-tetrahydrocortisol (5β-THF/ THF) by the membrane bound enzyme 5α-reductase (SRD5A1), or the cytosolic enzyme 5β-reductase (SRD5A2), respectively. In normal subjects, conversion by 5β-reductase predominates resulting in a 5β-THF: 5α-THF ratio of 2:1 (Arlt and Stewart, 2005). Additionally, 5β-reductase can catalyse the metabolism of cortisone into tetrahydrocortisone (THE). Although the majority of metabolism is to tetrahydros (50%), a smaller proportion (25%) of cortisol and cortisone is converted to α-/ β-cortol and α-/ β-cortone, respectively, by 20α- or 20β-hydroxysteroid dehydrogenase (20α- or 20β-HSD) (Arlt and Stewart, 2005). Active cortisol and inactive cortisone can be interconverted by the activity of the 11β-hydroxysteroid dehydrogenases (11β-HSDs, HSD11B1 and HSD11B2) via the oxidation of cortisol and the reduction of cortisone, which is discussed in further detail in section 1.1.4.5.2.

In humans the majority of cortisone circulates in the free form at approximately 50-100nmol/l. While this level is significantly less than that of cortisol during the diurnal peak (400-600nmol/l), approximately 95% of cortisol is bound to plasma proteins, notably cortisol binding globulin, and therefore biologically inactive (Meulenberg and

Hofman, 1990a; Meulenberg and Hofman, 1990b). The metabolites of cortisone and cortisol, which are detectable in urine, can be used as biomarkers of 11β-HSD1 activity, employing the equation: 5α-THF + 5β-THF: THE (Tomlinson et al., 2004). Any changes in GC metabolism and clearance are compensated for by the HPA axis via an alteration in ACTH secretion, so that circulating cortisol levels are maintained.

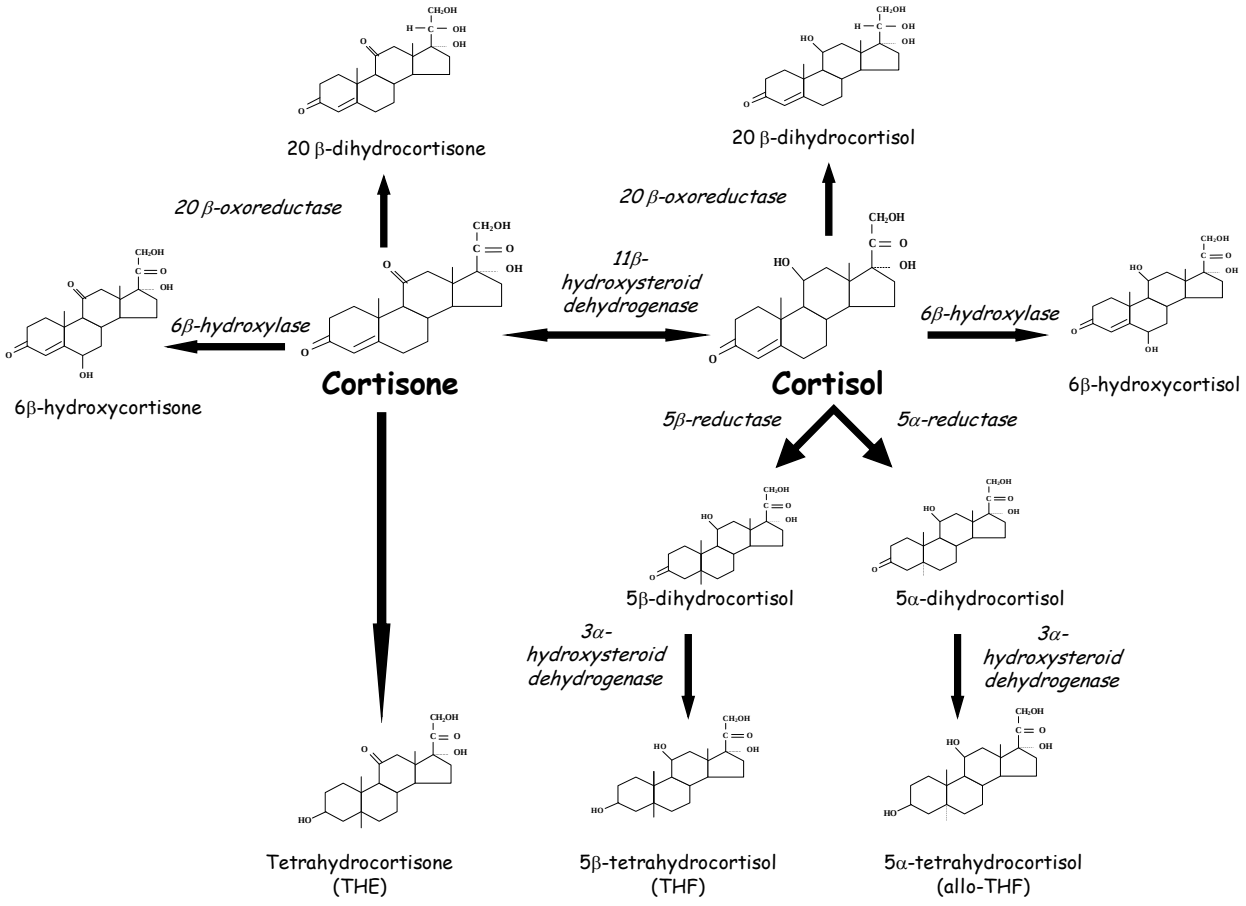

Figure 1-8 The key pathways of cortisol metabolism. *Cortisol can be interconverted to cortisone by 11β-HSD or to 5α-tetrahydrocortisol (allo-THF) and 5β-tetrahydrocortisol (THF) by 5α-reductase, or 5β-reductase, respectively. Additionally, 5β-reductase can catalyse the metabolism of cortisone into tetrahydrocortisone (THE). Cortisol can also be converted to 6β-hydroxycortisol by 6β-hydroxylase, or 20β-dihydrocortisol by 20β-oxoreductase.*

1.1.4.5 Pre-receptor regulation of glucocorticoids

The interconversion of active cortisone and inactive cortisol is catalysed by 11β-HSD, of which two isoforms have been cloned and characterised in human tissues: 11β-HSD type 1 (11β-HSD1, HSD11B1) and 11β-HSD type 2 (11β-HSD2, HSD11B2) (Stewart, 1996; Stewart and Krozowski, 1999; White et al., 1997). Both isoforms are members of the short chain dehydrogenase/ reductase (SDR) superfamily of oxidoreductases, comprising around 300 members, which share several distinct sequence motifs (Jornvall et al., 1995). Despite this the 11β-HSD isozymes are encoded for by different genes, have only 21% identity and display differential cofactor specificity, substrate affinity and importantly, direction of reaction that they catalyse (Albiston et al., 1994; Draper and Stewart, 2005; Tannin et al., 1991).

1.1.4.5.1 ***11β-Hydroxysteroid dehydrogenase type 1***

11β-HSD1 was first purified from rat liver by White and colleagues (Agarwal et al., 1989), and shown to act solely as a dehydrogenase (Lakshmi and Monder, 1988). However, subsequent studies revealed 11β-HSD1 to be a bi-directional enzyme, capable of catalysing both the inactivation of cortisol and the activation of cortisone. *In vivo* and in whole cell systems, this isoform acts predominately as an oxoreductase, catalysing the conversion of inactive cortisone to active cortisol (**Figure 1-9**) (Odermatt et al., 2006; Stewart and Krozowski, 1999; Tomlinson et al., 2004). Upon cellular disruption the reductase activity of 11β-HSD1 is lost and its dehydrogenase activity prevails (Tomlinson et al., 2004). The underlying mechanism for this 'switch' appears to depend on the intracellular redox content (see section 1.1.4.5.3) (Agarwal et al., 1990). Type 1 is principally expressed in glucocorticoid

target tissues such as liver, skeletal muscle and adipose tissue, gonad and bone where, via its oxoreductase activity, it amplifies the local effects of glucocorticoids (Draper and Stewart, 2005).

11β-HSD1 is a nicotinamide adenine dinucleotide phosphate (NAD(P)H)-dependent enzyme and has a much lower affinity for cortisol and corticosterone (the rodent form of cortisol) than 11β-HSD2 (Tomlinson et al., 2004). Biochemical analysis has revealed that the reductase reaction has co-operative rather than Michaelis-Menten kinetics (Maser et al., 2002), unlike the dehydrogenase, ensuring cortisol generation across a wide range of substrate concentrations.

1.1.4.5.2 ***11β-HSD2***

11β-HSD2 is a high affinity, nicotinamide adenine dinucleotide (NAD)-dependent dehydrogenase that rapidly inactivates F to E (**Figure 1-9**) (Stewart et al., 1995b). Although expressed in many tissues in the developing foetus, in adult life its localisation is principally classic mineralocorticoid target tissues, including the distal nephron of the kidney, sweat glands, salivary glands and colonic mucosa where this isozyme prevents the illicit occupation and activation of the MR by cortisol, which *in vitro* has an equal binding affinity for the MR as its natural ligand, aldosterone (Edwards et al., 1988; Stewart et al., 1995b). In addition, 11β-HSD2 is highly expressed in the placenta and the developing foetus, where it protects against exposure to maternal glucocorticoids (Seckl and Meaney, 2004). 11β-HSD2 is not expressed in human adipose tissue (Bujalska et al., 1997). Where 11β-HSD2 is congenitally absent, as in the condition apparent mineralocorticoid excess (AME), or inhibited, as following exaggerated liquorice ingestion, active glucocorticoid is able to

access the MR of the kidney, resulting in sodium retention, hypertension and hypokalemia (Stewart et al., 1995b; Ulick et al., 1979). In these patients the circulating concentration of cortisol are maintained within the normal range by intact regulation by the HPA axis. This 'experiment of nature' mirrors the phenotypic findings of 11β-HSD2 knockout mice (Kotelevtsev et al., 1999).

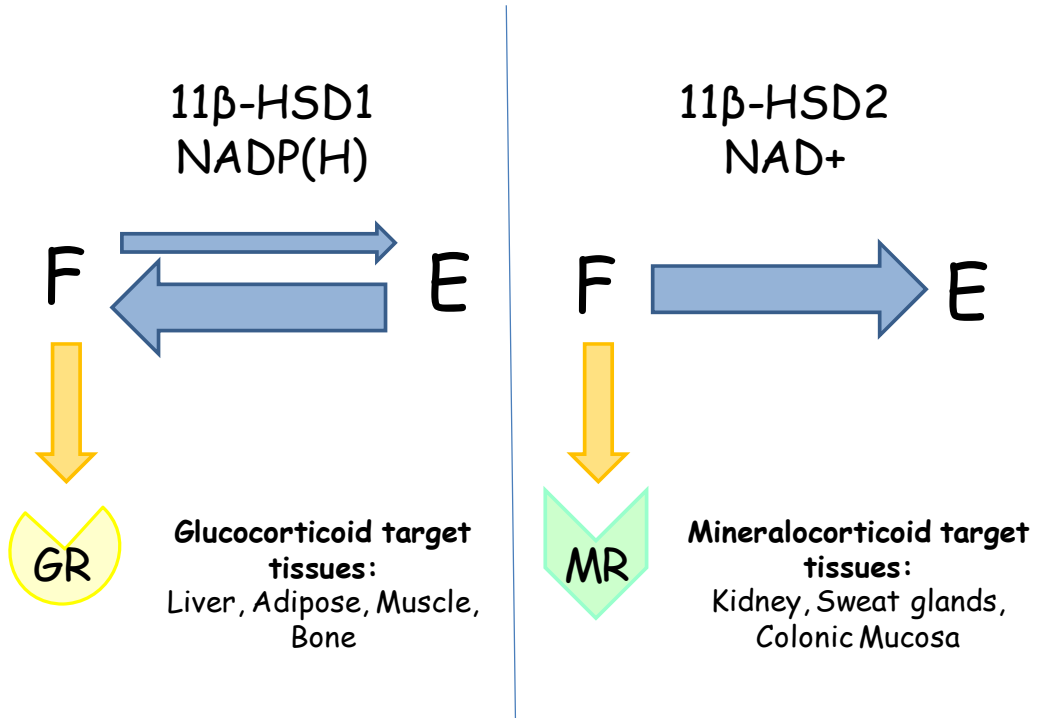

Figure 1-9 The pre-receptor regulation of glucocorticoid action. *In glucocorticoid target tissues 11β-HSD1 activates cortisone (E) to cortisol (F) which can bind and activate the glucocorticoid receptor (GR). In mineralocorticoid target tissues 11β-HSD2 inactivates cortisol to cortisone, preventing the illicit occupation of the mineralocorticoid receptor (MR) by cortisol. Adapted from (Arlt and Stewart, 2005).*

1.1.4.5.3 ***Hexose-6-phosphate dehydrogenase***

Hexose-6-phosphate (H6PDH) is co-expressed with 11β-HSD1 and is the rate limiting step in the microsomal pentose phosphate pathway, which is believed to exist within the ER lumen (Bublitz and Steavenson, 1988). H6PDH has dual nucleotide specificity for NADP+ and NAD+ but under physiological conditions, within the microsomal environment, G6P and NADP+ are believed to be its native substrates (Hewitt et al., 2005). It is responsible for catalysing the oxidation of glucose-6-phosphate (G6P) and other hexose-6-phosphates to 6-phospho-gluconolactone, thereby generating NADPH (Kimura et al., 1979). As described in section 1.1.4.5.1, NADPH is the co-factor required for the oxo-reductase activity of 11β-HSD1 which activates inactive cortisone to active cortisol. A supply of G6P is ensured by the G6P transporter of the ER, which is specific for G6P and a supply of NAD(P)+ is maintained through the functional co-operation of H6PDH and intraluminal reductases (Hewitt et al., 2005),

Bujalska et al have previously demonstrated that H6PDH expression is a crucial determinate of 11β-HSD1 oxoreductase activity in intact human adipocytes and Chinese hamster ovary cells and HEK cells transiently expressing 11β-HSD1 and H6PDH *in vivo* (Bujalska et al., 2005). Furthermore, H6PDH mRNA levels were found to positively correlate with 11β-HSD1 oxo-reductase activity in human omental adipocytes obtained from 15 women, independent of 11β-HSD1 mRNA expression levels (Bujalska et al., 2005).

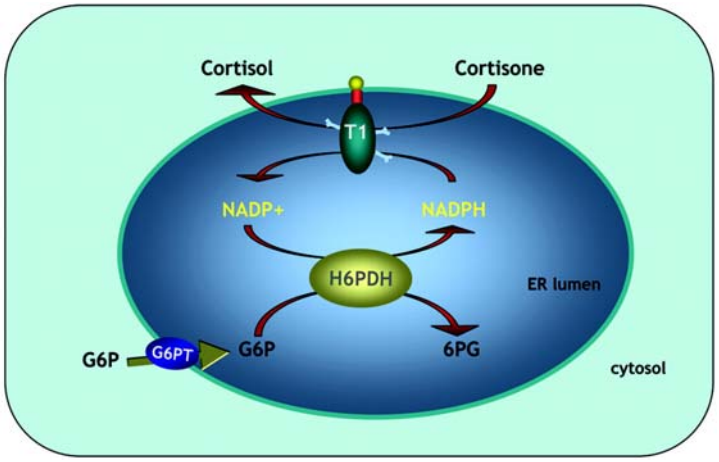

Figure 1-10 **Schematic representation of the interaction between H6PDH and 11β-HSD1 within the ER.** H6PDH converts glucose-6-phosphate (G6P) to 6-phosphogluconate (6PG), thus generating NADPH, within the ER. 11β-HSD1 (T1) uses the NADPH as a cofactor, converting cortisone to cortisol.

1.1.4.5.4 ***Cortisone reductase deficiency***

Failure to regenerate the active glucocorticoid cortisol from cortisone via the enzyme 11β-HSD1 results in the disease cortisone reductase deficiency (CRD). A lack of cortisol regeneration stimulates the HPA axis resulting in adrenal androgen excess. Consequently affected males present early in life with precocious pseudopuberty, while females present in midlife with a phenotype resembling PCOS, characterised by hirsuitism, oligoamenorrhea, and infertility (Lavery et al., 2008a). It originally appeared that mutations in *HSD11B1* may be responsible for CRD. However, large-scale population studies have failed to identify disease-causing mutations and have only identified polymorphic variants, with population frequencies that could not explain CRD. More recently it has become apparent that CRD can be explained by

mutations of the *H6PDH* gene, resulting in reduced generation of NADPH and consequently reduced 11β-HSD1 activity (Lavery et al., 2008a).

1.1.4.5.5 ***Animal models of 11β-HSD1 and H6PDH***

To investigate the role of 11β-HSD1 and H6PDH *in vivo*, knockout (KO) and overexpressing mice have been generated. 11β-HSD1 -/- mice appear to develop normally and are viable, fertile and normosensitive, but display protection from high fat diet induced dyslipidemia, glucose intolerance and obesity, a phenotype compatible with impaired intracellular glucocorticoid regeneration and reduced antagonism of insulin action (Kotelevtsev et al., 1997). These animals display a normal baseline expression of the gluconeogenic enzyme phosphoenopyruvate carboxylase (PEPCK) in the liver, however, induction of this enzyme is attenuated on fasting (Kotelevtsev et al., 1997). As both the liver and adipose play critical roles in whole body homeostasis it is difficult to assess the differential phenotypic effects due to the loss of GC action in these tissues in these animals. However, these animals do not have an obvious adipose phenotype (Kotelevtsev et al., 1997) possibly due to enhanced preadipocyte proliferation which may offset any potential benefits on adipocyte differentiation.

In contrast, a variety of transgenic models overexpressing 11β-HSD1 in a tissue specific manner have displayed detrimental effects (Masuzaki et al., 2001; Masuzaki et al., 2003). Mice overexpressing 11β-HSD1 under control of the adipose specific AP2 promoter have elevated cortisol levels in adipose tissue and the portal vein (which supplies the liver) but not in the systemic circulation, and display the full blown metabolic syndrome, including obesity, dyslipidemia and hypertension (Masuzaki et

al., 2001; Masuzaki et al., 2003). In this model, because the transgene was directed to the adipocyte-specific aP2 promoter, increases in adipose tissue mass were solely a consequence of increased lipid accumulation within pre-existing adipocytes. Similarly mice expressing 11β-HSD1 in liver under the ApoE promoter exhibit insulin resistance dyslipidemia, and hypertension, although these animals do not spontaneously develop obesity or glucose intolerance (Paterson et al., 2004), suggesting that adipose tissue may be more important than liver in determining the metabolic effects of 11β-HSD1. Overexpression of 11β-HSD2 in adipose tissue, where this isoform is not usually expressed, results in local GC inactivation and protects against high fat feeding induced obesity, compared to WT mice (Kershaw et al., 2005).

H6PDH KO mice have reduced generation of NADPH within the ER, resulting in a switch in 11β-HSD1 activity from reductase to dehydrogenase (Lavery et al., 2006). Similar to 11β-HSD1 KO mice, H6PDH KO mice display protection from high fat diet induced dyslipidemia, glucose intolerance and obesity, and elevated plasma corticosterone concentrations (**Table 1-1**)(Rogoff et al., 2007). However, in contrast to 11β-HSD1 KO mice, in H6PDH KO mice there is preserved induction and activity of the glucocorticoid responsive gluconeogenic enzymes PEPCK and glucose-6-phosphatase (G6Pase) (Lavery et al., 2007), suggesting that these animals partially retain glucocorticoid sensitivity in the liver. These animals display enhanced rates of glycogen synthesis, as has been observed in 11β-HSD1 KO mice, which has been proposed to be due to due to allosteric activation of glycogen synthase and inhibition of glycogen phosphorylase by G6P in these animals (Lavery et al., 2007). In contrast to fasted 11β-HSD1 KO mice, fasted H6PDH null animals were able to mobilise

stored glycogen, suggesting these animals have no defect in glycogenolysis (**Table 1-1**)(Lavery et al., 2007).

Interestingly H6PDH null animals also display severe skeletal myopathy, which is absent in 11β-HSD1 KO animals (Lavery et al., 2008b). The affected muscles of the animals have normal sarcomeric structure but contain large intrafibrillar membranous vacuoles and switching of muscle fibre type from type II to type I (Lavery et al., 2008b). It has been proposed that the molecular cause of this phenotype is the alteration of the redox state within the sarcoplasmic reticulum which results in the impairment of protein folding resulting in the activation of the unfolded protein response pathway (Lavery et al., 2008b). The lack of similar phenotype in 11β-HSD1 null animals, suggests that this phenotype is due to an 11β-HSD1 independent currently uncharacterised role of H6PDH.

Rodent models of obesity and diabetes interestingly elude to the tissue specific (dys)regulation of 11β-HSD1 in these conditions. In a model of genetic obesity, leptin resistant Zucker rats, obesity is associated with elevated type 1 mRNA expression in visceral adipose tissue, while liver expression is decreased compared control animals (Livingstone et al., 2000). Similar findings have been reported in leptin deficient ob/ob mice (Liu et al., 2003). However, in a model of diet induced obesity, short term feeding of Wistar rats with a high fat diet decreased 11β-HSD1 mRNA expression in both adipose and the liver (Drake et al., 2005). Although, following a longer period of high fat feeding expression levels were comparable to controls, indicating that the modulation of 11β-HSD1 levels may be an adaptive mechanism to protect against the short term effects of high fat feeding (Drake et al., 2005).

Table 1-1 Similarities and differences in the phenotype of 11β-HSD1 KO and H6PDH KO mice. *Phenotype refers to comparison with wild type animals.*

Phenotype	***11β-HSD1 KO mouse***	***H6PDH KO mouse***
Protection from diet induced obesity and dyslipidemia	***Yes***	***Yes***
Improved glucose sensitivity	***Yes***	***Yes***
Enhanced glycogen synthesis	***Yes***	***Yes***
Normal ability to metabolise stored glycogen	***No***	***Yes***
Normal Induction of gluconeogenic genes	***No***	***Yes***
Skeletal myopathy	***No***	***Yes***

1.1.4.6 Physiological and pathophysiological effects of glucocorticoids

The physiological effects of GC's can be summarised as being anti inflammatory/ immunosuppressive, metabolic or behavioural (**Figure 1-11**). In normal physiological conditions, acute stimulation of GC secretion, in times of illness or psychological stress, results in a beneficial stimulation of the anti-inflammatory response, and the catabolism and mobilisation of substrates for energy generation, thus restoring the homoeostasis of the organism. However, in cases of chronic GC excess, as in Cushing's disease or prolonged glucocorticoid treatment, the effects of GC can be detrimental (Stewart and Krozowski, 1999).

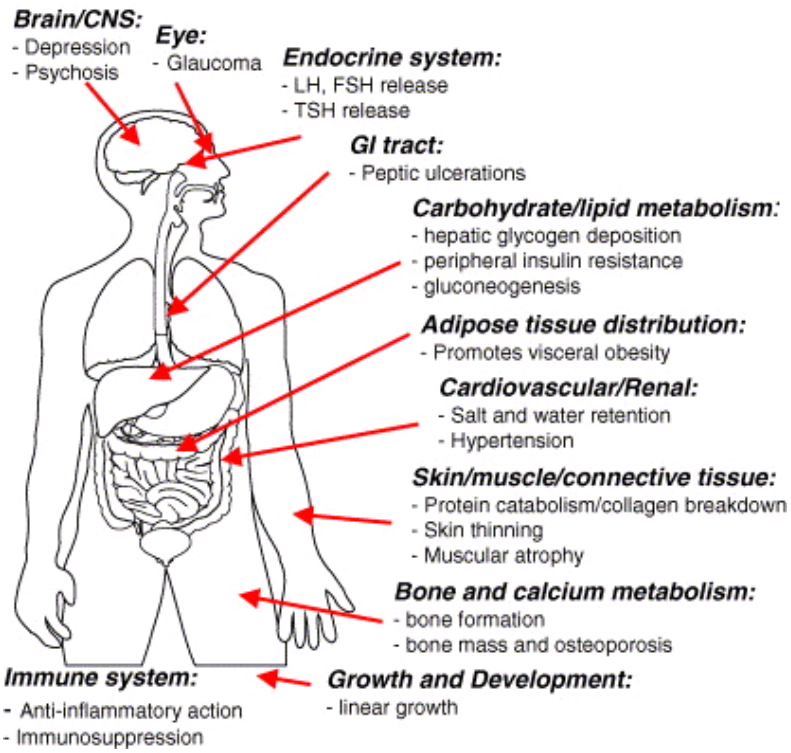

Figure 1-11 The key sites of glucocorticoid action. *Glucocorticoids act on a diverse range of tissue to cause numerous physiological effects which can be summarised as being anti inflammatory/ immunosupressive, metabolic or behavioural Taken from (Arlt and Stewart, 2005).*

1.1.4.6.1 ***Physiological effects***

1.1.4.6.1.1 Adipose

Glucocorticoids are potent modulators of adipose tissue adipogenesis, homeostasis and distribution, exemplified by the development of central obesity associated with Cushing's syndrome (Orth, 1995; Stewart et al., 1995a). The modulation of adipose tissue homeostasis by glucocorticoids appears to depend on nutritional status and adipose depot. In the fed state, glucocorticoids have been shown to enhance the rate of insulin induced lipogenesis (Wang et al., 2004), via induction of Acetyl CoA carboxylase (ACC) and fatty acid synthase (FAS) (Rumberger et al., 2003). However, in the fasted state, when insulin and glucose levels are low, GCs have been shown to enhance lipolysis, at least in part by stimulating hormone sensitive lipase (Slavin et al., 1994) and adipose triacylglycerol lipase (ATGL) and suppressing PEPCK expression, consequently reducing triglyceride re-esterfication and consequently increasing free fatty acid release (Chakravarty et al., 2005; Nechushtan et al., 1987). The effects of glucocorticoids on adipose tissue are also dependent on adipose depot and as observed in Cushing's syndrome, increase central (visceral, abdominal, facial and nape of neck) fat deposition while peripheral fat mass is reduced. This has led to the hypothesis that opposing effects of glucocorticoids may prevail in different tissues, and on the one hand increase lipolysis and downregulate lipoprotein lipase, thereby liberating free fatty acids from peripheral fat, but concurrently increase substrate flux into central adipocytes. In addition, glucocorticoids decrease glucose uptake and oxidation (Weinstein et al., 1995).

Glucocorticoids are potent regulators of adipogenesis by stimulating preadipocyte differentiation (Bujalska et al., 1999) and limiting preadipocyte proliferation (Gregoire et al., 1991; Rabbitt et al., 2002; Tomlinson and Stewart, 2002), which is discussed in section 1.2.3.1.

1.1.4.6.1.2Liver

Under normal physiological conditions, acute GC secretion, as observed during fasting, results in hepatic *de novo* glucose synthesis and gluconeogenesis, in order to provide glucose for extra hepatic tissues such as erythrocytes, brain and adrenal medulla (Consoli, 1992). At a molecular level GC's achieve this by the activation of key gluconeogenic regulatory genes including pyruvate carboxylase (PC), which catalyses the conversion of pyruvate into oxaloacetate (Yamada et al., 1999); PEPCK, the rate limiting step in the gluconeogenic pathway, which converts oxoloacetate to phosphopyruvate (Hanson and Reshef, 1997); and G6Pase, which hydrolyses glucose-6-phosphate into free glucose and inorganic phosphate (Saltiel and Kahn, 2001). However, chronically elevated GC levels result in the aberrant induction of gluconeogenic gene expression, and a consequential increase in hepatic glucose output, the development of hyperglycaemia and type II diabetes (Consoli, 1992). In addition, chronic GC levels have been shown to be associated with increased hepatic triglyceride synthesis, reduced hepatic fatty acid oxidation and the subsequent accumulation of lipids in the liver, termed 'fatty' liver or hepatic steatosis (Cole et al., 1982), as observed in patients with Cushing’s syndrome (see section 1.1.4.6.2.1)(Taskinen et al., 1983). The molecular mechanism(s) of this process are

not fully understood but are thought to involve the upregulation of the key lipogenic genes, fatty acid synthase (FAS), and acetyl coA carboxylase (ACC).

1.1.4.6.1.3 Skeletal muscle

In times of stress, such as fasting or infection, GCs stimulate skeletal muscle catabolism by direct and indirect mechanisms, mobilising amino acids which can be utilises as substrates for gluconeogensis and protein synthesis (Schacke et al., 2002). Concurrently GC's inhibit muscle glucose utilisation, increasing the availability of glucose to other tissues such as the brain and immune system. The catabolic effect of GC on muscle is exemplified by Cushing's syndrome and steroid therapy, both of which are associated with muscle atrophy (Schacke et al., 2002).

GCs have been shown to inhibit glucose uptake via reduced activation of the Insulin receptor/ PI3-kinase/ AKT signalling pathway. Treatment of rats or cultured C2C12 cells with the GR agonist dexamethasone (Dex) has been shown to result in reduced IR phosphorylation (Giorgino et al., 1993), PI3-kinase activity (Saad et al., 1993) and AKT phosphorylation and activation (Long et al., 2003; Sandri et al., 2004) in response to insulin. Reduced activation of this pathway results in the attenuation of insulin dependent glucose transporter, GLUT4, translocation to the plasma membrane and a subsequent reduction of insulin stimulated glucose uptake (Weinstein et al., 1995). In addition the GC-induced inhibition of AKT signalling results in suppression of glycogen synthase activity in muscle resulting in reduced glycogen synthesis (Ekstrand et al., 1996).

1.1.4.6.2 *Pathophysiological effects of glucocorticoids*

1.1.4.6.2.1 Cushing's syndrome

The pathology of GC excess, caused by a malfunction of the pituitary gland, was first described by Harvey Cushing in 1912, which he termed 'polyglandular syndrome' (Cushing H, 1932) and today is known as Cushing's syndrome. The eitiology of Cushing's syndrome can be ACTH dependent or independent (Orth, 1995). Autonomous ACTH secretion by pituitary corticotroph tumours (termed Cushing's disease) accounts for 80% of ACTH dependent causes of Cushing's syndrome, and demonstrates female preponderance (8:1) (Felig P, 2001). The remaining 20% of cases result from ectopic ACTH secretion, commonly from small cell lung carcinomas (Felig P, 2001). ACTH independent mechanisms include cortisol secreting adrenal tumours (Felig P, 2001). However the most common cause of Cushing's syndrome is treatment with exogenous GCs, which are estimated to be prescribed to 2.5% of the population (Van Staa TP, 2000).

Patients with Cushing's syndrome present with a dramatic phenotype, including hypertension (due to an increased activation of the MR in the distal nephron, as in AME), increased central adipose tissue mass (**Figure 1-12**), impaired glucose tolerance, insulin resistance, increased risk of cardiovascular disease, decreased bone mineral density, myopathy, and skin thinning (Orth, 1995).

1.1.4.6.2.2 Obesity

There are striking phenotypic similarities between Cushing's syndrome and the metabolic syndrome (visceral obesity, hypertension, dyslipidemia and

hyperglycaemia). However, in contrast to patients with Cushing's syndrome, who have elevated circulating levels of glucocorticoids, circulating cortisol concentrations are normal or possibly even reduced by 10-20% in patients with obesity and associated with a concomitant increase in daily cortisol secretion rates, an effect that is reversed upon weight loss (Dunkelman et al., 1964; Glass et al., 1981; Stewart, 1996). These findings led to the hypothesis that obesity, is associated with glucocorticoid excess via elevated 11β-HSD1 oxo-reductase activity, particularly at the omental depot representing 'Cushing's disease of the omentum' (Bujalska et al., 1997), and is supported by studies with genetically obese Wistar rats (see section 1.1.4.5.5). However, the majority of studies investigating global cortisol metabolism (assessed by urinary glucocorticoid metabolites, see 1.1.4.4) have shown reduced reductase activity with increasing adiposity (Rask et al., 2001; Rask et al., 2002; Stewart et al., 1999; Valsamakis et al., 2004). Although a limitation of this approach is that it most likely predominately reflects hepatic 11β-HSD1 activity and is influcenced by 11β-HSD2.

The adipose tissue level of 11β-HSD1 in humans remains controversial, possibly due to the use of inappropriate dehydrogenase assays on tissue homogenates in some studies (Rask et al., 2002). The majority of studies have been carried out on sc adipose samples and have shown an increase in 11β-HSD1 dehydrogenase activity compared to lean controls (Rask et al., 2002; Sandeep et al., 2005; Tomlinson et al., 2008; Wake et al., 2003). There have been a smaller number of studies investigating omental adipose tissue and the majority have shown no change or indeed an inverse correlation with fat mass (Tomlinson et al., 2002). However, all studies have agreed

that, as in rodent models, there is decreased hepatic 11β-HSD1 expression and activity in human obesity (Rask et al., 2001; Rask et al., 2002; Stewart et al., 1999).

Interestingly recent data seems to suggest that the decrease in global 11β-HSD1 activity that is seen in simple obesity with increasing fat mass is not observed in type 2 diabetes (Valsamakis et al., 2004). It has been proposed that a down regulation of 11β-HSD1 activity and/ or expression may represent a compensatory mechanism, preserving insulin sensitivity and preventing an increase in hepatic glucose output in the face of increasing fat mass (Tomlinson et al., 2008). Furthermore, failure to regulate 11β-HSD1 may result in relative tissue specific GC excess, perpetuating insulin resistance, hyperglycaemia and central adiposity.

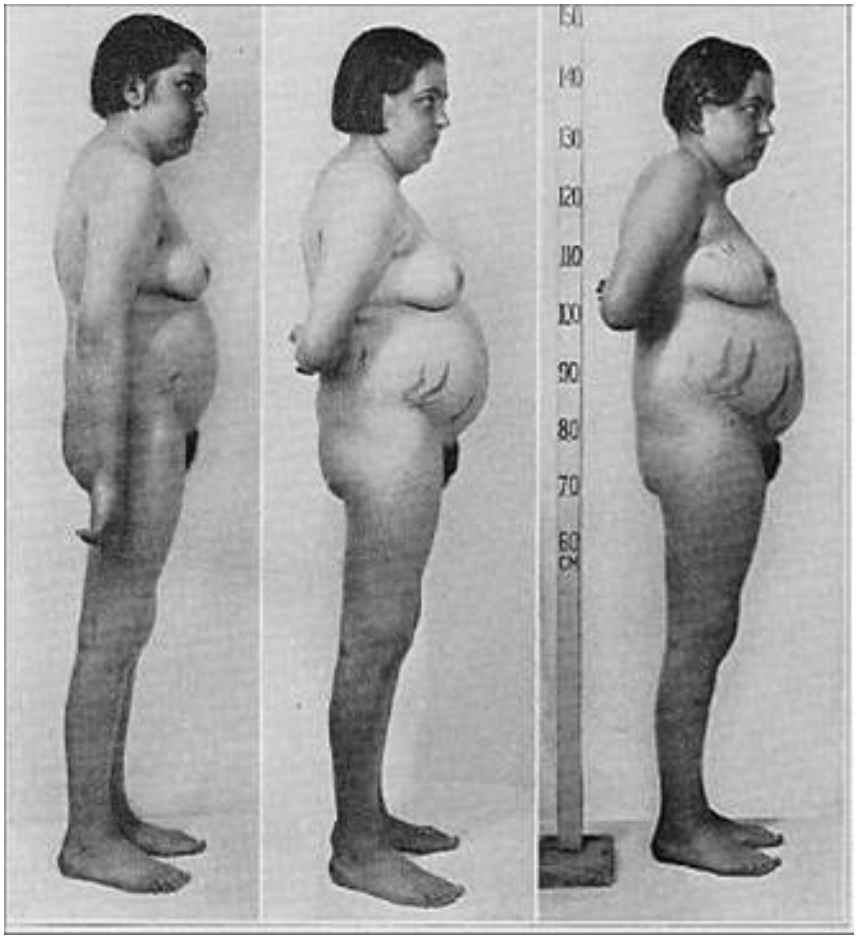

Figure 1-12 An early patient of Harvey Cushing with Cushing's Syndrome demonstrating the Cushingoid phenotype of increased central adipose tissue mass which is similar to that seen in patients with the metabolic syndrome. *The three photographs show the progression of the development of this disease in the patient.*

1.1.5 Adrenal sex steroids

1.1.5.1 Adrenal androgen synthesis- the synthesis of dehydroepiandrosterone

The innermost layer of the adrenal cortex, the zona reticularis, is the site of production of the metabolically active adrenal androgens, and their precursors, dehydroepiandrosterone (DHEA) and DHEA-sulfate (DHEAS), which are converted in peripheral target tissues to metabolically active sex hormones. The synthesis of DHEA occurs in a three step process, requiring the enzymes *CYP17A1* and *CYP11A*. The synthesis of adrenal androgens, unlike that of glucocorticoids and mineralocorticoids, is not solely regulated by differential zona enzyme expression. Indeed, *CYP17A1* and *CYP11A* are also expressed in the zona fasiculata and zona glumerolosa, and are required for glucocorticoid and mineralocorticoid expression and are expressed prior to adrenarche, a time when little DHEA is produced. Instead, adrenal androgen production relies on the modulation of the activity of these enzymes. In contrast to the zona fasiculata, the zona reticularis promotes both 17α-hydroxylase and 17,20-lyase activity of *CYP17A1*, driving steroid synthesis in the direction of C19 over C21 generation. The differential activity of *CYP17A1* is regulated via the co-factor cytochrome b5 (CYB), expression of which is distinct to the zona reticularis (Yanase et al., 1998). Expression of CYB increases during adrenarche (Suzuki et al., 2000), the onset of adrenal androgen production, characterised by a dramatic increase in serum DHT, DHEA, DHEAS and urinary 17-ketosteroids. It is thought that human CYB modulates adrenal androgen production by acting as an allosteric effector, optimising the interaction of *CYP17A1* with its

obligatory electron donor, P450 oxidoreductase, resulting in the stimulation of 17,20-lyase activity (Auchus et al., 1998b). The ratio of P450c17 17,20 lyase activity to 17-hydroxylase activity is also regulated by the concentration of P450 OR, with high molar ratios of POR to P450c17 promoting 17,20 lyase activity. Therefore, CYB can selectively augment 17,20-lyase activity, but only when OR is present (Gupta et al., 2001) In addition, phosphorylation of serine residues on P450c17 by a cAMP-dependent protein kinase also favours *CYP17A1* 17,20 lyase activity, however the specific kinase is yet to be identified (Auchus et al., 1998a; Auchus et al., 1998b).

In addition to *CYP17A1,* POR is the electron donor for all microsomal P450 enzymes, including P450c21 (encoded by *CYP21A2*), and aromatase (*CYP19A1*), key enzymes in glucocorticoid and sex steroid synthesis, respectively. Mutations in POR give rise to POR deficiency, a variant of congenital adrenal hyperplasia (CAH), which manifests as craniofacial malformations and disordered sex development in both sexes (Arlt, 2007). Interestingly, recent studies have provided evidence for a differential interaction of specific POR mutations with different electron-accepting P450 enzymes which begins to further explain the complex pathogenesis of this disease (Dhir et al., 2007).

Following the conversion of cholesterol to pregnenolone by *CYP11A1*, pregnenolone is converted to DHEA by *CYP17A1*. DHEA is predominately inactivated to DHEAS (Baulieu, 1996) by the action of the cytosolic enzyme SULT2A1, described in more detail in section 1.1.6. DHEA can also be converted to androstenedione by 3β-HSD2 (*HSD3B2*), and subsequently to active androgens and oestrogens. In addition, a significant amount of unmetabolised DHEA is secreted from the adrenal. An alternative pathway also exists by which pregnenolone can be converted to

androstenedione. In this secondary pathway pregnenolone is first converted into progesterone by 3β-HSD2 (*HSD3B2*) and then to 17α-hydroxy-progesterone by the 17α-hydroxylase activity of *CYP17A1*. 17α-hydroxy-progesterone is finally converted into androstenedione by *CYP17A1* 17,20-lyase activity. However, the hydroxylation of 17α-hydroxy-pregnenolone by *CYP17A1* is around 100 fold that of 17α-hydroxy-progesterone (Auchus, 2004). Therefore, in humans 17α-hydroxy-pregnenolone is the predominant substrate for DHEA generation under normal physiological circumstance and 17α-hydroxy-progesterone only contributes when there is an accumulation of this steroid due to an enzymatic block in steroidogenesis, for example, in 21-hydroxylase deficiency.

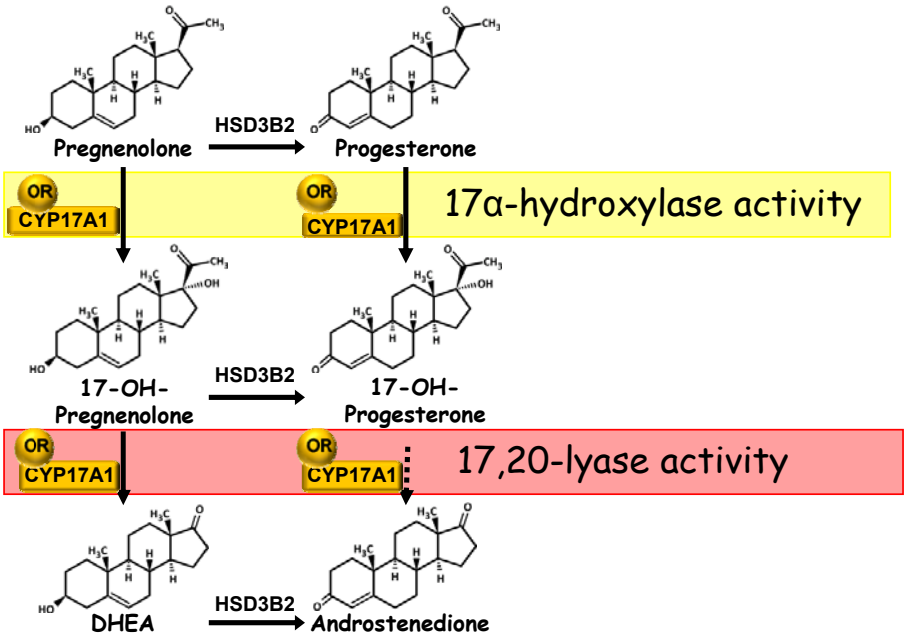

Figure 1-13 Schematic diagram of CYP17A1 activity. *CYP17A1 catalyses the 17α-hydroxylation of both pregnenolone and progesterone to 17-hydroxy-pregnenolone and 17-OH-progesterone, respectively, and the subsequent 17,20-lyase reaction to DHEA and androstenedione, respectively. The hydroxylation of 17α-hydroxy-pregnenolone by CYP17A1 is around 100 fold that of 17α-hydroxy-progesterone. Therefore, in humans 17α-hydroxy-pregnenolone is the predominant substrate for DHEA generation.*

1.1.5.2 Regulation of dehydroepiandrosterone synthesis and secretion

The human adrenal cortex synthesises and secretes approximately 4 mg and 25 mg of the active hormone DHEA, and the inactivated sulphated form, DHEAS, respectively, daily (Baulieu, 1996) making DHEA and DHEAS the most abundant steroid hormones in the circulation of human and some non-human primates (Cutler et al., 1978). Indeed, the plasma DHEAS levels in adult human men and women are 100-500 times those of testosterone, and 1000-10,000 times those of oestradiol (Labrie et al., 2005). The relatively high levels of DHEAS present in the circulation reflect the high degree of sulphotransferase activity of the human adrenal in addition to the relatively long half-life of DHEAS (10-12 hours), to DHEA (1-3 hours) (Cutler et al., 1978). Approximately 75%-90% of DHEA in the body is synthesised by the zona reticularis, while the remainder is produced by the testes and ovaries (Labrie et al., 2000b).

DHEA is distinct from the other major adrenal steroids in that it exhibits a characteristic age related pattern of secretion (Orentreich et al., 1984) (**Figure 1-14**). High levels of circulating DHEAS are detectable immediately following birth. However, during the first decade of life levels rapidly decline, as a consequence of the involution of the foetal zone of the adrenals (Allolio and Arlt, 2002). Circulating levels remain low until the onset of adrenarche, which occurs between the age of 6-8 years. Serum DHEAS then steadily increases until maximal levels are achieved between the second and third decade of life (Allolio and Arlt, 2002; Orentreich et al., 1984). Thereafter serum DHEAS levels decrease markedly, so that at 80 years of age, serum DHEAS levels are decreased to approximately 20% of their peak values

(Migeon et al., 1957). This process has been termed adrenopause, despite constant levels of cortisol and aldosterone secretion being maintained.

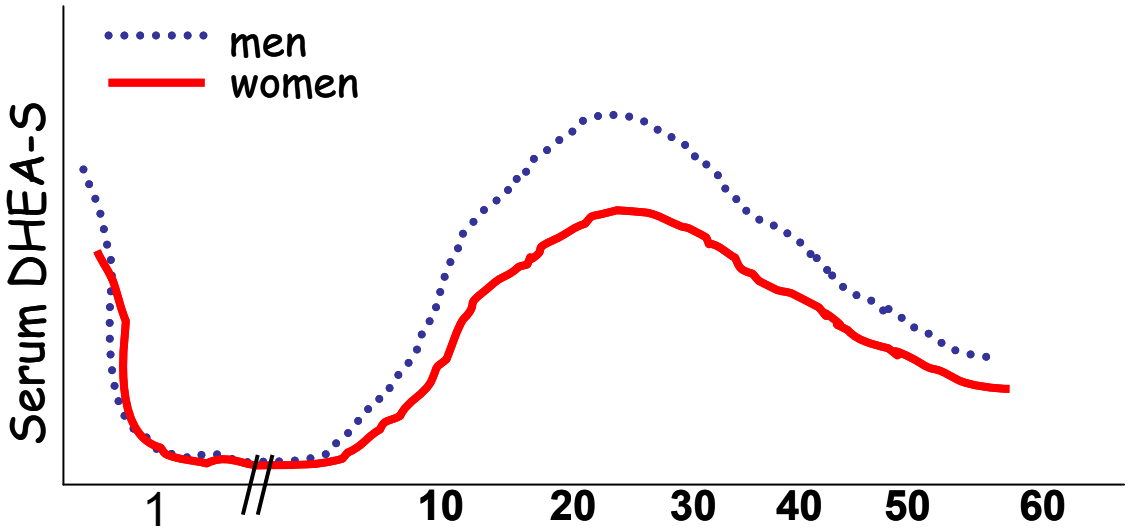

Figure 1-14 Serum DHEAS levels during human life*. Humans and other non-human primates express a characteristic pattern of DHEAS synthesis. Serum DHEAS levels are high immediately after birth due to production by the foetal adrenal. Levels rapidly decline and remain minimal until 8-10 years of age. Taken from (Arlt, 2004a).*

1.1.5.3 Mechanism of action

The effects of DHEA are known to be exerted indirectly, in peripheral target tissues of sex steroid action (following conversion to active androgens and/or oestrogens), or directly, as a neurosteroid (via interaction with neurotransmitter receptors in the brain). However, it is also becoming increasingly apparent that DHEA may elicit further direct effects.

1.1.5.3.1 ***Downstream metabolism of DHEA***

The principle way in which DHEA produces physiological effects is via its downstream conversion into potent androgens and oestrogens in peripheral target tissues (**Figure 1-15**). Only uncongugated DHEA can be metabolised in this way, whereas DHEAS has to first have the sulphate moiety removed to achieve biological activity. The local metabolism of DHEA, termed 'intracrinology', depends upon the level of expression of the various steroidogenic and metabolising enzymes in each of these tissues (e.g. *HSD3B2, HSD17B3, SRD5A2* and *CYP19A1*) (Martel et al., 1994a). In peripheral tissues, DHEA is predominantly converted into androstenedione by *HSD3B2* and subsequently to testosterone by *HSD17B3*. Testosterone can be further metabolised to the potent androgen, 5α-dihydrotestosterone (DHT), or aromatised to the active oestrogen, 17β-oestradiol (E2). DHT, however, cannot be aromatised (Miller, 2002).

Both testosterone and DHT can elicit androgenic effects, predominantly by binding to the androgen receptor (AR), a member of the nuclear receptor superfamily, although DHT has a 5 times greater affinity for the AR. Similarly, E2 exerts its effects by binding to its specific receptor, oestrogen receptor (ER), of which there are two isoforms, ERα and ERβ.

Figure 1-15 The principle downstream pathways of DHEA metabolism

1.1.5.3.2 ***Direct effects of DHEA***

In addition to its role as a precursor to active sex steroids there is growing evidence that DHEA can act via a direct mechanism. Although a specific receptor has not yet been isolated and cloned, high affinity binding sites for DHEA have been reported in several cell types of the vascular and immune system, including murine and human T lymphocytes (Meikle et al., 1992; Okabe et al., 1995), bovine aortic endothelial cells (BAEC) (Liu and Dillon, 2002; Liu and Dillon, 2004) and primary human umbilical vein endothelial cells (HUVECS). In a landmark paper, Liu et al (Liu and Dillon, 2002) described DHEA binding to BAEC cells which was of high affinity (Kd = 48.7 pM) and specificity (not inhibited by other sex steroids), saturable, within the physiological range of DHEA concentration (0-10 nM) and isolated to the plasma membrane. More recently this group and others have shown this specific binding to be to a G protein coupled receptor in BAEC cells, the activation of which, via a MAPK, ERK 1/2, results in the stimulation of endothelial nitric oxide synthase eNOS, nitric oxide (NO) production (Formoso et al., 2006; Simoncini et al., 2003), cellular proliferation, cell survival, cell migration and vascular tube formation in these cells. These findings may explain, at least in part, the beneficial effects of DHEA on the cardiovascular system observed *in vivo*. Although these studies provide support for a DHEA plasma membrane receptor, they have shown the effects of DHEA vary widely in time and dose- response characteristics. Therefore, the actions of DHEA are likely to occur via more than one specific receptor and/ or effector pathway, which remain to be elucidated.

1.1.5.3.3 *Metabolic effects of DHEA*

Sex steroids are known to play a role in adipose deposition and homeostasis, as described in section 1.2.3.2. In addition it is becoming clear that DHEA can modulate body composition and metabolic parameters directly, independent of the downstream conversion to active sex steroids. Several murine studies have demonstrated that DHEA administration blocks or retards fat accretion, and reduces weight gain in young rodents (Cleary et al., 1984; Cleary et al., 1988; Tagliaferro et al., 1986) and reduce fad pad weight, percentage body fat, adipocyte number and serum triglyceride levels in adult mice (Cleary and Zisk, 1986; Lea-Currie et al., 1997b; Mohan and Cleary, 1988; Shepherd and Cleary, 1984), without affecting food or water intake of these animals (Tagliaferro et al., 1986). In addition DHEA treatment has been show to prevent or attenuate the hyperglycaemia and/or hyperinsulinemia of diabetic (db/db) and obese (ob/ob) mice and obese Zucker rats (Coleman, 1988; Coleman et al., 1984; Leiter et al., 1987). *In vitro* data suggests that DHEA attenuates rodent adiposity via a direct effect on the adipocyte. Studies using the embryonic murine preadipocyte cell line, 3t3-L1 cells, and rodent isolated preadipocytes have demonstrated that DHEA attenuates the proliferation, differentiation and lipid accumulation of these cells (Gordon et al., 1987; Ishizuka et al., 1999; Lea-Currie et al., 1998; Shantz et al., 1989). However, the molecular mechanisms by which DHEA mediates these effects are unclear. In addition, DHEA has been demonstrated to increase adipocyte insulin stimulated glucose uptake in *ex-vivo* murine adipocytes (Ishizawa et al., 2001; Ishizuka et al., 1999; Ishizuka et al., 2007; Kajita et al., 2000; Labrie et al., 2000b). It has been suggested that DHEA may mediate this effect via activation of PI 3-kinase/ atypical PKC (Ishizawa et al., 2001;

Ishizuka et al., 1999; Kajita et al., 2000) or IRS-1/2/ P13-kinase / typical PKC signalling (Perrini et al., 2004).

The findings from human studies are less conclusive. The majority of clinical studies have shown that body composition after DHEA treatment remained either unaffected (Arlt et al., 2001; Diamond et al., 1996; Morales et al., 1994) or showed variable changes which were specific to men only (Morales et al., 1998; Yen et al., 1995). Furthermore, some studies have shown no effect of DHEA administration on insulin sensitivity or hyperglycaemia (Arlt et al., 2001; Christiansen et al., 2004; Hunt et al., 2000). However, many of these studies were short in duration and underpowered, which may explain the lack of significant effects. In contrast, a randomised control trial in elderly men and women demonstrated that the administration of 50 mg/day of DHEA for 6 months significantly reduced abdominal visceral and abdominal subcutaneous fat and increased insulin sensitivity, assessed by oral glucose tolerance test (OGTT) (Villareal and Holloszy, 2004). A further randomised double blind study where 1600 mg/day of DHEA was administered 28 days to healthy men demonstrated a significant reduction in body fat but no change in insulin sensitivity (Nestler et al., 1988). Conversely, a randomised double-blind cross over study has demonstrated that 50mg/day DHEA for 12 weeks to hypoadrenal women reduced plasma insulin and increased the amount of glucose required to maintain similar blood glucose levels while infusing the same insulin dosages (Dhatariya et al., 2005).

1.1.5.3.4 *Neuronal effects of DHEA*

In addition to the adrenal, DHEA can be synthesised *'de novo'* in neuronal tissues, as the necessary steroidogenic enzymes are expressed in a region specific fashion in

the brain (Compagnone and Mellon, 1998). Numerous studies have shown that DHEA and DHEAS can modulate several neurotransmitter systems, including the antagonism of γ-aminobut acid type A ($GABA_A$) receptors (Demirgoren et al., 1991; Majewska et al., 1990) and the stimulation of N-metyl-D-aspartate (NMDA) receptors, thereby suggesting a putative anti-depressant action of DHEA(S). Furthermore, pre-treatment with physiological concentrations of DHEA and DHEAS have been shown to protect murine primary hippocampal cell cultures from endocitoxin N-metyl-D-aspartic acid (NMDA) induced toxicity and DHEA (nM concentration range) has been shown to promote cortical neuronal growth and antagonise the suppressive effect of corticosterone on both neurogenesis and neuronal precursor proliferation in the rodent foetus. Studies suggest that DHEA may mediate this antiglucocorticoid action in the hippocpus, at least in part, by decreasing nuclear glucocorticoid receptor levels (Cardounel et al., 1999).

In addition, DHEA and DHEAS (nM range) have been shown to protect NMDA/$GABA_A$ negative neural crest derived PC12 cells *in vitro*, and rodent hippocampal cells *in vivo* against serum induced apoptosis via the activation of NF-κB and CREB, within minutes of DHEA administration, suggesting a non-genomic mechanism of DHEA action (Charalampopoulos et al., 2006b). As in human immune cells, high affinity binding sites for DHEA (Kd at the nanomolar range) have been detected in PC12 cells, human chromaffin and rat hippocampal cells (Charalampopoulos et al., 2006a; Charalampopoulos et al., 2006b). These findings suggest that DHEA, at physiological concentrations, may also exert its potent neuroprotective effects via specific membrane receptors, independent of NMDA and $GABA_A$ receptors.

Based on these findings it has been proposed that a relative deficiency of DHEA and DHEAS levels, as observed during aging and adrenal insufficiency, may represents a key cause of neuronal dysfunction and/or degeneration. In support of this hypothesis epidermiological studies have shown that patients with Alzheimer's disease have decreased DHEAS levels in specific regions of the brain, as compared to that of healthy age-matched controls (Huppert et al., 2000). Furthermore, DHEA has been consistently shown to improve impaired mood and well-being reported in patients with AI (Callies et al., 2001), depressive disorders (Bloch et al., 1999; Wolkowitz et al., 1999) and schizophrenia (Strous et al., 2004). In addition, DHEA and DHEAS have been shown to enhance memory in mice and rats (Flood and Roberts, 1988; Flood et al., 1988). However, to date there is no consistent *in vivo* data that DHEA influences memory, cognition, mood or wellbeing in healthy subjects (Arlt et al., 2001; Baulieu et al., 2000).

1.1.5.3.5 *Immune effects of DHEA*

In vitro and *in vivo* studies have suggested that DHEA stimulatory activity on the immune system, counteracting the immunosuppressive effects of glucocorticoids. Several studies have shown that DHEA administration increases host resistance to viral and bacterial pathogens in animal studies (Ben-Nathan et al., 1999; Danenberg et al., 1992; Loria et al., 1996). *In vitro* studies employing human immune cells have revealed that DHEA induces mitogen stimulated IL2 production from CD4+ cells (Suzuki et al., 1991), increase natural killer (NK) numbers and cytotoxicity (Casson et al., 1993; Solerte et al., 1999a; Solerte et al., 1999b) and inhibit release of the inflammatory cytokine IL-6 (Catania et al., 1999). However, whether some of these effects are mediated by DHEA directly or via conversion to active androgens and

oestrogens is controversial. Nonetheless, conversely glucocorticoids stimulate a shift to CD8+ T cells, suppressing IL-2 production (Dillon, 2005) and IL-6 secretion, and have been shown to suppress NK cell cytotoxicity (Gerra et al., 2003). Furthermore, in humans DHEAS, and in rodents DHEA, have been shown to attenuate cortisol induced suppression of neutrophil proliferation (Butcher et al., 2005). Consequently, a high cortisol to DHEA(S) ratio, as associated with aging, may create a negative milieu for immune function. Indeed, low serum DHEAS and high cortisol serum levels following trauma are correlated with high mortality in trauma patients (Beishuizen et al., 2002).

In a number of studies, DHEA supplementation has been used to modify immune functions and course of disease in patients with immunopathies. Clinical trials have demonstrated a beneficial effect of DHEA in systemic lupus erythematosus (SLE), increasing T lymphocyte IL-2 secretion (Suzuki et al., 1995), consequently decreasing the number of SLE flares, and reducing the requirement of glucocorticoids (van Vollenhoven et al., 1995). It remains to be seen if DHEA provides beneficial effects in other auto-immune disease states. In contrast, the DHEAge study involving DHEA treatment of healthy elderly subjects, did not reveal any effect of DHEA on NK cell cytoxicity, cytokine production, or T cell populations (Baulieu et al., 2000). It is likely that DHEA will be more efficacious in patients with immunopathies or an impaired immune system than healthy populations.

1.1.5.3.6 *Bone effects*

As sex steroids are potent regulators of bone remodelling, there has been interest on the influence of DHEA replacement on bone mineral density (BMD) and

homeostasis. DHEA replacement to healthy elderly individuals, has been shown to increase in BMD at the femoral neck (Baulieu et al., 2000) and in the spine (Weiss et al., 2009) in older women (≥70 years of age) but not in men. Similar findings were observed in studies involving patients with primary AI, where an increase in femoral neck BMD was also reported (Arlt et al., 2001). Taken together, current findings suggest the beneficial effects of DHEA on BMD are small and limited to women, possibly due to the transformation of DHEA to androgens. Further large scale studies need to be performed in this area.

1.1.6 Interconversion of DHEA and DHEAS

Only uncongugated DHEA can be metabolised intracellularly to androgens and oestrogens, while DHEAS first requires cleavage of its sulphate moiety, and is thought to act as a storage pool of hormone. DHEA can be sulfated to DHEAS by the cytoplasmic enzyme, DHEA sulphotransferase (SULT2A1) and conversely DHEAS can be hydrolysed to DHEA by the microsomal enzyme steroid sulfatase (STS, **Figure 1-16**). Based on previous studies, which determined the pharmokinetics of DHEA and DHEAS following oral DHEA administration, it was generally accepted that DHEA and DHEAS interconvert freely and continuously. However, a more recent study in which oral DHEA and intravenous DHEAS was administered to healthy young men indicates that the predominant direction of DHEA and DHEAS interconversion to be of sulfation (Hammer et al., 2005b). In this study, as expected, DHEA administration resulted in an increase in circulating DHEAS, whereas, administration of DHEAS surprisingly failed to result in any significant production of DHEA. This finding was endorsed *in vitro* utilising hepatic HEPG2 cells, despite

significant, comparable mRNA expression of STS and SULT2A1 by these cells. This finding suggests that the crucial rate limiting step regulating circulating DHEA levels to be that of DHEA sulphotransferase rather than STS. However, STS does play an important role in the regeneration of DHEA in select sex steroid target peripheral tissues, such as the breast and prostate (Labrie et al., 2003; Reed et al., 2005) which enables local sex steroid synthesis. In addition, STS is abundantly expressed in the placenta (Glass et al., 1998), enabling the biosynthesis of sex steroids important for foetal development.

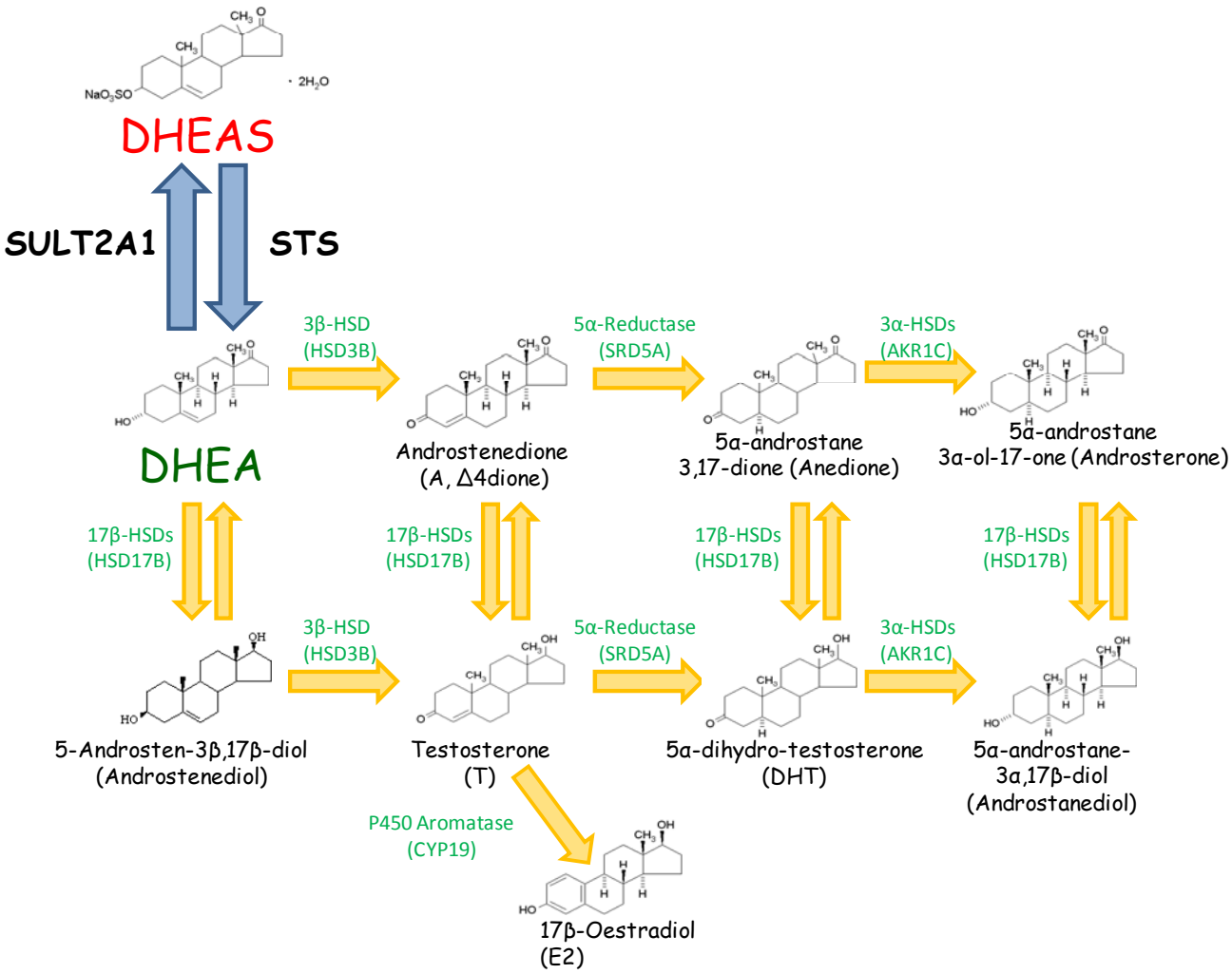

Figure 1-16 The interconversion of DHEA and DHEAS. *DHEA is metabolised by the cytosolic enzyme sulphotransferase (SULT2A1) to its sulphate ester, DHEAS. Conversely, DHEAS is hydrolysed by the microsomal enzyme steroid sulfatase (STS) to DHEA, which can be converted to active sex steroids in peripheral target tissues.*

1.1.6.1 Steroid sulphatase

In addition to those of adrenal origin, sex steroid precursors can be synthesised by the hydrolysis of inactive conjugated steroids, catalysed by the microsomal enzyme STS, prior to their local biosynthesis of biologically active androgens and oestrogens. STS hydrolyses DHEAS to DHEA (**Figure 1-16**), which is then converted to dihydrotestosterone (DHT), the most potent agonist of the androgen receptor, by the actions of *3HSD, 17HSD3* and 5α-reductases 1 and 2 (5R1/R2), as described in section 1.1.5.3.1. Additionally STS can catalyse the hydrolysis of estrone sulfate to estrone, which is subsequently reduced to 17β-estradiol by *17HSD1*. These pathways play a particularly important role in the maintenance of local levels of sex steroids in post-menopausal women (Labrie et al., 2000a; Labrie et al., 2000b).

STS is a member of the highly conserved arylsulfatase (ARS) family. The ARS family members catalyse the hydrolysis of sulfate ester bonds of a wide variety of substrates ranging from sulfated proteoglycans to conjugated steroids and sulfate esters of small aromatics. Seventeen human sulfatase proteins and their genes have been identified (Diez-Roux and Ballabio, 2005), with a sequence homology ranging between 20% and 60% (Ghosh, 2007). The catalytically active N-terminal residues are particularly highly conserved indicating a common catalytic mechanism between family members (Ghosh, 2007).

STS is a membrane bound microsomal enzyme, ubiquitously expressed in mammalian tissues (Martel et al., 1994b). The human *STS* gene contains ten exons comprising 583 amino acids located on the distal short arm of the X chromosome

and maps to Xp22.3-Xpter (Yen et al., 1987). Inactivation of the *STS* gene results in X-linked ichthyosis, a disease related to scaling of the skin (Alperin and Shapiro, 1997; Ghosh, 2004; Yen et al., 1992). In contrast, elevated levels of STS in breast carcinomas and STS dependent proliferation of breast cancer cells have been observed. Consequently, inhibitors of STS are being developed as a novel therapy for hormone dependant breast and endometrial cancer in women (Foster et al., 2008; Stanway et al., 2007; Stanway et al., 2006).

1.1.6.2 Sulphotransferase superfamily

The conversion of DHEA to DHEAS (**Figure 1-16**) is performed by a sulphotransferase, SULT2A1. Sulphotransferases transfer the polar sulpho moiety from the universal co-factor 5'-phosphoadenosine-3'-phosphosulphate (PAPS) to nucleophillic hydroxyl and amine groups of their specific substrates. In mammals two classes of sulphotransferases can be distinguished. The first comprises primarily membrane-bound sulphotransferases localised to the Golgi apparatus, which metabolise macromolecular endogenous structures, such as polysaccharides (Strott, 2002). The second class, of which SULT2A1 is a member, are soluble, predominantly localised to the cytoplasm, and metabolise hormones, such as DHEA and other small endogenous compounds or neurotransmitters (Strott, 2002).

As with the sulfation of DHEA, the transfer of a sulpho moiety to small molecules usually produces a product of increased aqueous solubility facilitating subsequent excretion and impairing passive membrane transport (Glatt et al., 2001). Consequently sulfation is generally associated with inactivation or detoxification. However, in some cases, sulfation promotes activation and sulphated products may

have a longer half life then the uncongugated compound. Indeed, a growing number of promutagens and procarcinogens are known to be activated by SULT's (Glatt et al., 1998; Glatt et al., 1994).

To date more than 50 mammalian and avian cytosolic sulphotransferases have been identified, cloned and sequenced, of which, 11 isoforms encoded by 10 genes have been identified in humans (Glatt and Meinl, 2004). Characterisation of these genes has revealed that cytosolic sulphotransferases, are members of a single gene superfamily, now termed SULT, which share considerable sequence and intron/exon homology (Nagata and Yamazoe, 2000; Yamazoe et al., 1994). In contrast, membrane bound sulphotransferases are genetically distinct. The human cytosolic SULT superfamily can be divided into four subfamilies SULT1, SULT2, SULT4 and SULT6 (Lindsay et al., 2008).

SULT enzymes have a widespread tissue distribution and are expressed in the liver, lung, brain, skin, platelets, breast, kidney and gastrointestinal tissue. Members of each family (indicated by the number after 'SULT') show at least 45% homology and each subfamily (letter after subfamily number) share at least 60% identity (Glatt and Meinl, 2004). The distinct genes are identified by a further number after the subfamily letter, and different translational products are identified by a letter following this number. Most SULT proteins appear to exist as homodimers, although the monomeric and tetromeric forms have been detected in rodents (Glatt and Meinl, 2004). The monomenic subunits of human SULTs consist of 284 and 365 amino acid residues and are not known to undergo posttranslational modification (Glatt and Meinl, 2004).

It is becomingly increasingly evident that the importance of DHEA sulfation may be even greater in humans than rodents, due to the inter-species differences in expression and function of SULTs. For example, to date, human is the only species in which a catecholamine specific SULT isoform (SULT1A3) has been identified (Glatt and Meinl, 2004). In contrast, rodents express several SULT2A isoforms, while only one has been characterised from humans (Glatt and Meinl, 2004).

1.1.6.3 SULT2A1

The *SULT2A1* gene is located on 19q13.3 at a distance of nearly 500kb to *SULT2B1*. SULT2A1 is the major isoform involved in the formation of steroid sulphate esters (Falany et al., 1995). DHEA is the principle substrate, however many other alcoholic steroids, including both the 3α-and 3β-hydroxysteroids, estrogens and testosterone, and non-steroidal alcohols can also act as substrates (Strott, 2002). SULT2A1 mRNA has been observed in many tissues. However, SULT2A1 protein is only highly expressed in the liver, adrenal cortex and duodenum, whereas no enzyme or extremely low levels of expression have been detected in other tissues. Currently relatively little is known about the regulation of SULT2A1 gene expression. Immunohistochemistry has revealed that SULT2A1 expression is high and localised to the zona reticularis in the adrenal, consistent with the abundant adrenal production and high circulating levels of DHEAS in humans. In addition SULT2A1 is an important role in the sulfation of secondary bile acids such as lithocholic acid and chenodeoxycholic acid (Strott, 2002).

Single nucleotide polymorphisms (SNPs) have been identified in most of the human SULT isoforms. Analysis of the liver SULT2A1 activity in 94 subjects revealed a

bimodal distribution, with SULT2A1 activity strongly correlating with SULT2A1 protein expression in these individuals (Aksoy et al., 1993; Wood et al., 1996), suggesting this distribution is via at least 1 genetic polymorphism. However, comparison of the nucleotide coding sequences revealed no variation between subjects displaying high or low SULT2A1 activity, suggesting the polymorphism may be present in the non-coding regions or outside the *SULT2A1* gene (Glatt et al., 2001). To date 10 non-synonyous cSNPs have been observed in the human SULTA1 gene (Glatt and Meinl, 2004). Three of these SNPs, which have been detected only in African-Americans (alloenzymes *VII,*VIII and *X), show significantly reduced levels of enzyme activity and immunoreactive protein when expressed in a mammalian cell model (Thomae et al., 2002), suggesting that SNPs in SULT2A1 may account for differences in sulfation between people *in vivo*.

1.1.6.4 3'-phosphoadenosine 5'-phosphosulfate (PAPS) synthesis

All sulfation reactions, such as that of DHEA catalysed by SULT2A1, require a ready supply of the active, high energy form of sulfate, 3'-phosphoadenosine 5'-phosphosulfate (PAPS). This is supported by the observation that sulfation does not proceed in the absence of PAPS *in vitro* or under conditions that limit PAPS synthesis (Klaassen and Boles, 1997). Inorganic sulfate (SO_4^{2-}) is usually available in copious amounts from the diet and the catabolism of proteins and sugar sulfates, and plasma levels are tightly regulated, such that sulfate deficiency is distinctly unusual (Huxtable RJ, 1986). The generation of PAPS from inorganic sulfate occurs in the cytosol or the nucleus (Li et al., 1995) as a result of the concerted action of two enzymes (Bandurski and Lipmann, 1956; Robbins and Lipmann, 1958a; Robbins and

Lipmann, 1958b), ATP sulfurylase and APS kinase, which in animal species are carried out by a bifunctional fusion protein termed PAPS synthase (PAPSS) (Lyle et al., 1994b), but in lower species are separate proteins (Strott, 2002). The presence of the bifunctional protein PAPS synthase in animals is thought to pose an advantage over lower species, in that the intermediate product APS can be shuttled from one active site to the other, increasing the efficiency of the process (Lyle et al., 1994b). Indeed, humans shuttling of the intermediate substrate, APS, has been shown to take place with remarkably high efficiency (96%) (Lyle et al., 1994a). It has been well established that the NH_2-terminal region of human PAPS synthase constitutes the APS kinase domain, whereas the ATP sulfurylase domain is located in the COOH-terminal portion of this bifunctional protein and when overexpressed and purified the domains can work independently of one another (Venkatachalam et al., 1998).

The biphasic reaction of PAPS synthesis is outlined in **Figure 1-17**. The first step is catalysed by ATP sulfurylase, in the presence of Mg^{2+}, and involves the reaction of inorganic sulfate with ATP to form adenosine 5'-phosphosulfate (APS) and inorganic phosphate. The reaction results in the formation of a high-energy phosphoric-sulfuric acid anhydride bond that is the chemical basis for sulfate activation (Leyh, 1993), and appears to be the rate limiting step in PAPS formation (Wong et al., 1991). Kinetic studies have established the order of reaction mechanism. First the binding of ATP-Mg and inorganic sulphate (SO_4^{2-}) occurs in a random order. Subsequently the products are released in an ordered fashion with PPi-Mg being released before PPi. The subsequent step is catalysed by APS kinase, again in the presence of Mg^{2+}, and involves the reaction of APS with a second molecule of ATP to yield PAPS and ADP. Similar to the ATP-sulfurylase domain, in the APS-kinase domain the synthesis of

PAPS proceeds in an ordered manner. First MgATP associates, which phosphorylates APS kinase, subsequently APS binds with high affinity, which is phosphorylated to form PAPS. PAPS then disassociates from APS kinase, followed by mgADP (Strott, 2002). Interestingly this enzyme undergoes pronounced uncompetitive substrate inhibition with APS (Sekulic et al., 2007), which is thought to occur by the rebinding of APS to the same site, before ADP dissociation.

The initial reaction, resulting in APS formation, is not favoured energetically with a Vmax of the forward and reverse direction as 6.6 and 50 units/ mg protein respectively (Klaassen and Boles, 1997; Seubert et al., 1985). In addition, as local levels of PAPS inhibit its own synthesis (Harjes et al., 2005), the subsequent hydrolysis or rapid utilisation of APS, and the consumption or translocation of PAPS out of the cytoplasm or nucleus are required for the reaction to proceed toward PAPS synthesis.

Each domain of the bifunctional protein possesses a conserved nucleotide-binding motif. Sequence analysis has revealed in the APS kinase domain this is in the form of a P loop motif (GxxGxGKS/T), which is involved in coupling of the phosphate moiety of ATP and cleavage of the β-γ phosphodiester bond (Strott, 2002; Walker et al., 1982). In contrast, the carboxy-terminal ATP sulfurylase domain contains a HxGH nucleotide binding motif, which catalyses the removal of the β-γ diphosphate of ATP and condensation of the formed AMP with inorganic sulfate to form APS (Bork et al., 1995). Mutational analysis of both nucleotide binding sites has confirmed their importance in PAPS generation (Deyrup et al., 1998; Venkatachalam et al., 1999).

1.1.6.4.1 ***PAPS synthase***

PAPSS exists as two isozymes, *PAPSS1* and *PAPSS2*, encoded by genes located, in humans, on chromosome 4q25-26 and chromosome 10q23-24, respectively. PAPSS 1 and 2 proteins are 106 and 85 kb in length, respectively, and share 77% identity (Strott, 2002) with very similar structures including 12 exons and virtually identical exon-intron splice junctions (Xu et al., 2000). PAPSS1 is highly expressed in brain and skin, while PAPSS2 is the predominant form in liver and cartilage (Fuda et al., 2002; Xu et al., 2000). *PAPSS1* has been cloned from several species, including human (Venkatachalam et al., 1998), mouse (Li et al., 1995), guinea pig (Fuda et al., 2002), marine worm (Rosenthal and Leustek, 1995) and drosophila (Jullien et al., 1997) and appears to be highly conserved between species, indicated by the 98% and 95% identity between human and mouse or guinea pig (Strott, 2002), respectively.

Two variants of the PAPSS2 isoform exist due to alternate splicing, PAPSS2a and PAPSS2b, which differ in an additional five amino acid segment (GMALP) in the ATP sulfurylase domain of the protein of the PAPSS2b variant (Strott, 2002). Rare mutations that inactivate PAPSS2 have been shown to be associated with human spondyloepimetaphyseal dysplasia (ul Haque et al., 1998) and murine brachymorphism (Kurima et al., 1998). In addition, more common genetic polymorphisms have been identified in both isoforms (Xu et al., 2002; Xu et al., 2003). To date twenty-one and twenty-two single nucleotide polymorphisms (SNPs) have been observed in the *PAPSS1* and *PAPSS2* genes respectively, including two non-synonomous coding regions SNPs in *PAPSS1* (Arg333Cys and Glu531Gln) (Xu et al., 2003) and four in *PAPSS2* (Glu10Lys, Met281Leu, Val291Met and Arg432Lys)

(Xu et al., 2002). Two of the non-synonomous SNPs in the *PAPSS2* gene were found to have reduced activity compared to WT, which was found to be due to reduced protein expression for 1 SNP, while neither of the SNPs in *PAPSS1* were shown to alter PAPSS activity. These findings give rise to the hypothesis that SNPs in these genes may be functionally significant and genetic polymorphisms might contribute to variations in sulfate conjugation *in vivo*.

The physiological significance of two isoforms of PAPSS, and furthermore, two splice variants of *PAPSS2*, which appear to catalyse the same reaction is currently unclear. Particularly as numerous tissues express the ubiquitously expressed *PAPSS1* and one or more of the isoforms of *PAPSS2*. The striking phenotype observed with the loss of one isoform as observed in brachymorphic mice (Kurima et al., 1998) and human spondyloepimetaphyseal dysplasia (ul Haque et al., 1998), further confounds this matter. However, in the case of *PAPSS2*, the splice variants are known to have differential tissue and, compared to *PAPSS1*, at least in the case of rodents, differential temporal expression (Stelzer et al., 2007). Additionally the isoforms display distinct catalytic activities, which in the PAPSS 2 variants are 10-15 times that of PAPSS1, and in the PAPSS2a variant is 30% less than that of PAPSS 2b (Fuda et al., 2002). In addition, the isoforms may have differential cellular localisation. Although PAPS synthesis had been assumed to occur in the cytosol, recent evidence indicates that PAPSS1 may be nuclear in its subcellular localization, as is PAPSS2 when coexpressed with PAPSS1 (Besset et al., 2000). Further studies are required to address if these proteins are truly redundant.

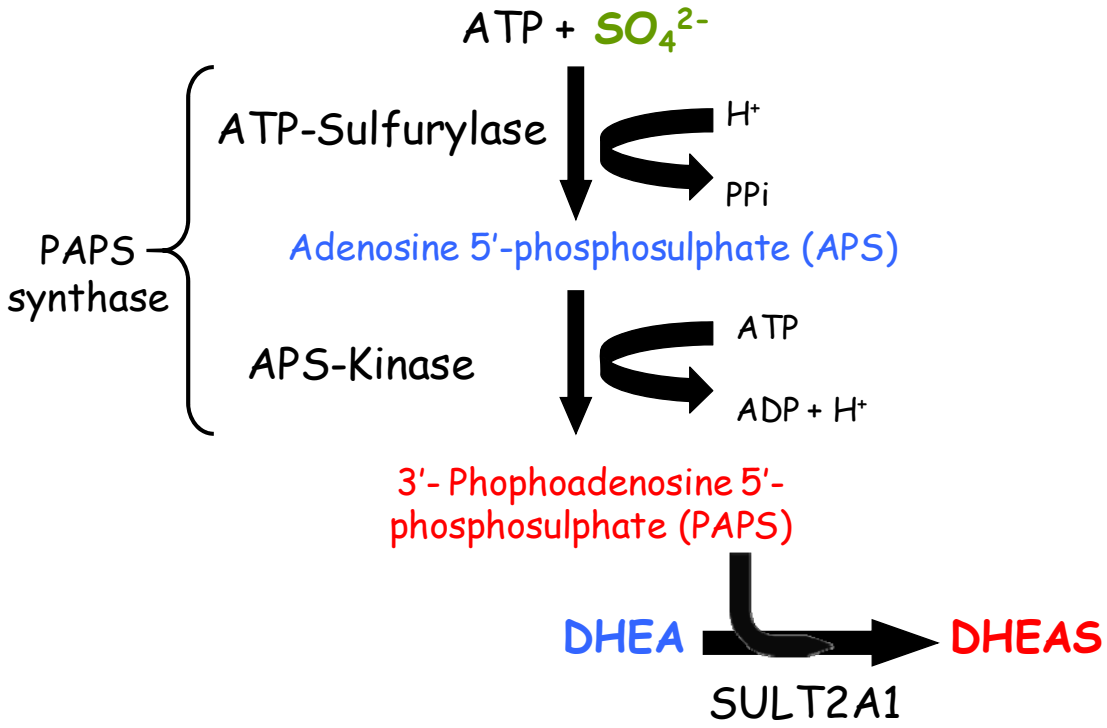

Figure 1-17 The synthesis of activated sulphate by PAPS synthase. *Inorganic sulphate (SO_4^{2-}) is converted by ATP-sulfurylase to adenosine 5'-phosphosulphate (APS), which in turn is converted to 3'-adenosine 5'-phosphosulphate by APS-kinase (PAPS). The enzymes are integral to a single bifunctional protein termed PAPS synthase. PAPS is the universal sulphate donor for all sulfation reactions, including that of DHEA to DHEAS catalysed by SULT2A1.*

1.1.7 Disorders associated with androgen excess

Androgen excess is the most common endocrine disorder, affecting 8-12% of adult women (Azziz et al., 2004; Carmina, 2006). The clinical manifestations of hyperandrogenism range in severity and can include hirtuism, acne, alopecia, central obesity, oligo or an-ovulation and frank viralisation. Numerous disorders such as cushing's syndrome, nonclassic 21 hydroxylase deficiency (NCAH), polycystic ovary

syndrome (PCOS), hyperprolactinemia and hyperandrogenic-insulin resistant – acanthosis nigricans (HAIR-AN) syndrome can present with similar hyperandrogenic phenotypes, although PCOS accounts for by far the majority (65-85%) of cases of hyperandrogenism (Maroulis, 1981; Rittmaster and Loriaux, 1987) and is estimated to affect 5-10% of females of reproductive age (Adams et al., 1986; Blank et al., 2008; Homburg, 2008). Indeed, PCOS is associated with 75% of all anovulatory disorders causing infertility, with 90% of cases of oligoamenorrhoea, and more than 90% with hirtuism and 80% with persistent acne (Blank et al., 2008; The Practice Committee of the ASRM, 2006).

The European Society for Human Reproduction and Embryology and the American Society of Reproductive Medicine at a meeting, Rotterdam 2003 (Galluzzo et al., 2008; Geisthovel and Rabe, 2007), redefined the criteria for the diagnosis of PCOS to the presence of any two of the following three observations, provided all other etiologies have been excluded: (a) polycystic ovaries on ultrasound scan, (b) oligo- and/or anovulation, (C) clinical and/or biochemical evidence of hyperandrogenism. As in the case of normal females, androgen production can originate from the adrenal or the ovary in hyperandrogenic disorders. Biochemical analysis is routinely used to identify the site of excess androgen production, with elevated DHEAS being regarded as indicative of adrenal origin and androstenediol indicative of ovarian origin (Carmina, 2006; The Practice Committee of the ASRM, 2006). However serum levels of DHEA, the active androgen precursor, are not usually examined. Studies have shown that serum DHEAS is increased, indicative of adrenal hyperandrogenism, in about 20-30% of women with classic anovulatory PCOS (Kumar et al., 2005). Although, the mean levels of DHEAS are shifted upward in most

patients with the disorder. Additional biomarkers of PCOS include raised concentrations of serum total and free testosterone and androstenedione; increased serum luteinizing hormone (LH) with low normal follicle stimulating hormone (FSH), giving rise to a characteristic high LH/FSH ratio; and low levels of serum hormone binding globulin (SHBG), hence the high concentrations of androgens. In addition to these criteria, insulin resistance and compensatory hyperinsulinemia, which are often associated with obesity and established as risk factors for the development of the metabolic syndrome, are common in PCOS patients (Barber et al., 2006; Galluzzo et al., 2008; Homburg, 2008).

Studies suggest that in some individuals the development of hyperandrogenism is associated with premature adrenarche (Ibanez et al., 2000; Ibanez et al., 1998a; Ibanez et al., 1998b). Precocious or premature adrenarche refers to an early increase in adrenal androgen production before the age of 8 years in girls and 9 years in boys, which usually manifests clinically as premature pubarche, with or without axillary hair development and pubertal odour(Auchus et al., 1998a; Kousta, 2006). Premature adrenarche occurs with increasing frequency between the ages of 3 and 8 years, although it may present as early as 6 months of age (Silverman et al., 1952). As with precocious puberty, girls are more frequently affected than boys, with a ratio of almost 10:1 (Sigurjonsdottir and Hayles, 1968; Silverman et al., 1952), although, there is currently no explanation for this unequal sex ratio. To date no single factor has been proven to regulate the onset of adrenarche. However, serine phosphorylation of P450c17 and access to CYB as a co-factor appear to be necessary for adrenarche to occur (Auchus et al., 1998a)(see section 1.1.5.1).

During pubertal development, leading to the attainment of full reproductive competence, the concerted effects of adrenarche and gonadarche give rise to a PCOS-like state. In the few years following adrenarche there is a relative hyperandrogenism, with high levels of androgens, relative to oestrogens and a significant decrease in SHBG. There is also a 20-fold increase in luteinizing hormone (LH) concentration and an increased LH to FSH ratio, with LH hyperpulsatility and a 30% decrease in insulin sensitivity with increased insulin secretion (Apter et al., 1994; Apter and Sipila, 1993; Pasquali et al., 1991; Venturoli et al., 1992). Consequently, in early puberty it is difficult to detect 'true' hyperandrogenism and PCOS as opposed to the normal physiological transient hyperactivity of the HPG axis. However, evidence is growing that anovulatory pubertal or postpubertal girls have higher testosterone and LH levels than their ovulatory counterparts (Ibanez et al., 1999) and that girls with early onset adrenarche are more likely to develop hyperandrogenism and the associated metabolic disturbances in adulthood (Ibanez et al., 2000; Kousta, 2006). Furthermore, an increased incidence of hirsutism and PCOS has been observed in postpubertal girls diagnosed with premature adrenarche during childhood (Ibanez et al., 2000; Kousta, 2006). Therefore it is suggested that premature adrenarche should not be considered a normal benign variant, but an indicator for the potential subsequent development of detrimental metabolic disease in some individuals.

The aetiology of PCOS is still unknown, although it is clear it is multifactorial involving genetic and environmental factors. The syndrome clusters in families and the prevalence rates in first degree relatives are five to six times higher than in the general population (Amato and Simpson, 2004). However, several candidate gene

approaches have not proved fruitful (Dumesic et al., 2007). Due to the emerging relationship between premature adrenarche and PCOS the aetiology of both conditions is proposed to be similar, although the majority of studies have investigated the latter. Hyperandrogenism and hyperinmsulinemia are known to be the primary underlying factors of the condition. However, it is not clear if insulin resistance depends on hyperandrogenism or visa versa.

It is likely that the pathogenesis of hyperandrogenism encompasses numerous derangements, and multiple pathways, which present with similar clinical manifestations and shared biochemical features. Therefore, both hyperandrogenism and insulin resistance may play initiating roles in some cases, or perpetuate the progression of others. Obesity and other antagonistic factors may be required in some patients to develop the disorder, or may not be required in more susceptible patients. In the future it is probable that further hyperandrogenic conditions or monogenic causes of PCOS will be unveiled, which will increase our understanding of the pathogenesis of this multifactorial syndrome.

1.2 Regulation of adipose tissue proliferation and differentiation

1.2.1 Adipose tissue embryology and morphology

Adipose tissue can be divided into two main categories; brown adipose tissue (BAT) and white adipose tissue (WAT). Brown adipose tissue is localised around the neck and scapulae and has a multi-ocular morphology, due to it containing a high number of mitochondria, and is involved in thermoregulation (**Figure 1-18**) (Gesta et al., 2007). The majority of BAT is lost in childhood, although it can exist at low amounts in adults. WAT differs from other tissues, in that it is forms at numerous, dispersed locations around the body (**Figure 1-18**) (Rosen and MacDougald, 2006). The majority of WAT forms at sites rich in loose connective tissues, such as the subcutaneous (sc) layers between the muscle and the dermis (Avram et al., 2007). However WAT deposits also form at intracellular depots, representing the main compartments of fat storage (Rosen and MacDougald, 2006)(**Figure 1-18**). The sc depot forms a continuous layer under the skin and in adulthood develops a sexually dimorphic distribution, with higher levels of abdominal fat in men, which has been termed ‘android’ or ‘apple’ distribution, and gluto-femoral fat in women, giving rise to ‘femoral’ or ‘pear’ adipose distribution (Lemieux et al., 1993).

In humans adipose tissue formation begins during the second trimester of pregnancy (Cornelius et al., 1994). However, WAT expansion does not take place until after birth via an increase in adipocyte cell size and an increase in adipocyte number. Contrary to previous dogma, it is now undisputed that the potential to acquire new fat cells from adipocyte precursors, in addition to the enlargement of current adipocytes,

persists in the human adult and occurs routinely as a consequence of normal cell turnover and the requirement for increased fat mass on significant calorie consumption (Miller et al., 1984; Prins and O'Rahilly, 1997). However, the adipogenic potential of preadipocytes depends on age, sex and depot (Lemieux et al., 1993; Rosen and MacDougald, 2006).

1.2.2 Adipose tissue growth

Adipose tissue development is dependent on two processes; hyperplasia and hypertrophy, with hypertrophy often preceding hyperplasia in a cyclic manner (Avram et al., 2007). Hyperplasia, hereafter termed adipogenesis, represents the complex process by which new fat cells are developed from adipocyte precursor cells and involves two major processes- the proliferation of adipocyte precursors and their differentiation into mature adipocytes (Gregoire et al., 1998; Hausman et al., 2001; Rosen and MacDougald, 2006). Although evidence from murine cell lines suggests that proliferation of a preadipocyte precedes its differentiation, studies using human preadipocytes suggest that partially differentiated cells are still capable of replication (Avram et al., 2007; Prins and O'Rahilly, 1997). Hypertrophy defines an increase in size of differentiated adipocytes due to lipid accumulation (Rosen and MacDougald, 2006).

The adipogenic process is regulated by an elaborate balance of stimulatory and inhibitory signals which can be nutritional, hormonal or paracrine in nature (Rosen and MacDougald, 2006). These stimuli co-ordinate the activation of a number of

transcription factors which regulate the expression of over 300 genes (Morrison and Farmer, 1999), responsible for establishing the mature fat-cell phenotype.

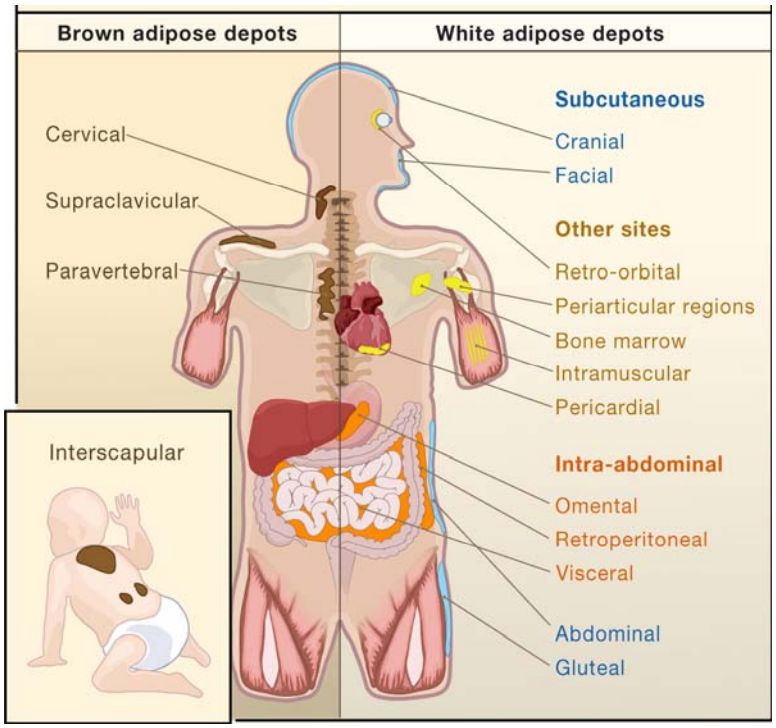

Figure 1-18 Human adipose tissue distribution. *Brown adipose tissue is present in babies and in smaller amounts in adults. White adipose tissue is present in dispersed locations around the body. Taken from Gesta et al, 2007.*

1.2.2.1 Adipocyte proliferation

WAT develops from multipotent stem cells of mesodermal origin that also give rise to muscle and cartilage lineages (MacDougald and Lane, 1995a). Human WAT-derived vascular cells have been shown to differentiate *in vitro* into myogenic, chondrogenic and osteogenic cells in the presence of lineage specific induction factors (Zuk et al., 2001) (**Figure 1-19**). Therefore, indicating that multipotent precursor cells are present

in adult human WAT. The first step in the adipogenesis process is the commitment of the multipotent stem cell (MSC) to the adipocyte lineage (**Figure 1-19**). Committed preadipocytes, have to withdrawal from the cell cycle, prior to the differentiation process (Amri et al., 1986; Gregoire et al., 1998). Growth arrest in G1/S phase is usually, with exception of certain conditions *in vitro*, achieved via contact inhibition. During this time preadipocytes appear morphologically similar to fibroblasts. The preadipocyte then requires a complex balance of proadipogenic and antiadipogenic signals, for the induction of differentiation to pursue (Gregoire et al., 1998). *In vitro* this is achieved via an 'induction cocktail' which can include a combination of dexamethasone, isobutylmethylxanthine (increases cAMP levels), supraphysiological concentrations of insulin, foetal bovine serum and an agonist of PPARγ, such as rosiglitazone (Gregoire et al., 1998). Stimulated preadipocytes subsequently re-enter the cell cycle and are thought to undergo at least one round of DNA replication and cell doubling, leading the clonal expansion of committed cells, prior to differentiation (Cornelius et al., 1994; MacDougald and Lane, 1995b). During this time there is an increase in the expression of prooncogenes, *c-fos*, *c-jun* and *c-myc*, which are thought to possess mitogenic properties (Avram et al., 2007; Cornelius et al., 1994; Zeng et al., 1997). Although clonal amplification is required for the differentiation of clonal cell lines (Amri et al., 1986; Tang et al., 2003), differentiation of human preadipocytes can occur without cell division at this stage (Entenmann and Hauner, 1996). It has been proposed that variation may be explained by the *in vivo* replication of human preadipocytes prior to cell harvesting (Avram et al., 2007), or that the clonal expansion may be an artefact of the *in vitro* process .

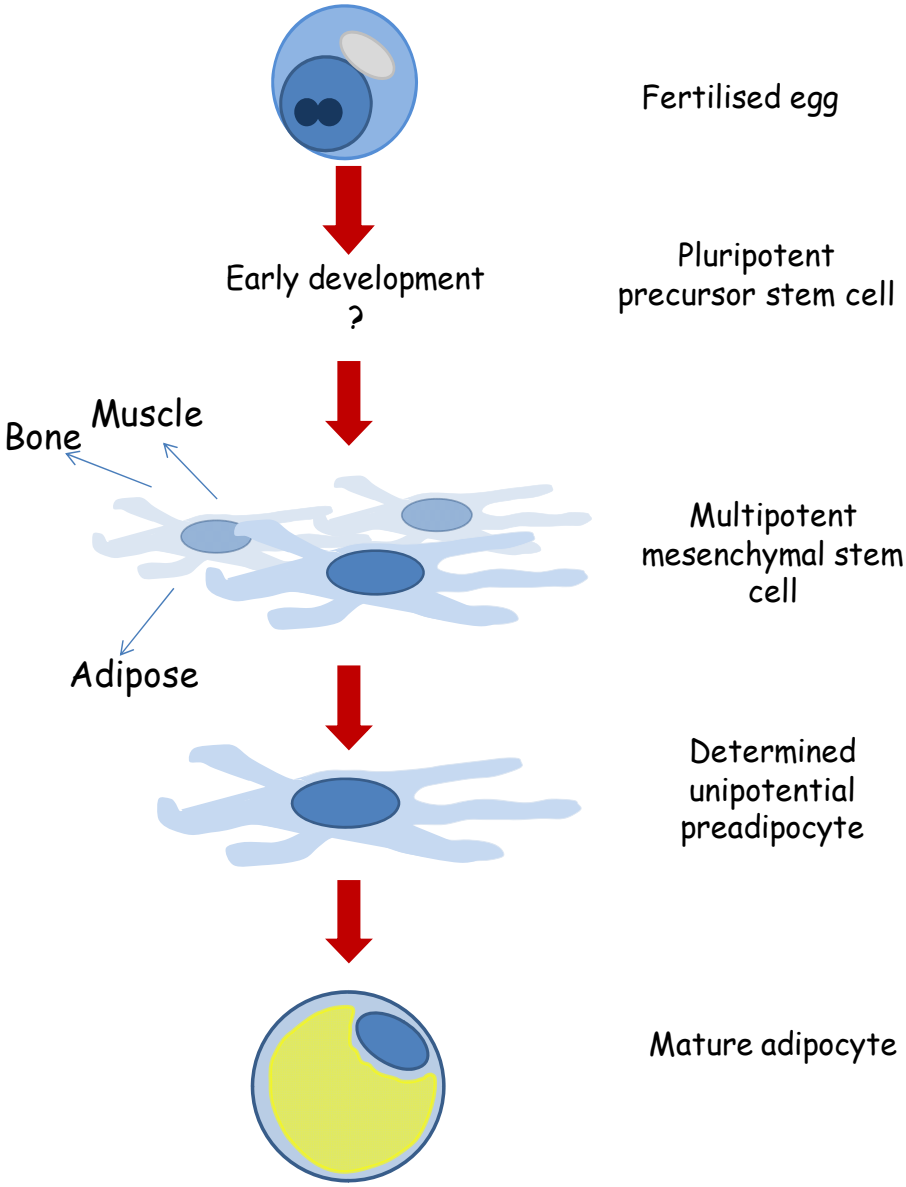

Figure 1-19 Adipose tissue determination and differentiation. *Multipotent mesenchymal stem cells have the potential to differentiate into muscle, bone and adipose. Under the correct stimuli, determined preadipocytes differentiate into mature adipocytes and accumulate unioccular lipid droplets which compress the nucleus to the cell membrane. Adapted from (Morrison and Farmer, 1999).*

1.2.2.2 Adipocyte differentiation

Immediately following exposure of the preadipocyte to adipogenic stimuli the gene expression of CCAAT/enhancer binding protein β (C/EBPβ) and C/EBPδ significantly and transiently increases (Morrison and Farmer, 1999) (**Figure 1-20**). This event enables the distinction between preadipocytes and nonadipogenic precursor cells (Cao et al., 1991). The importance of these proteins upon adipogeneseis is demonstrated by gain of function models have shown that C/EBPβ and C/EBPδ can accelerate differentiation in NIH-3T3 preadipocytes (Darlington et al., 1998). During the transient induction of C/EBPβ and C/EBPδ expression, preadipocytes undergo a second permanent period of growth arrest termed G_D (Scott et al., 1982) and at this stage preadipocytes are fully committed. G_D coincides with loss of E2F/DP, a central transcriptional regulator of many genes involved in cell growth (Altiok et al., 1997).

Along with cell-cycle regulators, C/EBPβ and C/EBPδ facilitate the expression of the nuclear hormone receptor peroxisome proliferator-activated receptor γ (PPARγ) (Clarke et al., 1997) and C/EBPα (**Figure 1-20**), which remain high throughout differentiation and within the mature adipocyte (Wu et al., 1999). This event marks the entry of committed cells into the process of terminal differentiation and is associated with the onset of lipid droplet accumulation. Once activated PPARγ and C/EBPα cross-regulate one another, maintaining their gene expression despite the ensuing decrease in C/EBPβ and C/EBPδ expression. The expression of PPARγ and C/EBPα In support of their regulatory role, the ectopic expression of C/EBPβ and C/EBPδ in 3t3-l1 preadipocytes (Cao et al., 1991), and C/EBPβ alone, or in combination with C/EBPδ in NIH 3T3 fibroblasts (Wu et al., 1996; Wu et al., 1995) induces C/EBPα and PPARγ expression, respectively. Furthermore, induction of the

adipogenic programme ensues, in the absence of extracellular hormones. Interestingly, both studies observed that C/EBPδ alone possesses minimal adipogenic activity (Cao et al., 1991; Wu et al., 1996). The finding that C/EBP regulatory elements are present in the promoters of C/EBPα and PPARγ further supports the important role of these proteins in inducing C/EBPα and PPARγ expression (Tang et al., 2004). However, there must be further uncharacterised, C/EBP independent, PPARγ and C/EBPα regulatory mechanisms, as C/EBPβ and C/EBPδ double-knockout mice express normal levels of these genes (Tanaka et al., 1997).

C/EBPα and PPARγ are recognised as the principle regulators of the differentiation process. In support of this notion, overexpression of C/EBPα or PPARγ in 3t3-l1 cells induces their differentiation into a mature adipocyte (Freytag et al., 1994; Lin and Lane, 1994). Furthermore, thiazolidinediones (TZD), high affinity synthetic ligands for PPARγ, are potent inducers of preadipocyte differentiation. PPARγ in particular is considered the master regulator; without it, precursor cells are incapable of expressing any known aspect of the adipocyte phenotype (Rosen and MacDougald, 2006). Indeed, WAT-hypomorphic PPARγ knockdown mice display severe lipodystrophy (Koutnikova et al., 2003). Furthermore, studies in which PPAR was ectopically expressed in nonadipogenic mouse fibroblasts showed that PPARγ alone can initiate the entire adipogenic programme (Tontonoz et al., 1994). However, cells deficient in C/EBPα are insulin resistant (El-Jack et al., 1999; Wu et al., 1999), indicating the requirement of C/EBPα for the accquistion of insulin sensivity (Wu et al., 1999).

Other factors are known to be important in the molecular regulation of differentiation, in both a positive and negative fashion (**Figure 1-20**). The upregulation of the helix-loop-helix transcription factor ADD1/SREBP-1c expression early on in the differentiation process is thought to be involved in the regulation of PPARγ expression (Fajas et al., 1999). Ectopic expression of a consitutively active form of ADD1/SREBP-1c enhances adipocyte gene expression in nonprogenitor NIH-3T3 fibroblasts under adipogeneic conditions (Tontonoz et al., 1993). Furthermore, evidence suggests that SREBP-1c may be involved in gene expression that leads to the production of endogenous PPARγ ligands (Kim and Spiegelman, 1996). In addition, cAMP response element, which also induces expression of PPARγ, regulates expression of fatty acid synthase (FAS), GLUT-4, and leptin (Klemm et al., 1998). STAT5A and STAT5B, which are involved in cytokine signalling, may also provide an additional pathway for regulating adipogenesis and double-knockout mice have 5-fold reduction in WAT mass as compared to wild type animals (Teglund et al., 1998) and ectopic expression of STAT5A in nonadipogenic fibroblasts induces preadipocyte differentiation (Floyd and Stephens, 2003).

In addition a number of factors are known to inhibit preadipocyte differentiation, and maintain the preadipocyte phenotype until adipogenic stimuli repress their expression, such as the AP2-α and SP-1 genes. Pre-adipocyte factor 1 (pref-1) is a plasma membrane protein expressed only in preadipocytes, which prevents differentiation by inhibiting PPARγ and C/EBPα expression (Smas and Sul, 1997). Accili et al have demonstrated that the forkhead transcription factor, FoxO1, when constitutively active inhibits the differentiation of 3T3-F422A preadipocytes by arresting the cells in clonal expansion (Accili and Arden, 2004). In addition,

constitutive expression of GATA binding protein transcription factors, GATA-2 and GATA-3, which are expressed in preadipocytes and suppresses differentiation, by binding the PPARγ promoter, inhibiting its transcription, and forming inhibitory complexes with C/EBPα and C/EBPβ (Tong et al., 2005).

During terminal differentiation the adipocytes markedly increase their ability to perform de novo lipogenesis, due to the induction of a number of genes involved in glucose and lipid metabolism. For example, during the final stages of differentiation, expression of the insulin receptor and glucose transporters increases, resulting in the adipocyte acquiring sensitivity to insulin (Garcia de Herreros and Birnbaum, 1989). The ability of adipocytes to synthesise TAG is increased by the expression of enzymes such as FAS and ACC and glycerol phosphate dehydrogenase, while the capacity for lipid uptake is increased by the induction of lipoprotein lipase expression. In addition, there is an increase in the expression of β2- and β3- adrenoreceptors, and as consequence and increase in the response to lipolytic stimuli (Knittle et al., 1979).

Based on *in vitro* models each stage of the adipocyte differentiation has been well established and associated with specific patterns of gene expression. The expression of such genes can be defined as early, such as lipoprotein lipase (LPL), or late, such as glycerol-3-phosphate dehydrogenase (G3PDH) or aP2. The identification of the expression of these genes is a commonly used tool to identify the differentiation state of adipocytes *in vitro*.

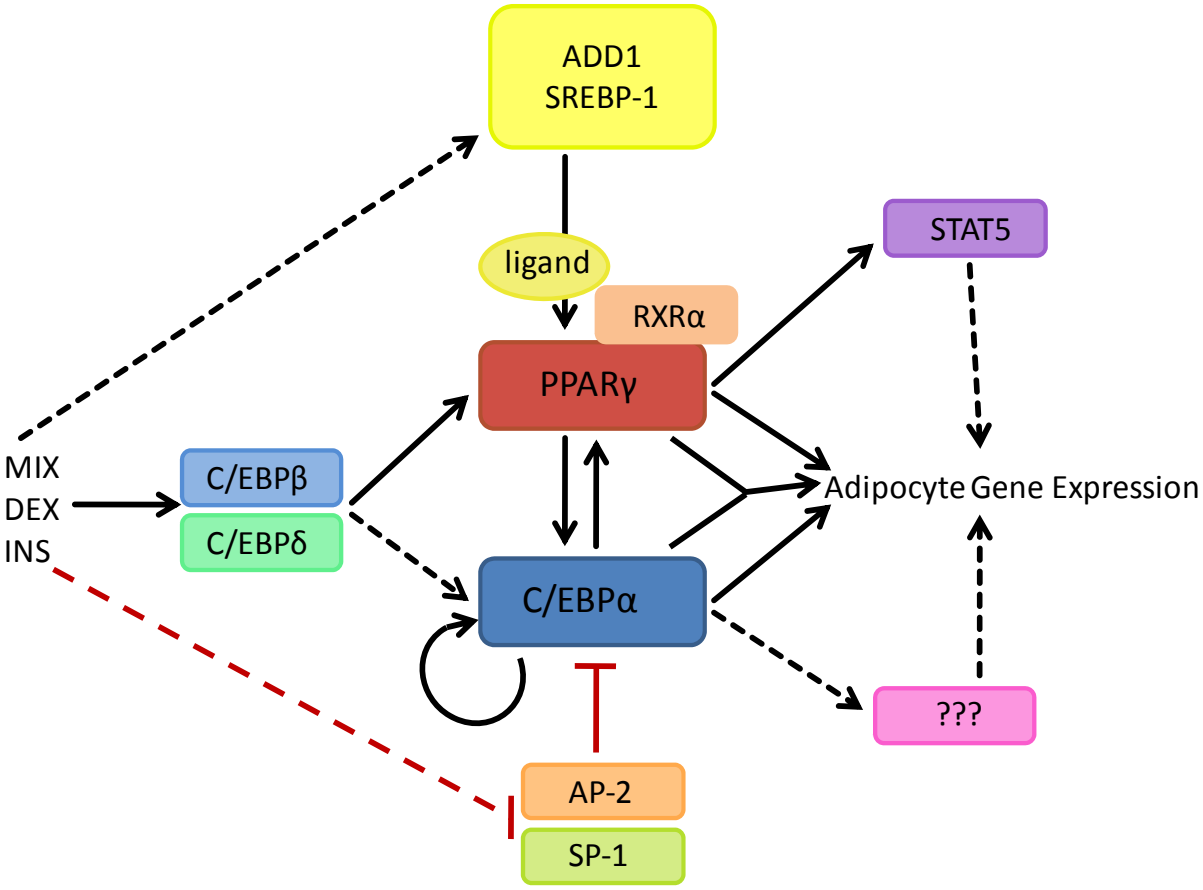

Figure 1-20 The transcriptional regulation of adipogenesis. *A complex signal of stimulatory and inhibitory stimuli induce differentiation. In vitro this is stimulated by (MIX), dexamethasone (DEX) and supraphysiological concentrations of insulin (INS). The factors induce the expression of key transcription factors including PPARγ and C/EBPα, which result in adipocyte differentiation. Adapted from (Morrison and Farmer, 1999)*

1.2.3 Hormonal regulation of adipogenesis and adipocyte homeostasis

1.2.3.1 Glucocorticoid regulation of adipose tissue

It is well established that glucocorticoids, or the synthetic glucocorticoid, dexamethasone (Dex), enhance preadipocyte differentiation *in vitro* and *in vivo* (Hauner et al., 1989; Hauner et al., 1987; Rubin et al., 1978). Depending on the cell model system, glucocorticoid treatment is either required for, or accelerates the differentiation process (Avram et al., 2007). Dex treatment induces C/EBPδ expression, which may account for some of its adipogenic activity (MacDougald et al., 1994; Wu et al., 1996). However, cells that overexpress C/EBPδ still require Dex to achieve their full adipogenic potential (Rosen and Spiegelman, 2000) indicating that DEX serves more than this purpose. Dex has also been shown to enhance the expression of the key regulators of the adipocyte process, C/EBPα and PPARγ (MacDougald et al., 1994; Wu et al., 1996). Furthermore, the activated GR also associates with Stat 5a, which as described in section 1.2.2.2, promotes adipocyte differentiation (Floyd and Stephens, 2003). Dex has also been shown to inhibit preadipocyte proliferation via a repression of the expression of pref-1, a negative regulator of adipogenesis and consistently anti-sense mediated repression of pref-1 decreases the dose of Dex required for adipogenesis to occur (Smas et al., 1999).

1.2.3.2 Sex steroid regulation of adipose tissue

There is a striking difference in body fat between men and women. Men tend to accumulate adipose tissue in the abdomen, and for a similar fat mass, have a two-fold higher visceral adipose tissue accumulation compared to women (Lemieux et al.,

1993). The fact that men have a higher risk of developing cardiovascular disease is well established. However, statistical adjustment for visceral adipose tissue area has been shown to abolish sex-related differences in cardiovascular disease risk factors (Lemieux et al., 1994) suggesting, visceral adipose tissue deposition is a responsible for the sex differences in cardiovascular disease risk factors (Despres and Lemieux, 2006; Yusuf et al., 2004). Such findings have led to the increasing understanding that testosterone, DHT and oestradiol, play important roles in the regulation of adipose distribution, development and homeostasis.

1.2.3.2.1 ***Androgen regulation of adipose tissue***

Numerous cross-sectional and longitudinal studies have shown that abdominal obesity correlates with low plasma testosterone levels in men (Khaw and Barrett-Connor, 1992; Pasquali et al., 1991). In these studies, waist circumference and waist hip ratio are also negatively associated with plasma sex hormone binding globulin (SHBG) (Khaw and Barrett-Connor, 1992; Pasquali et al., 1991). In support of these findings, Boyanov et al have shown that physiological testosterone administration decreases waist-to-hip ratio of hypogonadal men (Boyanov et al., 2003), whom without treatment have an increased incidence of cardiovascular disease. However, other studies investigating the effect of DHT or testosterone administration to unaffected men have observed no effect (Marin et al., 1992).

In contrast, abdominal obesity is thought to be associated with high plasma androgen levels in women. Women with PCOS (of which hyperandrogenism is a characteristic) and female-to-male transsexuals receiving testosterone treatment, often develop a more android adipose tissue distribution pattern (Dunaif, 1997; Elbers et al., 1999a),

and concurrent increase in the associated cardiovascular risk factors (Dunaif, 1997). As in men, in women SHBG levels are inversely correlated with waist to hip ratio and elevated SHBG levels are inversely associated with features of the metabolic syndrome (De Pergola et al., 1994; Ivandic et al., 2002).

Taken together these findings suggest that physiological concentrations of testosterone are associated with a favourable metabolic profile. Conversely, testosterone levels outside of the normal physiological range, as observed in hypogonadal men (sub-physiological), or female-to-male transsexuals (supraphysiological), may have adverse effects on adipose tissue development (Elbers et al., 1999a).

The effects of androgens on preadipocyte proliferation, differentiation, lipid synthesis and lipolysis have been studied *in vitro* and *in vivo*. Androgens have generally been shown to have no effect on preadipocyte proliferation in rodent and human studies (Anderson et al., 2001; Dieudonne et al., 2000). However, testosterone treatment was shown to prevent the increase in preadipocyte proliferation observed following castration in male mice (Garcia et al., 1999). Androgens are considered antiadipogenic and have been shown to inhibit preadipocyte differentiation in rodent *in vitro* studies (Dieudonne et al., 2000; Gupta et al., 2008; Singh et al., 2003), thought to be due to a reduced level of IGF-1 receptor and C/EBPα expression which has been observed in mesenteric and omental preadipocytes following DHT treatment (Dieudonne et al., 2000; Gupta et al., 2008) and interaction of the androgen receptor with the Wnt signalling pathway (Singh et al., 2006).

Androgens are also known to modulate adipose homeostasis. In men omental fat androgen content has been found to be positively correlated with adipocyte lipolytic responsiveness in this depot (Belanger et al., 2006). Basal lipolysis of abdominal adipose tissue was shown to be increased in female to male transsexuals under testosterone treatment (Elbers et al., 1999b). Conversely, hypogonadism in man is associated with a significant decrease in lipolytic response to catecholamines (Bjorntorp, 1996). In contrast, in SC adipocytes obtained from women T and DHT inhibited catecholamine-stimulated lipolysis associated with decreased expression of hormone sensitive lipase and β2-adrenoreceptors (Xu et al., 1990; Xu et al., 1993; Xu et al., 1991). Consistent with these findings only male androgen receptor knockout (ARKO) mice develop a late onset obesity phenotype (Yanase et al., 2008), presumed attributable to impaired lipolysis due to a decrease in HSL in these mice.

The effects of androgens on adipocyte lipid synthesis remain controversial. In subcutaneous adipocytes obtained from women, DHT has been shown to stimulate lipoprotein lipase expression (Anderson et al., 2002). Conversely, testosterone treatment of adipose tissue obtained from men and male rats was shown to reduce fatty acid synthesis, LPL levels and radioactive triglyceride uptake (Hansen et al., 1980; Marin et al., 1995).

It is becoming evident that in addition to the adrenal and gonads, adipose tissue can contribute to the synthesis and activation of androgens which via intracrine effects may modulate adipose tissue development and homeostasis. Quinkler *et al.* demonstrated the expression and activity of AKR1C3, a reductive 17β-HSD isozyme responsible for the conversion of androstenedione to testosterone, in human female adipose tissue (Quinkler et al., 2004). The expression of AKR1C3 was shown to be

site specific, being greater in sc than om depots, and to increases with adipocyte differentiation, suggesting a role for this enzyme in preadipocyte differentiation. Functional activity analysis confirmed predominant androgen activation in sc adipocytes, indicating that human adipose tissue is capable of androgen synthesis. Interestingly the mRNA expression of AKR1C3 was shown to positively correlate with BMI, and decrease upon weight loss, suggesting that AKR1C3 plays a site specific role in obesity. Furthermore, these findings suggest that the increase in AKR1C3 expression with differentiation and in sc depots relative to om depots may compensate for the reduced expression of the AR in sc adipocytes and highlights the importance of understanding the site-specific regulation of sex steroids synthesis and action on adipogenesis.

Consistent with the apparent differing effects of androgens *in vitro* it appears that androgen metabolism in adipose tissue may differ between men and women as Blouin et al have shown that in the adipose tissue the expression of AR and AKR1C1 is higher in the sc adipose depot (Blouin et al., 2003). In contrast the expression of 17β-HSD2, which was not shown to be expressed in women, was higher in the om depot. This study demonstrated higher inactivation of 5α-DHT in mature adipocytes compared to adipocytes, which was greater in the om depot. Furthermore, higher inactivation rates were observed in obese compared to lean men, again indicating that modulation of androgen synthesis may play a site specific role in obesity.

1.2.3.2.2 ***Oestrogen regulation of adipose tissue***

Women have approximately 10% more body fat than men (Chumlea et al., 1981b), which is generally localised to the gluteal site. The increase in adipose tissue mass

seen in women at puberty is associated with both an increase in both adipocyte hyperplasia and hypertrophy (Chumlea et al., 1981a). Indeed, subcutaneous gluteal fat has been shown to increase 45% in girls compared to boys at puberty (Chumlea et al., 1981a), suggesting that oestrogens may preferentially promote fat accumulation in the gluteal region. In contrast, the accumulation of central adipose tissue, which is associated with the menopause in women appears to be prevented by oestrogens and is reversed with hormone replacement therapy (Cooke and Naaz, 2004). Furthermore, ERα knockout (ERαKO) mice, or experimental animals following ovariectomy develop a large increase in adipose tissue mice adipose tissue accumulation (Simpson and McInnes, 2005; Wade et al., 1985).

The inhibitory effect of oestrogen has been shown to inhibit adipose deposition principally by decreasing lipogenesis by the direct inhibition of LPL expression via a negatively regulated oestrogen response element (Homma et al., 2000). In addition E2 can indirectly affect lipolysis in central adipocytes by inducing the lipolytic enzyme hormone sensitive lipase (HSL) and by increasing the lipolytic effects of epinephrine. In contrast, oestrogen site specifically attenuates the effects of α2A-adrenergic receptors in the subcutaneous adipocytes of humans, decreasing lipolysis (Negishi et al., 2001), which could account for some of the site specific effects of oestrogens.

1.3 Aims and Hypotheses

The aim of this thesis is to investigate the effect of DHEA, and the importance of DHEA metabolism, in human disease states. This will be examined in two studies investigating: a) the effect of DHEA on, and its metabolism in, human preadipocytes, described in chapter three. b) The effect of aberrant DHEA sulfation on DHEA downstream metabolism, examined in chapter four.

1.3.1 DHEA metabolism and action in human adipocytes

As described in section 1.1.5.3.3 numerous murine studies have demonstrated that DHEA has beneficial effects on obesity, preventing high fat diet-induced fat mass accretion or diminishing total fat mass of these animals. *In vitro* studies have suggested that these effects are, at least in part, via a direct effect on the adipocyte. However as rodents do not express *CYP17A1* in the adrenal and therefore have circulating levels of DHEA many orders of magnitude lower than that of humans the relevance of these findings to humans is questionable. To date no *in vitro* and limited *in vivo* human studies have been performed with largely inconsistent findings (see section 1.1.5.3.3). Recent studies have shown that DHEA inhibits 11β-HSD1 expression and oxoreductase activity. Therefore the aim of the study described in chapter three is to investigate, utilising a human subcutaneous preadipocyte cell line, Chub-S7:

- The metabolism of DHEA in human preadipocytes and adipocytes.
- The effect of DHEA on preadipocyte adipogenesis.

- The effect of DHEA on human adipocyte glucose uptake.
- The effect of DHEA on 11β-HSD1 activity and expression.

I hypothesise that DHEA will attenuate preadipocyte adipogenesis via an inhibitory effect on 11β-HSD1 expression and activity, resulting in the attenuation of glucocorticoid regeneration. In addition, based on the findings of previous human clinical studies I propose that DHEA will enhance human adipocyte glucose uptake.

1.3.2 Interconversion of DHEA and DHEAS and androgen excess

As described in section 1.1.6.4 all sulphation reactions, including that of DHEA by SULT2A1, require the ubiquitous sulphate donor, PAPS, which is synthesised by PAPS synthase of which in humans there are two isoforms, PAPSS1 and PAPSS2. In chapter four I describe a patient with compound heterozygous mutations in PAPSS2. I aim to confirm the disease causing nature of the mutations by bacterially expressing WT and mutant PAPSS2 and performing *in vitro* analysis of their activity. This will be achieved by exploiting the dependence of the enzyme SULT2A1 catalytic activity on PAPS bio-availabiliy.

I hypothesise that the two identified heterozygous mutations will have reduced or no activity and therefore explain the phenotype of the patient.

2 Chapter 2: Methods

This chapter contains all of the general techniques and protocols utilised in this thesis. Specific modifications made to these general protocols are included within the relevant chapters. All reagents were obtained from Sigma, Poole, UK all cell culture plasticware utilised had a Corning® CellBIND® surface, supplied by Appleton Woods Limited, Birmingham, UK, unless otherwise stated. All solutions and reagents were stored at room temperature, unless otherwise stated.

2.1 Cell culture techniques

2.1.1 General principles of cell culture

2.1.1.1 Chub-S7 cell line

The Chub-S7 cell line was derived from human subcutaneous adipose tissue by co-expression of human telomerase reverse transcriptase and papillomavirus E7 oncoprotein (HPV-E7) genes (Darimont et al., 2003). The cell line has an unlimited life span and the capacity to accumulate lipid without chromosomal alteration. This cell line has previously been well characterised by our group and by others (Bujalska et al., 2008; Darimont et al., 2003), and represents a human *in vitro* model. Under basal conditions, prior to confluence, these cells resemble preadipocytes. Post growth restriction, in chemically defined media, they differentiate into mature adipocytes demonstrated by the expression of classical markers of differentiation and the accumulation of lipid droplets (**Figure 2-1**).

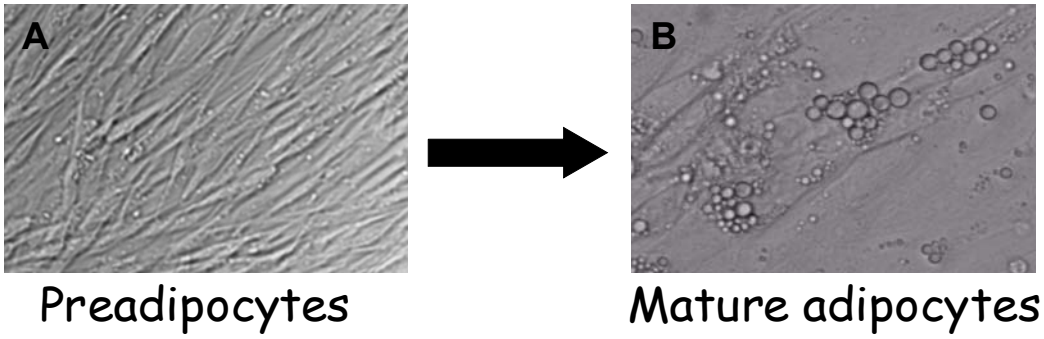

Figure 2-1 The morphological changes of Chub-S7 preadipocytes associated with differentiation. *Preadipocytes (A) have a fibroblast like morphology. Following differentiation mature adipocytes (B) accumulate lipid droplets and develop a more rounded appearance.*

2.1.1.2 Cryo-preservation of Chub-S7 cells

Cells to be preserved were grown in T75 cm^2 TC flasks until 70% confluence, as described in section 2.1.2.1. Upon reaching 70% confluence cells were trypsinised and centrifuged at 300g for 5 min (Centaur 2, MSE, London, UK). The resulting cell pellet was resuspended in FCS and the cell number determined, utilising a hematocytometer. Cells were then diluted with FCS to a concentration of 5 x 10^6 cells/ ml and DMSO was added dropwise, to prevent cellular osmotic shock, to a final concentration of 10%. The cell suspension was aliquoted into 1.5 ml cryovials and cooled at 1ºC/ min in a cryo-freezing container (Nalgene, Hereford, UK) at -80ºC. For long term storage cryo-stocks of cells were kept in liquid nitrogen.

2.1.1.3 Re-establishment of Chub-S7 cells after freezing

Cells were removed from liquid nitrogen and rapidly defrosted at 37ºC. The cell suspension was transferred to a falcon tube, diluted with 5 ml of fresh medium, and centrifuged at room temperature for 5 min at 1000 g (Centaur 2, MSE, London, UK). The resulting cell pellet was re-suspended in 5 ml of fresh growth media, and transferred to a T25 cm^2 flask. The following day the media was replenished.

2.1.1.4 Cell treatments

Prior to treatments all cells were washed with serum free medium (SFM) or the appropriate buffer. DHEA, androstenediol, faslodex, flutamide, cortisone (E) and cortisol (F) were all resuspended in absolute ethanol. DHEAS and RU486 were resuspended in dimethyl sulfoxide (DMSO). All control cells were incubated with the same concentration of ethanol and DMSO as treated cells, which did not account for greater than 0.5% of the total volume of any incubation.

2.1.2 Assessment of cell proliferation

2.1.2.1 Cell proliferation

Chub-S7 cells were cultured in 75 cm^2 tissue culture (TC) flasks in Dulbeco's minimal essential medium F-12 (DMEM-F12) containing 10% foetal calf serum (FCS) and 2mM glutamine (Gibco) at 37ºC in a humidified atmosphere containing 5% CO_2. At 70% confluence cells were trypsined and re- seeded into fresh 75 cm^2 TC flasks for maintenance of the cell line, or the appropriate format for subsequent assays.

2.1.2.1.1 ***Solutions***

- **DMEM F-12** (Gibco). L-Glutamine was added to a final concentration of 2 mM. Stored at 4˚C for up to three months.

2.1.2.2 ^{3}H Thymidine uptake assay

2.1.2.2.1 ***Principle***

^{3}H-Thymidine Uptake analysis is based on the principle that the amount of labelled thymidine which is incorporated into the DNA of actively dividing cells during S phase of mitosis (see **Figure 2-2**) is directly correlated to the rate of proliferation of the cells. During this procedure an optimised number of cells are incubated with ^{3}H-thymidine for a pre-determined time period. Following this incubation, whilst the cells are still in linear growth, the cellular protein is removed and the labelled DNA extracted in NaOH. The amount of ^{3}H-thymidine incorporated into the resultant solubilised nuclear material is determined by liquid scintillation counting and subsequently the relative rates of proliferation of sub-populations of cells can be determined.

2.1.2.2.2 ***Solutions***

- **1 X PBS**. 2 tablets of PBS dissolved in 400 ml of distilled water. Autoclaved.

- **0.1M NaOH**, diluted in H_20.

- **^{3}H-Thymidine,** (G. E. Healthcare, UK). Specific activity of 80 Ci/mmol. Stored at -20˚C for up to 6 months.

- **5% TCA**. 1M TCA diluted in distilled water and stored at 4ºC.

2.1.2.2.3 ***Method***

Cells were seeded in to 24 well tissue culture (TC) plates (2.5 x 10^5 cells/well). At the pre-optimised time-point (1,3 and 5 days) sub-confluent proliferating cells were washed with SFM to remove any traces of protein and 500 µl of SFM was added per well. 0.4 µCi of ^{3}H-thymidine (in 10 µL of SFM) was added per well and the cells cultured for a further 5 hr at 37˚C in a 5% CO_2 incubator to permit the incorporation of ^{3}H-thymidine. Following the incubation period unbound ^{3}H-thymidine was removed by washing the cells with PBS and inversion of the plates. Soluble protein was removed by the addition of 1 ml of 10% TCA per well for 10 min while on ice. The TCA was aspirated and the cells washed with PBS. 200 µL of 0.1 M NaOH was added to each well and the assays incubated at room temperature for 30 min. Cells were scrapped and the resulting cell lysate transferred to a scintillation vial. To ensure the removal of any remaining residue from the TC plates, a further 200 µl of 0.1 M NaOH was added to each well, pipetted up and down, and transferred to the corresponding scintillation vial. 4 ml of scintillant was added to each vial and the amount of ^{3}H-thmidine determined by liquid scintillation counting (Packard 2500 TR Liquid Scintillation Analyzer, Perkin Elmer, UK).

2.1.2.3 Colorimetric proliferation assay

2.1.2.3.1 ***Principle***

The number of viable cells in culture can be determined utilising commercially available proliferation assays such as the CellTiter 96 Aqueous One Solution Cell Proliferation assay, supplied by Promega. This assay exploits the fact that viable, metabolically active cells express dehydrogenase activity and reduce NADP and

NAD to NADPH and NADH respectively. The CellTiter 96 Aqueous One Solution contains a tetrazolium compound [3-(4,5-dimethylthiazol-2-yl)-5-(3-carboxymethoxyphenyl)-2-(4-sulfophenyl)-2H-tetrazolium, inner salt; MTS] and an electron coupling reagent (phenazine ethosulphate; PES). The MTS tetrazolium compound is bioreduced by cellular NADH/NADPH to a coloured formazan product that is soluble in cell culture media. Thus, the quantity of formazan product, as measured at 490nm, is directly proportional to the number of viable cells in culture.

2.1.2.3.2 ***Method***

Cells were seeded into a 96 well plate (1 x 10^4 cells /well in 100 µl of medium) and allowed to adhere overnight before treatment. Following treatment, at the timepoints, 1, 3, 5 and 7 days 20 µl of cellTiter 96 Aqueous One Solution was added to each well using a repeat pipette and incubated at 37˚C, 5% CO_2, for 2 hr. Following the incubation period, absorbance of the colorimetric reagent was measured at 490nm with a Victor3 1420 multilabel counter (Perkin Elmer, Beconsfield, Buckinghamshire).

2.1.2.4 FACS cell cycle analysis

2.1.2.4.1 ***Principle***

Cell cycle analysis relies on the principle of flow cytometry, which enables the analysis of individual cells or particles as they travel in suspension one by one past a sensor. Utilising different fluorescent DNA binding dyes this technique enables the distinction of the 3 discrete phases of the cell cycle: namely G1 (gap 1), S (synthesis) and G2/M (gap 2/ mitosis), based on the differing nuclear DNA content of each phase. As shown in **Figure 2-2**, cells in G1 phase have a normal complement of

DNA, whilst cells in G2 possess twice the normal content, and cells in S phase, while undergoing DNA synthesis, contain a varying DNA content between normal to double. To distinguish between these different proliferative phases, the nuclei of permeablised cells are stained with a fluorescent DNA binding dye, propidium iodine. The fluorescence of the individual cells is subsequently analysed by flow cytometry. The intensity of florescence of each nuclei correlates to the content of DNA within the nuclei and thus the corresponding phase of cell cycle. Therefore, it is possible to determine the percentage of cells at each phase of the cell cycle in a given population of cells, providing an indication of their proliferative activity.

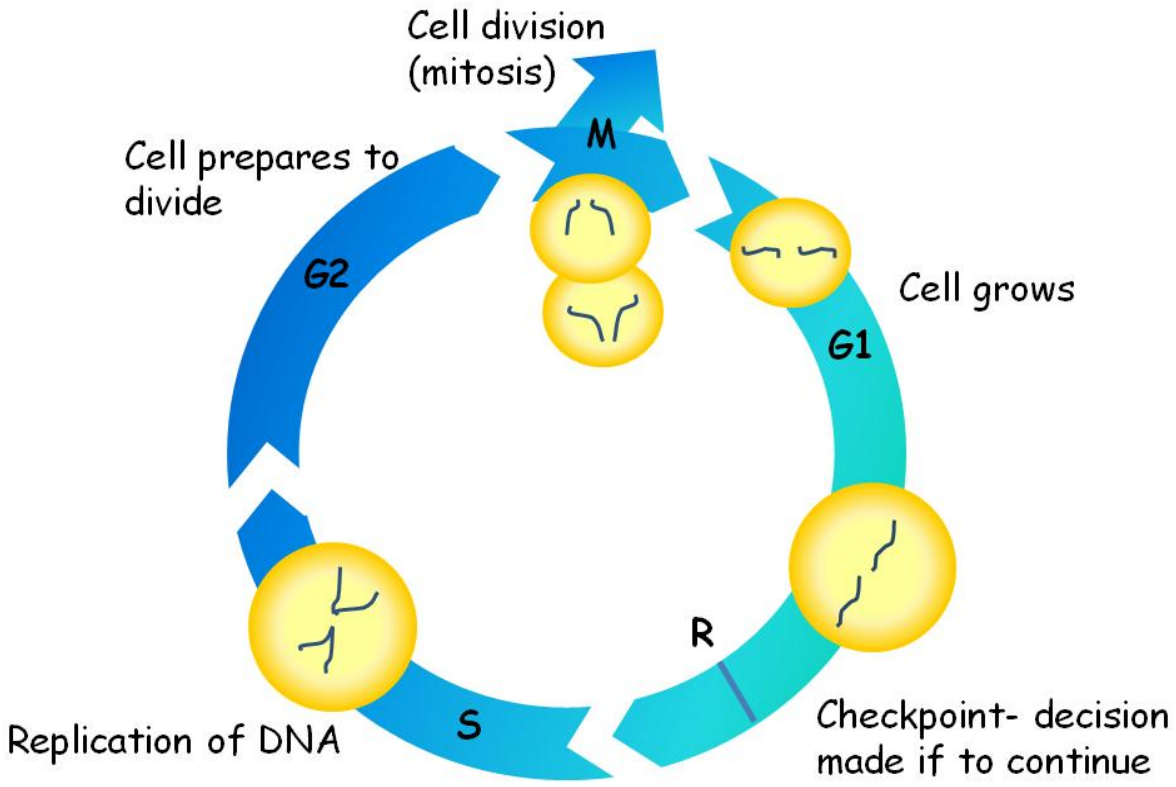

Figure 2-2 Phases of the cell cycle. *In the G1 phase cells have a normal complement of DNA, whilst cells in G2 phase possess twice the normal content, and cells in S phase, while undergoing DNA synthesis, contain a varying DNA content between normal to double.*

2.1.2.4.2 ***Solutions***

- **FACS buffer**, 25 µl NaCl (100 µM), 1 ml sodium citrate (1%), 25 µl Triton-X-100 (0.1%), 25 µl propridium iodine (10 µg/ml), 24 ml dH_20. Stored, protected from light, at 4˚C for up to 7 days.

- **1 X PBS**. 2 tablets of PBS dissolved in 400 ml of distilled water. Autoclaved.

2.1.2.4.3 ***Method***

Chub-S7 preadipocytes were seeded into 6 well TC plates (2.5 x 10^6 cells/well). and cultured overnight at 37˚C, 5% $C0_2$, to allow the cells to adhere. The following day, cells were treated with 25 μM DHEA and cultured for a further 24 hrs. Prior to cell cycle analysis, cells were washed 3 times with PBS. Subsequently cells were incubated with 500 μl of FACS buffer, containing propidium iodide, on a shaker for 30 min at room temperature, protected from light. The resulting cell lysate was disaggregated by repeat pipetting, transferred to a FACS tube, and analysed immediately using a FACS IV Flow cytometer at a wavelength of 488 nm. Approximately 10,000 cells were analysed per injection.

2.1.3 Assessment of preadipocyte differentiation

2.1.3.1 Differentiation

2.1.3.2 Solutions

- **Cell culture trypsin,** (Gibco). 10 x stock diluted to 1 x with PBS/ EDTA, pH 8.0. Stored at 4ºC.

- **Human insulin**. Diluted to 1mg/ml in glycine buffer (20 mM, pH 2). Stored at 4˚C for up to six months. Human insulin was added fresh to media on the day of use.

- **GW1929**, (Camlab, Cambridge, UK). Dissolved in DMSO to a final concentration of 1 mM. Stored at -20ºC. GW1929 was added fresh to media on day of use.

- **3,3',5 Triiodothyronine (T3).** Dissolved in NaOH to 0.2 µM and stored at -20ºC. T3 was added to differentiation media to a final concentration of 0.2 nM.

- **Biotin**. Dissolved in NaOH, stored at 4ºC. Biotin was added to differentiation media to a final concentration of 33 µM.

- **Calcium D-Pantothenate**. Dissolved in dH_20 and stored at -20ºC. Added to differentiation media to a final concentration of 17 µM.

- **DMEM F-12** (Gibco). Add L-Glutamine to a final concentration of 2mM. Store at 4˚C for up to 3 months.

2.1.3.3 Principle

For differentiation experiments, cells were seeded into 24 well TC plates (5 x 10^6 cells/well) and cultured until 2 days post confluence. Preadipocytes were differentiated (up to 21 days) according to Hauner et al (Hauner et al., 1989; Hauner et al., 1987), with 166 nM human insulin, 1 µM rosiglitazone (PPARγ agonist) , 0.2 nM T3, 17 µM Pantothenic acid, 33 µM Biotin and, as specified, 500 nM cortisone (E) or cortisol (F). For all experiments, cells utilised were between passage 23 and 30.

2.1.4 Analysis of glucose uptake

2.1.4.1 2-Deoxy-D-[1-^{3}H] glucose uptake assay

2.1.4.1.1 ***Principle***

This assay enables the functional analysis of glucose uptake of a population of cells. Briefly, following treatment cells are incubated with radiolabelled glucose (2-Deoxy-D-[1-^{3}H]glucose) for a predetermined optimum incubation period. As with unlabelled glucose, 2-Deoxy-D-[1-^{3}H]glucose can enter the cell by facilitated diffusion, mediated by glucose transporters (predominantly GLUT4 and GLUT1 in adipose tissue, see **Figure 2-3**). The cells are subsequently washed to remove 2-Deoxy-D-[1-^{3}H]glucose which remains in the culture medium and the amount of 2-Deoxy-D-[1-^{3}H]glucose which has been taken up into the adipocytes can be assessed by scintillation counting. As cellular glucose influx can be independent or dependent of insulin this

assay is generally performed with and without an insulin 'spike', prior to the addition of 2-Deoxy-D-[1-^{3}H]glucose. Subsequently, for a given population of cells, insulin dependent glucose uptake can be assessed by subtracting glucose uptake which occurs in the absence of insulin (basal glucose uptake) from glucose uptake which occurs in the presence of insulin.

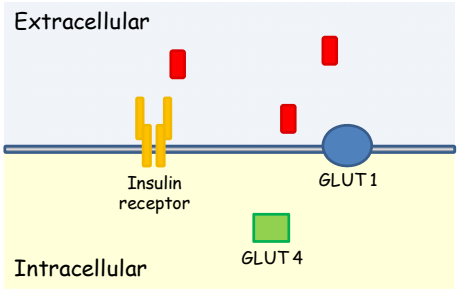

1. The assay is performed in the absence or presence of insulin. The predominant insulin independent glucose transporter GLUT 1, and insulin dependent glucose transporter are both expressed by adipocytes.

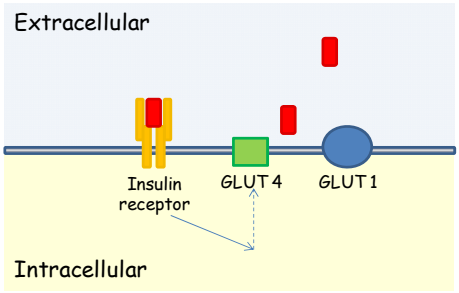

2. Insulin binds to its cognate receptor, resulting in the rapid translocation of GLUT 4 to the plasma membrane.

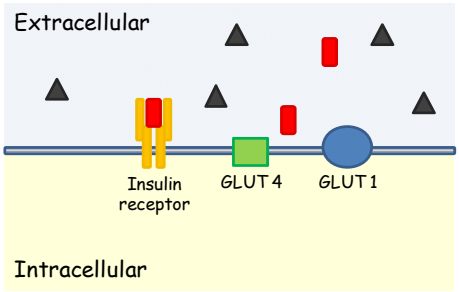

3. ^{3}H glucose is added to the culture medium for the predetermined optimised time period.

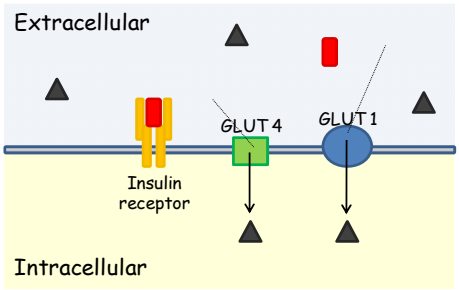

4. ^{3}H glucose is transported across the cell membrane via facilitated diffusion, mediated by both GLUT1 and GLUT4.

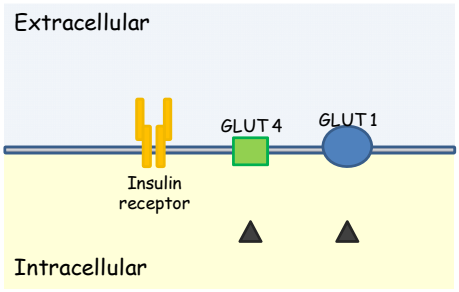

5. The cells are washed to remove ^{3}H glucose which remains in the culture medium. The relative amount of ^{3}H glucose which has been taken up by the adipocytes is assessed by scintillation counting.

Figure 2-3 The principle of glucose uptake analysis. *Cells are incubated with 2-Deoxy-D-[1-^{3}H]glucose in the presence or absence of insulin. The amount of 2-Deoxy-D-[1-^{3}H]glucose taken up by the adipocyte is assessed by scintillation counting.*

2.1.4.1.2 ***Solutions***

- **1 X PBS**. 2 tablets of PBS dissolved in 400 ml of distilled water. Autoclaved.

- **Krebs-Ringer-Hepes (KRP) buffer**, 136 mM NaCl, 4.7 mM KCl, 1.25 mM $CaCl_2$, 1.25 mM $MgS0_4$, 10 mM sodium phosphate buffer, pH 7.4. Autoclaved and stored at 4ºC for up to 3 months.

- **Insulin**, diluted to 1 mg/ ml in glycerine buffer (20 mM, pH 2.0). Stored at 4ºC for up to 6 months.

- **2-Deoxy-D-[1-^{3}H]glucose** (G. E. Healthcare, UK). Specific activity Ci/mmol. Stored at -20˚C for up to 6 months.

- **1% Triton X 100**, diluted in distilled H_20.

2.1.4.2 Method

Fully differentiated adipocytes, cultured in a 24 well TC plate, were washed with PBS and pre-treated with various concentrations of DHEA (0-25 µM) in SFM for 2 hr prior to the assay. Following pre-treatment, cells were washed with KRP and incubated with 0.40 ml or 0.45 ml of KRP (depending on subsequent insulin treatment). 50 µl of insulin was added to a final concentration of 12 nM to cell subject to insulin treatment and all cells were incubated at 37˚C, 5% CO_2, for 20 min. Glucose uptake was initiated by the addition of 50µl of KRP containing glucose, to give a total volume of 0.5 ml, and final concentrations of 0.1 mM glucose and 37MBq/l 2-Deoxy-d-[1-^{3}H]glucose, and the cells were incubated at 37˚C for the optimised time period. Following the incubation period, glucose uptake was terminated by the aspiration of

the KRP solution and the cells washed with ice cold PBS. The cells were lysed by the addition of 700 µl of 1% triton to each well and incubated for 20 min at 37˚C, 5% CO_2. Cells were then scrapped and the cell lysate transferred to a scintillation tube, to which 5ml of scintillant was added. The amount of 2-Deoxy-d-[$^{1\text{-}3}$H]glucose in each cell lysate was determined by scintillation counting (Packard 2500 TR Liquid Scintillation Analyzer, Perkin Elmer, UK). For all treatments, analysis of both basal and insulin stimulated 2-Deoxy-d-[$^{1\text{-}3}$H]glucose uptake was performed.

2.2 DNA methods

2.2.1 DNA extraction from agarose gels

2.2.1.1 Method

DNA was extracted from agarose gels using the 'QIAquick Gel Extraction Kit' (Qiagen), following the manufacturers protocol. All centrifugation steps were performed utilising an Eppendorf chilled table-top centrifuge, model 5415R (Cambridge, UK) at 21˚C. Following the separation of the PCR product by gel electrophoresis, the band of interest was visualized under UV light (Syngene G:Box, Geneflow, UK) isolated with a scalpel and weighed. The gel was melted by incubation with 3 x volume/ weight of QG buffer, containing guanadine thiocyanate to denature the DNA, at 50ºC for 10 min. The dissolved gel was loaded into a 'QIAquick Spin Column' and centrifuged for 1 min at maximum speed 13,000 g. The flow-through was discarded and subsequently 0.75 ml of PE buffer, containing ethanol, was added onto the column and centrifuged twice for 1 min at maximum speed, to

wash the DNA sample. The flowthrough was discarded and the sample was centrifuged again for 1 min to ensure the complete removal of PE buffer. The DNA was eluted by the addition of 30 µl of NFW, and the sample was stored at -20º until use.

2.2.2 DNA plasmid purification

2.2.2.1 Principle

Vector DNA was purified from bacterial cell culture using the QIAprep Miniprep system (Qiagen). This procedure is uses the modified alkaline lysis of bacterial cells of Birnboim and Doly. Bacteria are lysed under alkaline conditions to release cytoplasmic plasmid DNA. The lysate is subsequently neutralised and adjusted to high salt conditions to enable the selective adsorption of DNA onto the silica membrane in the miniprep column. Protein, RNA and metabolites are not retained on the membrane and are found in the flow-through. The DNA is washed, while bound to the column, with a buffer that efficiently removes endonucleases, ensuring that plasmid DNA is not degraded. Purified DNA is subsequently eluted utilising a low-salt buffer or water. This method has advantages over other methods in that it is simpler and quicker as it does not utilise loose resins or slurries and there is no need for phenol extraction or ethanol precipitation.

2.2.2.2 Method

The procedure was carried out according to the manufacturer's protocol. All steps were carried out at room temperature and all centrifugation steps were at 18000 g, using an Eppendorf chilled table-top centrifuge, model 5415R (Cambridge, UK), unless otherwise stated. Briefly, 5 ml overnight cultures of E. coli in LB were pelleted by centrifugation at 6800 g for 3 min. The supernatant was discarded and the bacterial cell pellet resuspended in 250 µl of buffer P1. 250 µl of buffer P2, containing NaOH, was added to each sample and mixed by gentle inversion to lyse the bacterial cells. 350 µl of buffer N3 was added to each sample and mixed by inversion, to neutralise the pH of the sample and precipitate the bacterial debris, proteins, and genomic DNA, which were subsequently pelleted by centrifugation for 10 min. The supernatant containing the plasmid DNA were applied to a QIAprep spin column by decanting and centrifuged for 60 sec. The plasmid DNA, bound to the silica membrane, was washed twice by the addition of 500 µl of buffer PB and centrifugation for 30 sec, followed by 750 µl of buffer PE and a further 60 sec centrifugation. Following both washes the flow through was discarded. Residual buffer was removed by centrifuging for a further 1 min. Plasmid DNA was eluted by the application of 50 µl of nuclease free water to the centre of each QIAprep spin column, which was left to stand at room temperature for 1 min and then centrifuged for 1 min. The concentration of eluted DNA was calculated using the Nanodrop spectrometer (ND-1000, Nanodrop, Wilmington, USA). Plasmid DNA integrity was verified by running 4µl on a 2% agarose gel containing 0.15 µl/ml ethidium bromide.

2.2.3 DNA sequencing

2.2.3.1 Principle

In this thesis, DNA sequencing was performed utilising fluorescent dye-terminator cycle sequencing, a method based on the original Sanger technique, devised in 1980. The principles are the same as with Sanger sequencing; fluorescently labelled dideoxynucleotides (ddNTPs) are incubated with a DNA template, a sequence specific primer and further unlabelled nucleotides, and a polymerisation reaction is initiated. ddNTPs lack a 3'OH, such that, when they are incorporated into a growing nucleotide chain they terminate the reaction, resulting in the production of a set of DNA fragments of differing lengths, with a ddNTP at the 3' terminus of each fragment. Due to the high number of DNA molecules included in the reaction, synthesised nucleotide chains will include a fragment with a terminal ddNTP at all possible bases of the template DNA. The resulting PCR products are subsequently separated by gel electrophoresis on a polyacrylamide gel, with the larger nucleotides progressing faster. As the different ddNTP bases (ddATP, ddGTP, ddCTP, ddUTP) are tagged with different fluorescent labels, the order of the migrating nucleotides as they pass a sequencing laser (corresponding to the 5' to 3' template DNA nucleotide sequence), can be detected. Subsequently the data is compiled and the identified DNA sequence expressed as a chromatogram. The key advantage over the original Sanger technique is that cycle sequencing employs a thermostable DNA polymerase, which, as described in section 2.4.3, allows for the sequencing reaction to be repeated numerous times. Therefore, sequencing can be performed to a higher degree of accuracy, with less DNA than with conventional sequencing reactions.

2.2.3.2 Plasmid DNA sequencing

2.2.3.2.1 ***Method***

Plasmid DNA was purified by Miniprep as described in section 2.12. 3 µg of purified plasmid DNA was mixed with 3.2 pmol of sequencing primer (**Table 2-1**) and subjected to direct sequencing on an automated sequencer (ABI 377) at the University of Birmingham sequencing facility. Traces were analyzed manually using ChromasPro Version 1.5 software (Chromas, UK).

Table 2-1 Primers used for sequencing of genomic DNA and plasmid DNA

Primer pair number	*Gene*	*Forward*	*Reverse*
Genomic sequencing primers			
1	SULT2A1 Exon 1	ggtggctacagttgaaaccc	tgcactgaatggacaggaac
2	SULT2A1 Exon 2	gcgtgagccaccatgtc	ggcatatcagtgtttgaaaggc
3	SULT2A1 Exon 3	tcaaaaagagtgaggattgactg	gggtgtcaaaagaggtcgg
4	SULT2A1 Exon 4	tagactggatgcctgctctc	taaggatggtggtgagaggg
5	SULT2A1 Exon 5	gcccagccttgtctttctc	catgcatgccgtgtattctg
6	SULT2A1 Exon 6	ggtggagacaggtcaaggag	caaggacaggagaatcaatgtc
7	PAPSS1 Exon 1	gccctcctcttgctac	gttcttcccacgaacg
8	PAPSS1 Exon 2	gtggaaagcagtaaacac	gttatatgtcgtgatgctc
9	PAPSS1 Exon 3	gcagagcaagactcttg	aacaaagagatggtagctg
10	PAPSS1 Exon 4	cactaaattggatgagaag	tccaagtcactccaatc
11	PAPSS1 Exon 5	gcgcagatactaacttc	cacaacacctcacacac
12	PAPSS1 Exon 6	tagcactcacagccttc	gctaataccacccctg
13	PAPSS1 Exon 7	ctcatccttacactgtttg	agtcttataatgctacctc
14	PAPSS2 Exon 1	aagggaagtgcgacgtgtc	cactcttactcctcctc
15	PAPSS2 Exon 2	catgtatcagtttcgcaattaaaag	catctcccagcctccttctaatg
16	PAPSS2 Exon 3	gtcatcttaaactatccaggccg	cttgcactgtgtgtgggaatcg
17	PAPSS2 Exon 4	ggctattgaaaaccaaagtacacag	caaggaagatttctgaggacag
18	PAPSS2 Exon 5	gtcaaggatggctgtttgacc	gaaatgaaacagcattggtaaaaac
19	PAPSS2 Exon 6	ggtaggtgaaccggttgtc	ggagaagaggttaaaaataacttgg
20	PAPSS2 Exon 7	catagaaggttctgccctcatc	acactgtaaatgatccaaacag
21	PAPSS2 Exon 7b	tgctgtaagattcgtttggt	gaactaatagcgattccaactg
22	PAPSS2 Exon 8	cttggatttgggtcttaatgcttc	cattcttccacctaatcccag
23	PAPSS2 Exon 9	ctgaaggcagttctttaactgtaac	gttgcagtgagctgagatcg
24	PAPSS2 Exon 10	gccagtggataatgaatgcacag	cagaaaggatcccagagactca
25	PAPSS2 Exon 11	gttgactcacattgctgaattac	gagagtttttcaaagggccc
26	PAPSS2 Exon 12	ccattatttcccttctcttctg	agcacttcagaaagaaactc
Plasmid sequencing primers			
27	PAPSS2a	atgtcggggatcaagaag	ctggtctgcattaccagc
28	PAPSS2a	cctgaaactcctgagcgtgtgc	ccaatttgtccacagtgagtgac
29	PAPSS2a	ggagggtagctatcttacgagac	gaccaataccgtctgacacctc
30	PAPSS2a	gatgtgcctctagactggcgg	

2.2.3.3 Genomic DNA sequencing

2.2.3.3.1 ***Method***

Genomic DNA was extracted from peripheral blood leukocytes of EDTA blood, after written informed consent from the patient with approval of the South Birmingham Research Ethics Committee. The coding sequences, including exon-intron boundaries, of the genes to be sequenced were amplified employing specific primers. PCR products were purified, as described in section 2.2.1. 6 ng of purified PCR product was mixed with 3.2 pmol of primer and subjected to direct sequencing on an automated sequencer (ABI 377) at the University of Birmingham sequencing facility. Traces were analyzed using Lasergene sequence analysis software (DNASTAR) and identified mutations were independently verified, and numbered according to the amino acid position in the relevant GenBank protein sequence.

2.3 Generation and cloning of expression constructs

2.3.1 PGEX-6P-3 expression vector

The pGEX-6P vectors possess a multiple cloning site that contains six restriction sites, facilitating the unidirectional cloning of cDNA inserts. In addition, the pGEX-6P vectors contain a GST gene, so that expression in Eschericia coli (E. coli) yields fusion proteins with the 26 kDa glutathione S-transferase (GST). The GST gene, which is located upstream of the multiple cloning site, contains an ATG and ribosome-binding site and is under control of the tac promoter, which is induced by isopropyl beta-D thiogalactosidase (IPTG), and the lac gene product, described in greater detail in section 2.5.2. A translational terminator is present downstream from

the multiple cloning site. In addition, the pGEX-6P-3 expression vector has also been engineered to contain an ampicillin resistance gene, Amp, enabling the selection of successfully transformed E. coli cells.

2.3.2 PGEX-6P-3 expression vector wild type and mutant construction

pGEX-6P-3-PAPSS2 and pGEX-6P-3-SULT2A1 wild type (WT) plasmids were kindly provided by Dr Charles Strott, NIH, Bethesda, USA. To generate these constructs, human full length PAPSS2 and SULT2A1 cDNA were inserted into the *Sal*I and *BamH*I sites or SalI and NotI sites of the pGEX-6P-3 expression vector (G E Healthcare) as previously described (Fuda et al., 2002). To confirm the presence of the insert restriction digests were performed as described in section 2.3.3. To ensure the correct in frame alignment of the insert and the absence of any sequence variations sequence analysis was performed as described in section 2.2.3.2. Utilising the pGEX-6P-3-PAPSS2-WT vector as a template, the PAPSS2 mutants (T48R, R329X and S475X) were generated using the Quickchange XL site-directed mutagenesis kit (Stratagene, Germany), as described in section 2.3.3.3. Resultant constructs were sequenced to confirm the successful generation of mutant constructs and the absence of any other sequence alterations during this procedure.

2.3.3 Restriction digestion

2.3.3.1 Principle

Restriction endonucleases are enzymes that cut double-stranded or single stranded DNA at specific recognition nucleotide sequences known as restriction sites. Since the isolation of the first restriction enzyme *Hind*II from bacteria in 1970, more than 3000 restriction enzymes have been identified and more than 600 of these are available commercially. Restriction enzymes recognize a specific sequence of nucleotides and produce a double-stranded cut in the DNA. Recognition sequences differ for each restriction endonuclease and vary widely with differing strand orientation and lengths between 4 and 8 nucleotides. However, many of the sequences are palindromic, nitrogenous base sequences that read the same backwards and forwards. Restriction endonucleases which cut double stranded DNA at a base pair produce DNA with 'blunt ends'. While restriction endonucleases which cut between unpaired bases produce a stretch of unpaired nucleotides, termed cohesive ends or sticky ends.

Restriction enzymes are exploited during gene cloning and protein expression to enable the insertion of DNA into plasmid vectors. To clone a gene fragment into a vector both plasmid DNA and gene insert are typically cut with the same endonuclease to produce ends which can be 'glued' together utilising the enzyme DNA ligase. Restriction enzymes are also commonly used for restriction fragment length polymorphism (RFLP) analysis, a technique which enables the distinction of gene alleles by specifically recognizing single base changes in DNA known as single

nucleotide polymorphisms (SNPs), without the need for relatively expensive gene sequencing.

2.3.3.2 Method

In this thesis both dual restriction digestions and sequential digestions were performed. For dual restriction digestions a 50 µl reaction was prepared comprising 1 µg of plasmid DNA, 10 units of each restriction enzyme, 5 µl of 10X buffer, made up to 50 µl with NFW, and incubated at the enzyme dependent temperature for 4 hours. For sequential digestion reactions a 50 µl reaction was prepared comprising 1 µg of plasmid DNA, 10 units of the first restriction enzyme, 5 µl of 10X buffer, made up to 50 µl with NFW and incubated at the enzyme dependant temperature for two hours. Following this incubation the digest was diluted 1:1 with a 50 µl reaction containing 20 units of the second restriction enzyme, 5 µl of 10X buffer made up to 50 µl with NFW, and the 100 µl reaction was incubated at the second restriction ezyme dependant temperature for a further two hours. To inactivate the enzymes the reaction was heated to 80˚C for 10 min. An aliquot of the digestion was assayed by agarose gel electrophoresis versus non-digested DNA, to confirm successful digestion.

2.3.3.3 Site directed mutagenesis

2.3.3.4 Principle

Site-directed mutagenesis is a technique by which a mutation (point-mutation, deletion or insertion) can be generated at a defined site in a DNA molecule, usually a

plasmid. There are several approaches by which this can be achieved, but the most common technique, which was utilised in this thesis, employs PCR (described in section 2.4.3). Complementary oligonucleotide primers of at least 20 bases in length are designed, which contain the desired sequence alteration in the centre, flanked by the known WT sequence. Mutageneic oligonucleotides incorporate at least one base change but can be designed to generate multiple substitutions, insertions or deletions. Briefly, template DNA is denatured by heating to produce single stranded DNA. The reaction is subsequently cooled to permit the mutagenic oligonucleotide to anneal to the template DNA. T4 DNA polymerase, using the parental DNA as a template synthesises a new complementary strand, which contains the desired mutation. Unlike the template DNA, as the DNA containing the DNA is produced *in vitro* it is not methylated. This can be exploited to eliminate the parental DNA by enzymatic digestion with a restriction enzyme specific for methylated DNA (*Dpn* I). The synthesised DNA containing the desired mutation is transformed into XL1-Blue supercompetent cells to repair nick between the end of the DNA strand and the oligonucleotide. The plasmid can subsequently be isolated and used for further applications.

2.3.3.5 Method

Mutagenesis reactions were carried out using QuikChange XL Site-Directed Mutagenesis kit (Stratagene, UK), following the manufacturers protocol, as shown in **Figure 2-4**. For each mutation to be synthesised two oligonucleotide primers were designed, which annealed to the same sequence on opposite strands of the plasmid and contained the desired mutation in the centre, flanked by the unmodified

nucleotide sequence (**Table 2-1**). Primers were designed between 25-30 bases in length, with a melting temperature equal to or greater than 78˚C; a GC content ≥40% and one or more G or C bases on the 3' end. A master mix was prepared for n+1 reactions as follows; 5 µl of 10X reaction buffer, 25 ng of dsDNA template, 125 ng of each oligonucleotide primer, 1 µl of dNTP mix, 1µl of Pfu Turbo polymerse (25U/µl), made up to final concentration of 50 µl with dH_20. The reaction was then placed in a GeneAmp 9700 thermal cycler on heated to 95ºC for 95 sec, and then 16 cycles of 95ºC for 30 sec, 55ºC for 1 minute, and 68ºC for 1 min per kb of plasmid length.

Following thermal cycling the reaction was placed on ice for 2 min. 1µl of Dpn1 restriction enzyme was added to each sample and incubated at 37˚C for 1 hr, to digest the parental template supercoiled DNA. Subsequently, 2µl of the sample was transformed into 100µl of XL-1 blue super competent cells (Stratagene, UK), following the transformation protocol described in section 2.5.1. The plasmid DNA was purified as described in section 2.2.1 and subjected to plasmid sequencing (section 2.2.3.2).

Table 2-2 Mutagenic primers used for site directed mutagenesis to generate mutant DNA constructs of PAPSS2a (T48R, R329X and S475X).

Primer pair number	Mutation	Forward Primer	Reverse Primer
57	**T48R**	TGTACCGTGTGGCTAAGAGGTCTCTCTGGTGCTG	CAGCACCAGAGAGACCTCTTAGCCACACGGTACA
58	**R329X**	GAGGGTAGCTATCTTATGAGACGCTGAATTCTATG	TCATAGAATTCAGCGTCTCATAAGATAGCTACCCTC
59	**S475X**	GGTCCTGGATCCCAAGTAAACCATTGTTGCCATCT	AGATGGCAACAATGGTTTACTTGGGATCCAGGACC

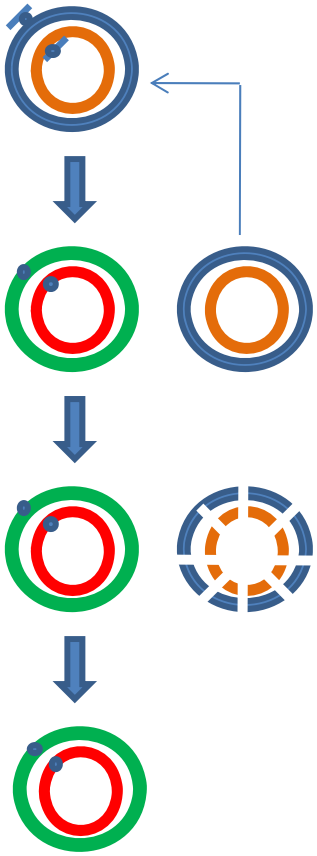

1. **Mutant strand synthesis**
   Perform thermal cycling to:
   - denature template DNA
   - anneal muatagenic primers containing desired mutation
   - extend and incorporate primers with *PfuUltra* DNA polymerase

2. **Dpn1 digestion of template**
   Digest parental methylethylated and hypermethylethylated DNA with Dpn1

3. **Transformation**
   Transform mutated molecule into competent cells for nick repair

Figure 2-4 A schematic of the principle of site-directed mutagenesis. *Mutagenic primers are designed which contain the desired mutation in the centre flanked by wild type sequence. The mutant primers are utilised in a PCR reaction which results in their incorporation and extension. The methylated parental DNA is digested with Dpn 1. The mutant DNA constructs are transformed into competent cells for nick repair.*

2.4 RNA methods

2.4.1 RNA extraction

2.4.1.1 Principle

The guanidinium thiocyanate-phenol-chloroform method for total RNA extraction was originally described by Piotr Chomczynski & Nicoletta Sacchi in 1987. This method relies on phase separation upon centrifugation of an organic phase (containing chloroform, water-saturated phenol and a denaturing solution (Guanidinium)) and an aqueous phase (containing phenol). In this thesis, total RNA was isolated from cells using a commercially available modified single step extraction reagent, TRI reagent, based on the guanidinium thiocyanate-phenol-chloroform method. This modified method is more time consuming than extraction using a column, but has the major advantage in that the RNA yield is not reduced.

2.4.1.2 Solutions

- **70% Ethanol**, diluted in dH_20.

2.4.1.3 Method

Total RNA was extracted from cell monolayers according to the manufacturers protocol, with all steps performed on ice. All centrifugation steps were performed utilising an Eppendorf chilled table-top centrifuge, model 5415R (Cambridge, UK) at 4˚C .Cells were washed with PBS and 0.5ml of TRI reagent added per $10cm^2$ of

monolayer cells. The resulting cell lysate was passed through a pipette several times to form a homogenous cell lysate and transferred to a fresh eppendorf. 0.2 ml of chloroform was added per 1 ml of TRI reagent, the sample mixed by inversion, and incubated at room temperature for 10 min to allow the complete dissociation of nucleotides. The solution was centrifuged at 8500 g for 15 min at 4˚C to separate the aqueous phase (containing RNA) from the organic phase (containing DNA) and the interface (denatured proteins). The aqueous phase was transferred to a fresh eppendorf and an equal volume of isopropanol added. RNA was precipitated at -20˚C overnight to ensure the maximal yield. RNA was pelleted by centrifugation at 4˚C, 1100 g, for 15 min. The supernatant was aspirated and the remaining RNA pellet washed with 70% ethanol and centrifuged at 1100 g for 5 min. The ethanol was aspirated and the pellet air dried before being resuspended in 30 µl of NFW and stored at -80˚C.

RNA was quantified by measuring the absorbance at OD_{260}, based on the equation 1 OD_{260} unit = 40 µg of RNA/ ml, using a nanodrop spectrometer (ND-1000, Nanodrop, Wilmington, USA). RNA integrity was confirmed by gel electrophoresis on a 1% agarose gel with 0.15 µg/ml ethidium bromide. Intact RNA exhibits defined 28S and 18S rRNA bands, with the 28S band being twice as intense as the 18S.

2.4.2 Reverse transcription

2.4.2.1 Principle

Reverse transcription is the process of synthesising single stranded complimentary DNA (cDNA) from single stranded RNA. The enzyme responsible for this process,

reverse transcriptase, was discovered independently by Howard Temin and David Baltimore in 1970. The process, outlined in **Figure 2-5**, involves the heating of extracted RNA to denature secondary structures, and the subsequent cooling to allow primers (random hexamers or oligo dT primers) to anneal to the single RNA strands. Once annealed, the primers are extended by reverse transcriptase in the presence of an RNase inhibitor. The resultant single stranded cDNA can then be used in a PCR reaction.

2.4.2.2 Method

Reverse transcription was performed using the Promega Reverse transcriptase kit, following the manufacturer's instructions. Nuclease free H_20 was added to 1 µg of RNA, to a final volume of 10 µl, and the sample was incubated at 70ºC for 10 min, to denature the RNA. A master mix was prepared, for n + 1 reactions, containing, 2.5 µl of 10x reaction buffer, 6 µl of $MgCl_2$ (25 nmol/l), 5µl dNTPs (10 nmol/l), 1.25 µl of random hexamers, 0.5 µl RNase inhibitor, 1.55 µl Avian myoblastosis virus (AMV) reverse transcriptase, made up to 25µl with NFW. 15 µl of master mix to each sample and the reaction incubated in a thermal cycler (Applied Biosystems GeneAmp PCR system 2700, California, USA) at 37ºC for 1 hour, to allow the synthesis of cDNA by reverse transcriptase, and subsequently, 95ºC for 5 min, to denature the reverse transcriptase, terminating the reaction. RNA was stored at -20ºC until use, or at -80ºC for long-term storage.

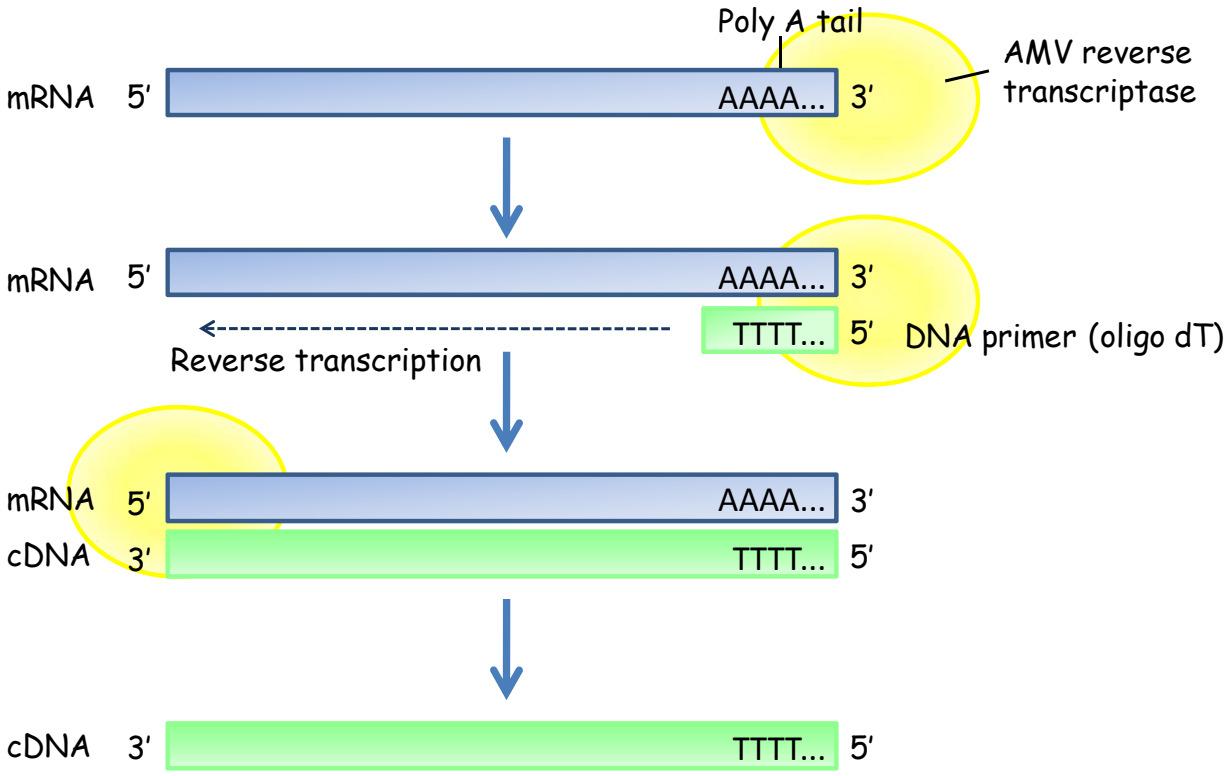

Figure 2-5 The principle of reverse transcription. *The reaction is heated to permit DNA primers (oligo dT or random hexamers) to anneal to the single RNA strand. The binding of oligo dT primers to the poly A tail of mRNA is shown in the diagram. Random primers bind randomly along the length of mRNA. The reaction is cooled to the optimum temperature for reverse transcriptase (AMV) activity and the DNA primers are extended by reverse transcriptase to generate cDNA.*

2.4.3 Polymerase chain reaction

2.4.3.1 Principle

PCR is a method by which nucleic acid sequence can be amplified exponentially *in vitro*. As shown in **Figure 2-6**, when performing PCR, small nucleotide sequences (primers) complementary to the 3’ and 5' ends of the target sequence for amplification are annealed to the template DNA and form an initiation point for the elongation of the complementary daughter strand. This process exploits the thermostable nature of thermostable bacterial DNA polymerases, which, unlike mammalian polymerases can tolerate the relatively high temperatures required for separation of DNA double strands. Taq polymerase, an enzyme originally derived from the bacterium Thermus aquaticus, was used for all PCR reactions described in this thesis. In this thesis conventional PCR has been used to amplify genomic DNA prior to sequence analysis and conventional and real-time semi-quantitative PCR have been used to evaluate mRNA expression, both of which are described below. A modified form of conventional PCR reaction using fluorescently labelled ddNTPs is utilised to perform DNA cycle sequencing. This procedure is described in section 2.2.3.

2.4.3.2 Conventional PCR

The principle of conventional PCR is outlined in **Figure 2-6**. When performing conventional PCR, the reaction is heated to 95ºC, above the melting point for double stranded DNA, to promote the separation of the two strands of the DNA template.

The reaction in then heated to the primer specific temperature, to allow the primers to anneal to the complementary single strand of DNA, and then to 72ºC, for an optimised duration, to allow for the synthesis of the new complementary strand by Taq polymerase. The reaction is subsequently cycled an optimised number of times to allow the exponential generation of specific target DNA fragments. After the final cycle the samples are incubated at 72ºC to promote the terminal elongation of the daughter strands.

2.4.3.2.1 ***Method***

All conventional PCR reactions were performed using Bioline reagents. A PCR mastermix was prepared on ice for n + 1 reactions containing, reaction buffer (1x), MgCl2 (1-2.5 µM), deoxy-NTPs (0.5 µM), Taq polymerase (0.05 U/µl), forward and reverse primers (0.6 µM, **Table 2-3**), made up to a specific total volume per reaction with nuclease free water (depending on the volume of DNA). The master mix was aliquoted and 1 µl of synthesised cDNA or 100ng of extracted DNA was added to make a final reaction volume of 25 µl. In a thermal cycler (Applied Biosystems GeneAmp PCR system 2700, California, USA) the samples were incubated at 95ºC for 5 min and then heated, for an optimised number of cycles to; 95ºC for 30 sec, the primer specific annealing temperature for 30 sec and 72ºC for a variable duration, depending on the size of the product. Samples were then incubated for 72ºC for 5 min.

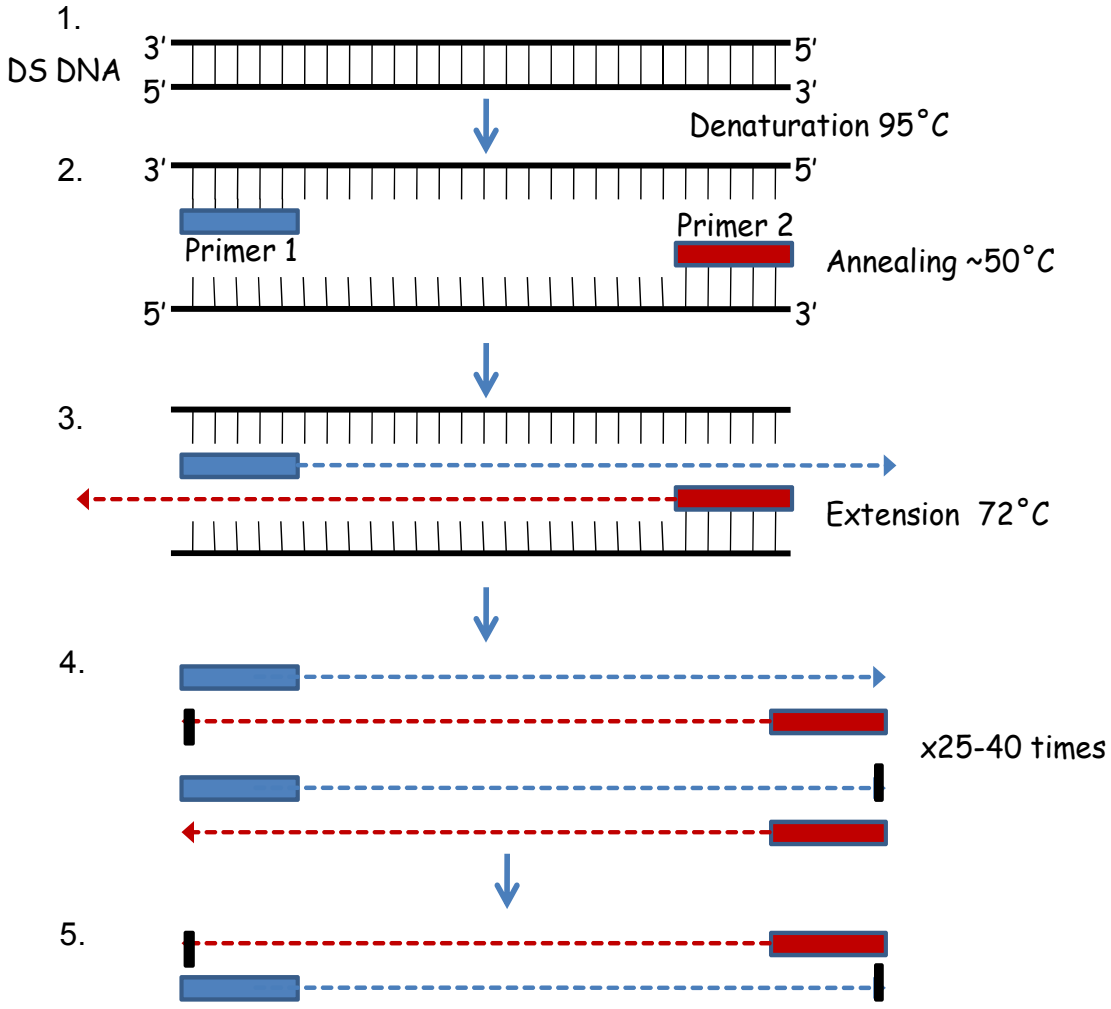

Figure 2-6 The principle of PCR. *1. The double stranded (DS) DNA is denatured by heating the reaction to 95˚C. 2. The reaction is cooled to allow the two complementary primers to anneal to the DNA template. 3. The reaction is heated to 72˚C, the optimal temperature for extension by Taq polymerase, which proceeds in the 5' to 3' direction. 4. These steps are repeated 25-40 times, resulting in the amplification of DNA. 5. Subsequent extensions are precisely limited to the region of interest.*

Table 2-3 Primer sequences used for conventional PCR

Primer pair number	***Gene***	*Forward primer*	*Reverse primer*
31	SULT2A1	caggaagaaccatagagaagatctg	Gtcttacacaatgaccccagtc
32	STS	aggacttcccaccgatgagattacctttg	Aaaagggtcaggattagggctgctaggaa
33	PAPSS1	ctgctggcatgcctcatc	Gtggtcccctcttgttactag
34	PAPSS2	cactcccctcaaaggtttc	Cagcgtctcgtaagatagc
35	11β-HSD1	accagagatgctccaaggaa	Atgcttccattgctctgctt
36	AKR1C3	acttcatgcctgtattgggatttg	Ctgcctgcggttgaagtttgata
37	17β-HSD4	agttctctctctttcttgttggctctgga	Gcgtcctatttcctcaaatacaaaggtactct
38	HSD3B1	ggaatctgaaaaacggcggc	Ctgagatatagtagaactgtcctcggatg
39	HSD3B2	gatcgtccgcctgttggtg	Ctcttcttcgtggccgttctggatgat
40	OATP-A	ccacaagatttatatgtggaaaatg	Catatatccaggtatggcagcc
41	OATP-B	catgggacccaggatagggcca	Ggcctggccccatcatggtcactg
42	OATP-C	gttcaacctgaattgaaatcac	Gatgtggaattatatgtcctacatgac
43	OATP-D	gctgagaacgcaaccgtggttcc	Gacttgagttcagggctgactgtcc
44	OATP-E	gccatgccactgcagggaaatg	Ttctggtacaccaagcaggagccc
45	OATP-F	cagaaagacaatgatgtcc	Cacatcttttaaatccccatttgaggc
46	OATP-8	gaataaaacagcagagtcagcatc	Gcaatatagctgaatgacagg
47	OAT-4	ctctgcggtttccacaaacatgacc	Ccaccatcagtgtcagtgaactcag

2.4.3.3 Real-time PCR

Compared to conventional PCR, Real-time PCR has the advantage in that the specific PCR product can be detected as it accumulates during the PCR reaction, thereby allowing the quantification of mRNA transcripts. To perform real-time PCR an oligonucleotide probe is synthesised containing a fluorescent reporter dye on its 5' end and a quencher dye on its 3' end (see **Figure 2-7**). The proximity of the quencher dye to the reporter dye in this synthesised structure reduces the florescence emitted by the reporter dye by fluorescence resonance energy transfer (FRET). During the PCR reaction the probe anneals downstream from one of the primer sites, and is cleaved by the 5' nuclease activity of Taq polymerase during primer extension, without inhibiting complimentary strand synthesis. The cleavage of the probe allows the reporter dye to produce a signal. During each cycle of the PCR

reaction additional annealed probe molecules are cleaved, resulting in an increase in the fluorescence intensity directly proportional to the amount of PCR product produced. The fluorescence produced is monitored throughout the PCR reaction, enabling the identification of the cycle number at which the product is first produced (and fluorescence exceeds the calculated threshold value) which is termed the Ct value, as shown in **Figure 2-8**. Therefore the Ct value of a gene is inversely proportional to the amount of original template of that gene. Measuring the Ct value of a housekeeping gene, of which the expression is kept constant within cells, and comparing it to the Ct value of the gene of interest, produces the ΔCt value. By comparing the ΔCt between different groups, the relative expression of a gene can be calculated.

Table 2-4 Primer sequences used for real-time PCR

Primer pair number	***Gene***	***Forward primer***	***Reverse primer***	***Probe***
48	HSD11B1	AGGAAAGCTCATGGGAGGACTAG	ATGGTGAATATCATCATGAAAAAGATTC	CATGCTCATTCTCAACCACATCACCAACA
49	H6PDH	CAGGTGTCCTAGTGCACATTGAC	GTAGCCCACTCTCTCGTCCAA	AAGGCACGCCCTCCCAGCG
50	GPD1 (G3PDH)	AGGGCCATCTGAAGGCAAACGCC	CCATCAGTTCATCGGCAAGAT	TCGTCTACCCCCTTAATAAGAGATATG
Assay on demand (Applied Biosystems)		***Identification number***		
51	LPL	Hs00173425_m1		
52	PAPSS1	Hs00193745_m1		
53	PAPSS2	Hs00190682_m1		
54	SULT2A1	Hs00234219_m1		
55	STS	Hs00165853_m1		
56	AKR1C3	Hs00366267_m1		

2.4.3.3.1 ***Method***

In this thesis real-time PCR was carried out using Applied Biosystems reagents and expression assays (Applied Biosystems, Warrington, UK), in separate reactions for the housekeeping gene and the gene of interest. To analyse housekeeping gene expression each reaction contained 10 µl of 2x MasterMix, 18S primers and probes (to a final concentration of 25 nM each), 1 µl of cDNA and NFW to a final volume of 20 µl. To analyse expression of the gene of interest each reaction contained 10 µl of 2x MasterMix, 1 µl of 20x 'assay on demand' gene expression assay (**Table 2-4**), 1 µl of cDNA and NFW to a final volume of 20 µl. PCR reactions were run utilising a 7500 real-time PCR system (Applied Biosystems, Warrington, UK). Ct values (cycle number at which logarithmic plot crosses the calculated threshold line) were used to determine ΔCt values, (Ct of gene of interest – Ct of housekeeping gene) and used to perform statistical analysis. To calculate relative gene expression the ΔCt of the control reaction was subtracted from the ΔCt of the treatment reaction to give the ΔΔCt. The ΔΔCt value was subsequently transformed through the equations, gene expression = $2^{-\Delta\Delta Ct}$, to calculate relative gene expression as fold change.

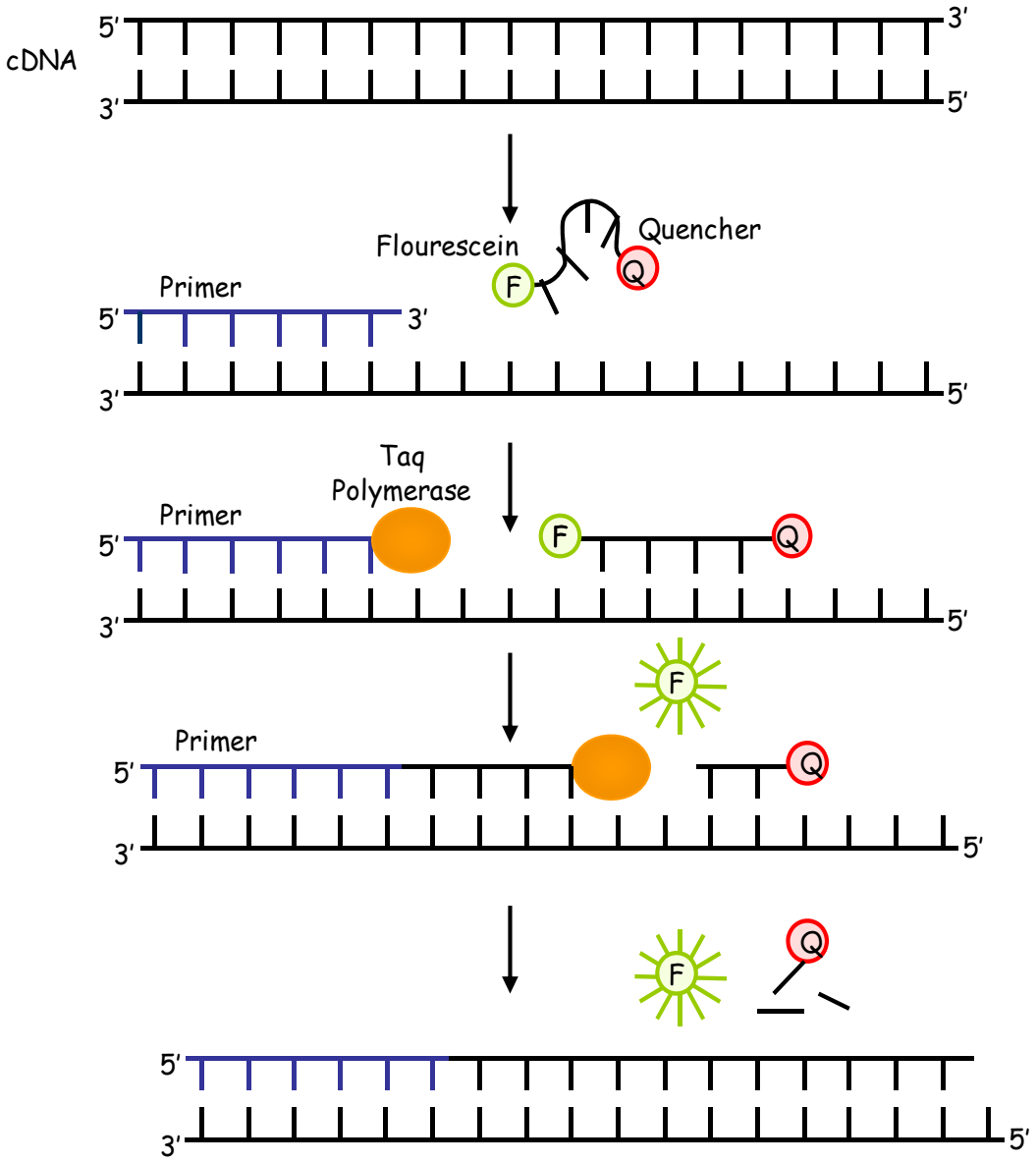

Figure 2-7. The principle of TaqMan Real-time PCR. 1*. The RT step synthesises a double stranded cDNA copy of the RNA template.* ***2****. The reaction is heated to permit the denaturation of the double stranded cDNA template and the target specific primers and probes to anneal. The probe contains a flourescein dye at the 5' end and a quencher at its 3' end.* ***3****. The reaction is cooled to allow Taq polymerase to synthesise the complementary strand. The 5' nuclease activity of Taq polymerase cleaves the probe, physically separating the flourescein and quencher dyes, resulting in reporter fluorescence. The increase in signal is directly proportional to the number of molecules released during that cycle.*

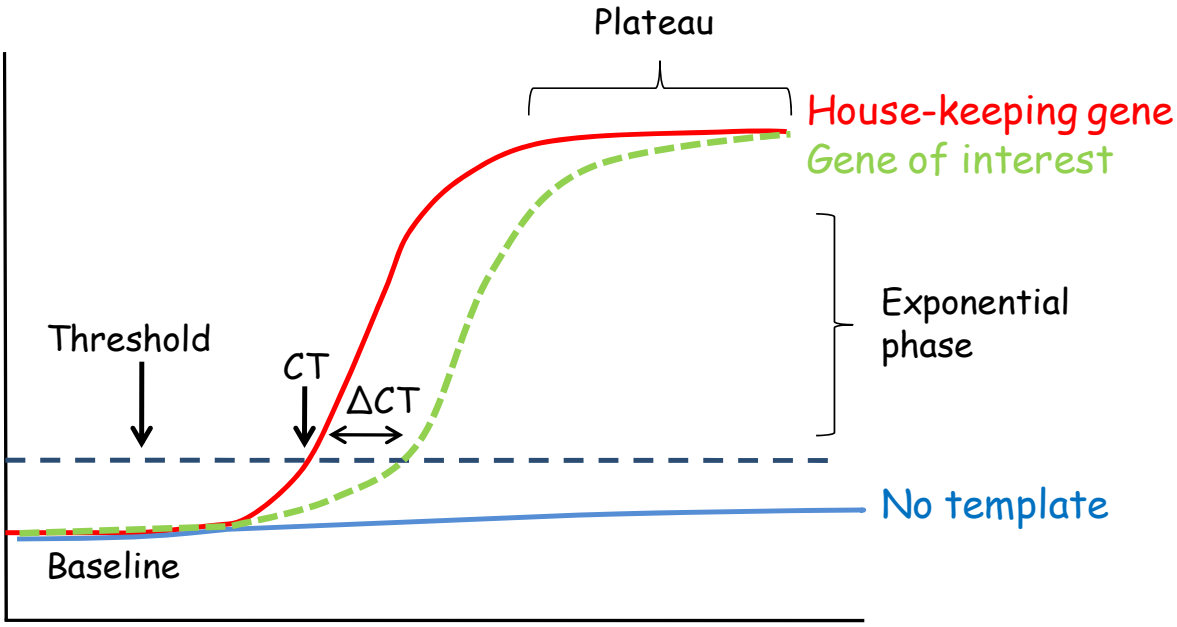

Figure 2-8 The analysis of Real-time PCR amplification curves. *The Real-time PCR amplification curves plot fluorescence signal versus cycle number. Representative curves for a 'housekeeping' gene and gene of interest are shown. The Ct values represent the cycle at which the instrument can first reliably detect fluorescence derived from the amplification reaction, and is relative to the amount of template. The curve continues to increase over the threshold value due to the accumulation of amplified product until the reaction is limited by lack of reagents and reaches a plateau. The difference between the Ct value of the gene of interest and the 'houskeeping' gene is termed the ΔCt value. By comparing the ΔCt between different treatments, the relative expression of a gene between different treatments can be calculated.*

2.5 Protein methods

2.5.1 Bacterial plasmid transformation and propagation

2.5.1.1 Description and genotypes of E.coli host strains

2.5.1.1.1 ***α-select bronze efficiency competent cells***

Genotype: F- deoR endA1 recA1 relA1 gyrA96 hsdR17(rk -, mk +) supE44 thi-1 phoA Δ(lacZYA argF)U169 Φ80lacZΔM15 λ-

Alpha–select bronze efficiency competent cells were used for maintenance of the vectors. This strain of E. coli has a medium level of competency, resulting in a mediocre transfection efficiency. Alpha–select competent cells have a mutation in the rec A gene (recA1), which is involved in recombination. The mutant gene limits recombination of the plasmid with the E. coli genome, improving insert stability. This strain also carries an inactivating mutation in the endonuclease I (endA) gene, which rapidly degrades plasmid DNA isolated by most miniprep procedures, thus enhancing plasmid purification.

2.5.1.1.2 ***BL21-Gold (DE3)***

Geneotype: E. coli B F– ompT hsdS(rB– mB–) dcm+ Tetr gal λ(DE3) endA Hte

BL21-Gold(DE3) cells were used for all protein expression applications. Derived from Escherichia coli B, this strain naturally lack the Lon protease, which can degrade recombinant proteins. In addition, BL21-Gold(DE3) cells are engineered to be deficient for a second protease, the OmpT protein and therefore, once transformed,

produce a high level of protein expression and stability. BL21-Gold(DE3) cells incorporate major improvements over the original BL21 strain the Hte phenotype, which increases the transformation efficiency of the BL21-Gold cells. In addition, similar to alpha-select competent cells, in BL21-Gold(DE3) cells the endonuclease I (endA) gene, is inactivated, improving the quality of DNA purification.

2.5.1.2 Principles

Transformation is the genetic alteration of a cell resulting from the uptake, and expression of foreign naked DNA molecules. Transformation of eukaryotic cells in tissue culture is usually termed transfection. The ability of a cell to take up exogenous DNA from the environment is referred to as competence. Some bacteria have natural competence, in that they are naturally capable of taking up DNA, however in the majority of species of bacteria, to perform transformation, artificial competence has to be induced. The most common way to induce bacterial competence is chilling cells in the presence of divalent cations such as Ca^{2+} (In $CaCl_2$). This causes holes to form in the cell membrane of bacterial cells, thus making them permeable to hydrophilic DNA.

2.5.1.3 Solutions

- **LB**, 25 g of LB dissolved in 1 L of dH_20. Autoclaved and stored at 4ºC

- **Carbenicillin**, diluted to 50 mg/ml in dH_20 and stored at -20ºC. Added fresh to LB to a final concentration 50 µg/ml.

2.5.1.4 Method

Transformation of alpha-select and BL21 strains of E coli were performed as described in the Bioline manual. Immediately prior to transformation β-ME was added to BL21 cells to a final concentration of 25 mM, to increase transformation efficiency. 50 µl of cells, thawed on ice, were gently mixed with 1 µl of plasmid DNA and incubated on ice for 30 min. Cells were 'heat shocked' at 42˚C for 30 sec and then incubated on ice for a further 2 min. Reactions were diluted by the addition of 200 µl of LB and incubated at 37˚C for 60 min. The cell transformation mixture was spread on LB agar plates containing the appropriate antibiotic and incubated at 37˚C overnight.

A single colony was picked and used to inoculate 10ml of Luria broth (LB) supplemented with 50 µg/L of Carbenicillin, a more stable ampicillin analogue. Alpha-select cells were cultured overnight at 37 ˚C in an elliptical incubator, prior to mini-prep plasmid DNA extraction as described in section 2.12. BL21-Gold (DE3) cells were cultured overnight at 26˚C in an elliptical incubator and subsequently diluted to 1 L with LB containing amplicillin (50 µg/l), until the OD60 of the cultures reached 0.4

2.5.2 Induction of fusion protein expression

2.5.2.1 Principle

Expression of inserts cloned into a pGEX vector is under the control of the inducible tac promoter. All pGEX vectors are also engineered with an internal LacIq gene, the product of which is a repressor protein that binds to the operator region of the tac

promoter preventing 'leaky' gene expression. This inhibition can be relieved by the lactose analogue, IPTG, which allosterically interacts with the repressor molecule, resulting in a 300 fold reduction in the repressor molecule's affinity for the operator sequence. Thereby the PGEX vectors allow high levels of expression in the presence of IPTG, while maintaining tight control over expression of the GST-fusion protein in the absence of IPTG.

2.5.2.2 Solutions

- **IPTG,** diluted to 1M in NFW and stored at 4˚C.

2.5.2.3 Method

BL21 cells were transformed and propagated in 1L cultures, as described in section 2.5.1, until the OD60 of the cultures reached 0.4. The induction of PAPSS2A-GST and SULT2A1-GST fusion protein expression was carried out as previously established. Briefly, IPTG was added to the bacterial cultures to a final concentration of 50mM or 1 μM for PAPSS2a and SULT2A1, respectively. Cultures were incubated for 16 hr at 26˚C to minimise the expression of proteins as inclusion bodies. The following day the cellular cytosolic fraction was isolated and the target fusion protein purified as described in section 2.5.4.

2.5.3 Preparation of cytosolic bacterial cell lysates

2.5.3.1 Principle

Expression of pGEX constructs in E.coli usually yields fusion proteins which accumulate in the cytoplasm of the host cell. Therefore, to assess the functional enzymatic activity of the fusion proteins, the cells have to be lysed and the cytoplasmic fraction, where the proteins reside, isolated. Bacterial cell lysis can be performed using commercially available lysis reagents or methods such as freeze-fracture, french pressing or sonication. The use of the total cell lysate for further assays is methodologically much quicker and easier than protein purification. However, it has the disadvantage that you cannot quantify specific protein expression and in some cases the enzymatic activity of the protein can be lost when fused to the GST tag.

2.5.3.2 Solutions

- **Lysis buffer- PBS/triton**. 2 tablets of PBS dissolved in 400 ml of dH_20 and autoclaved. 1 Complete Mini, EDTA-free, protease inhibitor tablet (Roche) was added per 10ml of PBS and Triton X 100 was added to 0.1%.

- **Lysis buffer- Commercially available**. 1 Complete Mini, EDTA-free, protease inhibitor tablet (Roche) was added per 10ml of Bugbuster (Merck, Nottingham, UK).

2.5.3.3 Method

Transformed BL21 cells were cultured and GST fusion protein expression was induced, as described in sections 2.5.1 and 2.5.2, respectively. A 1 L bacterial cell culture was centrifuged at 6,500 g for 15 min at 4ºC (Avanti J-20XP centrifuge, Beckman Coulter, High Wycombe, UK). The supernatant was discarded and the remaining cell pellet was lysed in PBS/1% Triton X 100 or 10 ml of Bugbuster (Merck, Nottingham, UK), containing protease inhibitors. Cell lysate was transferred to 15 ml falcon tubes and rapidly 'freeze-thawed' twice in a dry ice/methanol slurry and at 37ºC in a waterbath, and subsequently subjected to two cycles of sonication (2 x 10 Sec; Diagenode Bioruptor, Diagenode, Belgium) and cooling on ice. The cytosolic fraction of the cell lysate was isolated by centrifugation at 16,000 g for 15 min at 4ºC (Avanti J-20XP centrifuge, Beckman Coulter, High Wycombe, UK). The resulting cytoplasmic cell lysate was aliquoted and stored at -80ºC until use. Cell lysates subjected to subsequent fusion protein purification were handled as described in section 2.5.4. The cell membrane fraction was retained if to be analysed by subsequent western blot analysis, as described in section 2.5.8.

2.5.4 Purification of GST fusion proteins

2.5.4.1 Principle

The use of the glutathione affinity tag was first introduced in 1988 and is now widely used for the purification of recombinant proteins. In most organisms glutathione S-transferase (GST) occurs as a natural protein that can catalyse the conjugation of reduced glutathione via the sulfhydryl group to electrophillic centres on a wide variety

of substrates. In vivo, this activity is useful in the detoxification and metabolism of endogenous compounds and xenobiotics. In vitro, this property can be exploited to purify GST fusion proteins from bacterial lysates by affinity chromatography using glutathione immobilised to a matrix such as sepharose (**Figure 2-8**). When applied to the affinity medium, fusion proteins bind to the ligand, and impurities are removed by washing with binding buffer. The binding of fusion proteins to the ligand is reversible and can be eluted from the glutathione sepharose under mild, non-denaturing conditions that preserve both protein antigenicity and function. Expression of a pGEX-insert construct in E. coli yields fusion proteins with *Schistomsoma japonicum* GST, which has a Mr of 26,000.

2.5.4.2 Solutions

- **50% Glutathione Sepharose 4B slurry**. 1.33 ml of the original 75% Glutathione Sepharose 4B slurry (G.E.Healthcare) washed with 1 x PBS and resuspended in 1 ml 1 x PBS.

- **Wash buffer**, 50 mM Tris-HCl (pH 7.0), 150mM NaCl. Stored at 4˚C.

- **Elution buffer**, 50 mM Tris-Hcl, 10 mM reduced glutathione, (pH 8.0). Stored at 4˚C.

2.5.4.3 Method

Transformed BL21 cells were cultured and GST fusion protein expression was induced, as described in section 2.5.2. The bacterial cytosolic cell fraction was isolated utilising Bugbuster, a commercially available lysis buffer as described in

section 2.5.3. The cell membrane fraction was retained for subsequent western blot analysis and the cytosolic fraction was incubated with 1 ml of pre-washed Glutathione Sepharose 4B (GE Healthcare) 50% slurry, under constant agitation for between 1 and 14 hr. Following the incubation period the fusion protein was cleaved as described in section 2.5.5 or purified as follows. The gel with adsorbed protein was transferred to a disposable column and the flowthrough collected for subsequent SDS-PAGE and western blot analysis. The column was then washed with 5 ml of wash buffer and then 2 ml of PBS. The protein was then eluted in 3 ml of elution buffer. Samples were collected at all stages of the purification in 1 ml fractions to prevent the dilution of the protein and analysed by SDS-PAGE coomassie staining and western blot analysis.

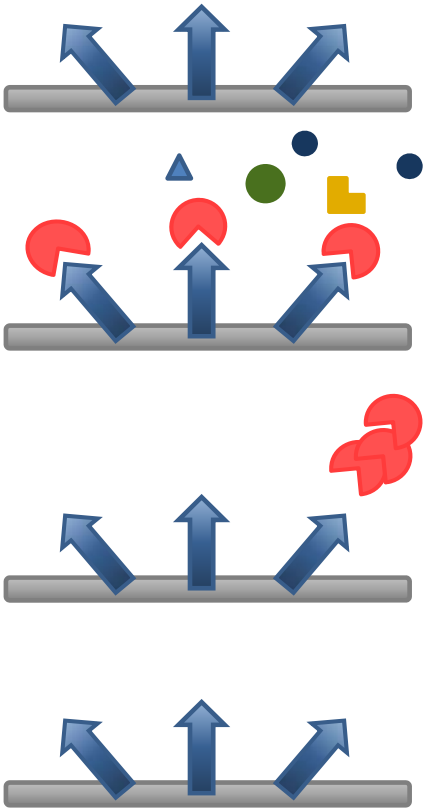

Figure 2-9 The mechanism of affinity chromatography. *The affinity medium is equilibrated in the column in binding buffer. The sample is applied to the column under conditions that favour the specific but reversible binding of the target molecule. Unbound sample is washed through the column. The concentrated target protein is eluted from the column with an elution buffer which contains a competitive ligand or different pH. Adapted from www.gelifesciences.com.*

2.5.5 Removal of GST fusion tag by enzymatic cleavage

2.5.5.1 Principle

If removal of the GST affinity tag is desired, the fusion protein can be digested with an appropriate site-specific protease while the fusion protein is bound to the glutathione sepharose or following elution from the medium. The specific protease compatible with the pGEX-6P-3 expression vector is PreScission Protease (GE Healthcare). PreScission Protease is a fusion protein of GST and human rhinovirus 3C protease. The protease specifically recognises the amino acid sequence Leu-Glu-Val-Leu-Phe-Gln‖Gly-Pro, cleaving between the Gln and Gly residues. Since the protease is fused to GST it can be removed from cleavage reactions using glutathione sepharose. The protease is maximally active at 4ºC so cleavage can be performed at low temperatures, improving the stability of the target protein.

2.5.5.2 Solutions

- **PreScission Protease buffer**, 50 mM Tris-HCl, 100 mM NaCl, 1mM EDTA, 1mM DTT, pH 8.0.

2.5.5.3 Method

In this thesis removal of the GST tag was performed while the fusion protein was bound to glutathione sepharose, as recommended in the manufacturers manual.

GST-fusion protein was bound to glutathione sepharose 4B as described in section 2.4.5. Following this incubation, the fusion-protein bound glutathione sepharose was loaded onto a column and washed with 5 ml of PreScission Protease buffer and subsequently incubated with 80 µl (160 units) of PreScission Protease in 920 µl of PreScission Protease buffer, at 4ºC for between 1 hr and 16 hr. Following incubation, the gluathione sepharose suspension was centrifuged at 10000 x g for 5 min at 4˚C (Eppendorf chilled table-top centrifuge, model 5415R, Cambridge, UK) to pellet the glutathione sepharose, and the elute, containing the protein of interest, transferred to a new tube. The elute, alongside samples taken at various stages of the procedure were analysed by SDS-PAGE analysis to verify the presence of the protein (in the elute) and to estimate the yield, purity and the extent of the digestion.

2.5.6 Protein extraction from cell culture

2.5.6.1 Principle

The extraction of proteins from monolayer cells can be achieved by lysing the cells in a buffer which preserves protein integrity. The cellular lysate is subject to freeze thaw cycles to further aid lysis. The membrane and the soluble fractions can be subsequently isolated by centrifugation.

2.5.6.2 Solutions

- **RIPA buffer**, 50 mM Tris pH 7.4, 1% NP40, 0.25% SDS, 150 nM NaCl, 1 mM EDTA. Store at -20ºC. Add 1 tablet of complete protease inhibitor cocktail (Roche) per 10 ml of RIPA buffer on before use.

2.5.6.3 Method

All steps of this procedure were performed on ice. Monolayer cells were washed with PBS before the addition of 30 µl of RIPA buffer per well of a 24 well plate. Cells were scraped and the cell lysate transferred into an eppendorf. Cell lysates were incubated at -80ºC for 10 min and then thawed on ice. The cytosolic fraction was obtained by centrifugation at 8000g for 5 min, and the supernatant containing the soluble proteins, transferred to a fresh eppendorf. The protein concentration was determined as described below (2.5.7), aliquoted, and stored at -80ºC until use.

2.5.7 Quantification of protein concentration

2.5.7.1 Principle

The total soluble protein concentration of a sample can be measured using a colourimetric assay. In this thesis the Bio-Rad DC protein assay (Bio-Rad Laboratories, GmbH, Germany); a modified version of the well documented Lowry assay (Lowry et al., 1951) was used to measure the total soluble protein concentration of cell extracts. The Lowry assay employs two colour forming reactions. The first being a Biuret reaction, in which, under alkaline conditions divalent copper ions react with the peptide bonds of proteins to produce monovalent copper ions (Cu+), resulting in the formation of a purple colour. The second exploits Folin-Ciocalteu chemistry, in which monovalent copper ions and the radical groups of tyrosine, tryptophan and cysteine react with phosphomolybdotungstate to produce an unstable product that becomes reduced to molybdenum/tungsten blue with absorption maximum of around 660 nM. Thus the concentration of protein in a

sample is directly proportional to the colour produced via these two reactions and can be quantified by measuring the absorbance at 650-750 nM. The Lowry assay is superior to other protein assays as it has a low sensitivity limit (10 µg/ ml). Furthermore, the Biorad assay contains SDS which separates membrane proteins from contaminating membrane constituents and denatures the proteins allowing more reproducible results.

2.5.7.2 Method

Mammalian monolayer cellular protein or bacterial cellular protein was obtained as described in sections 2.5.3 and 2.5.4, respectively. 5 µl of sample was added, in duplicate, to a 96 well plate. A range of protein concentrations of BSA standard were made (0 mg/ ml, 0.25 mg/ ml, 0.5 mg/ ml, 1.0 mg/ ml and 2.0 mg/ ml) and were added in duplicate to a 96 well plate adjacent to the protein samples to be quantified. Using an automated pipette, 25 µl of reagent A and 200 µl of reagent B were added to each well. The plate was then placed on a shaker for 10 min to allow a uniform reaction to take place and resulting colour formation to occur. Absorbance at OD_{690} nm was measured using a Victor3 1420 multilabel counter (PerkinElmer, Beconsfield, Buckinghamshire). A standard curve was plotted as µg of protein (x axis) against OD_{690} (Y axis). The protein concentrations of samples were then determined using the standard curve coefficients. To ensure that the protein concentrations were within the standard curve range a predetermined dilution of protein extract was used.

2.5.8 Western blot analysis

2.5.8.1 Principle

Western blotting is a technique by which the relative amounts of a specific protein can be measured, from a heterogeneous protein extract. In this thesis, proteins have been separated utilising SDS-PAGE, which denatures the proteins so that they are separated dependant on their size. The separated proteins are then transferred to a membrane, usually nitrocellulose or polyvinylidene diflorise (PVDF). The membrane is then blocked by incubation with a dilute solution of protein, typically non-fat dry milk or bovine serum albumin, to prevent non-specific binding of antibody to the membrane. To detect the protein of interest the membrane is first incubated with a primary antibody which specifically binds to the protein. The membrane is then washed to remove the excess primary antibody and subsequently incubated with a secondary antibody, which specifically binds the primary antibody. The secondary antibody is conjugated to an enzyme, usually horseradish peroxidase, which in the presence of a chemiluminescent agent results in the generation of light, proportional to the amount of protein on the membrane. This reaction can be recorded by various methods, such as the use of photographic film or camera, and the signal strength semi-quantified by imaging software. If this technique is being used to analyse the relative expression of a protein between samples, the same membrane can be re-probed with an antibody against a housekeeping gene, to ensure the quantity of protein loaded has been kept constant.

2.5.8.2 Solutions

- Loading buffer (4X). 50 mM Tris-HCl pH 6.8, 2% SDS, 10% glycerol, 1% 14.7 M β-mercaptoethanol, 12.5 mM EDTA, 0.02% bromophenol blue.

- Running buffer, 20 X NuPAGE MOPS SDS running buffer (Invitrogen). Dilute 1:20 with dH_20.

- Transfer buffer 10X. 30.3 g Tris base, 144g glycine diluted in I L of distilled H_20, adjusted using HCL to pH 8.3.

- Transfer buffer (working solution), for 1 L, 100 ml 10X, 200 ml absolute methanol, 700 ml H_20

- Washing solution, 0.1% tween in PBS.

- Blocking solution, 5% non-fat resuspended dried milk (Marvel), in washing solution.

- Stripping solution, 100 mM 2-βmercaptoethanol, 2% SDS, 62.5 mM Tris-HCL Ph 6.7.

2.5.8.3 Method

SDS-PAGE and protein transfer were carried out using Xcell *Sure Lock*™ Mini-Cell (Invitrogen), according to the manufacturer's instructions. A pre-determined quantity of protein sample was added to the appropriate amount of 4 x protein loading buffer and boiled at 95ºC for 7 min. Samples were loaded onto a pre-cast 1.0mm thick 10%

NuPAGE® Bis-Tris SDS-PAGE gel (Invitrogen), and run at 200V for 50 min, immersed in running buffer. Proteins were subsequently transferred onto a Hybond ECL nitrocellulose membrane (G.E Healthcare) at 30V for 1 hour, immersed in transfer buffer. To confirm successful and efficient running and transfer, protein was visualised by incubation of the membranes with a reversible protein stain, ponceau S red at room temperature for 1 min. Excess ponceau was decanted and the membrane washed with H_20 to visualise bands of protein. The membrane was blocked for 1 hr on a horizontal shaker, prior to repeated washing with PBS 0.1% tween and incubation of the membrane with the primary antibody at an optimised dilution, overnight at 4ºC under constant agitation. The membrane was repeatedly washed with PBS 0.1% tween and then incubated with the appropriate secondary antibody for 1 hour at room temperature, under constant agitation. The membrane was washed as above and incubated with 1 ml of ECL chemiluminescent detection reagents (G.E. Healthcare) for 1 min, according to the manufacturer's instructions. The resultant luminescent signal was recorded by exposure of the membrane to light sensitive kodak MXB photographic film (G.R.I, Rayne, UK) for between 2 sec and 1 hour. Photographic film was developed using a compact X4 developer (Xenograph Imaging Systems, Gloucestershire, UK). If the relative quantification of samples was to be performed the membranes were stripped by incubating the sample in stripping buffer at 50˚C for 30 min. The membrane was then washed once and re-probed with an antibody against β-actin, as described above.

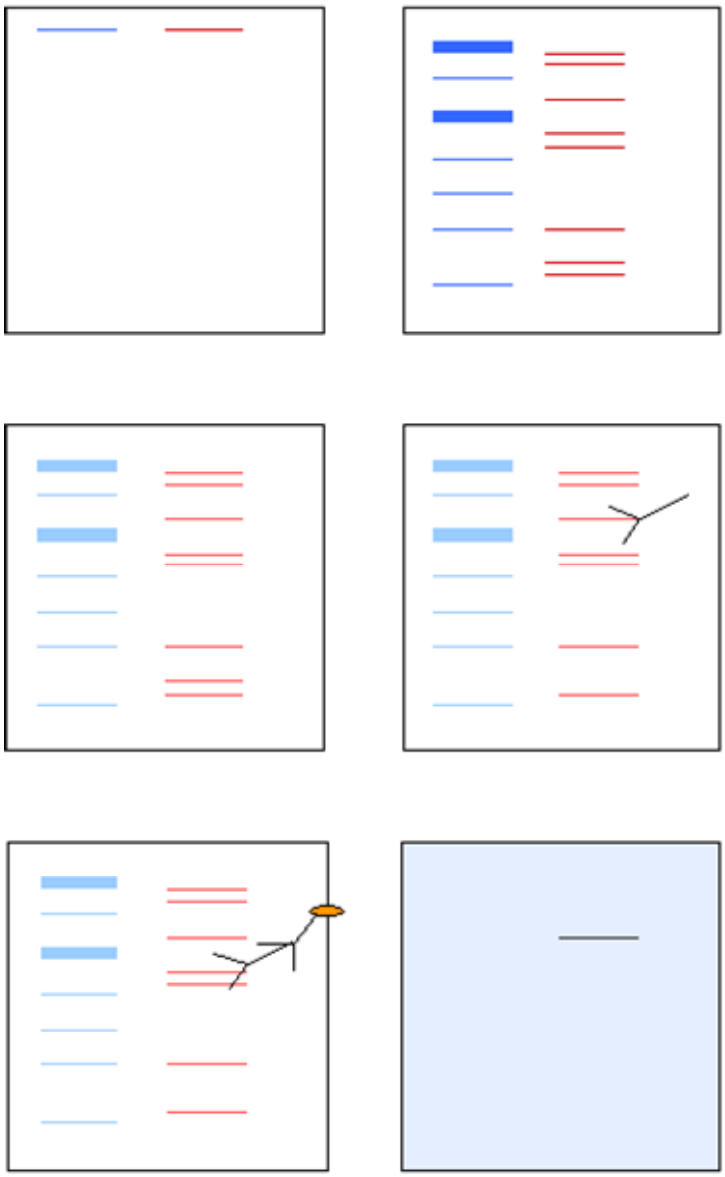

Figure 2-10. Schematic of the principle of western blot analysis. 1*. The protein sample (red) is loaded onto the gel, parallel to a protein ladder (blue).* ***2.*** *The mixed protein sample and ladder are separated by electrophoresis.* ***3.*** *The proteins are transferred onto nitrocellulose membrane.****4.*** *The membrane is first incubated with a primary antibody which recognises and binds the protein of interest, and subsequently (****5****) with a fluorescently tagged secondary antibody, which binds to the primary antibody.* ***6.*** *The antibody is detected by exposure to x-ray film.*

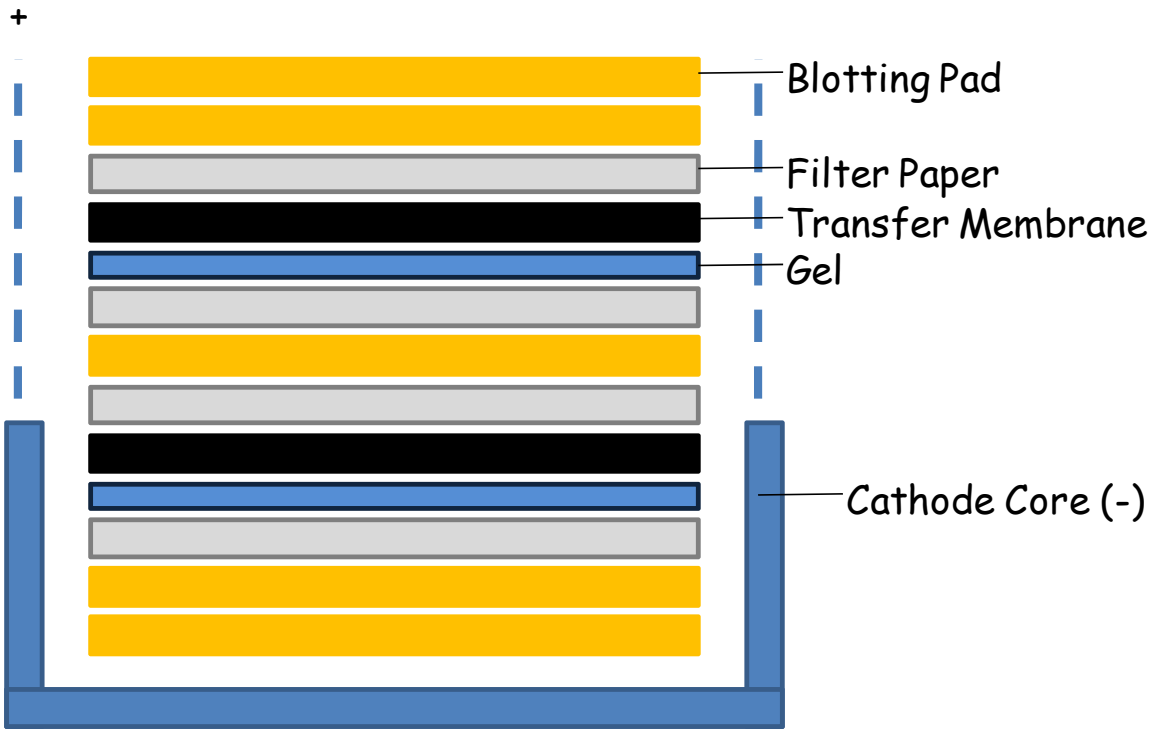

Figure 2-11 Schematic diagram of transfer procedure. *The diagram shows how the transfer procedure is set up for a double transfer using the X Cell II Blot Module (Invitrogen). While submerged in transfer buffer the SDS-gel the transfer membrane is lay on top of the gel, sandwiched between blotting paper and filter paper. The gel is placed in the module closest to the anode(+), with the transfer membrane nearer the cathode (-), resulting in the transfer of proteins from the gel to the membrane.*

2.5.9 Coomassie staining

2.5.9.1 Solutions

- Coomassie blue. 0.2% coomassie blue, 7.5% acetic acid, 50% ethanol, made up with H_20.

- Destain. 40% glacial acetic acid, 10% methanol, 50% H_20. Solution can be recycled by passing through activated carbon. Store at room temperature.

2.5.9.2 Method

Proteins were separated by SDS-PAGE as described in section 2.5.8. Following electrophoresis the gel was submerged in coomassie blue, under constant agitation, overnight. The following day the gel was repeatedly incubated in de-satin solution until distinct bands were visible.

2.6 Enzymatic activity assays

2.6.1 Principle

The functional activity of an enzyme in intact cells, or purified protein, can be quantified by incubation of the sample with the substrate and necessary co-factors of that enzyme, and measuring the amount of product produced. Steroids can be extracted from a reaction mixture using an organic solvent and separated from one another by thin layer chromatography (TLC) using an optimised mobile phase. If a known concentration of radiolabelled substrate is used, the amount of product produced can be quantified by measuring the radiation of the separated steroid. Below is a sample trace obtained by the analysis of a TLC plate with a Bioscan imaging detector (Bioscan, Washington, DC, USA). The protein content of the sample can be calculated and the fractional conversion of the cells calculated as pmols of product per mg of protein per hour.

This principle can also be applied to cases where the primary functional enzyme(s) in a cell are not known. The unknown product(s) of the reaction can be identified by TLC by co-migration with unlabeled steroid standards. The location of the steroids on

the TLC plate can be identified by visualisation under UV light, or using Lieberman-Buchard reagent, as described in section 2.6.6. This technique therefore enables the identification of functional enzymes within the target cells.

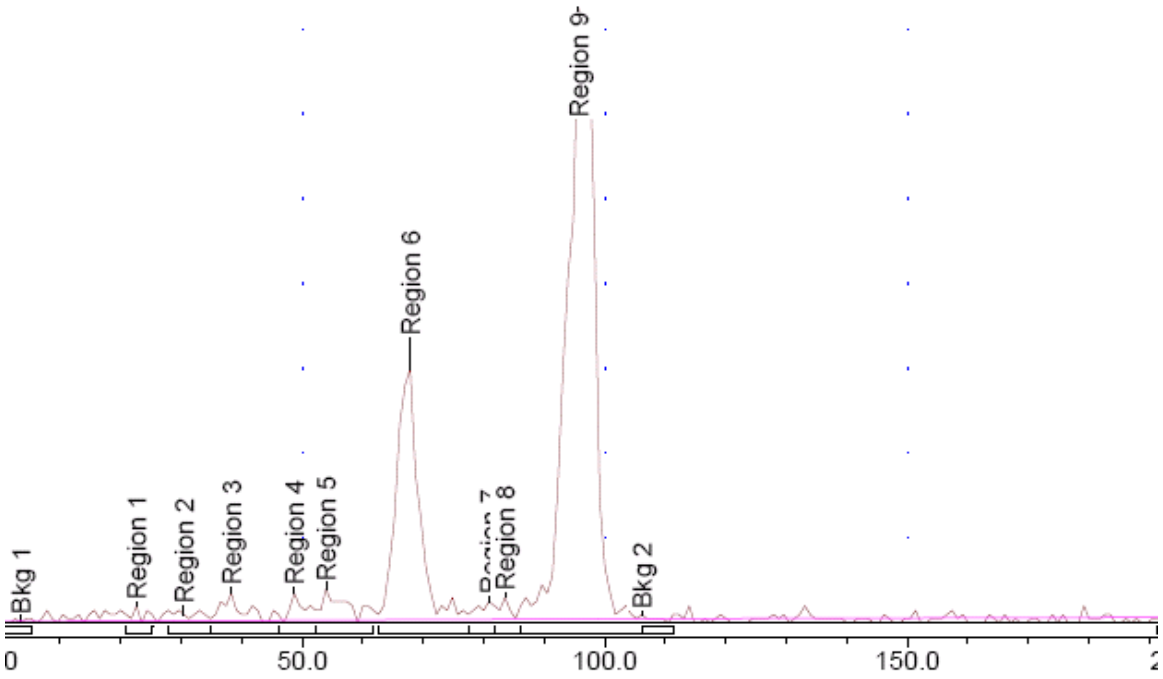

Figure 2-12 Representative TLC trace. *Extracted radiolabelled unknown steroids were spotted on TLC plate adjacent to known steroids, and developed using a solvent system consisting of chloroform/methanol/acetone/acetic acid/water (8:2:4:2:1). Steroids were quantified using a Bioscan 2000 image analyzer (Lablogic, Sheffield, UK). Due to the differing retention distance of steroids, each steroid produces a distinct peak.*

2.6.2 11β-HSD1 activity assay

2.6.2.1 Solutions

- **10-2 M cortisone/cortisol stock**, dilute 3.6mg of cortisol/cortisone in 1 ml of absolute ethanol, stored at 4˚C for up to 2 months. Steroids were diluted to a desired concentration in medium on the day of the experiment.

- **^{3}H-Cortisol stock**, Specific activity 100Ci/mmol (Du Pont, NEN, The Netherlands). Store at -20 ˚C for up to 2 months.

- **^{3}H-Cortisol working solution**, 5µl of 1mCi/ml stock of ^{3}H-cortisol into 200µl ethanol, store at -20 C for up to 2 months.

- **^{3}H-Cortisone working solution**, synthesised as described in section 2.24 to a concentration of 1000 cpm/ µl. Store at -20 ˚C for up to 2 months.

2.6.2.2 Method

Confluent monolayers of Chub-S7 mature adipocytes were washed with PBS, and 11β-HSD1 dehydrogenase activity was assessed by incubating cells in 1 ml of serum free DMEM/F12 supplemented with 100 nM F (for dehydrogenase activity) or E (for oxo-reductase activity) with appropriate tritiated tracer – ^{3}H F (Du Pont, Stevenage, UK) or ^{3}H E (0.02 µCi/reaction) for 3 hours at 37˚C in 5% CO_2. Following incubation culture medium was transferred to 10 ml borosilicate glass tubes and steroids were extracted with 8 ml of dichloromethane, by shaking horizontally for 15 min and

centrifugation for 15 min at room temperature at 100g, to separate the aqueous and organic phases. The aqueous phase and protein containing interphase were aspirated, leaving the inorganic phase, containing the steroids. Steroids were subsequently concentrated by evaporating the dichloromethane at 55˚C for 45 min under a constant stream of air. Steroids were then resuspended in 80 µl of dichloromethane and spotted on silica TLC plates (Silica gel/TLC plates; Fluka) along with one drop of unlabelled standard steroid solution (1 x 10^{-2} M of cortisol or cortisone in ethanol). The steroids were separated by TLC using chloroform: ethanol (92:8) as the mobile phase in a total volume of 200 ml, for 1 hour, and the retention factor of the unlabelled steroid standards determined by visualisation using UV light. The location and amount of radiation on the TLC plate was assessed using a Bioscan imaging detector (Bioscan, Washington, DC, USA), and the fractional conversion of steroids calculated. Percentage conversion was calculated using the regional counts of the individual peaks. The protein content of individual wells was quantified as described in section 2.5.7 and activity was calculated as pmol per mg of protein per hr.

2.6.3 DHEA metabolism assay

2.6.3.1 Solutions

- 10-2 M steroid stock (DHEA metabolites) stored at 4 ˚C.
- ^{3}H-DHEA stock, Specific activity 100Ci/mmol (Du Pont, NEN, The Netherlands). Store at -20 ˚C for up to 6 months.

- ^{3}H-DHEA working solution, 5µl of 1mCi/ml stock of ^{3}H-cortisol into 200µl ethanol, store at -20˚C for up to 6 months.

2.6.3.2 Method

Confluent monolayers of Chub-S7 preadipocytes or mature adipocytes were washed with PBS, and incubated with serum free DMEM supplemented with cold DHEA (20nM) and radiolabelled DHEA (0.2µCi per well) at 37˚C, 5% CO_2 for 24 hrs. Following incubation, culture medium was transferred to 10 ml borosilicate glass tubes and steroids were extracted with 8 ml of dichloromethane, by shaking horizontally for 15 min and centrifugation for 15 min at room temperature at 100g, to separate the aqueous and organic phases. The aqueous phase and protein containing interphase were aspirated, leaving the inorganic phase, containing the steroids. Steroids were subsequently concentrated by evaporating the dichloromethane at 55˚C for 45 min under a constant stream of air. Steroids were then resuspended in 80 µl of dichloromethane and spotted on silica TLC plates (Silica gel/TLC plates; Fluka), adjacent to a mixture of unlabelled steroid standards, with known retention factors. (1 x 10-^{2} M in ethanol). The steroids were separated by TLC using using n-hexane/1-hexanol (75:25) as the mobile phase in a total volume of 200 ml. The location and amount of radiation of individual peaks on the TLC plate was assessed using a Bioscan imaging detector (Bioscan, Washington, DC, USA). The retention factor of the unlabelled steroid standards was visualised by exposure to UV light or Lieberman-Buchard reagent, enabling the identification of the products, and the fractional conversion of steroids to be calculated.

2.6.4 PAPSS activity assay

2.6.4.1 Method

Purified bacterially expressed SULT2A1-GST and PAPSS2a-GST fusion proteins were prepared as described in section 2.5.4 or the cytosolic fractions of WT SULT2A1 and WT and mutant (T48R, R329X and S475X) PAPSS2 expressing BL21 E.Coli cells were prepared as described in section 2.5.3. The total protein content of the samples was quantified using a BioRad Bradford protein assay, as described in section 2.5.7 and samples were subsequently diluted with PBS to achieve the same protein concentration. Consistent expression of PAPSS2A between the samples was ensured by western blot analysis, section 2.5.8.

For functional activity assays a master mix was prepared on ice containing assay buffer (150 nM Tris-HCl (pH 7.0), 50 mM KCl, 15 mM $MgCl_2$, 3 mM EDTA, 45 mM dithiothreitol), supplemented with ATP (final concentration 5mM) and sodium sulphate (final concentration 10mM). 145 µl of master mix was aliquoted into glass tubes. To each tube ^{3}H DHEA was added to a final concentration of 5 µM and reactions were initiated by the addition of 25 µl of WT SULT2A1-GST and WT or mutant PAPSS2a-GST (T48R, R329X and S475X) for 1 hour at 30˚C. Steroids were extracted with 8 ml of dichloromethane, by shaking horizontally for 15 min, vortexing for 20 seconds and centrifugation for 15 min at room temperature at 100g, to separate the aqueous and organic phases. The aqueous phase and protein containing interphase were aspirated, leaving the inorganic phase, containing the steroids. Steroids were subsequently concentrated by evaporating the dichloromethane at 55˚C for 45 min under a constant stream of air. Steroids were

then resuspended in 80 µl of dichloromethane and spotted on PE SIL G/UV silica gel plates (Whatman, Maidstone, Kent, UK). Steroids were separated by TLC using a solvent system consisting of chloroform/methanol/acetone/acetic acid/water (8:2:4:2:1). Steroids were quantified using a Bioscan 2000 image analyzer (Lablogic, Sheffield, UK).

2.6.5 Synthesis of ^{3}H cortisone

In contrast to tritiated cortisol (^{3}H-F), tritiated cortisone (^{3}H-F) is not available commercially. Therefore a protocol has been optimised for the in-house synthesis of ^{3}H-E ([1,2,6,7-^{3}H]-E) from ^{3}H-F (1,2,6,7-^{3}H]-F), utilising the high 11β-HSD2 dehydrogenase activity of human placenta.

2.6.5.1 Solutions

- **0.1M Phosphate buffer (pH 7.4)**. Mix 57 ml of 0.2 M sodium phosphate monobasic and 243 ml of 0.2 M sodium phosphate dibasic heptahydrate. Make up to 600ml with dH_20.

2.6.5.2 Method

20 µl of ^{3}H-F was incubated with 250 µg of protein from homogenised human term placenta in a 500 µl total volume of 0.1 M phosphate buffer (pH 7.4), with 500 µM NAD+ as a cofactor, for 3 hr at 37ºC. Tritiated steroids were then extracted in 7 ml of dichloromethane by shaking tubes for 15 min followed by centrifugation for 15 min at 1000g to separate the aqueous and organic phases. The upper aqueous phase was

aspirated and the remaining organic phase was evaporated at 55ºC under air using a sample concentrator. Tritiated steroids were then resuspended in 80µL dichloromethane and spotted on a silica TLC plate (Silica gel/TLC plates; Fluka) adjacent to E and F standards. Steroids were separated by TLC with chloroform: ethanol (92:8) as the mobile phase until the solvent front had reached the top of the plate (~1 hour). The plate was placed under a UV lamp to visualise the location of the standard steroids and then scanned using the Bioscan 200 imaging scanner (Lablogic, Sheffield UK) to detect the retention factor of the extracted steroid, which was compared against the steroid standard to confirm the conversion to ^{3}H-E. Once the location of ^{3}H-E had been established the silica in that location was scrapped into a glass tube and ^{3}H-E was eluted from the silica for 12 hr at 4ºC in 300 µl of ethanol. Following the incubation the silica and eluted ^{3}H-E were separated by centrifugation at 100g for 5 min and the ^{3}H-E solution transferred to a fresh glass tube. To determine the concentration of synthesised ^{3}H-E, 5 µl of the solution was spotted onto a TLC plate and separated and analysed as described above (section 2.6.2). The solution was subsequently diluted in ethanol to 1000 cpm/ µl and stored at -20ºC until use.

2.6.6 Visualisation of steroids utilising Liberman Buchard reagent

2.6.6.1 Principle

The use of Lieberman-Burchard reagent enables the identification of steroids which cannot be visualised by other methods, such as under UV light. When concentrated sulfuric acid is added to a steroid derivative of cholesterol, the steroid is oxidised,

resulting in a polymer product containing a chromophore, which produces a colouration. For example, the addition of sulphuric acid to cholesterol results in the removal of a water molecule from C3 of cholesterol molecule, and it is oxidised to form, 3,5-cholestadiene, containing a chromophore, which produces a green colour. The resultant chromophore, and thus the colour produced, differs between steroids, and can therefore facilitate the identification of unknown steroid products. An example of steroids separated by TLC and visualised utilising Lieberman-Burchard reagent is shown in **Figure 1-12**.

2.6.6.2 Solutions

- Lieberman-Burchard reagent (for 100ml; 2ml acetic Acid, 8ml sulfuric acid, 24ml ethanol)

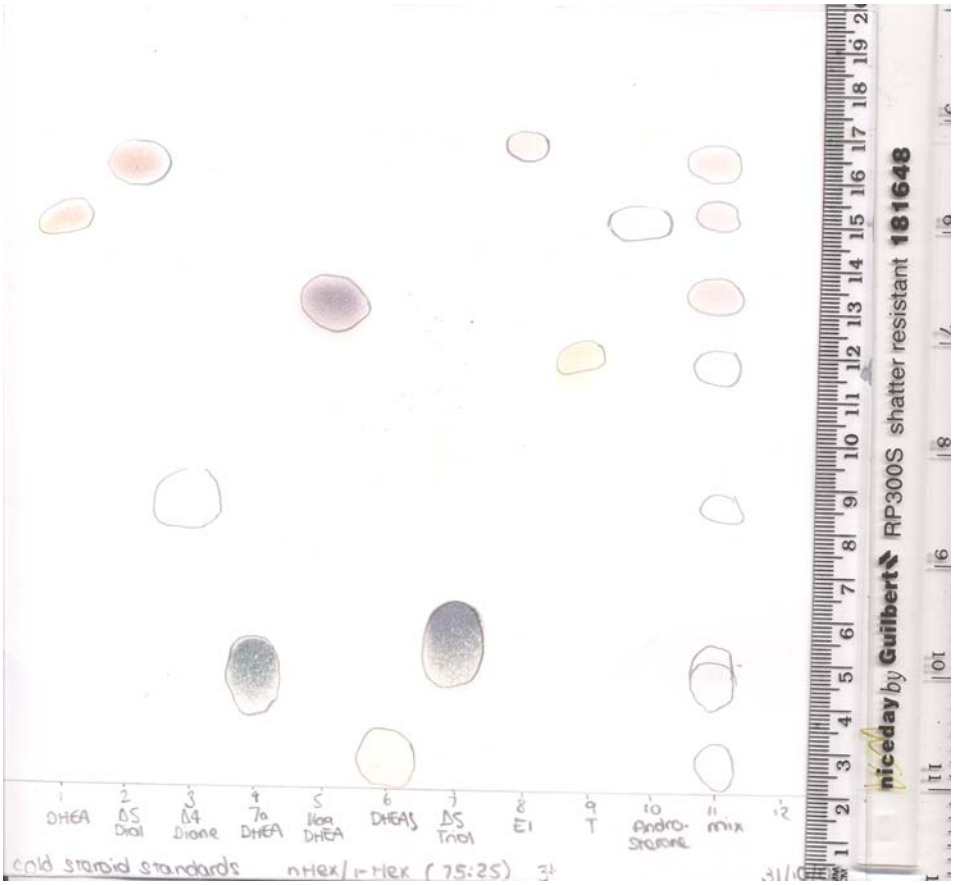

Figure 2-13 A representative photograph of a steroids separated by TLC and visualised by Lieberman-Burchard reagent. *Known reference steroid samples were spotted on to a TLC plate and separated by TLC using n-hexane/ 1-hexanol as the solute for 3 hours. The TLC plate was sprayed with Lieberman-Burchard reagent and heated at 100˚C, which oxidises the steroids resulting in a colour to be produced. The distance migrated of a known steroid in a given solute phase can be used to identify unknown steroids. The chromophore of a steroid, and thus the colour produced differ between steroids, which also aids identification.*

2.6.6.3 Method

A TLC plate (Silica gel/TLC plates; Fluka) was spotted with known reference steroid metabolites of DHEA which were then separated by TLC as described in section 2.6.3. Plates were sprayed with a thin layer of Liberman-Burchard reagent and

heated to 100ºC, until the resultant coloured regions could be visualised. The location and colour of the known reference spots were used to identify unknown steroid when this procedure was repeated on subsequent TLC plates.

3 Chapter 3: DHEA metabolism and action in human adipocytes

3.1 Introduction

As described in section 1.2.3, the development of adipose tissue is potently regulated by hormonal factors that include glucocorticoids and sex steroids. Glucocorticoids are well characterised key regulators of adipose tissue hyperplasia, hypertrophy and insulin sensitivity, playing a permissive role in adipose tissue differentiation. Consequently, glucocorticoid excess is characteristically associated with central obesity and insulin resistance, as exemplified in Cushing's syndrome (section 1.1.4.6.2.1). The local reactivation of glucocorticoids represents an important mechanism mediating glucocorticoid action. As described in section 1.1.4.5, the enzyme 11β-hydroxysteroid dehydrogenase type 1 (11β-HSD1) efficiently converts inactive cortisone to active cortisol via its oxoreductase activity in a variety of tissues, importantly including liver and adipose, major sites involved in the regulation of insulin sensitivity. The clinical significance of local glucocorticoid activation in the context of the metabolic syndrome has been conclusively demonstrated during recent years by a multitude of *in vitro*, *in vivo* and clinical studies (Tomlinson et al., 2004). In addition, the selective inhibition of 11β-HSD1 activity emerges as an exciting, novel therapeutic approach in type 2 diabetes and the metabolic syndrome (Stewart and Tomlinson, 2009).

As described in section 1.2.3.2 the effects of active sex steroids on adipocyte development are also relatively well established. In addition, evidence is emerging that the sex steroid precursor, DHEA, may also regulate adipose tissue development. Several *in vitro* studies have demonstrated that in contrast to glucocorticoids, DHEA

has inhibitory effects on preadipocyte proliferation (Gordon et al., 1987; Lea-Currie et al., 1998) and differentiation (Gordon et al., 1986; Lea-Currie et al., 1999; Lea-Currie et al., 1998; Lea-Currie et al., 1997b) while enhancing glucose uptake (Ishizawa et al., 2001; Ishizuka et al., 1999; Ishizuka et al., 2007; Kajita et al., 2000; Perrini et al., 2004). Furthermore murine *in vivo* studies have revealed that DHEA treatment attenuates weight gain and ameliorates hyperglycaemia and hyperinsulinemia in murine models of obesity and diabetes (Cleary and Zisk, 1986; Coleman, 1988; Coleman et al., 1982). Interestingly, recent studies have demonstrated that DHEA may modulate 11β-HSD1 (Apostolova et al., 2005; Gu et al., 2003), suggesting an anti-glucocorticoid mechanism by which DHEA may act. Apostolova *et al* have demonstrated that DHEA inhibits 11β-HSD1 expression and oxoreductase activity in 3T3-L1 cells and murine adipocytes (Apostolova et al., 2005). While, a recent cDNA analysis has revealed that 11β-HSD1 is one of the genes whose expression is inhibited by DHEA in the liver of treated animals (Gu et al., 2003). However, the above studies employed almost exclusively rodents or the murine preadipocyte cell line 3T3-L1. As rodent adrenals lack the ability to synthesize DHEA and consequently have circulating DHEA levels several orders of magnitude lower than that of humans, the relevance of these findings to human physiology is questionable.

Therefore, we have examined the effects of DHEA on adipocyte proliferation, differentiation and glucose uptake, employing a human cell model, the subcutaneous preadipocyte cell line Chub-S7, with the aim of investigating the underlying mechanisms.

3.2 Results

3.2.1 The metabolism of DHEA human adipose cells

3.2.1.1 The mRNA expression of steroidogenic enzymes in human preadipocytes and adipocytes

The key pathways of DHEA metabolism include its sulfation to inactive DHEAS catalysed by SULT2A1 and the conversion of DHEA towards the active androgen precursors, androstenediol and androstenedione, by 17β-HSDs and 3β-HSD, respectively (Figure 1-15). Therefore, I first examined the potential intracellular conversion of DHEA by analyzing the mRNA expression of key DHEA metabolizing enzymes in our cellular model, the human preadipocyte cell line Chub-S7, and human subcutaneous and omental primary adipocytes. Total RNA was extracted from Chub-S7 cells and human subcutaneous and omental primary preadipocytes and adipocytes as described in section 2.4.1. Reverse transcription and conventional PCR were performed as described in section 2.4.2 and 2.4.3.2 respectively utilising gene specific primers (**Table 2-3**, primer pairs 31-32 and 35-39). Following amplification, PCR reactions were assayed by agarose gel electrophoresis as described in section 2.4.3.2.

PCR amplification of SULT2A1 failed to produce any detectable product in all of the samples analysed, indicating that human subcutaneous preadipocytes and adipocytes and our cellular model do not express SULT2A1. This confirms that DHEA cannot be inactivated by sulfation to DHEAS within preadipocytes or adipocytes (**Figure 3-1**). In contrast, the successful amplification of STS was

confirmed by the identification of a band of the expected size in all of the samples, indicating there is abundant expression of STS, responsible for the conversion of DHEAS to DHEA, in both preadipocytes and mature adipocytes (**Figure 3-1**).

DHEAS is hydrophilic and therefore requires active trans-membrane influx transport, which is facilitated by members of the organic anion transporter polypeptide (OATP) family. I studied mRNA expression of all OATP isoforms previously implicated in DHEAS trans-membrane transport, including OATP–A, -B, -C, -D, -E and -8. Amplification of OATP-D resulted in a band of the correct size for all of the samples (**Figure 3-1**), whereas products were not detected for any other reaction (data not shown), confirming the selective expression of OATP-D in preadipocytes and adipocytes.

DHEA can be converted downstream to active androgens via two mechanisms: the conversion to androstenedione via 3β-HSD activity or conversion to androstenediol via oxidative 17β-HSD activity (**Figure 1-15**). Amplification of the genes encoding the two human 3β-HSD isoforms, *HSD3B1* and *HSD3B2*, resulted in no detectable products, indicating that human preadipocytes and adipocytes do not express 3β-HSD1 and 3β-HSD2. In contrast, the amplification of *AKR1C3* produced a band of the correct size, indicating the expression of 17β-HSD type 5 in all the samples examined (**Figure 3-1**). To further investigate *AKR1C3* expression I performed quantitative mRNA expression analysis as described in section 2.4.3.3 using gene specific primers and probe (**Table 2-4**, primer pair number 56). Data obtained from three independent triplicate experiments are presented as arbitrary units (AU), calculated using the equation AU = $2^{-\Delta Ct}$ x 1000. The mRNA expression of *AKR1C3* in preadipocytes was relatively low and greatly increased following adipocyte

differentiation (**Figure 3-2**). This was observed in all three cell lines examined, i.e. primary human sc and om preadipocytes and Chub-S7 preadipocytes, further confirming Chub-s7 as a suitable model to study human adipogenesis.

3.2.1.2 DHEA metabolism in human preadipocytes and adipocytes

I subsequently assessed the functional significance of the observed steroidogenic gene expression in the Chub-S7 human cell line. Enzymatic activity assays were performed as described in section 2.6.3, investigating the conversion of DHEA, during a 24 hour incubation period in both preadipocytes and mature adipocytes. Metabolites were identified by co-migration with unlabelled reference steroids which were visualised by exposure to Lieberman-Burchard reagent as described in section 2.6.6. Activity was normalised to cellular protein content, assessed as described in section 2.5.7, and calculated per hour of incubation. Data obtained from four independent triplicate experiments are expressed as mean pmol/mg protein/ hour conversion.

While there was no appreciable conversion of DHEA in preadipocytes, significant conversion of DHEA to androstenediol was detected in fully differentiated adipocytes ($p<0.001$; **Figure 3-3**), in consistence with our mRNA expression data (**Figure 3-2**). Interestingly, despite the detection of mRNA transcripts encoding STS in both preadipocytes and mature adipocytes, a lack of functional activity of STS was noted, evidenced by no detectable conversion of DHEA to DHEAS.

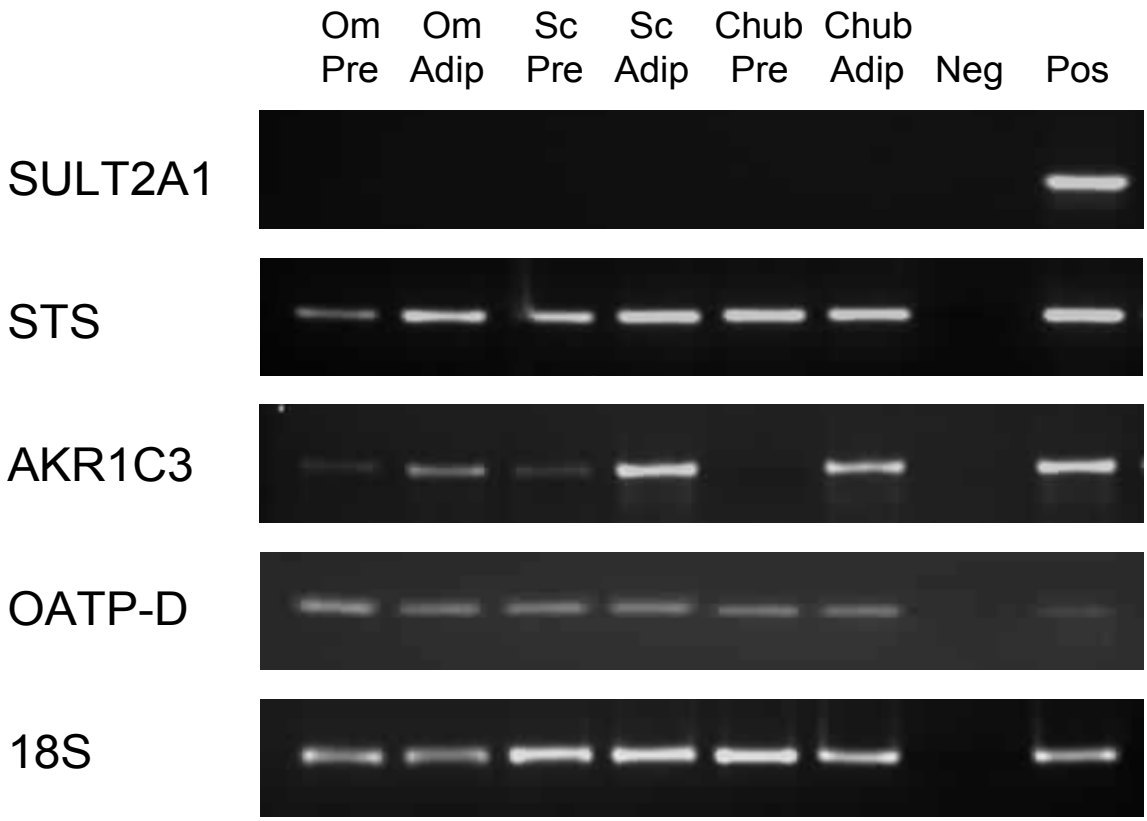

Figure 3-1 The mRNA expression analysis of steroidogenic genes in human adipocytes*. The expression of key steroidogenic enzymes and transporters was assessed by conventional PCR in human omental preadipocytes (Om Pre) and adipocytes (Om Adip); human subcutaneous preadipocytes (Sc Pre) and adipocytes (Sc Adip); and Chub-S7 preadipocytes (Chub Pre) and adipocytes (Chub Adip). No expression of SULT2A1 was observed in any cells. In contrast transcripts for STS, OATP-D and 17β-HSD5 encoded for by AKR1C3 were detected in all cells examined. Positive control (Pos) reactions, utilising cDNA in which the gene of interest is expressed, confirmed amplification. Negative control (Neg) reactions, in which cDNA was excluded, confirmed the bands visualized were not artefacts.*

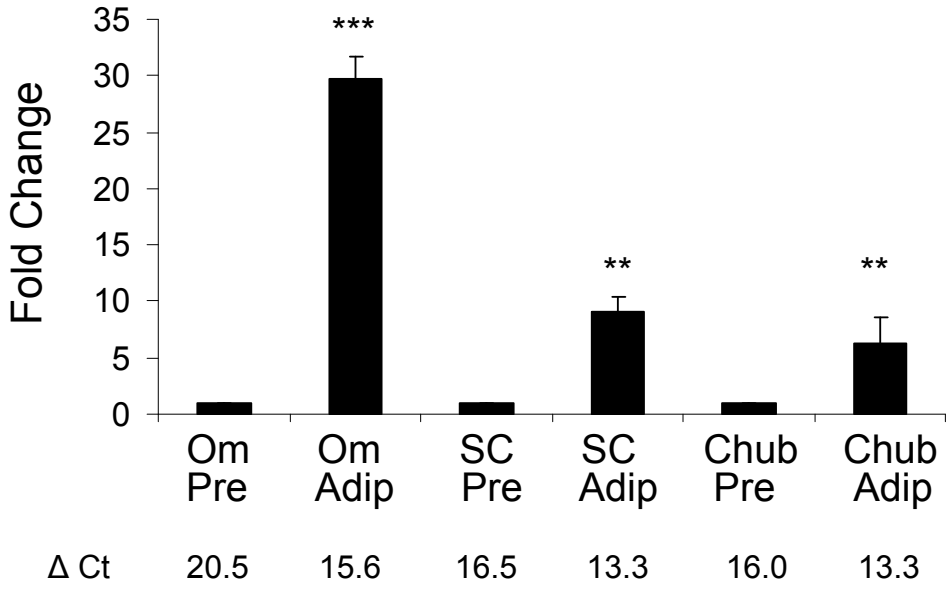

Figure 3-2 The mRNA expression of AKR1C3 in human preadipocytes and adipocytes. *The mRNA expression of AKR1C3 in human omental preadipocytes (Om Pre) and adipocytes (Om Adip); human subcutaneous preadipocytes (Sc Pre) and adipocytes (Sc Adip); and Chub-s7 preadipocytes (Chub Pre) and adipocytes (Chub Adip) was examined by real-time PCR. The expression of AKR1C3 in chub-S7 and human adipose tissue was increased in differentiated adipocytes relative to preadipocytes. Data obtained from three independent triplicate experiments are presented as arbitrary units, with ΔCt given in the table. Statistical significance of expression by adipocytes vs. preadipocytes was assessed utilising Student's t-test. **, P< 0.01; ***, P< 0.005*

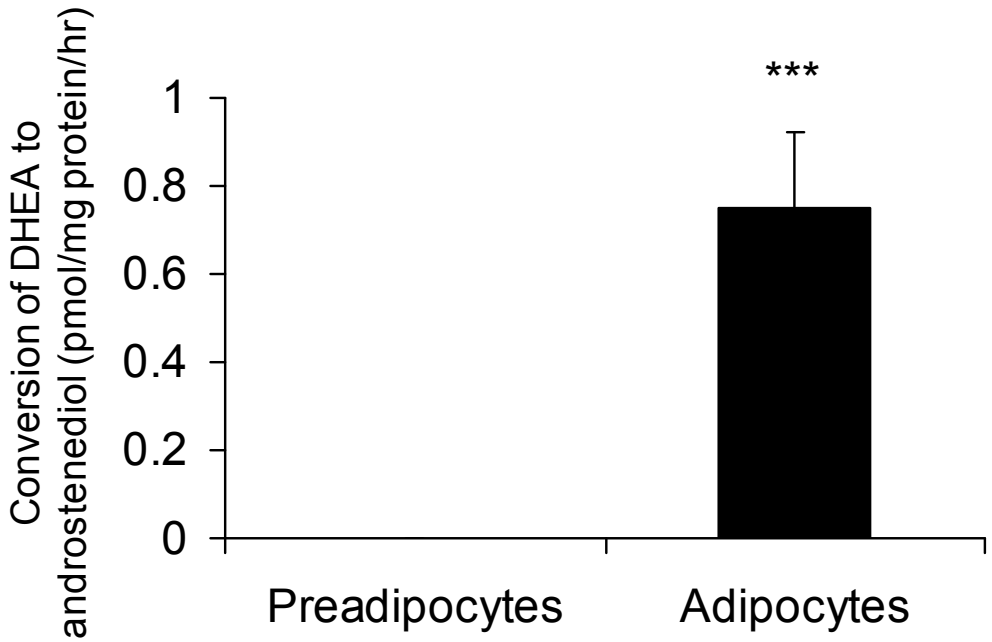

Figure 3-3 The activity of AKR1C3 in Chub-S7 preadipocytes and adipocytes. *The conversion of DHEA in Chub-S7 preadipocytes and adipocytes was assessed via co-incubation with ^{3}H DHEA for 24 hours and extraction, separation and identification of the metabolites. Appreciable conversion of DHEA to androstenediol was observed in adipocytes, but not proliferating preadipocytes. Data are presented as mean conversion in pmol/ mg of protein/ hour, obtained from four independent triplicate experiments. Statistical significance was assessed utilising unpaired Student's t-test. ***, P<0.005*

3.2.2 The effect of DHEA, androstenediol and DHEAS on human preadipocyte proliferation

3.2.2.1 DHEA and androstenediol inhibit preadipocyte proliferation

As the acquisition of adipose mass *in vivo* requires both preadipocyte proliferation and differentiation, the effects of DHEA on both of these processes were examined. Sub-confluent preadipocytes were incubated with various concentrations (100 nM, 1 μM, 10 μM, 100 μM) of DHEA, DHEAS or androstenediol for up to 120 hrs. Preadipocyte proliferation was assessed by thymidine uptake analysis or colorimetric analysis as described in sections 2.1.2.2 and 2.1.2.3 respectively. Thymidine uptake analysis revealed that DHEA (≥1μM) significantly reduced the amount of tritiated thymidine incorporated into actively proliferating cells during the incubation period, indicating that DHEA inhibits preadipocyte proliferation (**Figure 3-4, A**). Androstenediol (≥10μM) inhibited preadipocyte proliferation to a lesser, but still notable, extent (**Figure 3-4, B**) whereas DHEAS had no effect (**Figure 3-4, C**). The inhibitory effects of DHEA and androstenediol were time and dose dependent, with maximal inhibition being observed following 120 hrs incubation with the maximum concentrations of steroid (**Figure 3-4**).

Similar findings were observed utilising colorimetric assay analysis (**Figure 3-5**). DHEA (≥1μM) significantly inhibited the number of viable cells in culture (assessed by absorbance at 490nm), compared to control incubations, indicating that DHEA inhibited preadipocyte proliferation (**Figure 3-5, A**). Androstenediol treatment (≥10μM) resulted in a significant but lesser effect (**Figure 3-5, B**), while DHEAS had

no significant effect (**Figure 3-5, C**). Again, the effects of DHEA and androstenediol were dose and time dependent.

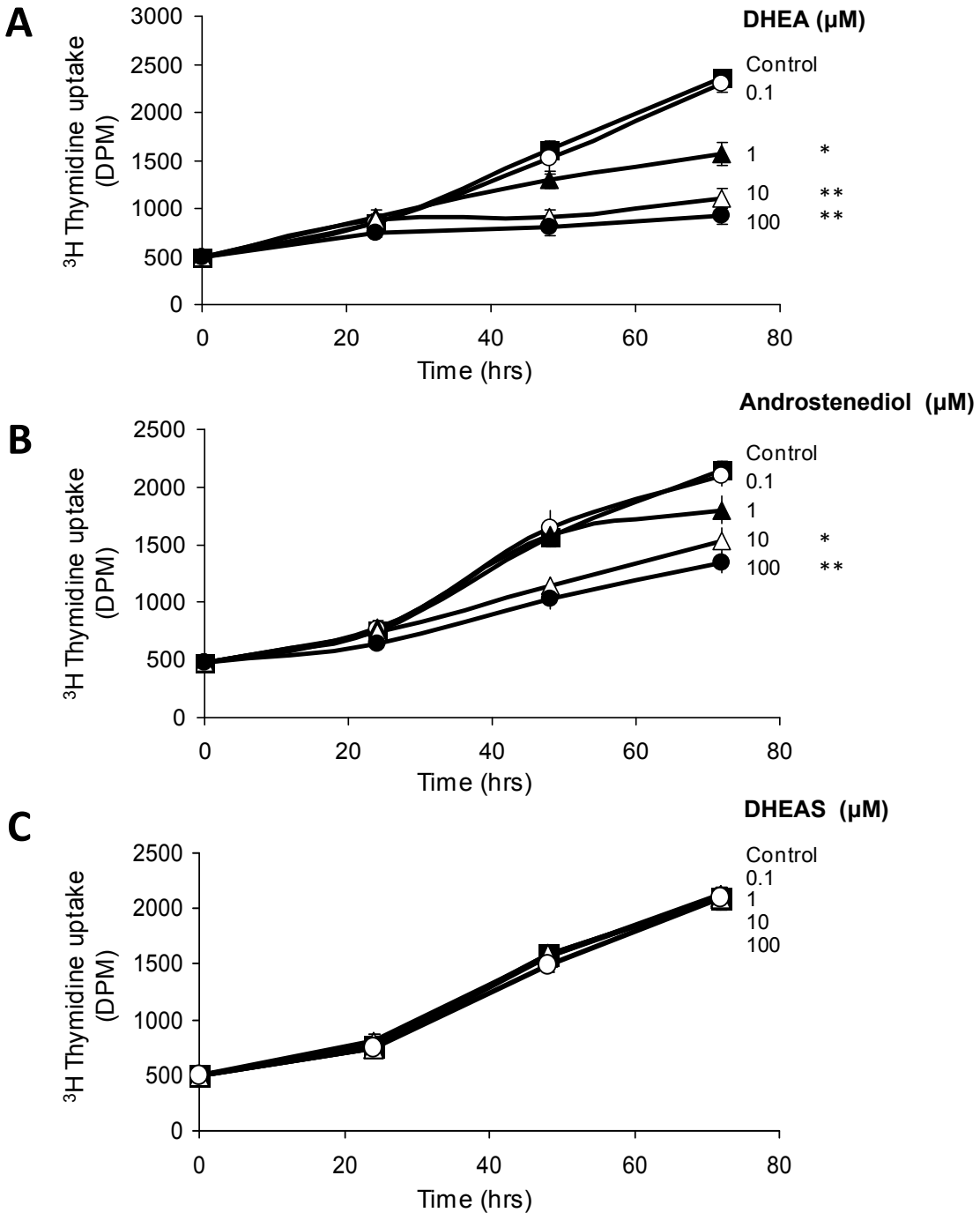

Figure 3-4 Dose-dependent inhibition of Chub-S7 preadipocyte proliferation by DHEA and androstenediol. *Sub-confluent Chub-S7 preadipocytes were incubated with DHEA, androstenediol or DHEAS (0-100 µM) for 24, 48 or 72 hours. Proliferation was analysed by incubation with incubated with 0.2µCi ^{3}H-thymidine for the last 6 hours of culture incubation. At 72 hrs, DHEA (≥1µM, panel A) and androstenediol (≥10µM, panel B) significantly inhibited preadipocyte proliferation. DHEAS did not significantly affect proliferation, (panel C). Statistical significance was assessed using one way ANOVA on ranks. *, P< 0.05; **, P< 0.01.*

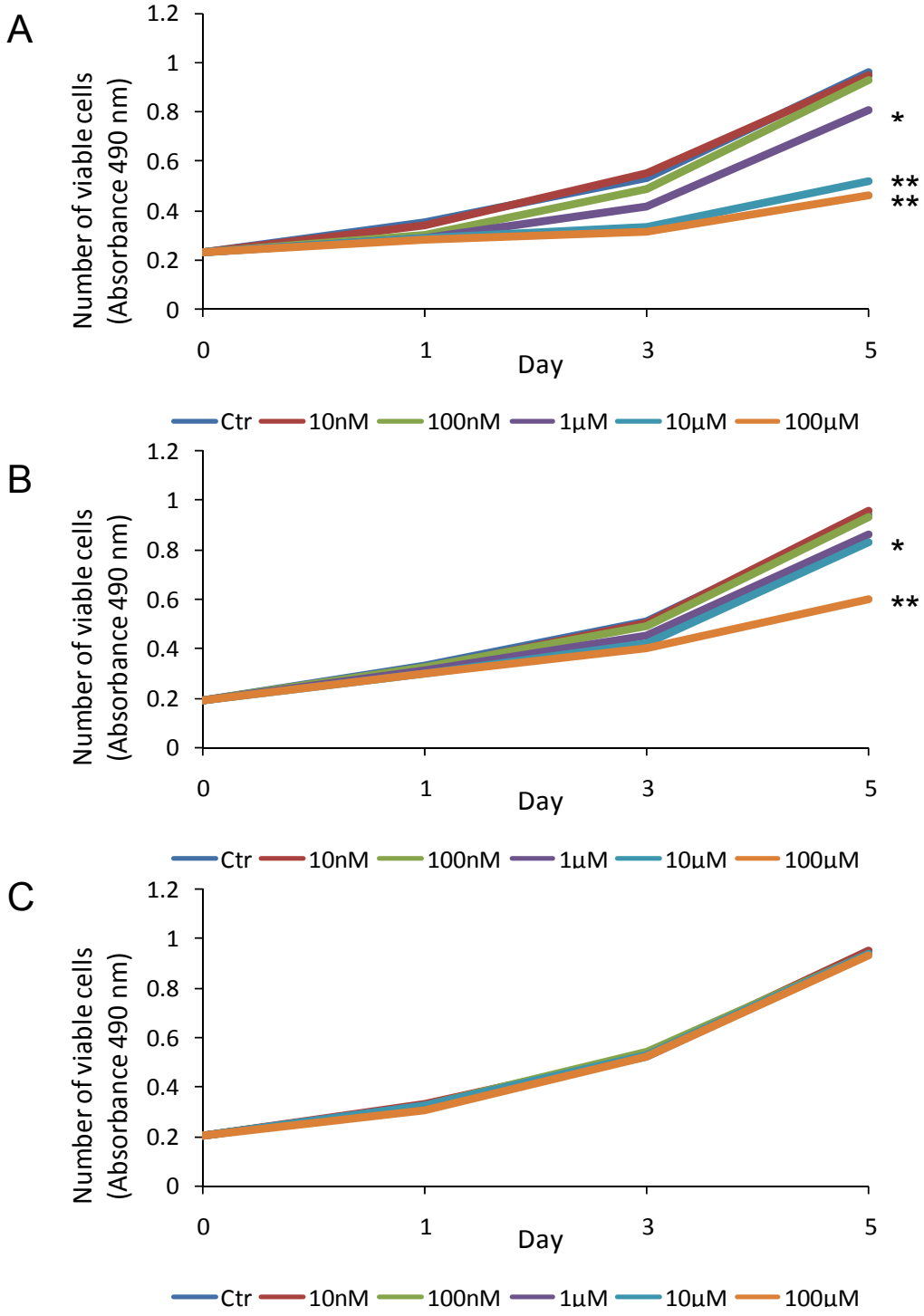

Figure 3-5 The dose-dependent inhibition of Chub-S7 preadipocyte proliferation by DHEA and androstenediol, assessed by colorimetric analysis *Sub-confluent Chub-S7 preadipocytes were incubated with DHEA, DHEAS or androstenediol for 24, 72 or 120 hrs. At 120 hrs DHEA (≥1µM; A) and androstenediol (≥10µM; B) significantly inhibited preadipocyte proliferation. DHEAS (C) produced no significant effect. Data represent the means ± SE and were obtained from three independent experiments. Statistical significance was assessed using one way ANOVA on ranks. *, P< 0.05; **, P< 0.01.*

3.2.2.2 The effect of DHEA on preadipocyte proliferation in the presence of sex steroid antagonists

To assess if the inhibitory effect of DHEA on preadipocyte proliferation was mediated by sex steroid receptors, Chub-S7 preadipocytes were treated with an androgen receptor antagonist, flutamide, and an oestrogen receptor antagonist, ICI 182780 (Faslodex) , 2 hrs prior to and during DHEA treatment. Preadipocyte proliferation was assessed by colourimetric analysis following 24, 72 and 120 hours incubation, as described in section 2.1.2.3. Co-incubation with the AR and ER antagonists failed to reverse the inhibitory effect of DHEA on preadipocyte proliferation at any timepoint (120 hrs, **Figure 3-8**) indicating that the observed effects are not mediated via DHEA downstream conversion to sex steroids. Treatment with the antagonists alone did not affect preadipocyte proliferation, confirming that the inhibition of proliferation observed was not due to the addition of the antagonists to the culture medium.

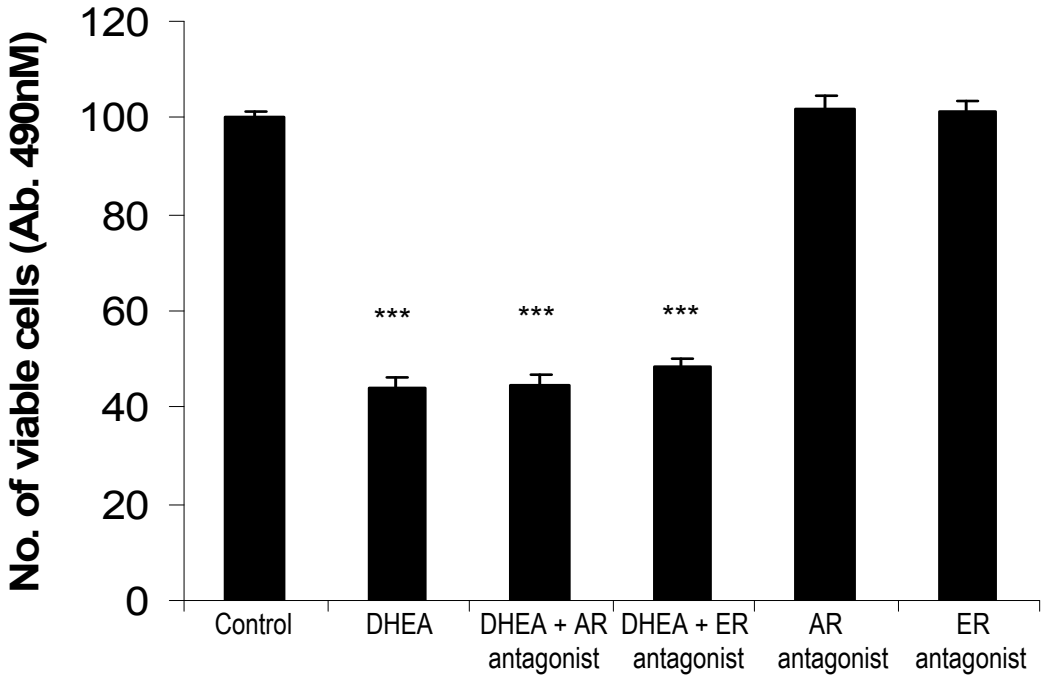

Figure 3-6 The inhibitory effect of DHEA on preadipocyte proliferation is independent of the AR and ER. *Sub-confluent Chub-S7 preadipocytes were co-incubated with DHEA and an antagonist of the androgen receptor, or oestrogen receptor and proliferation was assessed by colorimetric analysis at 120 hours. The inhibitory effect of DHEA was not diminished when cells were co-incubated with either antagonist. Incubation of cells with the androgen receptor or oestrogen receptor alone did not effect proliferation compared to control. Data represent means ± SE obtained from at least three independent experiments. Statistical significance (vs. ctr) was assessed by Student's t-test. ***, P< 0.005.*

3.2.2.3 The effect of DHEA on the cell cycle

As cellular toxicity was not evident following steroid treatment it was hypothesized that the inhibitory effect of DHEA was due to aberrant cell cycle progression. To test this hypothesis sub-confluent preadipocytes were incubated with 25 μM DHEA and the number of cells in each stage of the cell cycle quantified by FACS utilising flow cytometery as described in section 2.1.2.4. DHEA treatment caused a significant increase in the number of cells in the G1 phase (treatment, 63% of cells vs. control, 54% of cells), while concurrently significantly reducing the proportion of cells in G2 phase (19 vs. 21%) and S phase (16 vs. 27%) (**Figure 3-7**).

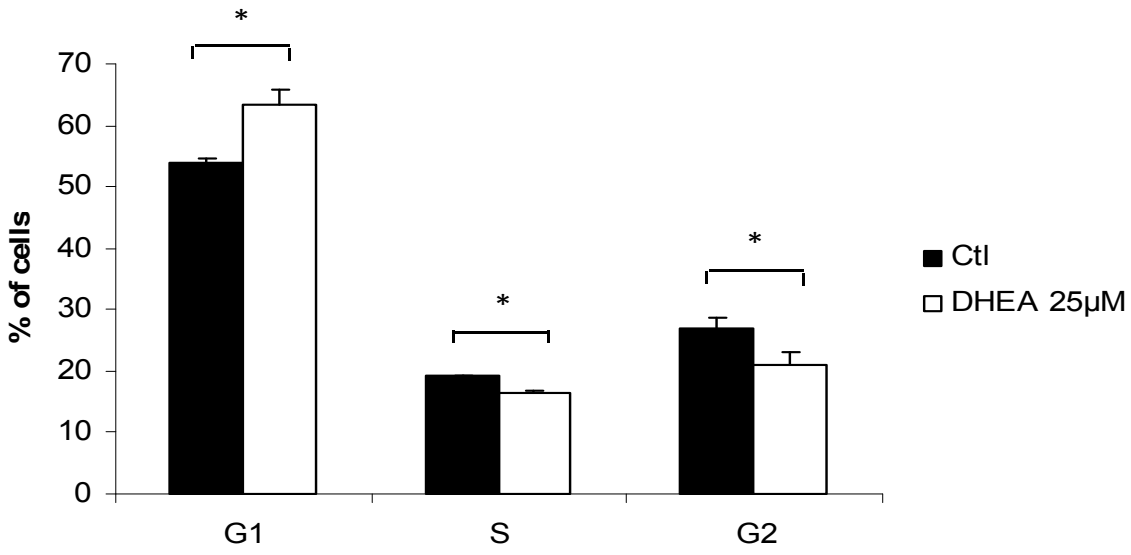

Figure 3-7 DHEA results in inhibition of preadipocyte proliferation via growth arrest in G1 phase. *Treatment of sub-confluent proliferating Chub-S7 cells with 25μM DHEA significantly increased the number of cells in G1 phase (63 vs. 54% in untreated control cells) and decreased the number of cells in S phase (16 vs. 27%) and G2 phase (19 vs. 21%). Data represent means ± SE derived from five independent triplicate experiments. Statistical significance was assessed by Student's t-test.* P< 0.05.*

3.2.3 The effects of DHEA, androstenediol and DHEAS on preadipocyte differentiation

3.2.3.1 The effect of DHEA on cell morphology during preadipocyte differentiation

The effect of DHEA on preadipocyte differentiation was assessed by observing cell morphology. Cells were cultured to 100% confluence in 24 well plates and differentiated for 21 days in chemically defined medium, including 500nM cortisone, as described in section 2.1.3.1. Cells were treated with various concentrations of DHEA (10 nM, 100 nM, 1 μM, 10 μM, 25 μM, 50 μM, 100 μM) throughout the differentiation procedure. Photographs were taken of the cells at 7, 14 and 21 days to document their morphology. Control cells (**Figure 3-8, B**) displayed a differentiated morphology, with the acquisition of lipid droplets and the loss of a fibroblast- like appearance. Cells treated with ≤10μM DHEA (**Figure 3-8 , C**) did not appear to differ morphologically from control cells. In contrast, cells treated with 25 μM DHEA (**Figure 3-8, D**) appeared more fibroblast-like than control cells, with an elongated shape and displayed less lipid accumulation. However, cells treated with 50μM DHEA or greater, appeared spherical and un-attached cells were visible in the media (**Figure 3-8, E**), suggesting that DHEA at these high concentrations was producing toxic effects. Therefore, 25μM was the highest concentration used for all further experiments.

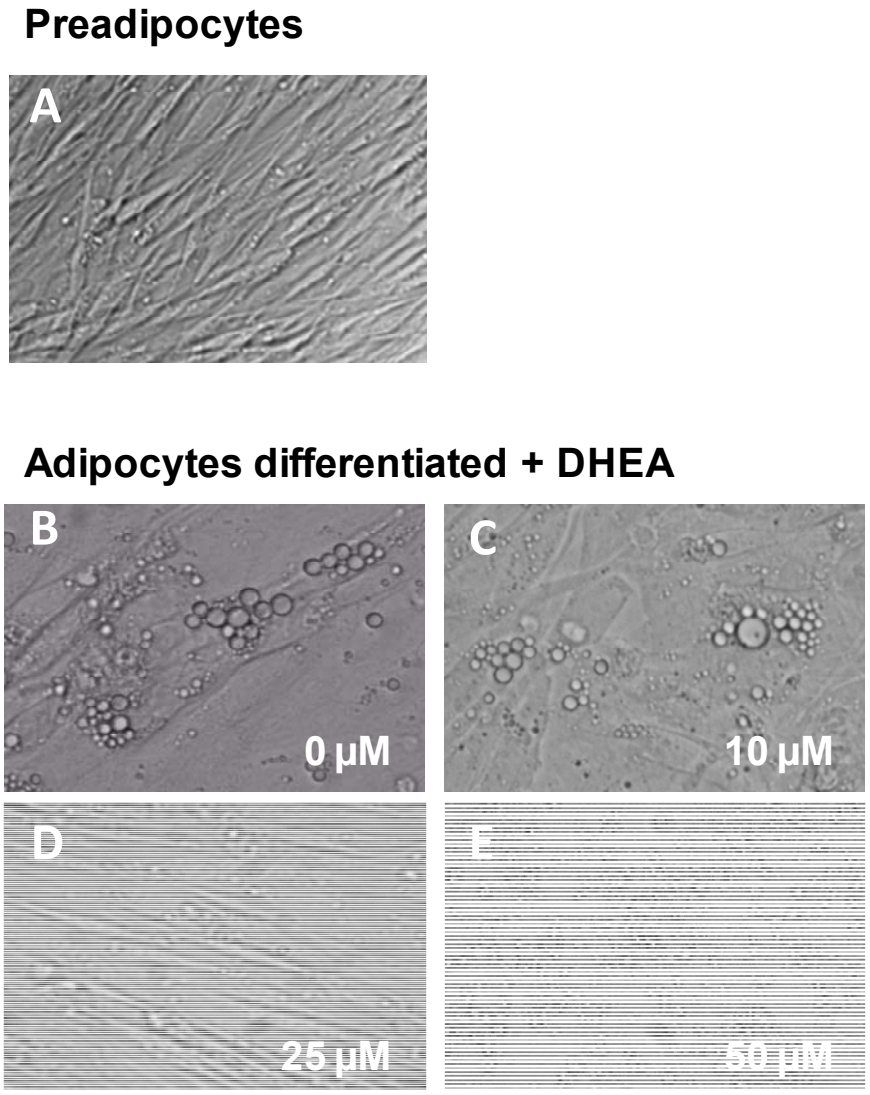

Figure 3-8 DHEA attenuates morphological changes associated with preadipocyte differentiation in Chub-S7 cells. *Confluent Chub-S7 preadipocytes (A) were differentiated in chemically defined media for 21 days in the presence of DHEA (0-50µM). Control cells (B) displayed a differentiated morphology, with the acquisition of lipid droplets and the loss of a fibroblast- like appearance. Cells treated in 10µM DHEA (C) did not appear to differ morphologically from control cells. In contrast, cells treated with 25 µM DHEA (D) appeared more fibroblast-like than control cells, with an elongated shape and contained much fewer lipid droplets. Treatment with ≥ 50 µM DHEA (E) induced toxicity.*

3.2.3.2 The effect of DHEA, androstenediol and DHEA on the expression of adipocyte differentiation markers

To gain further insight into the apparent inhibitory effect of DHEA on preadipocyte differentiation I analyzed the mRNA expression of the early adipocyte differentiation marker lipoprotein lipase (LPL), the late differentiation marker glycerol-3-phosphate dehydrogenase (G3PDH) and the expression of hexose-6-phosphate dehydrogenase and 11β-hydroxysteroid dehydrogenase type 1 (11β-HSD1), which play a key role in mediating the effects of glucocorticoids on preadipocyte differentiation. Cells were cultured to 100% confluence in 24 well plates and differentiated for 21 days in chemically defined medium, including 500nM cortisone, as described in section 2.1.3.1. Cells were treated with various concentrations (10 nM, 100 nM, 1 μM, 10 μM and 25 μM) of DHEA, androstenediol or DHEAS throughout the differentiation procedure. At days 7, 14 and 21 total RNA was extracted as described in section 2.4.1, reverse transcribed to cDNA as described in section 2.4.2, and the mRNA expression of adipocyte differentiation markers was assessed by real-time PCR as described in section 2.4.3.3, utilising gene specific primers and probes, (**Table 2-4**, 48-51). DHEA co-incubated with cortisone significantly inhibited the mRNA expression of all LPL (≥10μM), G3PDH (≥10μM) and even more pronounced of H6PDH (≥100nM) and 11β-HSD1 (≥1μM) in a dose dependent manner. Interestingly, androstenediol treatment also resulted in a significant inhibition of differentiation markers, albeit less pronounced (LPL, G3PDH, 11β-HSD1 ≥25μM) while differentiation assays with DHEAS did not produce any detectable effect.

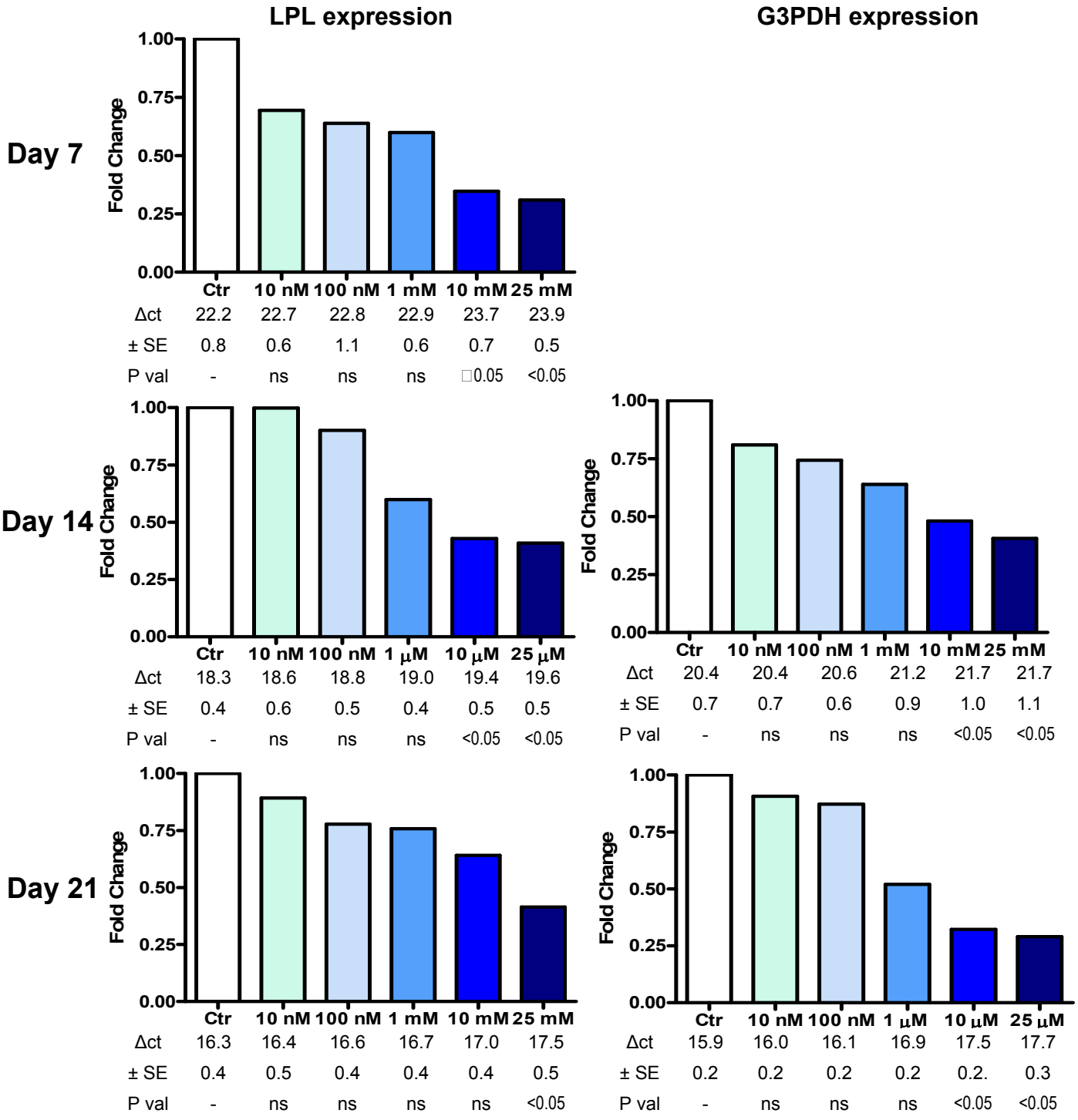

Figure 3-9 DHEA inhibits the induction of LPL and G3PDH mRNA expression during preadipocyte differentiation. *The expression of the early differentiation marker LPL and the late differentiation marker G3PDH was analysed by real-time PCR in Chub-S7 preadipocytes differentiated in the presence of DHEA and 500 nM cortisone for 7, 14 or 21 days. Data are presented as mean ΔCt obtained from four independent triplicate experiments. At day 7 G3PDH expression was not detectable by real-time PCR. Statistical significance (vs. control) was assessed by one way ANOVA on ranks.*

Day 7

Day 14

	Ctr	10 nM	100 nM	1 mM	10 mM	25 mM
Δct	16.7	16.7	16.8	17.1	17.5	17.6
± SE	0.2	0.3	0.3	0.3	0.3	0.3
P val	-	ns	ns	ns	<0.05	<0.05

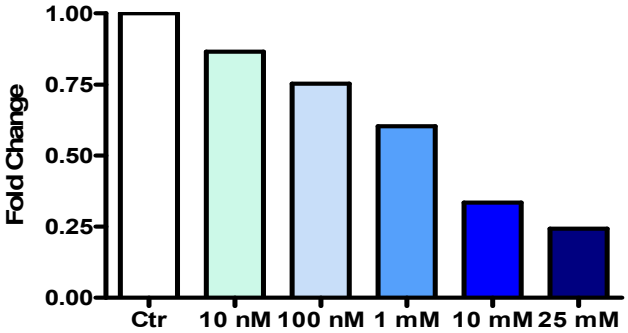

	Ctr	10 nM	100 nM	1 µM	10 µM	25 µM
Δct	14.5	14.9	15.6	15.7	16.4	16.2
± SE	0.5	0.5	0.5	0.5	0.6	0.6
P val	-	ns	>0.05	<0.05	<0.05	<0.05

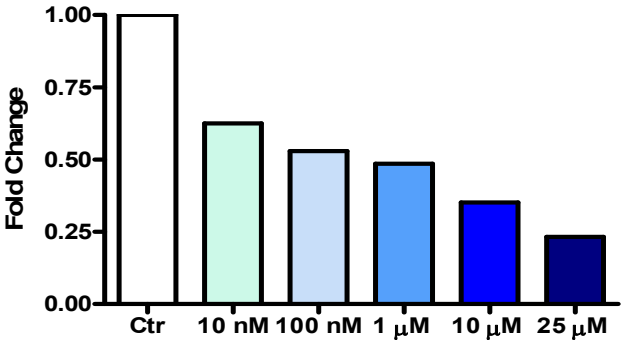

	Ctr	10 nM	100 nM	1 mM	10 mM	25 mM
Δct	13.9	14.1	14.3	14.7	15.5	16.0
± SE	0.2	0.4	0.3	0.3	0.4	0.5
P val	-	ns	ns	<0.05	<0.05	<0.05

Day 21

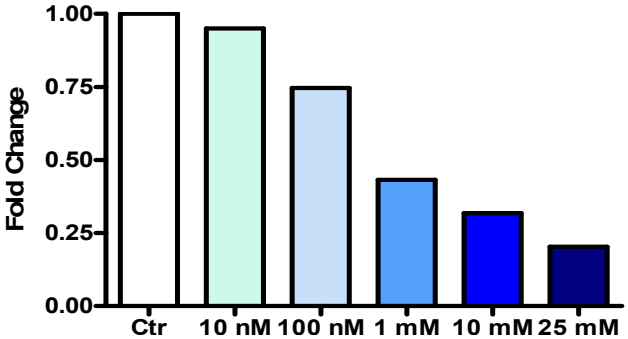

	Ctr	10 nM	100 nM	1 µM	10 µM	25 µM
Δct	15.0	15.6	15.9	15.9	16.5	16.9
± SE	0.3	0.2	0.3	0.3	0.4	0.5
P val	-	ns	<0.05	<0.05	<0.05	<0.05

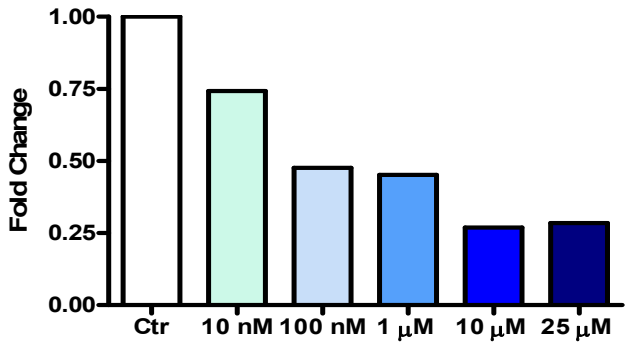

	Ctr	10 nM	100 nM	1 mM	10 mM	25 mM
Δct	13.2	13.6	13.6	14.4	14.9	15.5
± SE	0.4	0.4	0.3	0.4	0.6	0.9
P val	-	ns	ns	<0.05	<0.05	<0.05

	Ctr	10 nM	100 nM	1 µM	10 µM	25 µM
Δct	16.2	16.5	16.8	17.2	17.5	17.4
± SE	0.3	0.3	0.5	0.3	0.2	0.2
P val	-	ns	<0.05	<0.05	<0.05	<0.05

Figure 3-10 DHEA inhibits the induction of 11β-HSD and H6PDH mRNA expression during preadipocyte differentiation. *The expression of 11β-HSD1 and H6PDH was analysed by real-time PCR in Chub-S7 preadipocytes differentiated in the presence of DHEA and 500 nM cortisone for 7 , 14 or 21 days. Data are presented as mean ΔCt obtained from four independent triplicate experiments. Statistical significance (vs. control) was assessed by one way ANOVA on ranks.*

LPL expression

G3PDH expression

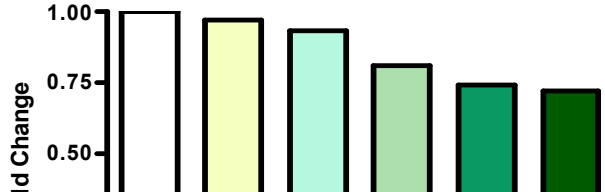

Day 7

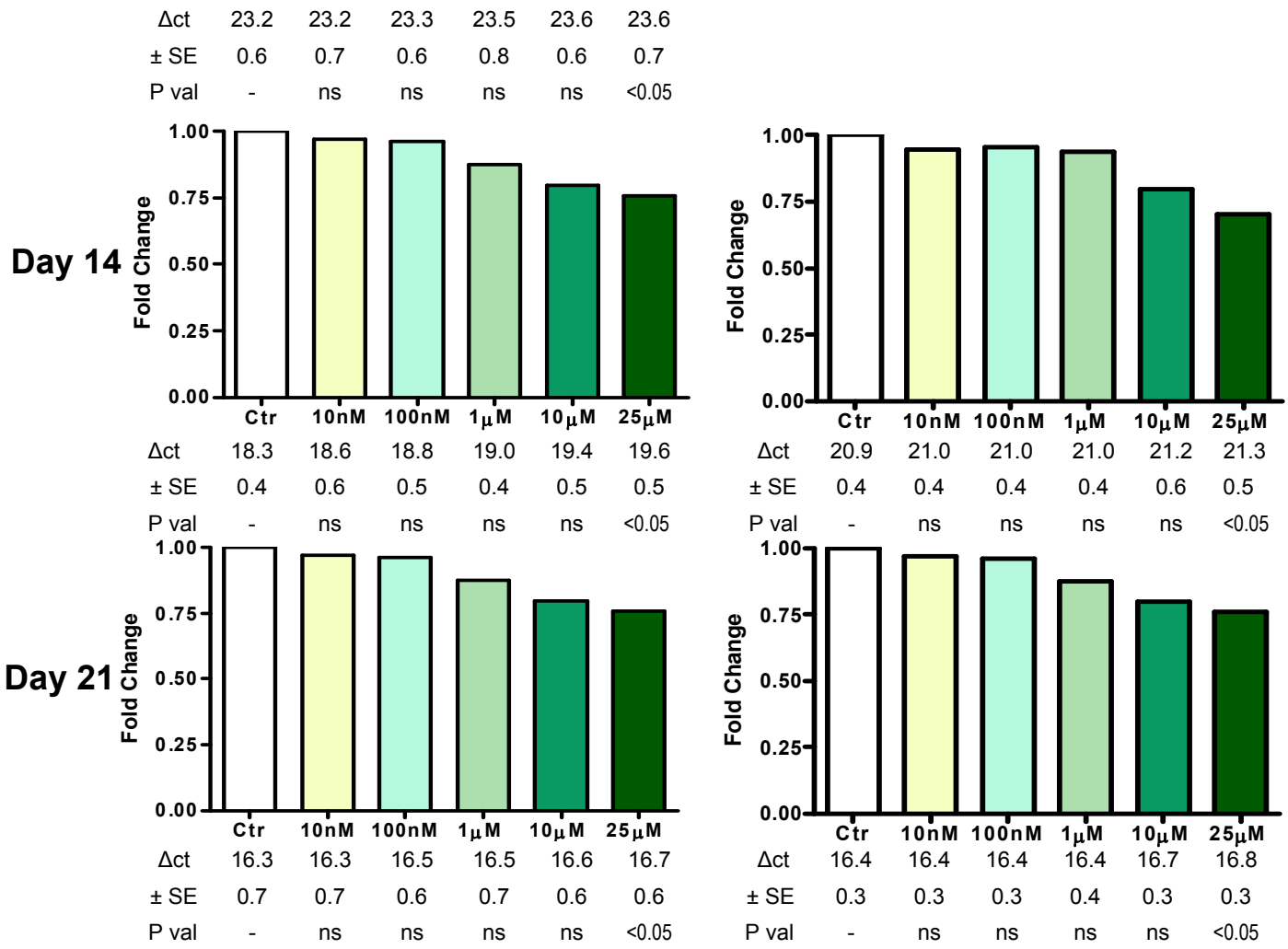

Figure 3-11 Androstenediol inhibits the induction of LPL and G3PDH mRNA expression. *The expression of the early differentiation marker LPL and the late differentiation marker G3PDH was analysed by real-time PCR in Chub-S7 preadipocytes differentiated in the presence of androstenediol and 500 nM cortisone for 7, 14 or 21 days. Data are presented as mean ΔCt obtained from four independent triplicate experiments. At day 7 G3PDH expression was not detectable by real-time PCR. Statistical significance (vs. control) was assessed by one way ANOVA on ranks. *, P<0.05; **, P<0.01.*

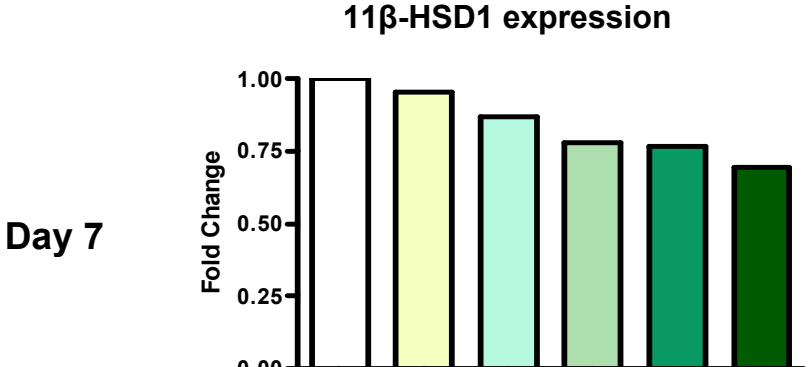

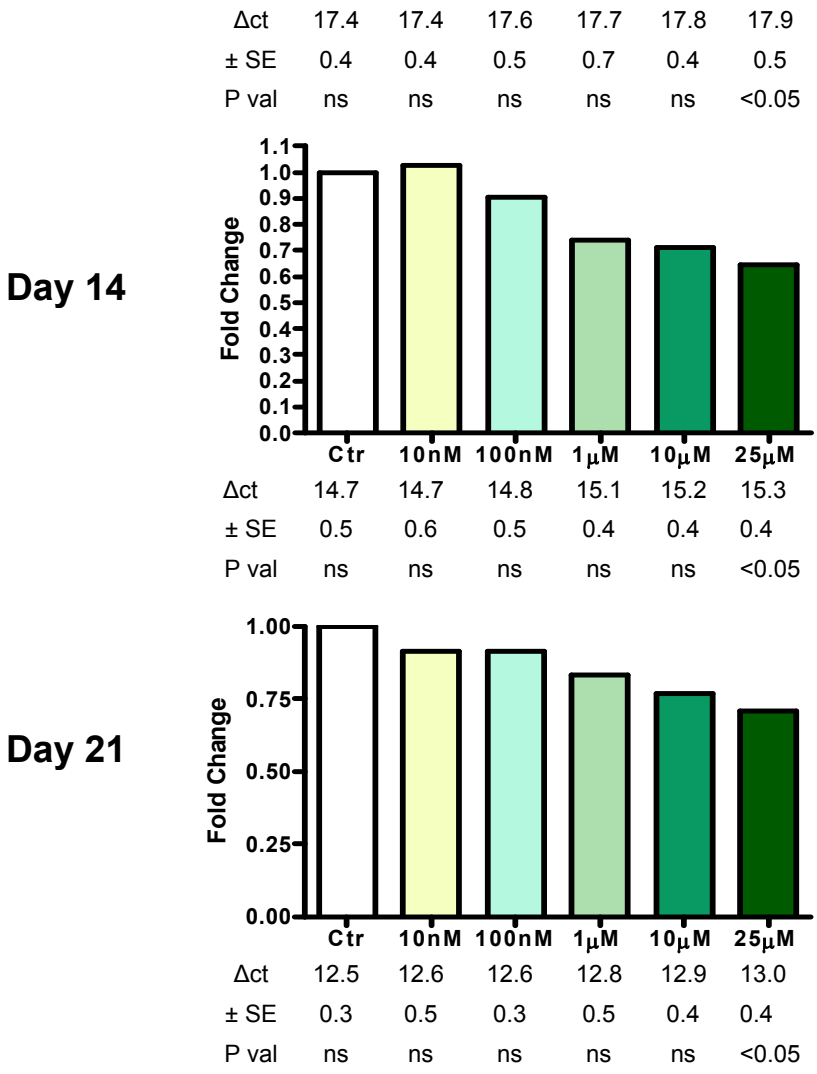

Figure 3-12 Androstenediol inhibits the induction of 11β-HSD mRNA expression during preadipocyte differentiation. *The expression of 11β-HSD1 was analysed by real-time PCR in Chub-S7 preadipocytes differentiated in the presence of various concentrations of androstenediol (0- 25 μM) and 500 nM cortisone for 7, 14 or 21 days. Data are presented as mean ΔCt obtained from four independent triplicate experiments. At day 7 G3PDH expression was not detectable. Statistical significance (vs. control) was assessed by one way ANOVA on ranks.*

Table 3-1 DHEAS does not effect 11β-HSD1 expression during preadipocyte differentiation. *The expression of 11β-HSD1 was analysed by real-time PCR in Chub-S7 preadipocytes differentiated in the presence of various concentrations of DHEAS (0- 25 μM) and 500 nM cortisone for 7 (A), 14 (B) or 21 (C) days. DHEAS treatment failed to produce any significant effects.*

		LPL		***G3PDH***		***11β-HSD1***	
		Δct	**SE ±**	**Δct**	**SE ±**	**Δct**	**SE ±**
Day 7	**Ctr**	23.4	0.5	Undetected		17.9	0.6
	10 nM	23.4	0.3			18.0	0.9
	100 nM	23.3	0.6			18.1	0.8
	1 μM	23.4	0.3			18.0	1.4
	10 μM	23.4	0.7			18.1	1.4
	25 μM	23.5	0.6			18.1	0.9
Day 14	**Ctr**	19.2	1.2	20.7	0.6	15.7	1.2
	10 nM	19.2	1.1	20.7	0.4	15.8	0.7
	100 nM	19.1	0.8	20.9	0.6	15.7	0.7
	1 μM	19.3	1.4	20.8	0.9	15.7	0.7
	10 μM	19.2	0.7	20.7	0.4	15.8	0.6
	25 μM	19.2	1.1	20.7	0.6	15.6	1.0
Day 21	**Ctr**	16.3	0.8	16.4	0.8	13.4	1.4
	10 nM	16.4	0.9	16.4	0.6	13.6	1.6
	100 nM	16.3	0.8	16.3	0.9	13.5	1.1
	1 μM	16.3	1.4	16.5	0.8	13.5	0.6
	10 μM	16.5	0.9	16.6	0.5	13.6	1.2
	25 μM	16.4	0.9	16.6	0.7	13.5	1.0

3.2.3.3 The effect of DHEA on basal and insulin dependent glucose uptake

In the mature adipocyte, cross-membrane glucose influx is a process critical for the provision of glucose, which via the pentose phosphate pathway is an important substrate for triglyceride synthesis, therefore contributing to adipocyte hypertrophy. The effect of DHEA on adipocyte glucose uptake, in both the basal and insulin stimulated states was therefore examined.

Preadipocytes were differentiated for 21 days as described in section 2.1.3.1. Cells were treated with DHEA for 2 hrs prior to and during 2-deoxy-D-[1-^{3}H]-glucose uptake analysis, performed as described in section 2.1.4.1. DHEA treatment (≥ 1μM) significantly increased glucose uptake in the absence and presence of insulin (P<0.05; **Figure 3-13**). Glucose uptake in the presence of insulin accounts for both basal and insulin stimulated uptake. Therefore insulin stimulated uptake was calculated by subtracting basal glucose uptake from total glucose uptake in the presence of insulin and is shown in **Table 3-1**. There was no significant effect of DHEA on insulin stimulated glucose uptake. Data were obtained from five independent triplicate experiments and statistical significance vs. control was assessed by one way ANOVA on ranks.

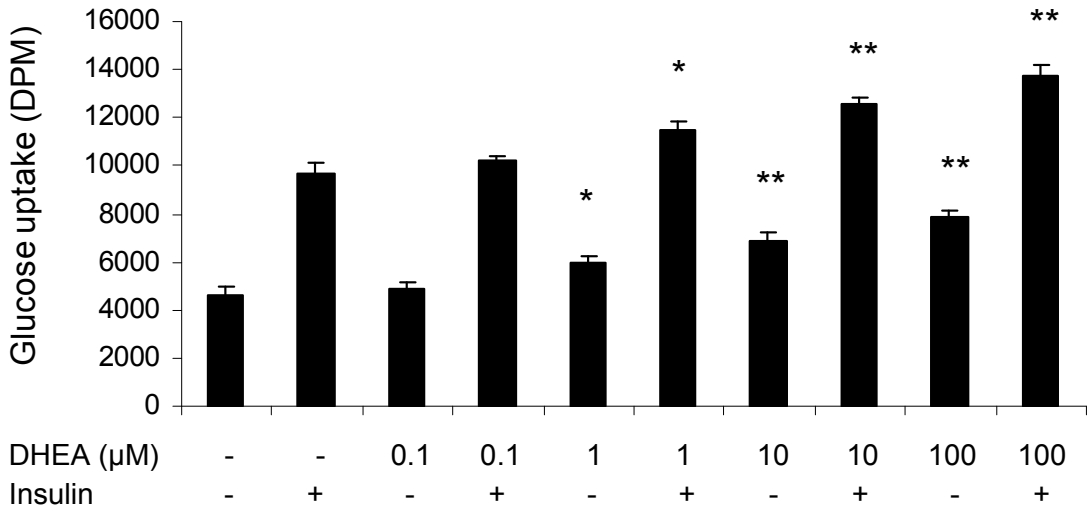

Figure 3-13 DHEA stimulates basal glucose uptake. *Preadipocytes were treated with DHEA for 2 hrs prior to and during, 2-deoxy-D-[1-^{3}H]-glucose uptake analysis, which was performed in absence (-) or presence (+) of insulin. DHEA (≥ 1μM) significantly increased basal glucose uptake and glucose uptake in the presence of insulin. Data are presented as mean glucose uptake (in DPM) ± SE, obtained from five independent triplicate experiments. Statistical significance vs. control was assessed by one way ANOVA on ranks. *, P<0.05; **, P<0.01 vs. control with corresponding insulin treatment.*

Table 3-2 DHEA does not modulate insulin stimulated glucose uptake*. Insulin stimulated glucose uptake for each DHEA treatment was calculated by subtracting glucose uptake in the absence of insulin (basal) from glucose uptake in the presence of insulin. DHEA treatment had no significant effect on insulin stimulated glucose uptake. Data are presented as mean insulin stimulated glucose uptake (in DPM) ± SE, obtained from five independent triplicate experiments. Statistical significance vs. control was assessed by one way ANOVA on ranks. ns, not significant.*

DHEA Treatment	Mean insulin stimulated glucose uptake ± SE	Statistical significance versus control
Ctr	5245 ± 634	ns
0.1 µM	5004 ± 523	ns
1 µM	5732 ± 732	ns
10 µM	5622 ± 691	ns
100 µM	5843 ± 644	ns

3.2.3.4 The effect of DHEA on adipocyte 11β-hydroxysteroid dehydrogenase type 1 oxo-reductase and dehydrogenase activity

Glucocorticoids (GC), key regulators of adipose differentiation are reactivated locally by 11β-HSD1 oxidoreductase activity, the expression of which increases with adipocyte differentiation. As I have shown that DHEA inhibits 11β-HSD1 expression and adipocyte differentiation, I postulated that DHEA may mediate its inhibitory effect on differentiation via the attenuation of the local regeneration of GC. I therefore assessed the effect of DHEA on 11β-HSD1 activity, to find out if the observed reduction of 11β-HSD1 mRNA expression by DHEA had functional significance. Preadipocytes were differentiated in chemically defined medium, including 500 nM cortisone and co-incubated with various concentrations of DHEA (10 nM, 100 nM, 1 μM, 10 μM, 25 μM), as described in section 2.1.3.1. 11β-HSD1 enzymatic activity was assessed by co-incubation with 100 nM cortisone or cortisol and the respective radiolabelled steroid (50,000 cpm/well) for three hours as described in section 2.6.2. Activity was normalized to cellular protein content, assessed as described in section 2.5.7, and calculated per hour of incubation. Data, obtained from four independent triplicate experiments, are expressed as mean pmol/mg protein/ hour conversion. DHEA treatment (≥1μM) resulted in a marked reduction in the conversion of ^{3}H E to ^{3}H F, in a dose dependent manner, indicating that DHEA attenuated the 11β-HSD1 oxo-reductase activity. (**Figure 3-14, A**). 11β-HSD1 is a bi-directional enzyme, possessing both oxo-reductase and dehydrogenase activity. However, *in vivo* this isoform acts predominantly as an oxo-reductase, converting cortisone to cortisol. Concurrent to the DHEA induced inhibition of 11β-HSD1 oxo-reductase activity, a

significant increase in the conversion of ^{3}H F to ^{3}H E was observed, indicating that DHEA (≥25μM) increases 11β-HSD1 dehydrogenase activity (**Figure 3-14, B**).

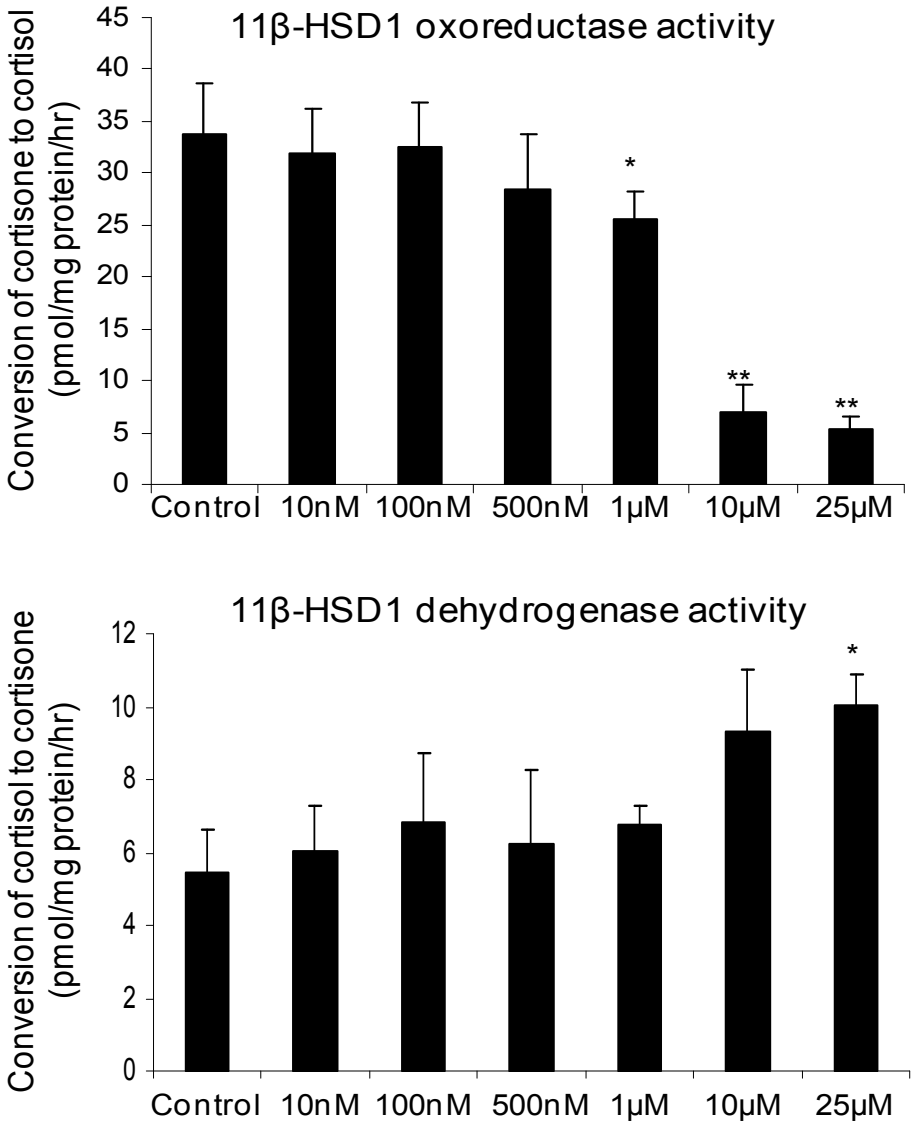

Figure 3-14 DHEA attenuates Chub-S7 11β-HSD1oxo-reductase activity. *Cells differentiated for 21 days in the presence of DHEA (0-25μM) were incubated with serum-free DMEM containing 100 nM cortisone or cortisol and ^{3}H-cortisone or ^{3}H-cortisol, respectively (50,000 cpm/ml) for 3 hours. Individual well protein concentrations were calculated and used as an internal control. DHEA (≥ 1 μM) significantly inhibited 11β-HSD1 oxoreductase activity, while DHEA (25 μM) significantly increased 11β-HSD1 dehydrogenase activity. Data is expressed as the means ± SEM of three independent triplicate experiments. Statistical significance was assessed by one way ANOVA on ranks. * P < 0.05, ** P < 0.01 vs. control*

3.2.3.5 The effect of DHEA co-incubated with cortisol on preadipocyte differentiation.

To further test the hypothesis that DHEA attenuates adipocyte differentiation via an inhibitory effect on 11β-HSD1, I analysed the effect of DHEA on adipocytes differentiated in the presence of the active glucocorticoid, cortisol, thus negating the requirement for 11β-HSD1 activity for differentiation. Preadipocytes were differentiated in chemically defined medium as previously, but with 500 nM cortisol substituted for cortisone (section 2.1.3.1). Cells were differentiated for a shorter period with cortisol (18 days vs. 21 days with cortisone) due to the greater adipogenic potency of cortisol. At days 9 and 18 total RNA was extracted as described in section 2.4.1 and reverse transcribed to cDNA as described in section 2.4.2. The mRNA expression of adipocyte differentiation markers was assessed by real-time PCR as described in section 2.4.3.3, utilising gene specific primers and probes (**Table 2-4**, primer pairs 48-51). DHEA co-incubated with cortisol significantly inhibited the mRNA expression of all genes analysed, LPL (25 μM), G3PDH (25 μM) H6PDH (≥100nM) and 11β-HSD1 (25 μM) at both timepoints analysed (day 9 and day 18). However, consistent with our hypothesis, the inhibitory effect of DHEA was significantly less than achieved by DHEA co-incubated with the inactive glucocorticoid cortisone, again at both time-points. Expression analyses for the two treatments were compared at the time-point when the control group of each treatment had comparable gene expression, suggesting a similar differentiation state of the control cells. No significant difference in gene expression between control groups was confirmed using unpaired Student's t-test. At 10μM DHEA, LPL expression was reduced by 52% in differentiation assays with cortisone as compared to 28% when co-incubated

with cortisol; similar effects were observed for G3PDH (DHEA+ cortisone 68%, DHEA+ cortisol 37%) and 11β-HSD1 (DHEA+ cortisone 68%, DHEA+ cortisol 43%) (**Figure 3-15**). Interestingly, co-incubation with cortisol did not significantly alter the level of DHEA-induced inhibition of H6PDH expression (**Figure 3-15**).

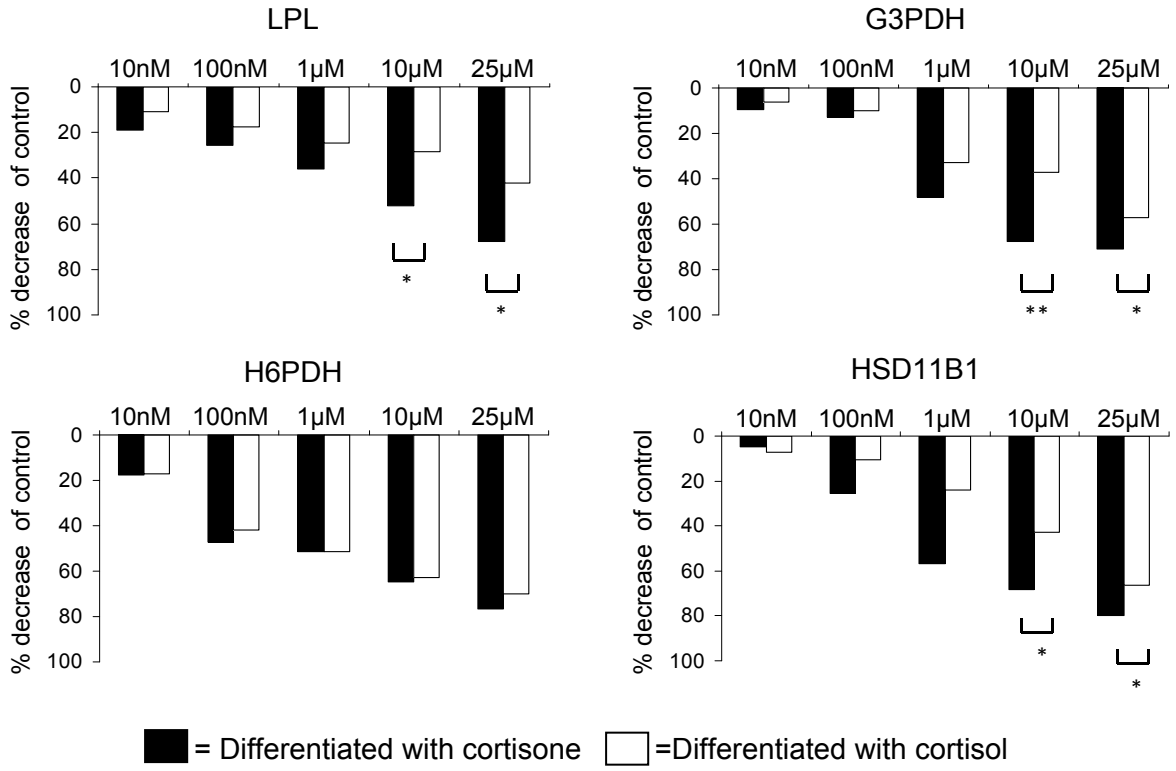

Figure 3-15 DHEA inhibits preadipocyte differentiation via inhibition of 11β-HSD 1 oxo-reductase activity. *Chub-S7 cells were differentiated in the presence of DHEA (0-25μM) and 500nM cortisone (black bars) or 500 nM cortisol (white bars). mRNA expression analysis is presented at the timepoint where the most significant effect of DHEA co-incubated with cortisone was observed; LPL and H6PDH, day 14; G3PDH and 11β-HSD1, day 21. The mRNA expression of the corresponding gene was determined by quantitative PCR and expressed as percentage decrease of control. Data was obtained from three independent experiments. Statistical analysis was performed on Δct values. DHEA co-incubated with inactive cortisone significantly inhibited LPL, G3PDH and 11β-HSD1 expression to a greater extent than when co-incubated with active cortisol. In contrast, there was no significant difference in H6PDH expression between treatments. * P < 0.05, ** P < 0.01*

3.3 Discussion

Previous murine studies have demonstrated beneficial anti-adipogenic and anti-diabetic effects of DHEA both *in vitro* and *in vivo*. However, as rodent adrenals lack the ability to synthesize DHEA and consequently have circulating DHEA levels several orders of magnitude lower than that of humans, the relevance of these findings to human physiology is questionable. Despite this significant discrepancy, to date no *in vitro* and limited *in vivo* human studies have been performed (Arlt, 2004b; Arlt and Allolio, 2003; Arlt et al., 1999; Gurnell et al., 2008; Johannsson et al., 2002; Lovas et al., 2003; Villareal and Holloszy, 2004). Here, utilising a human immortalised subcutaneous preadipocyte cell line, Chub-S7 (Darimont et al., 2003) I have demonstrated that DHEA attenuates preadipocyte proliferation and differentiation, and increases adipocyte glucose uptake, opposing the effects of glucocorticoids. To our knowledge, this is the first time the effect of DHEA on these parameters has been investigated in a human model. I have demonstrated that the Chub-S7 cell line, which has previously been extensively characterised by us and others, exhibits a level of expression of steroidogenic enzymes comparable to that of human primary subcutaneous adipocytes. This further confirms that this cell line is a suitable and valuable model for our studies, particularly due to the relative difficulty in obtaining the required number of human adipocytes for primary culture.

I have shown that DHEA (≥1μM) and androstenediol (≥10μM) attenuate preadipocyte proliferation, while the sulphate ester of DHEA, DHEAS, produced no significant effect. I have shown that the subcutaneous preadipocytes express OATP-D, a member of the OATP superfamily, implicated in the cross membrane transport of DHEAS (Hsiang et al., 1999; Kullak-Ublick et al., 1998; Ugele et al., 2003). This

finding, in contrast to previous studies, implies that the differential effect of hydrophilic DHEAS is not due to its inability to cross the cell membrane. Our finding for DHEA is similar to those of previous murine *in vitro* studies (Lea-Currie et al., 1999; Lea-Currie et al., 1998) which have shown that DHEA inhibits the proliferation of 3T3-L1 cells at 5 μM or greater. I have shown the anti-proliferative effect of DHEA to be, in part, via growth arrest in the G1 phase of the cell cycle. Interestingly, Schultz et al (Schulz et al., 1992) have demonstrated that DHEA treatment of a human colonic adenocarcinoma cell line results in G1/S phase cell cycle arrest, suggesting that this inhibitory effect of DHEA may not be tissue specific.

Previous studies have proposed that the anti-adipogenic actions of DHEA are mediated by its downstream conversion to active metabolites. However I have shown the inhibitory effect of DHEA to be direct as no significant conversion of DHEA within Chub-S7 preadipocytes was detected. Furthermore, failure of antagonists of the androgen and oestrogen receptor to relieve the inhibitory effect of DHEA, exclude the possibility that DHEA acts via these receptors.

Interestingly the observed anti-proliferative effect of DHEA opposes that of glucocorticoids. Evidence is emerging that glucocorticoids may stimulate preadipocyte proliferation in a depot specific manner, enhancing preadipocyte proliferation in the subcutaneous depot ((Bader et al., 2002), our own unpublished observations). However, an anti-glucocorticoid mechanism of DHEA regulating proliferation has failed to be identified.

In contrast to preadipocytes, significant metabolism of DHEA to androstenediol was observed in mature adipocytes, putatively catalysed by the observed increase in

AKR1C3 expression with differentiation of Chub-S7 cells. This finding is consistent with one previous study which examined the conversion of DHEA in human adipocytes by LCMS analysis. I have demonstrated that DHEA, and to a lesser extent androstenediol, attenuate human preadipocyte differentiation. DHEA treatment resulted in marked retardation in differentiation, characterised by a more fibroblast-like cellular morphology, a reduction in the accumulation of lipid droplets, and reduced expression of LPL and G3PDH- well characterised markers of adipocyte differentiation. Some previous murine studies have also alluded to an inhibitory effect of DHEA on preadipocyte differentiation. Lea-Curie et al observed that 30 μM DHEA attenuated TAG accumulation in differentiating 3t3-L1 cells. While, Kajita et el have reported that DHEA treatment of rodents decreased the expression of PPARγ, a regulator of adipocyte differentiation, in the adipose tissue of these animals. However these previous studies have failed to provide a mechanistic insight into the effects of DHEA.

I propose that the inhibitory effect of DHEA on preadipocyte differentiation is via an anti-glucocorticoid mechanism. It is well recognised that glucocorticoids, which are reactivated locally by the oxo-reductase activity of 11β-HSD1, play a vital permissive role in inducing preadipocyte differentiation (Bujalska et al., 1999; Gregoire et al., 1991; Hauner et al., 1987; Wolf, 1999). I have demonstrated that DHEA attenuates the local regeneration of glucocorticoids in adipocytes by two concerted mechanisms- attenuation of the induction of 11β-HSD1 during differentiation, and inhibition of expression of H6PDH, the enzyme which regenerates the co-factor NADPH, required for 11β-HSD1 oxo-reductase activity (Hewitt et al., 2005). Inhibition of 11β-HSD1 oxoreductase activity was associated with concurrent increase in

dehydrogenase activity, suggesting the specific inhibition of the oxo-reductase activity of 11β-HSD1, which I propose to be due to the observed inhibition of H6PDH. However, the increase in dehydrogenase activity was only significant at the highest concentration of DHEA treatment (25 μM), while and inhibition in 11β-HSD1 oxoreductase activity was observed at 1 μM DHEA, suggesting that the observed reduction in 11β-HSD1 mRNA expression is also likely to contribute.

Co-incubation with the active glucocorticoid cortisol confirmed that DHEA mediates the inhibition of adipocyte differentiation at least in part via the attenuation of the local amplification of glucocorticoids. However, it is also clear that DHEA additionally acts via glucocorticoid independent mechanisms. Co-incubation with cortisol still resulted in inhibition of preadipocyte differentiation, although the effect of DHEA was significantly diminished.

In addition, I have shown DHEA to stimulate basal glucose uptake, mimicking the action of insulin, consistent with the amelioration of hyperglycaemia and insulin resistance observed upon DHEA treatment *in vivo*. Again this effect of DHEA opposes that of glucocorticoids, which are well known to induce insulin resistance in preadipocytes. The underlying mechanisms by which glucocorticoids modulate insulin signalling remain unclear but appear to involve the conventional PKCs. In direct contrast, it has been demonstrated utilising rat adipocytes that DHEA may mimic or enhance insulin action via PI3-kinase and atypical PKC activation (Kajita et al., 2000). In support of our finding that DHEA predominately mimics rather than enhances the actions of insulin, DHEA has been shown to activate the insulin signalling pathway at the level of P13-kinase, independent of either the insulin receptor or AKT phosphorylation. This has been shown to result in increased

translocation of the glucose transporters, GLUT1 and GLUT4 to the plasma cell membrane (Perrini et al., 2004). Furthermore these findings are consistent with the rapid (2 hrs) stimulatory effect of DHEA observed in this study, which suggests that DHEA is acting via a non-genomic mechanism.

In summary our findings establish that DHEA exerts anti-glucocorticoid action in the adipocyte compartment, antagonizing the effects of cortisol on proliferation, differentiation and glucose uptake. Our findings are consistent with those of previous murine *in vivo* studies, suggesting a potential beneficial effect of DHEA on adipocyte proliferation and differentiation and insulin sensitivity in humans that warrants further studies, e.g. employing human primary cells and *in vivo*. Of particular interest is the conversion and effect of DHEA in adipocytes from PCOS patients, who have elevated DHEA levels, yet display central obesity and insulin resistance. It is currently unclear if the expression of DHEA metabolizing enzymes differs in this population, as has been previously shown to occur in PBMC cells with aging.

4 Chapter 4: Interconversion of DHEA and DHEAS and androgen excess

4.1 Introduction

The principle way in which DHEA produces physiological effects is via its downstream conversion into potent androgens and oestrogens in peripheral target tissues. As described in section 1.1.5.3, only uncongugated DHEA can be metabolised in this way, whereas conversion of DHEAS to androgens first requires cleavage of the sulfate moiety, catalysed by the microsomal enzyme STS. Conversely, DHEA can be inactivated by sulfation, catalysed by the cytosolic enzyme SULT2A1. Therefore the expression and activity of STS and SULT2A1 determines the bioavailability of DHEA.

Based on previous studies, which determined the pharmokinetics of DHEA and DHEAS following oral DHEA administration, it was generally accepted that DHEA and DHEAS interconvert freely and continuously. However, a more recent study in which oral DHEA and intravenous DHEAS was administered to healthy young men indicates that the predominant direction of DHEA and DHEAS interconversion to be of sulfation (Hammer et al., 2005b). In this study, as expected, DHEA administration resulted in an increase in circulating DHEAS, whereas, administration of DHEAS surprisingly failed to result in any significant production of DHEA. Therefore the crucial rate limiting step regulating circulating DHEA levels appears to be that of DHEA sulphotransferase rather than STS. If this paradigm is correct, increased sulfation of DHEA to DHEAS can be predicted to limit the amount of DHEA available for androgen synthesis, whilst impaired sulfation would increase DHEA and consequently the level of active androgens.

As described in section 1.1.7, androgen excess is the most common endocrine disorder and a key diagnostic trait of PCOS, which accounts for the majority of cases and is estimated to affect 5-10% of women of child-bearing age (Franks, 2006; Norman et al., 2007; Trivax and Azziz, 2007). PCOS is associated with a range of metabolic and endocrine dysregulations including obesity, type II diabetes mellitus, arterial hypertension and infertility (Barber et al., 2006; Norman et al., 2007). Recent studies have suggested that premature adrenarche, defined by an early increase in DHEA/DHEAS circulating levels, and its clinical manifestation, premature pubarche, may be early clinical predictors of the subsequent development of PCOS and its co-morbidities (Blank et al., 2008; Ibanez et al., 2000; Ibanez et al., 1998a; Ibanez et al., 1998b).

All sulfation reactions, including that of metabolically active DHEA to inactive DHEAS, catalysed by SULT2A1, require the universal sulphate donor 3'-phosphoadenosine 5'-phosphosulfate, PAPS. In humans, PAPS is synthesised by two isoforms of PAPS synthase, PAPSS1 and PAPSS2 (Xu et al., 2000). Two variants of the PAPSS2 isoform exist due to alternate splicing, PAPSS2a and PAPSS2b, which differ in an additional five amino acid segment (GMALP) in the ATP sulfurylase domain of the PAPSS2b protein. As described in section 1.1.6.4.1 a homozygous mutation in the human PAPSS2 enzyme (S475X) has previously been described in several individuals from large Pakistani kindred (ul Haque et al., 1998). This mutation has been shown to be linked with spondyloepimetaphyseal dysplasia (SEMD) Pakistani type (OMIM +603005) (ul Haque et al., 1998), thought to result from impaired sulfation of cartilage proteoglycan in growth plate chondrocytes, an essential process for normal bone development.

In this chapter I describe the case of a girl with androgen excess, premature pubarche, hyperandrogenic anovulation, and serum DHEAS levels below the limit of detection. Using an *in vitro* DHEA/DHEAS shuttle model I have investigated the molecular cause of the observed androgen excess in this patient, hypothesizing that a defect in DHEA sulfation may explain her phenotype.

4.2 Case report

An 8 year old girl, the daughter of nonconsanguineous parents of Turkish origin, was referred to the Endocrine Unit of the Department of Paediatrics, Radboud University Nijmegen Medical Centre, for evaluation of premature pubarche based on pubic and axillary hair growth which had been observed since the age of 6 years. Pubic-hair development was classified as Tanner stage 4 and breast development as Tanner stage 2. Blood pressure was normal at 115/85 mm Hg. The patient's bone age was advanced without evidence of accelerated growth velocity in the growth curve.

Biochemical analysis revealed DHEAS was below the lower limit of detection, while plasma DHEA was close to the upper limit of the normal range (**Table 4-1**) and circulating androstenedione and testosterone were both increased approximately 2-fold (**Table 4-1**). Dexamethasone (0.5 mg administered every 6 hours for 48 hours) suppressed the plasma cortisol level to less than 0.02 nmol per litre and reduced the DHEA level from 15.0 to 1.6 nmol per litre and reduced the androstenedione level from 4.1 to 2.9 nmol per litre, findings that ruled out autonomous steroid production by adrenal or gonadal tumour. Plasma 17-hydroxyprogesterone was normal at baseline and 60 min after cosyntropin 250 µg i.v. excluding 21-hydroxylase deficiency. Gonadotrophins were within the normal prepubertal range at baseline (LH

<0.2 U/L, FSH 0.7 U/L) and after GnRH 100 µg i.v. (LH 4.5 U/L, FSH 8.5 U/L) as was 17β-estradiol (36 pmol/l, normal range <18-52 pmol/L). The absence of a clearly pubertal response of levels of oestradiol or luteinizing hormone to the administration of gonadotrophin-releasing-hormone, as well as the short history of breast budding argued against the possibility that central precocious puberty was a major contributor to the patient's advanced bone age. Magnetic resonance imaging of the adrenals revealed normal size, shape and location of both adrenal glands. Following this initial presentation there was progression of pubic hair growth and breast development and menarche occurred at the age of 11 years.

The findings of a follow up assessment were largely similar to those made at 8 years of age, with a 2-fold increase in 2-fold increased androstenedione and testosterone levels, DHEA at the upper limit of normal and again DHEAS levels below the limit of detection (**Table 4-1**). Reassessment with a more sensitive assay showed plasma DHEAS levels at 0.27 µmol per litre (99.5 ng per litre). DHEAS remained below 0.4 µmol per litre throughout a cosyntrophin stimulation test, whereas plasma DHEA levels increased during the test. Analysis of urinary steroid metabolites over a 24-hour period showed increased excretion of the major androgen metabolite androsterone (5376 µg per 24 hours; normal range 287 to 2215).

At 12 years the patient had pubic-hair development at Tanner stage 5, breast development at Tanner stage 4 and clinically significant hirtuism and acne. Her bone age was 16.5 years, her height was 139.0 cm, short for her chronological age and bone age (standard deviation score, for chronological age, -2.4, and for bone age, -4.6). Her body mass index (the weight in kilograms divided by the square of the height in meters) was 30.2. X-rays revealed mild lumbar sclerosis, flattened vertebrae

(platyspondyly) with irregular vertebral end plates in the thoracolumbar region (**Figure 4-1**).

At 13 years of age she developed secondary amenorrhea, but polycystic ovaries were not evident. Her thyroid function, fasting plasma glucose and insulin levels all to be normal and all known conditions which present with hyperandrogensim were excluded. The patients height at 14.5 years remained at 139.0 cm (standard deviation score, -4.1). The father reported having had normal height and pubertal development and the mother reported normal pubarche and menarche. But when she was in her early 30's, obesity, oligomenorrea and hirsutism had developed.

All clinical and biochemical analyses were performed by the team of Dr Cees Noordam from the Department of Paediatrics- Metabolic and Endocrine Disorders and the Department of Chemical Endocrinology, Radboud University Nijmegen Medical Center, Nijmegen, The Netherlands.

Table 4-1 Circulating hormone concentrations and respective sex- and age-specific reference ranges in the patient as measured at the initial assessment (8 years of age) and at the follow-up assessment (12 years of age). GnRH denotes gonadotrophin releasing hormone.

Serum hormone parameter	Patient at age 8 years	Sex- and age-specific reference range	Patient at age 12 years	Sex- and age-specific reference range
DHEAS (µmol/L)	<0.40	0.6-4.6	<0.40	1.4-10.4
DHEA (nmol/L)	15.0	1.3-18.0	20.0 (43.0)*	2.0-22.0
Androstenedione (nmol/L)	4.1	0.14-2.4	27.0	<12.0
Testosterone (nmol/L)	1.2	0.03-0.65	2.1	0.51-1.26
Dihydrotestosterone (nmol/L)			0.36	0.05-0.25
LH (IU/L)	<0.2 (4.5)†	<0.2-1.3	3.2	<0.05-20.2
FSH (IU/L)	2.0 (8.5)†	<0.2-3.7	5.2	0.14-8.8
17β-estradiol (pmol/L)	36	<18-52	220	110-370
Estrone (pmol/L)			260	65-220
17-hydroxyprogesterone (nmol/L)	1.30 (3.1)*	0.2-5.8 (<20)*		
17-hydroxypregnenolone (nmol/L)			2.9 (15.1)*	0.3-6.1 (<40)*
11-deoxycortisol (nmol/L)			<0.17 (1.70)*	<0.17 (<7)*
Cortisol (nmol/L)			140 (650)*	100-500 (>500)*

* at baseline (60 min after cosyntropin 250 µg i.v.)
† at baseline (30 min after GnRH 100 µg i.v.)

Figure 4-1 Skeletal X-rays taken in the patient at the age of 12 years. *Spinal x-ray depicting flattened vertebrae (platyspondyly) with reduced intervertebral disk space and slightly irregular end plates within the thoraco-lumbar region. By contrast x-ray analysis of the long bones did not (B and C, left leg; D, left arm) did not reveal any evidence of metaphyseal or epiphyseal changes.*

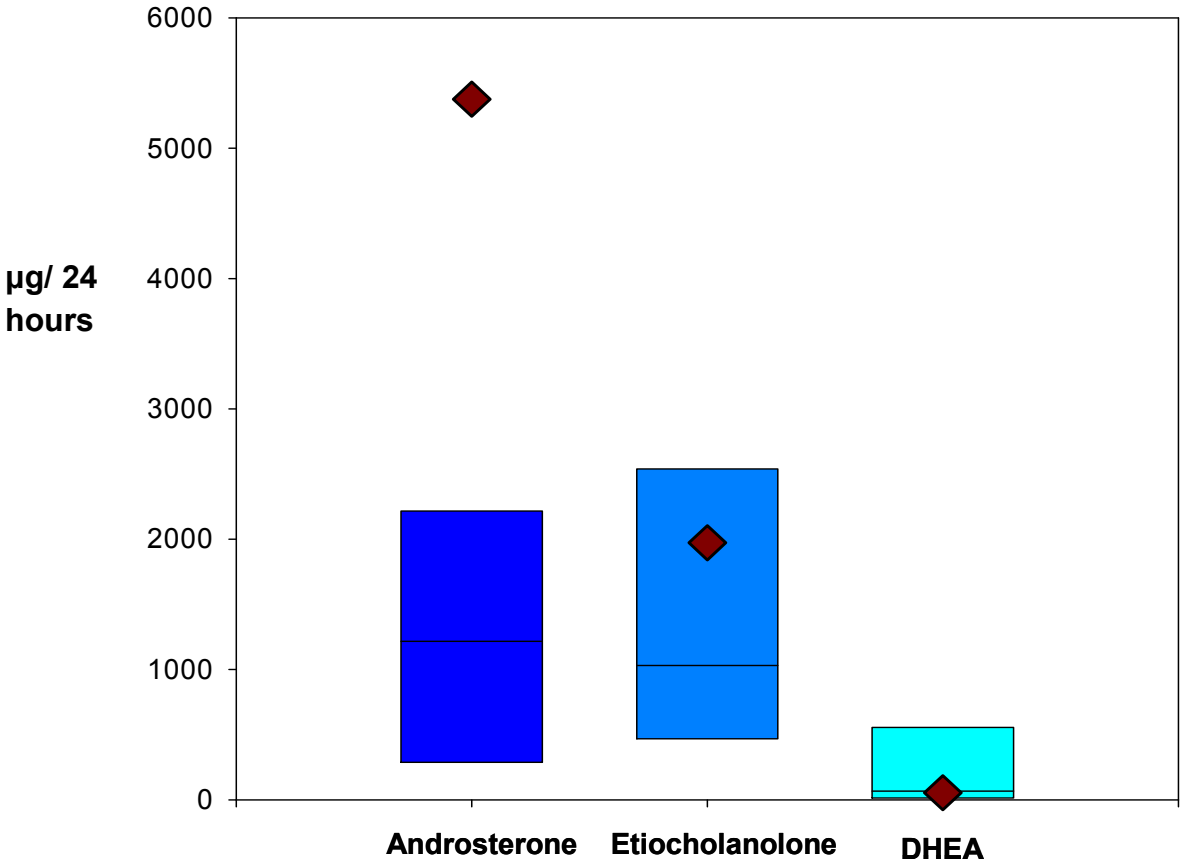

Figure 4-2 Urinary androgen metabolite excretion. *Analysis of urinary steroid metabolites of the patient (at age 12 years) over a 24-hour period showed increased excretion of the major androgen metabolite androstenedione (5376 µg per 24 hours, represented as red diamond; normal range, 287- 2215 µg per 24 hours, represented as blue box). Etiocholanolone and DHEA excretion was in the upper-normal and normal range, respectively.*

4.3 Results

4.3.1 Genetic analysis of the genes encoding the human DHEA sulfation system

We hypothesised that the patient's phenotype of androgen excess and concurrent low DHEAS levels may be due to a defect in DHEA sulfation. Therefore I sequenced the genes encoding the key enzymes involved in this process (*SULT2A1, PAPSS1* and *PAPSS2*) in the affected individual and her immediate family. Genomic DNA was isolated from peripheral blood leucocytes of the patient, her parents and her sibling, following written informed consent from the parents and verbal consent from the patient, with approval of the South Birmingham Research Ethics Committee.

The coding sequences of human *SULT2A1*, *PAPSS1* and *PAPSS2* including exon-intron boundaries were amplified and subsequent automated sequence analysis was performed as described in section 2.4.3.2 and section 2.2.3.3 respectively, employing gene specific primers (listed in **Table 2-1**, 1-26). Initial sequencing of *SULT2A1*, revealed previously identified single nucleotide polymorphisms (SNPs), which have been shown to not affect enzyme function, but no mutations. Likewise, sequencing of *PAPSS1* failed to identify any mutations. However, sequencing of *PAPSS2* gene revealed a heterozygous substitution of cytosine for guanine at nucleotide position 143 (143C>G) in exon 2 of genomic DNA obtained from the patient and her father (**Figure 4-3, A**). This missense mutation substitutes an arginine for threonine at position 48 of the PAPSS2 protein (T48R), which is located in immediate proximity to the P loop structure within the APS kinase domain of the enzyme. This region has previously been identified as critical for APS kinase activity and is highly conserved

across species (**Figure 4-3, B**). In addition, sequencing analysis revealed a heterozygous substitution of cytosine for thymidine in position 985 (c.985C>T) in exon 8 of the *PAPSS2* gene in genomic DNA obtained from the patient and mother. This mutation introduces a premature stop codon within the ATP sulfurylase domain of the PAPSS2 protein and truncating the protein at position 329 (R329X). The proposed crystal structure of these mutant proteins, in addition to WT PAPSS2a and the previously Identified mutation in PAPSS2 (S475X, see section 1.1.6.4.1) are shown in **Figure 4-4**. The mutation which I refer to as S475X was originally reported as S438X, but translates to S475X according to the current PAPSS2a protein sequence NP_004661. Identified mutations were independently verified and numbered according to the amino acid position in the protein sequence of the human PAPSS2a protein (GenBank accession number NP_004661).

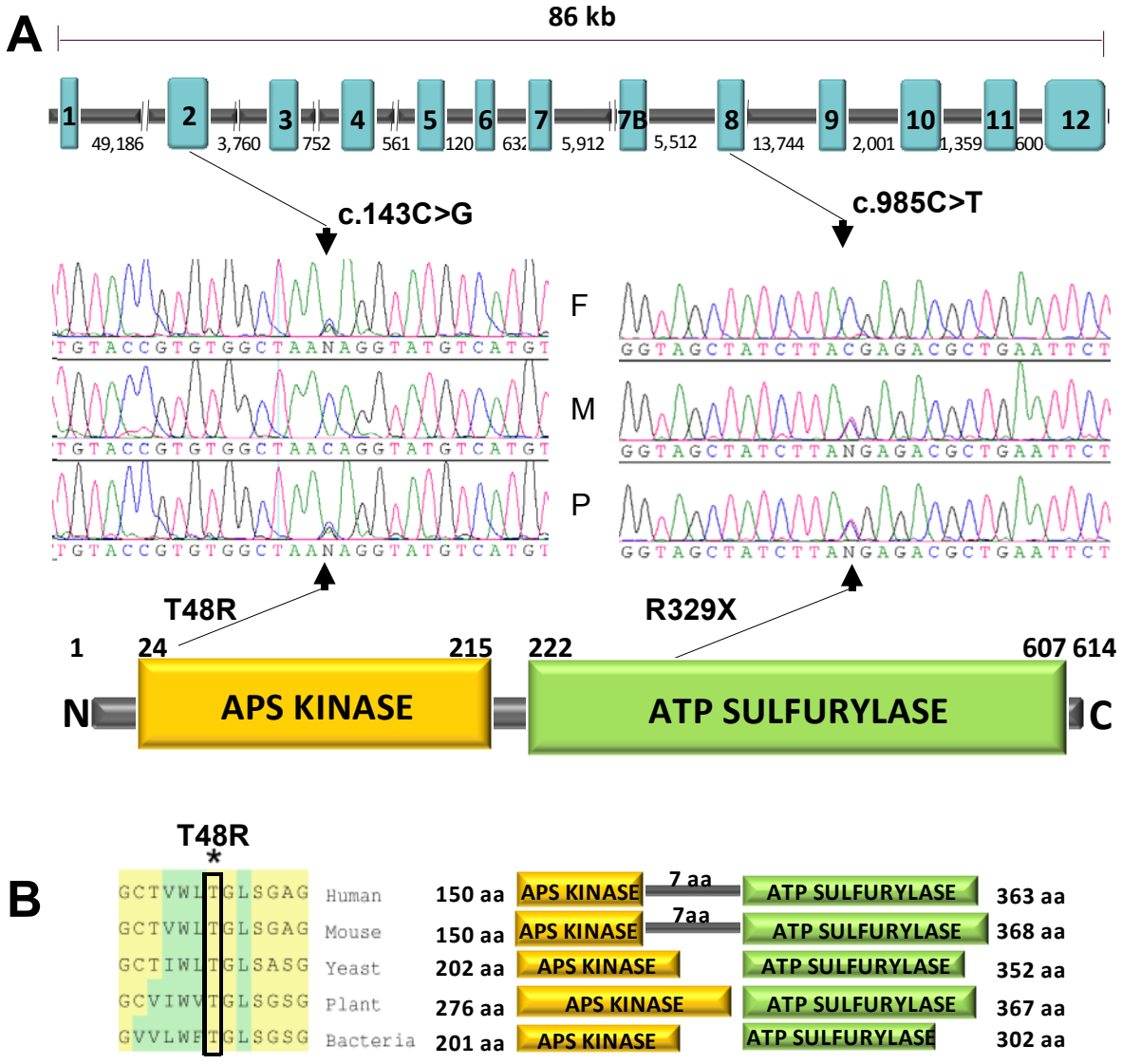

Figure 4-3 A, Location of the identified PAPSS2 mutations within the PAPSS2 gene locus *and the two functional domains of the PAPSS2 protein. The patient (P) is compound heterozygous while father (F) and mother (M) are heterozygous carriers.* ***B, Cross-species alignment of the PAPSS2 region*** *containing missense mutation T48R and schematic depiction of the respective protein secondary structures. Protein sequence alignments were generated using clustalX2 (www.clustal.org) and the deposited sequences for Human (NP_004661), Mouse (NP_035994), Yeast (CAA46252; CAA60932), Bacteria (A1AEU4; AAG57859) and Plant PAPSS2 (CAA53426; CAB78510).*

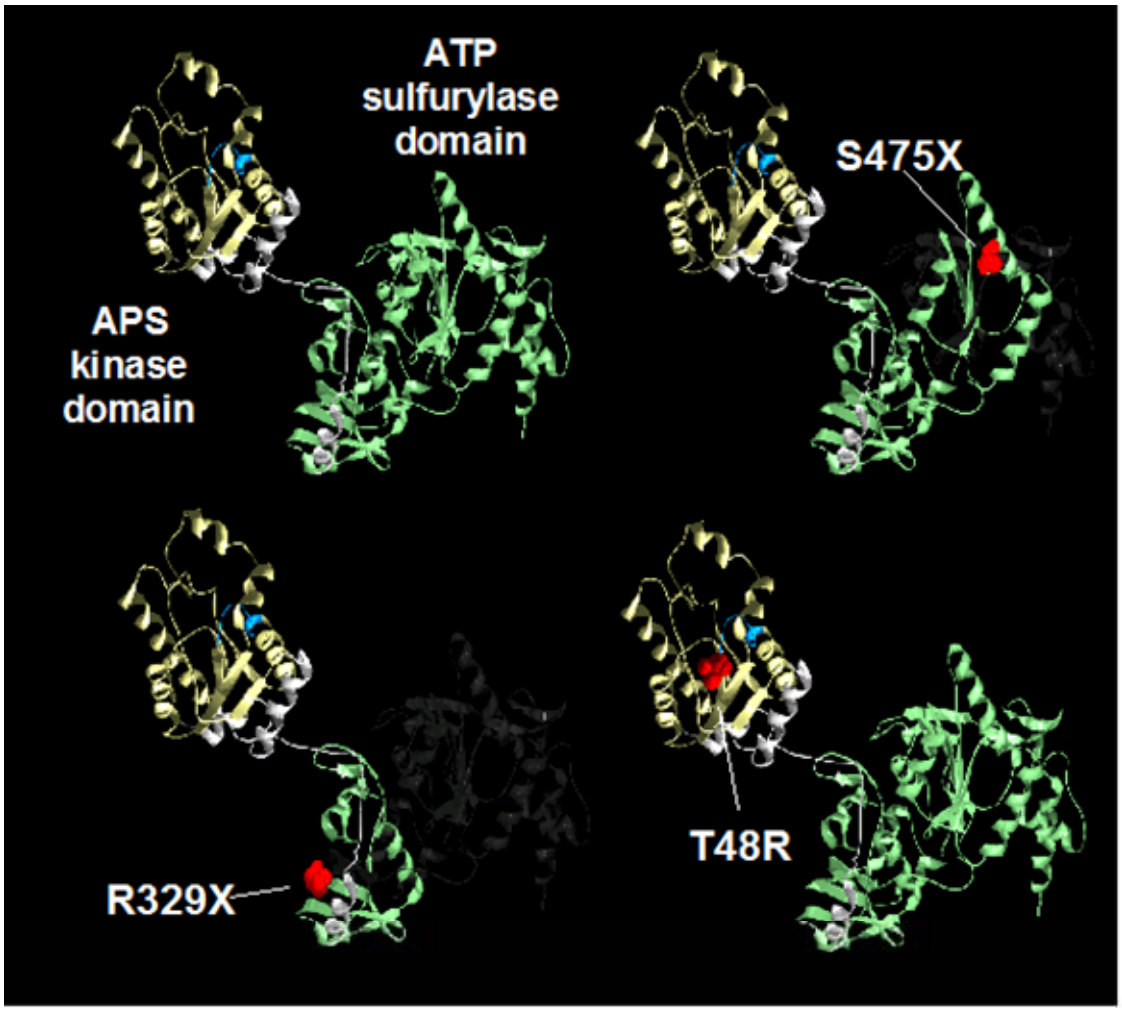

Figure 4-4 Three-dimensional modelling of wild-type and mutant PAPSS2 proteins. *PAPSS2 contains two functional domains, ATP sulfurylase and APS kinase. Previously reported mutant S475X and R329X on the maternal PAPSS2 allele in our patient result in early truncation of the ATP sulfurylase domain while the paternally inherited missense mutation T48R affects an amino acid immediately adjacent to the central P loop structure (highlighted in blue) within the APS kinase domain, an area crucial for ATP cleavage and thus APS kinase activity. The x-ray structure of human PAPSS1 (*http://www.expasy.org/cgi-bin/dbxref?SMRO*95340), which shares 80% sequence identity to human PAPSS2, served as the template for three-dimensional modelling of human PAPSS2 wild-type and mutant proteins, generated using DeepView/Swiss-PDB Viewer (www.expasy.org/spdbv/) and POVRAY (www.povray.org). Generated by Dr Vivek Dhir*

4.3.2 In vitro constitution of the DHEA sulfation system

With the aim of confirming the disease causing nature of the identified mutations I generated an *in vitro* model of the DHEA/DHEAS shuttle, as described in section 2.6.4, by co-incubating bacterially expressed wild type (WT) SULT2A1 and WT or mutant PAPSS2a proteins. In this system the dependence of SULT2A1 activity (the sulfation of DHEA to DHEAS) on the provision of PAPS by PAPSS can be exploited to determine the functional activity of bacterially expressed WT and mutant PAPSS2a.

4.3.2.1 ***Confirmation of pGEX-construct sequences***

WT plasmids (pGEX-6P-3-PAPSS2a and pGEX-6P-3-SULT2A1), kindly provided by Dr Charles Strott, NIH Bethesda, USA, were used to bacterially express SULT2A1 and PAPSS2. To generate these constructs, human full length PAPSS2a and SULT2A1 cDNA were inserted into the *Sal*I and *BamH*I sites or the *Sal*I and *Not*I sites, respectively, of the pGEX-6P-3 expression vector (G.E Healthcare) as described previously (Fuda et al., 2002) or via personnel communication.

Restriction digestion of the vectors was executed as described in 2.3.3 employing 1 µg of plasmid DNA, to confirm the presence of the insert. A dual digest was performed to digest pGEX-6P-3-SULT2A1, employing the restriction enzymes *Sal*I and *Not*I; the optimal buffer for these enzymes, buffer D and optimum enzyme specific reaction temperature of 37˚C for 4 hours. Sequential digestion reactions were performed to digest pGEX-6P-3-PAPSS2a, as described in section 2.3.3 using the restriction enzymes *Sal*I and *BamH*I; their respective optimal buffers, buffer D and

buffer 3, and optimum enzyme specific reaction temperature of 37˚C for 2 hours for each reaction. Assay of the digestions by gel-electrophoresis, alongside undigested vector, confirmed the presence of the inserts. Analysis of the pGEX-6P-3-PAPSS2a digestion revealed a band of the appropriate size for PAPSS2a, 1,600 bp, and a band of 5,000 bp, which correlated to linear pGEX vector (**Figure 4-4, A**). Undigested vector revealed bands corresponding to nicked and supercoiled DNA. Analysis of the pGEX-6P-3-SULT2A1 digestion revealed a band of the appropriate size for SULT2A1, 850 bp, and a band of 5,000 bp corresponding to the linear pGEX vector (**Figure 4-4, B**). Again, analysis of undigested vector revealed bands corresponding to nicked and supercoiled DNA.

Sequence analysis of the constructs was performed as described in section 2.2.3.2 utilising 3 µg of purified plasmid DNA and 3.2 pmol of primer (**Table 2-1**, primer pairs 27-30) per reaction. Comparison of plasmid sequences to WT sequences confirmed the correct in frame alignment of the insert and the absence of any sequence variations.

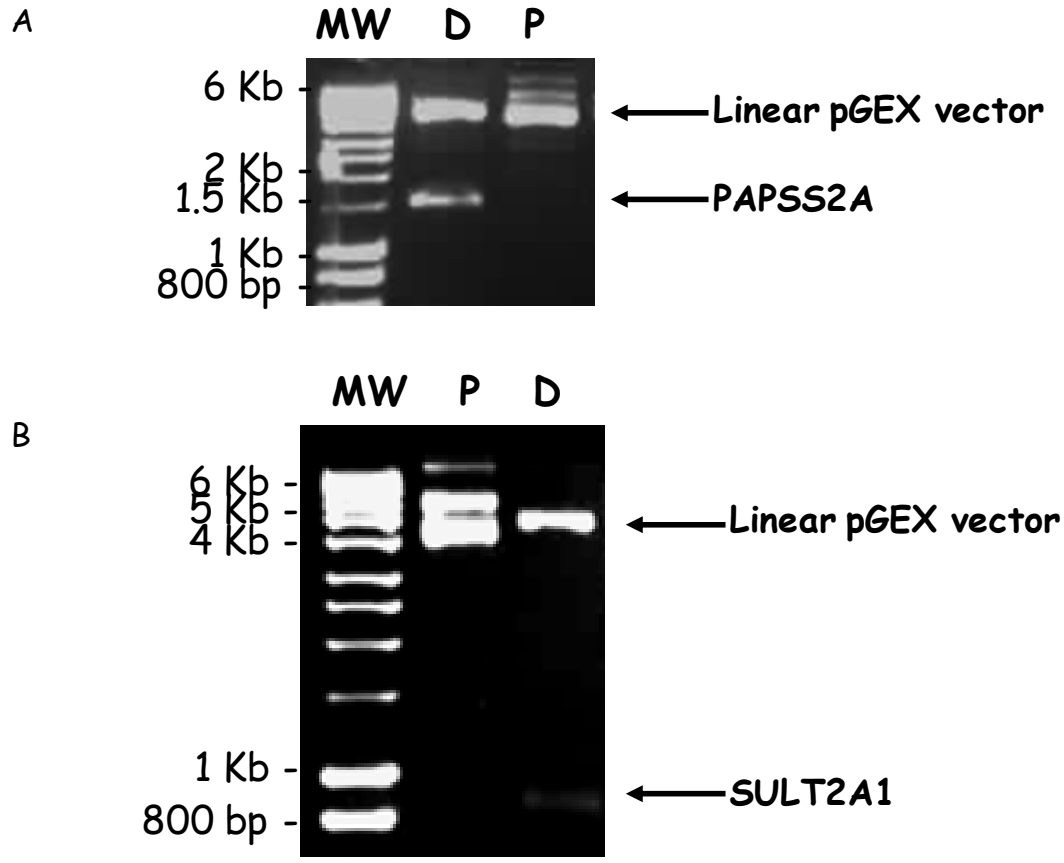

Figure 4-5 Restriction digestion of the WT pGEX-PAPSS2 and WT pGEX-SULT2A1 vector constructs. A, *Restriction digestion of pGEX-PAPSS2 vector (D) revealed a band of 1,600 bp, the appropriate size for PAPSS2a, and a band of 5,000 bp, corresponding to the linear pGEX vector.* ***B,*** *Restriction digestion of pGEX-SULT2A1 vector (D) revealed a band of 850 bp, the appropriate size for SULT2A1, and a band of 5,000 bp corresponding to the linear pGEX vector, confirming that both vectors contained an insert. Analysis of the undigested plasmids revealed bands corresponding to nicked and supercoiled DNA.*

4.3.2.2 ***Confirmation of generation of PGEX-mutant PAPSS2 constructs.***

Utilising the pGEX-6P-3-PAPSS2a-WT vector as a template, the PAPSS2a mutants (T48R, R329X and S475X) were generated using the Quickchange XL site-directed mutagenesis kit, as described in section 2.3.3.3. Specific primers were designed with the desired mutation in the centre, flanked each side by the unmodified WT sequence, as described in section 2.3.3.3 and are listed in (**Table 2-2**, primer pair 57-59). SDM reactions were performed utilising primer specific annealing temperatures and a final elongation of 68˚C for 5 minutes. Resultant constructs were sequenced as described in section 2.2.3.2, and compared to WT PAPSS2a, confirming the successful generation of mutant constructs and the absence of any other sequence alterations during this procedure.

4.3.3 Expression of WT-pGEX-6P-3-PAPSS2 and WT-pGEX-6P-3-SULT2A1 proteins

To amplify the WT constructs *E. coli* strain Alpha-select were transformed with WT-pGEX-PAPSS2a and WT-pGEX-SULT2A1 and cultured as described in section 2.5.1. Plasmid DNA was purified, as described in section 2.2.2. In order to express the fusion proteins the purified vectors were subsequently transformed into *E. coli* BL21 (DE3) cells (section 2.5.1), and protein expression induced by incubation with 50 nM or 1 mM IPTG, for the PAPSS2 and SULT2A1 cultures, respectively for 16 hours (section 2.5.1). For initial experiments bacterial cells were lysed utilising a commercially available lysis reagent (BugBuster, Novagen) and the cytosolic and membrane fractions isolated via centrifugation as described in section 2.5.3.

The induced soluble fractions were assayed by western blot analysis as described in section 2.5.8, utilising polyclonal specific antibodies for PAPSS2 and SULT2A1. Samples were assayed by SDS-electrophoresis adjacent to mouse adrenal total protein, which expresses SULT2A1 but not PAPSS2a, as a positive and negative control, respectively. Soluble fractions from both cultures were incubated with both specific antibodies (against PAPSS2 and SULT2A1). A distinct band of the correct size (~62 KDa; SULT2A1 protein 36 KDa, GST 26 KDa) was visualised in the supernatant fraction of the SULT2A1 culture (**Figure 4-6, A**), confirming the expression of the fusion protein, in this fraction. A larger band of ~70 KDa was also observed. No band of the appropriate size was observed in the mouse adrenal total protein negative control, however an unspecific band was visable (~62 KDa). Similarly, a distinct band of the expected size (~96 KDa; PAPSS2a protein 70 KDa, GST 26 KDa) was visible in the supernatant fraction of the PAPSS2a culture (**Figure 4-6, B**), confirming the successful expression of the fusion protein in this fraction. A smaller band (~75 KDa), which was of the expected size for native mouse PAPSS2 protein, without a GST tag, was visible in positive control. The absence of visible bands in the soluble fraction incubated with the alternate antibody (i.e, PAPSS2a incubated with the specific antibody against SULT2A1 and visa versa) confirmed that the antibodies were specific and did not cross-react with the GST tag present on both fusion proteins (**Figure 4-6**).

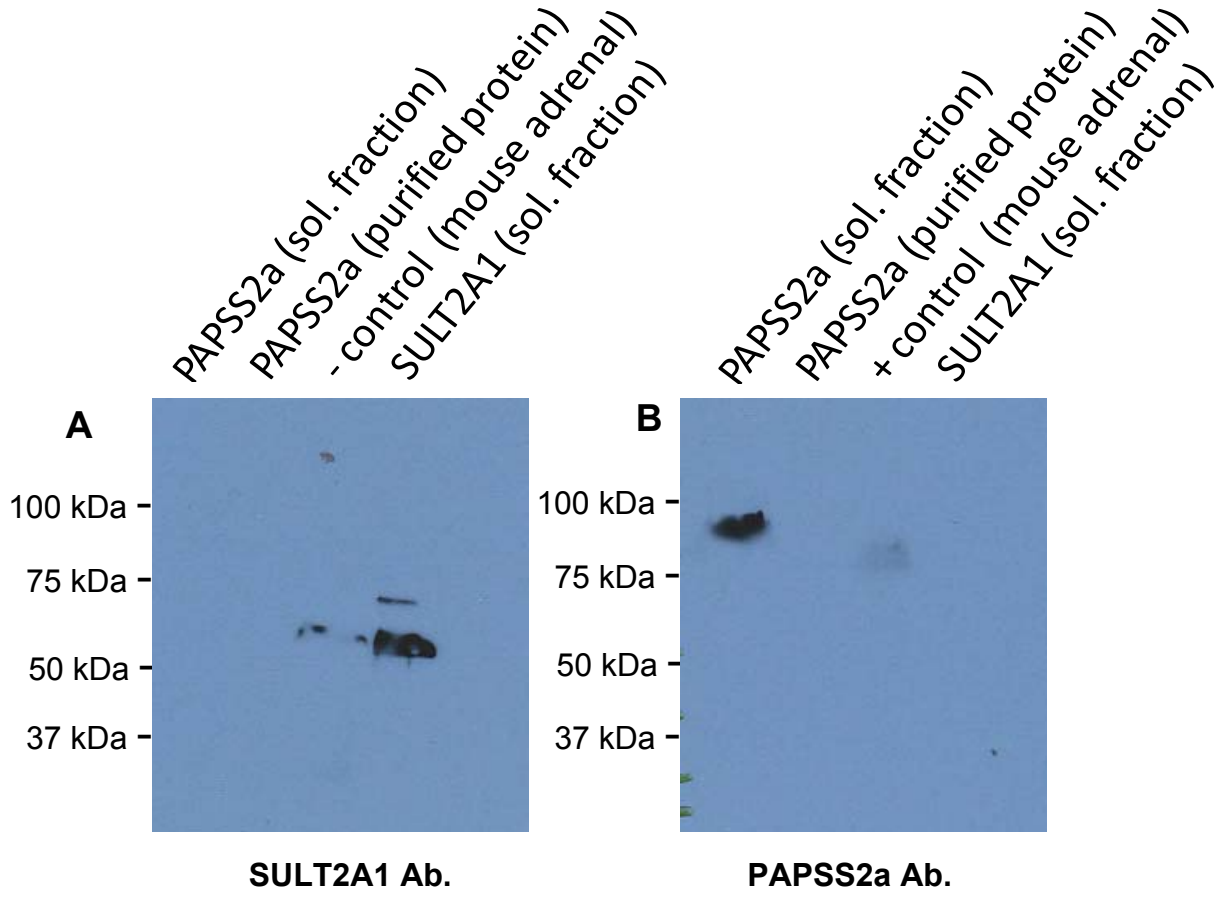

Figure 4-6 Western blot showing WT SULT2A1 and WT PAPSS2a expression. Panel A, Incubation with antibody against SULT2A1*. A distinct band of ~60 KDa, the expected size of SULT2A1-GST fusion protein, was detected in the induced soluble fraction of SULT expressing cells, confirming the expression of SULT2A1-GST fusion protein in this fraction. No band of the appropriate size was visible in the SULT2A1 negative (-) control. However, an unspecific band of ~62 KDa was observed. No band was visible in the soluble fraction of PAPSS2a-GST expressing cells, indicating that the antibody is specific and does not cross react with GST.* ***Panel B, Incubation with antibody against PAPSSA.*** *Similarly, a distinct band of ~96 KDa, the expected size of PAPSS2a-GST fusion protein, was visible in the soluble fraction of PAPSS2a-GST expressing cells and a smaller band of ~80 KDa, the expected MW of native mouse PAPSS2 protein (without GST tag), was detected in the PAPSS2a positive (+) control. This confirms expression of the PAPSS2a-GST fusion protein in the soluble fraction of PAPSS2a expressing cells. Again no band was visible in the soluble fraction of PAPSS2a-GST fusion protein expressing cells, indicating that the antibody is specific.*

4.3.4 ***Purification of the WT fusion proteins***

The SULT2A1-GST and PAPSS2a-GST fusion proteins were isolated from bacterial cell lysates as described in section 2.5.4, exploiting the affinity of the GST tagged fusion proteins for glutathione. Samples were washed with 4 ml of wash buffer and eluted into 2 ml (section 2.5.4). Samples were collected in 1 ml fractions during the purification procedure to prevent the dilution of the protein. Fractions were analysed by SDS-PAGE and coomassie blue staining (2.5.9). Analysis of fractions isolated from the soluble fraction of SULT2A1-GST expressing bacterial cells revealed a distinct band at ~62 KDa, the expected MW of SULT2A1-GST fusion protein in the elute and PBS wash fractions. This confirmed the presence a single isolated protein, which was thought to be SULT2A1-GST in these fractions (**Figure 4-7**). Similarly, analysis of the fractions isolated from the soluble lysate of PAPSS2a-GST expressing cells revealed a band of the appropriate MW of PAPSS2a-GST (~96 KDa) in the second elute and PBS wash fractions, (**Figure 4-8, A**), confirming the presence of a single isolated protein in these fractions. Western blot analysis of the fractions, using a polyclonal specific antibody against PAPSS2a (section 2.5.8) confirmed the protein in this fraction to be PAPSS2a (**Figure 4-8, B**).

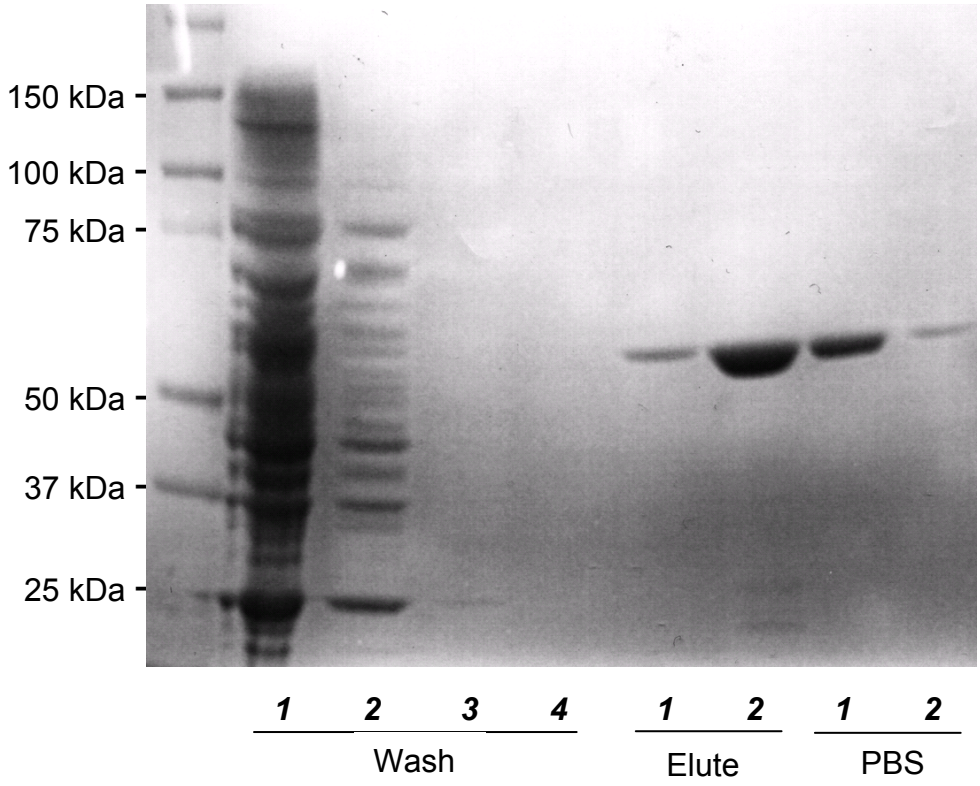

Figure 4-7 Purification of SULT2A1-GST fusion protein. *Purification fractions isolated from the soluble fraction of SULT2A1-GST expressing bacterial cells were assayed by SDS-electrophoresis and coomassie blue staining. A distinct band of the expected size of SULT2A1-GST (~62 KDa) was visible in the elute and PBS wash fractions, confirming the presence of a single isolated protein in these fractions.*

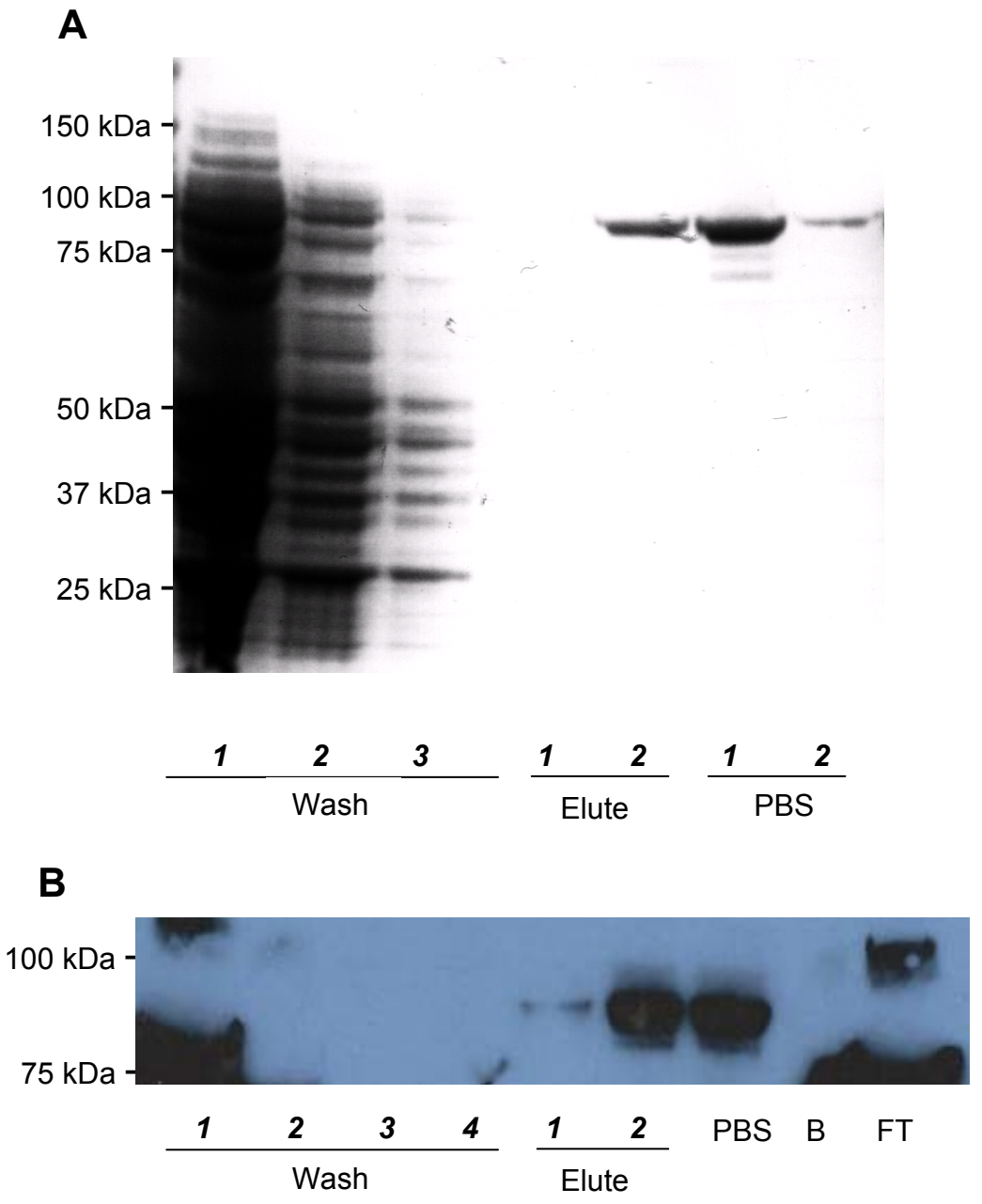

Figure 4-8 Purification of PAPSS2a -GST fusion protein. A*, Purification fractions isolated from the soluble fraction of PAPSS2a-GST expressing bacterial cells were assayed by SDS-electrophoresis and coomassie blue staining. A distinct band of the expected size of SULT-2A1-GST (~96 KDa) was visible in the elute and PBS wash fractions, confirming the presence of a single isolated protein in these fractions.* ***B****, Western blot analysis, utilising a specific antibody against PAPSS2a, confirmed the purified protein identified by coomassie staining to be PAPSS2a. B= beads following purification; FT= flow through.*

4.3.5 ***Functional analysis of purified WT SULT2A1-GST fusion protein***

The functional activity of the purified bacterially expressed putative WT SULT2A1-GST fusion protein was assessed via co-incubation with a tritiated form of the enzymes principle substrate, DHEA, and commercially available PAPS as described in section (2.6.4). Analysis of extracted steroids revealed production of the sulphated product, ^{3}H DHEAS (**Figure 4-9**), confirming that the purified protein was as expected SULT2A1 and that the purified protein retained enzymatic activity. Negative control reactions were performed in parallel, as other reactions but without the addition of SULT2A1-GST, which revealed no conversion of ^{3}H DHEA to ^{3}H DHEAS, confirming that SULT2A1 is required for conversion.

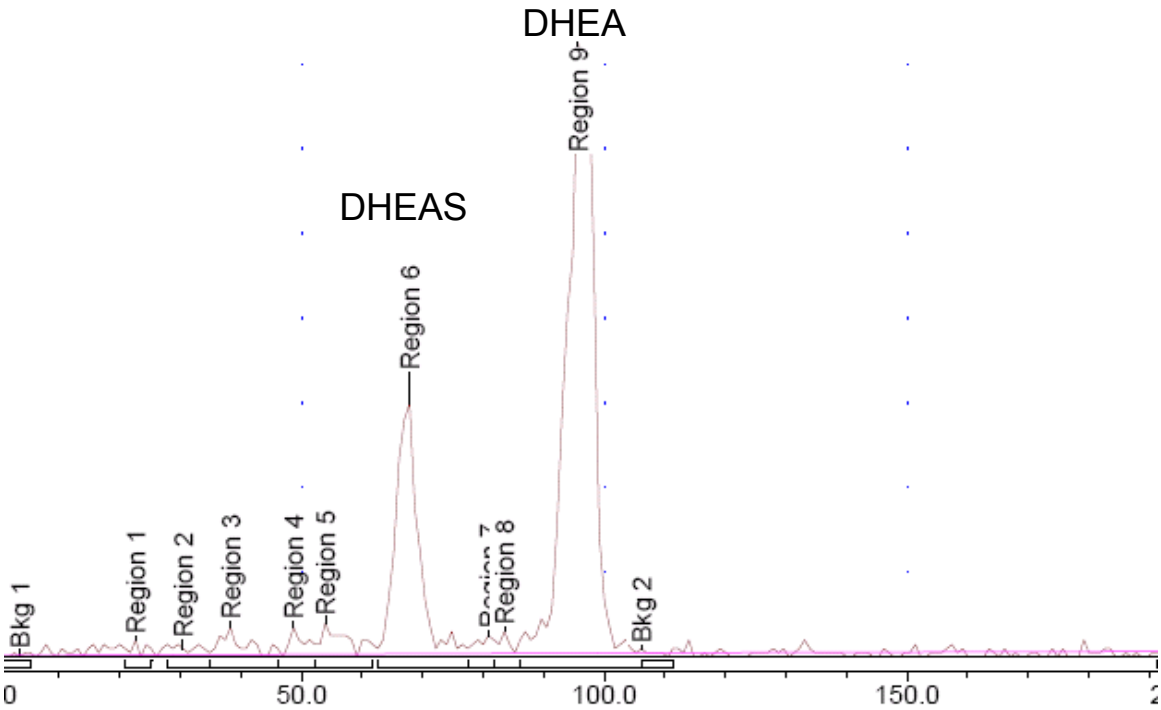

Figure 4-9 Enzymatic activity of purified SULT2A1-GST fusion protein. *The enzymatic activity of the isolated putative SULT2A1-GST protein was assessed via a DHEAS generation assay. Co-incubation of the isolated protein and ^{3}H DHEA resulted in the generation of ^{3}H DHEAS, confirming that the protein was SULT2A1 and that the isolated protein preparation retained functional activity.*

4.3.6 ***Functional analysis of purified WT PAPSS2-GST fusion protein***

Similarly, the functional activity of WT PAPSS-GST fusion protein was assessed by co-incubation with the confirmed active WT SULT2A1-GST purified fusion protein and a source of sulphate (S_2SO^4) as the substrate for the sulfation reaction. This coupled assay exploits the dependence of the catalytic activity of SULT2A1 on PAPS bio-availability, as described in section 2.6.4. However, following co-incubation of the purified fusion proteins, extraction and analysis of the steroids revealed the absence of DHEAS in the reaction mixture indicating that conversion of DHEA to DHEAS had not occurred. This suggested that the purified PAPSS2-GST fusion protein was inactive (**Figure 4-10**). Unfortunately PAPSS protein or APS (the intermediate product of PAPS synthesis) are not available commercially, so a positive control reaction could not be performed. However, as described above (section 4.3.5) SULT2A1 activity assays confirmed that the second step of the coupled reaction (the sulfation of DHEA to DHEAS) to be functional and the successful extraction and identification of DHEA and DHEAS, suggesting that a failure of the initial step of the reaction (the synthesis of PAPS by PAPSS2a, catalysed by PAPSS) was accountable for the lack of DHEAS generation.

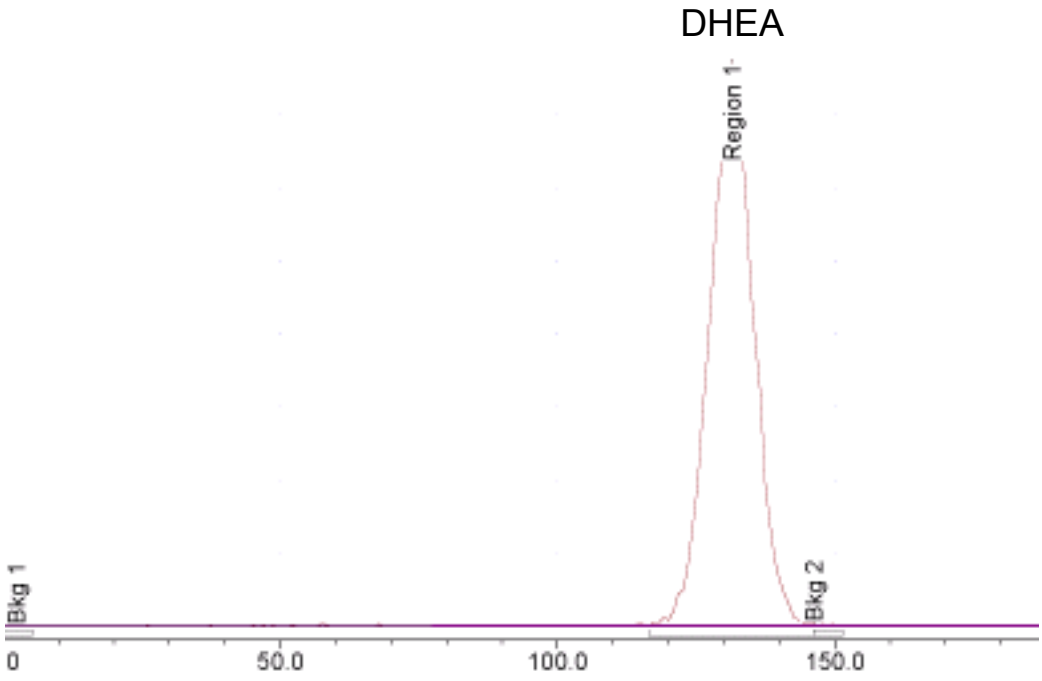

Figure 4-10 Purified WT PAPSS2a lack enzymatic activity. *The enzymatic activity of purified PAPSS2a-GST fusion protein was assessed via a coupled assay. Co-incubation of equal amounts of purified PAPSS2a-GST and SULT2A1-GST did not result in the generation of DHEAS from DHEA, confirming that the purified PAPSS2a protein was inactive.*

4.3.7 ***Cleavage of the WT PAPSS2a-GST fusion protein***

I hypothesised that the purified PAPSS2-GST fusion may not have functional activity due to the presence of the GST tag, which may result in incorrect protein folding. Therefore I attempted to cleave the fusion protein utilising a specific protease, to result in the purified unlabeled protein moiety. Recombinant PAPSS2-GST was induced and purified as above and described in section 2.5.1. Whilst still bound to glutathione sepharose the purified protein was co-incubated with PreScission protease (the specific protease for the pGEX system) as described in section 2.5.5, utilising 80 units of PreScission protease in 960 µl of PreScission protease buffer (see 2.5.5.2) (per 1 L of original bacterial culture). The reaction was incubated at 4˚C for four hours, as recommended by the supplier (G.E. Healthcare). The beads and supernatant were separated by centrifugation (section 2.5.5) Analysis of the fractions by SDS-electrophoresis and coomassie blue staining indicated the absence of unlabelled protein in the supernatant fraction (***Figure 4-10***).

A band of ~26 KDa, correlating to free GST, was detected in the pelleted fraction, suggesting that cleavage of the fusion protein had been successful. However, no band was visible at ~70 KDa, the MW of free PAPSS2a protein. In addition, some uncleaved PAPSS2a-GST fusion protein (~96 KDa) was identified in the pelleted fraction, showing that the reaction was not efficient. In an attempt to optimize the reaction the procedure was repeated with different incubation times (2 hours, 8 hours, 16 hours) and an increased concentration of PreScission protease (160 units/ reaction). However, all further reactions were also unsuccessful, producing similar

findings (data not shown). For all time-points analysed control reactions (which did not include precision protease) were performed and analysed as described above, adjacent to samples. A band of ~96 KDa correlating to uncleaved PAPSS2a-GST fusion protein was visible in the pelleted fraction of control reactions. However, no band at ~26 KDa was identified, indicating the absence of cleaved GST in the pelleted fraction. This confirmed that, as expected, in the absence of PreScission protease a cleavage reaction did not occur.

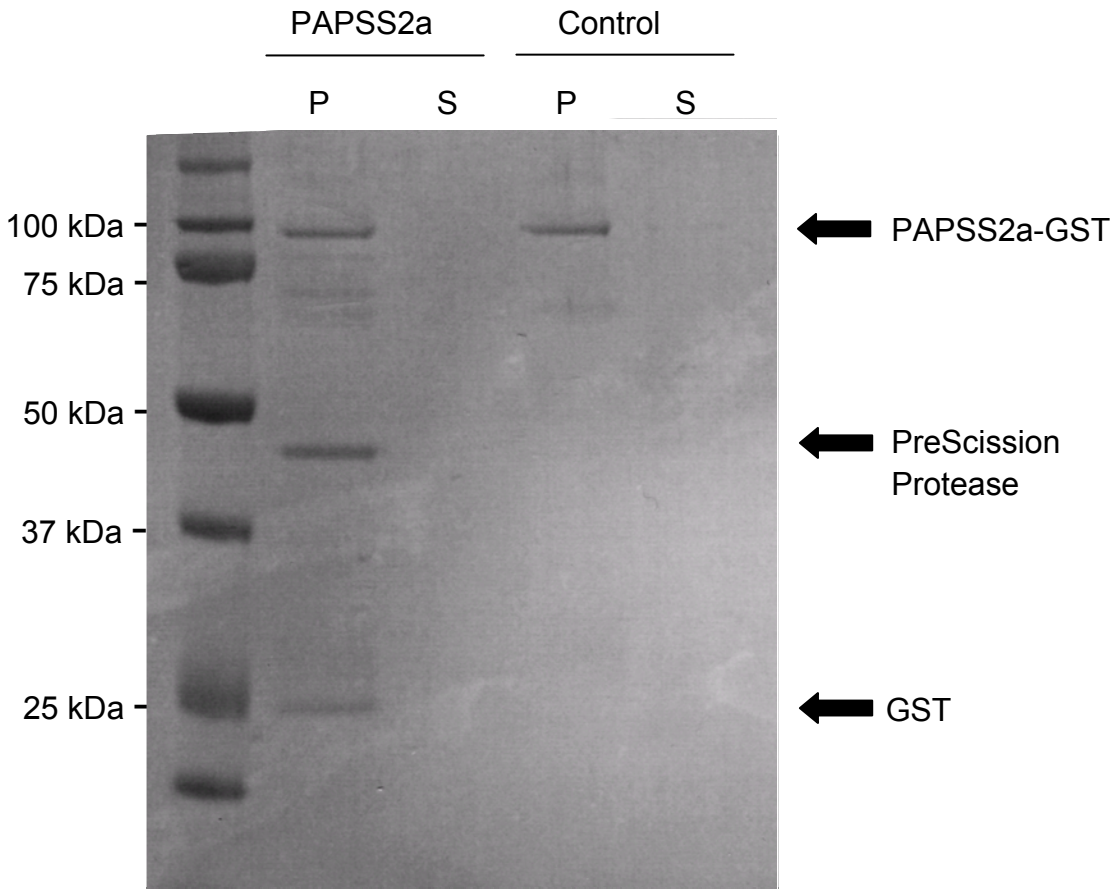

Figure 4-11 Cleavage of GST-PAPSS2a fusion protein. *PAPSS2a-GST fusion protein bound to glutathione sepharose beads was incubated with PreScission protease for 4 hours at 4˚C. The supernatant fraction (S), where uncleaved protein should reside, and the pelleted fraction (P), containing glutathione beads and bound protein, were isolated by centrifugation. A band of ~26 KDa, correlating to free GST, was detected in the pelleted fraction, suggesting that cleavage of the fusion protein had been successful. However, no band was visible at ~70 KDa, the MW of free PAPSS2a protein. In addition, some uncleaved PAPSS2a-GST fusion protein (~96 KDa) was identified in the pelleted fraction. Control reactions, performed as other experiments but without the addition of PreScission protease, had only one detectable band at ~96 KDa, correlating to uncleaved PAPSS2a-GST fusion protein, confirming that the protease was necessary for cleavage to occur.*

4.3.8 ***Functional activity of WT PAPSS2a expressing bacterial cell lysates***

Following the absence of observed functional PAPSS2a-GST fusion protein activity via the *in vitro* co-incubation assay and the unsuccessful cleavage of the GST moiety from the PAPSS2a-GST fusion protein, co-incubation assays were performed with the soluble fractions of PAPSS2a expressing *E.coli*. This decision was based on the hypothesis that the functional activity of the proteins may be lost during the purification procedure, and not as a consequence of the presence of the GST tag. In addition, consistent with this decision, we had previously detected PAPSS2a fusion protein in the soluble fraction of the bacterial cell lysates (section 4.3.3).

E.coli strain BL21 were transformed with pGEX-6P-3-PAPSS2a and pGEX-6P-3-SULT2A1, cultured and induced as described above and section 2.5.1. To enable the direct use of bacterial cell lysates in subsequent reactions, the cells were lysed with PBS/triton, and the soluble and membrane fractions separated by centrifugation as described in section 2.5.3. The total protein content of the bacterial soluble cell lysates were quantified (section 2.5.7) and 25 µg of each bacterial cell lysate (from WT PAPPS2a-GST and WT SULT2A1-GST expressing bacterial cells) was utilized to analyse PAPSS2a enzyme activity. This was performed, as described in 2.6.4, exploiting the dependence of the catalytic activity of SULT2A1 on PAPS bio-availability. Identification of extracted steroids revealed the generation of detectable ^{3}H DHEAS (**Figure 4-12**), indicating that the enzymes were both active. The soluble fraction of BL21 cells transformed with empty pGEX-6P-3 vector and cultured and induced as described above and in section 2.5.1, were utilised for negative control reactions, which were performed in parallel to experiments. The extraction and

identification of steroids from the negative control reaction revealed a lack of conversion of DHEA to DHEAS, confirming that the observed functional activity was not of bacterial origin.

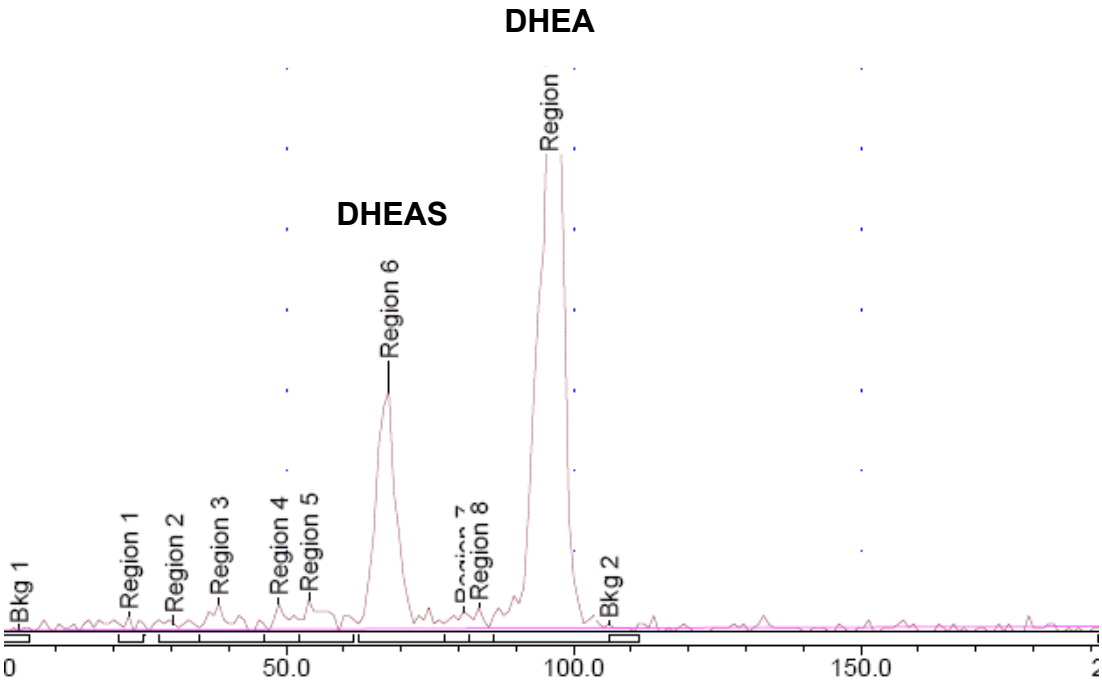

Figure 4-12 Enzymatic activity of bacterially expressed PAPSS2a-GST and SULT2A1-GST fusion proteins. *The soluble fractions of bacterial cells expressing PAPSS2a-GST and SULT2A1-GST were isolated by centrifugation. The activity of PAPSS2a-GST fusion protein, present in the bacterial soluble fraction, was assessed via a DHEAS generation assay, exploiting the requirement of SULT2A1 activity on the provision of PAPS by PAPSS. Extraction and identification of steroids following the reaction confirmed the conversion of DHEA to DHEAS, indicating that both PAPSS2a-GST and SULT2A1-GST proteins had functional activity.*

4.3.9 ***Functional activity of bacterially expressed mutant PAPSS2a***

To confirm the disease causing nature of the mutations identified in the affected patient (T48R and R329X) and assess the effect of the previously described PAPSS2a mutation (S475X) on DHEA sulfation, *E.coli* strain BL21 were transformed with the generated mutant constructs and cultured and induced as described in section 2.5.1. The soluble fractions of the bacterial cultures were isolated as described above and in section 2.5.3. To ensure the use of similar amounts of PAPSS2a proteins for *in vitro* analysis, the total protein content of the samples was quantified (section 2.5.7) and western blot analysis was performed as described in section 2.5.8, utilising a monoclonal human antibody to GST (**Figure 4-13**).

To assess the activity of the mutant proteins (T48R, R329X and S475X) co-incubation assays were performed as described in section 2.6.4 including 25 µg of WT or mutant PAPSS2a protein and 25 µg SULT2A1 protein. Quantification of the extracted steroids revealed reduced conversion of DHEA to DHEAS by the mutant proteins, confirming the inactivating nature of the mutations. No activity was detected for R329X and S475X and only minor residual activity for T48R (6.0±0.6% of wild-type PAPSS2 activity; **Figure 4-13**).

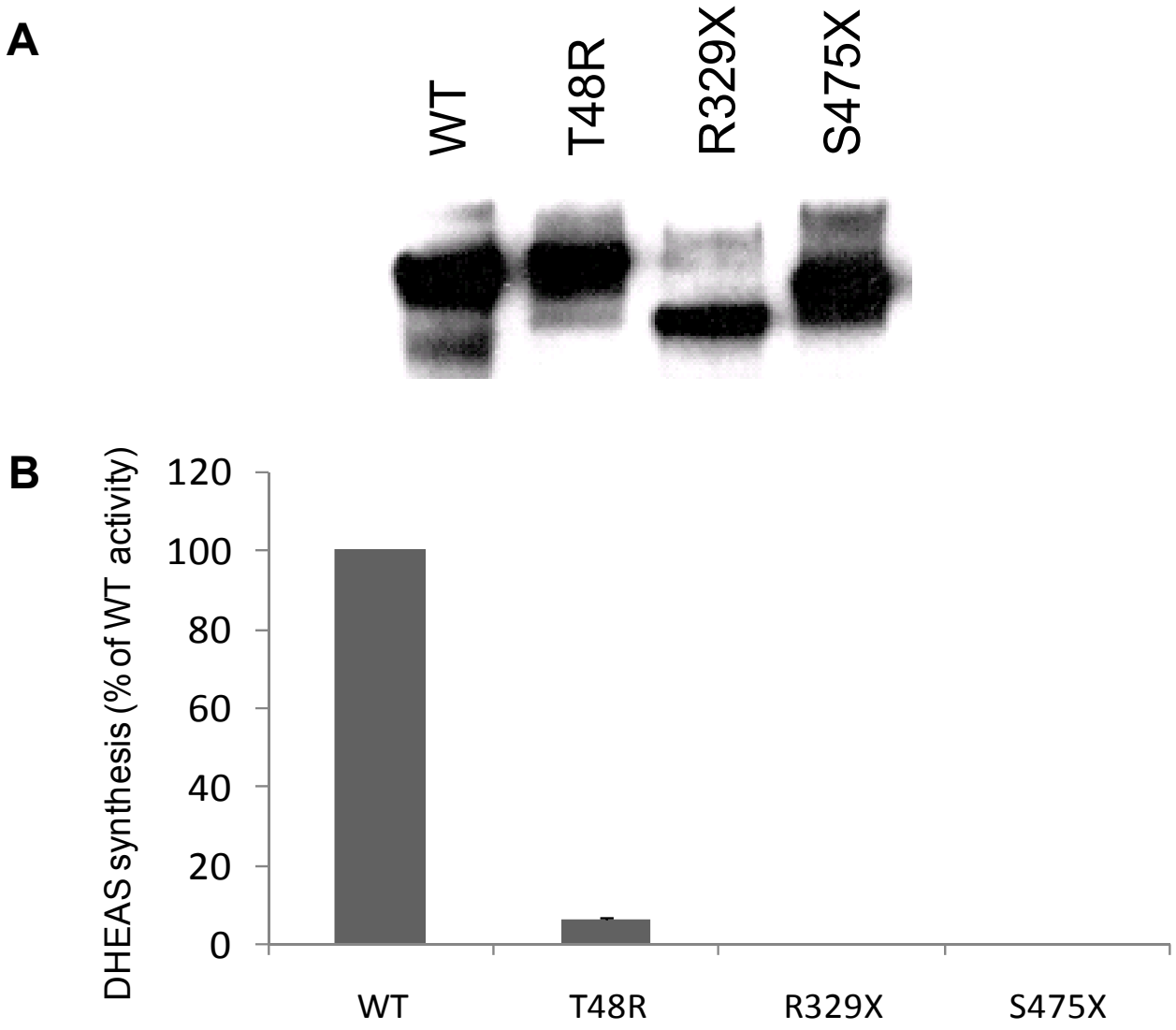

Figure 4-13 Confirmation of the inactivating nature of the PAPSS2 mutants by an in vitro DHEAS generation assay. *A, a representative Western Blot confirming equal PAPSS2 protein content for wild-type and mutant PAPSS2a preparations. Mutants R329X and S475X result in shorter proteins due to truncations within the early ATP sulfurylase domain of PAPSS2a. B, The enzymatic activity of bacterially expressed WT and mutant PAPSS2a was assessed using a coupled assay. Equal amounts of human DHEA sulfotransferase (SULT2A1) protein and human wild-type or mutant PAPSS2a proteins were co-incubated and the generation of DHEAS assessed. No activity was detected for R329X and S475X and only minor residual activity for T48R (6.0±0.6% of wild-type PAPSS2 activity), confirming the inactivating nature of the mutations.*

4.3.10 Analysis of PAPSS and SULT2A1 mRNA expression in foetal chondrocytes

The previously identified homozygous PAPSS2 mutation, S475X, manifests in affected individuals as Spondyloepimetaphyseal dysplasia (SEMD), Pakistani type (ul Haque et al., 1998),thought to be due to impaired proteoglycan sulfation in chondrocytes. However the expression of key enzymes of the DHEA/DHEAS shuttle have not been characterised within human chondrocytes. Therefore I examined the mRNA expression of SULT2A1, PAPSS1 and the two splice variants of PAPSS2, PAPPSS2a and PAPSS2b, in human foetal chondrocytes, in addition to human adult liver and adult and foetal adrenal, key sites of DHEA sulfation. Total RNA extraction was performed as described in section 2.4.1 and reverse transcribed as described in section 2.4.2. Conventional PCR was performed as described in section 2.4.3.2 using gene specific primers and conditions **Table 2-3**, primer pairs 52-54. Reactions were assayed by agarose gel electrophoresis as described in section 2.4.3.2. Amplification of PAPSS2 results in two distinct bands, corresponding to the two splice variants, PAPSS2a and PAPSS2b, which differ in size by five amino acids.

Amplification of PAPSS1 resulted in a band of the expected size for in all samples, indicating that this isoform is expressed in all tissues examined. Amplification of SULT2A1 resulted in a band of the correct size in adult liver and adult and foetal adrenal reactions, indicating that this enzyme is expressed in these tissues. A single band of the expected size for PAPSS2b was observed in adult liver, while a single band for the alternate isoform PAPSS2a, confirming only one splice variant is exclusively expressed in these tissues. In contrast, the amplification of PAPSS2

resulted in two detectable bands in the adult and foetal adrenal samples, indicating that the adrenal expresses both splice variants.

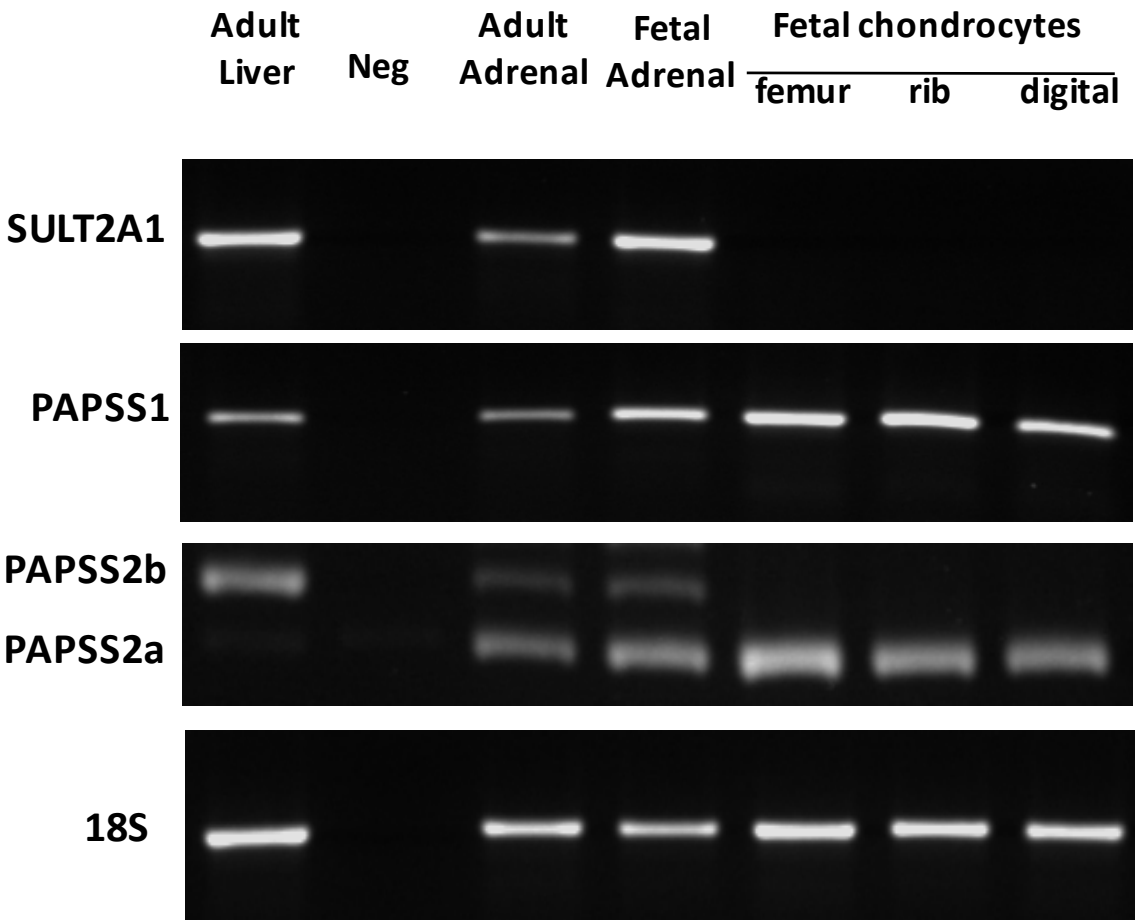

Figure 4-14 Tissue specific expression of the DHEA sulfation system. *The mRNA expression of key enzymes of the DHEA sulfation system was analysed by conventional PCR in human adult liver, adult and foetal adrenal, and foetal chondrocytes from three sites (femur, rib, digital). PAPSS1 expression was observed in all tissues examined. PAPSS2b was exclusively expressed in adult liver, while foetal chondrocytes express exclusively PAPSS2a. In contrast adult and foetal adrenal express both splice variants of PAPSS2. SULT2A1 expression was observed in adult liver and adult and foetal adrenal but not chondrocytes.*

4.3.11 Analysis of PAPSS and SULT2A1 mRNA expression in human tissues

I have demonstrated that the identified mutations in PAPSS2 impair SULT2A1 activity, resulting in the phenotype of the patient. However, it is unclear why PAPSS1, which is unaffected in the patient, cannot compensate for the loss of PAPSS2, preventing the clinical manifestation of androgen excess. I hypothesised that a possible explanation was the differential tissue expression of the two isoforms of PAPSS and SULT2A1.

The expression of SULT2A1 and the two PAPSS isoforms, PAPSS1 and PAPPS2 was examined in human adrenal, liver, ovary and testis. For these tissues commercially available pooled adult total RNA was obtained from Clontech, USA and reverse transcription was performed as described in section 2.4.2. Quantitative expression analysis was performed as described in section 2.4.3.3, utilising gene specific primers and probes, given in **Table 2-4**, primer pairs 29-32.

I observed that the adrenal and liver express abundant levels of SULT2A1 (dct ± SD; adrenal, 11.9 ± 0.1; liver, 11.3 ± 0.1), while the testis and ovary express relatively low levels (dct ± SD; testis, 18.6 ± 0.0; ovary, 20.8 ± 0.1). A similar expression pattern was observed for PAPSS2 (dct ± SD; adrenal, 12.7 ± 0.0; liver, 15.6 ± 0.1, testis, 16.5 ± 0.1; ovary, 14.9 ± 0.0) confirming the adrenal and liver are key sites of DHEA sulfation, co-expressing PAPPS2 and SULT2A1 at high levels. Conversely, I found the level of PAPSS1 expression to be highest in the gonads (dct ± SD; testis, 16.0 ± 0.0; ovary, 16.3 ± 0.0), while the adrenal and liver expressed relatively low levels (dct ± SD; adrenal, 17.4 ± 0.0; liver, 19.7 ± 0.2) of this isoform.

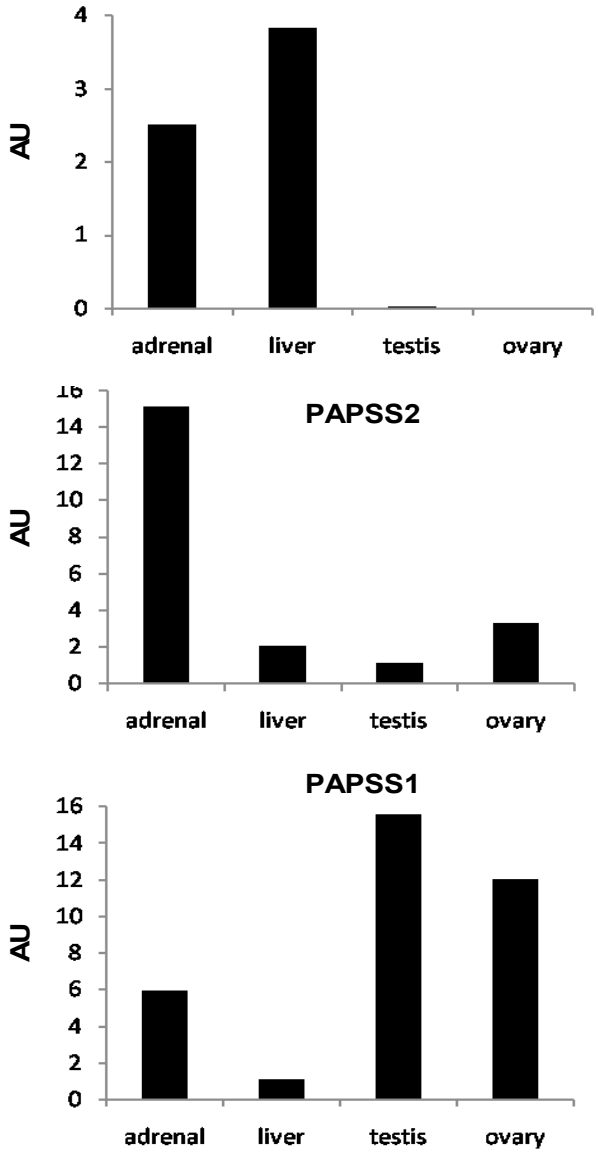

	SULT2A1	PAPSS2	PAPSS1
Adrenal	11.9 ± 0.1	12.7 ± 0.0	17.4 ± 0.0
Liver	11.3 ± 0.1	15.6 ± 0.1	19.7 ± 0.2
Testis	18.6 ± 0.0	16.5 ± 0.1	16.0 ± 0.0
Ovary	20.8 ± 0.1	14.9 ± 0.0	16.3 ± 0.0

Figure 4-15 Quantitative analysis of mRNA expression of SULT2A1, PAPSS1 and PAPSS2. *Adrenal and liver co-express relatively high levels of SULT2A1 and PAPSS2, confirming these tissues as key sites of DHEA sulfation. Conversely, ovary and testis express relatively low SULT2A1 and PAPSS2 mRNA levels, but contain high levels of PAPSS1 mRNA, that is found at much lower abundance in adrenal and liver. Results are expressed as arbitrary units (AU); ΔCt values are given in the table.*

4.4 Preliminary results

4.4.1 siRNA mediated knockdown of PAPSS1 and PAPSS2

I have shown that mutations in PAPSS2 may manifest as the phenotype of our patient due to the inability of PAPSS1 to compensate, possibly because of the tissue specific expression of the isoforms and SULT2A1. Another potential mechanism is that the relative importance of the PAPSS isoforms on DHEA sulfation could differ. In our future project I aim to further explore the potentially differential dependence of SULT2A1activity on the two PAPSS isoforms in a mammalian model system, utilising a shRNA approach. As I have shown the human adrenal expresses the complete DHEA sulfation system (PAPSS1, PAPSS2a, PAPSS2b and SULT2A1), making it a suitable model for our study, an adrenal cell line, NCI H295R has been used.

To validate DNA target sequences for subsequent shRNA knockdown, transient transfections were been performed using siRNA against PAPSS1 and PAPSS2. 48 hours post transfection, cells were harvested and total RNA was extracted as described in section 2.4.1, and reverse transcribed as described in section 2.4.2. Gene expression of PAPSS1 and PAPPS2 was assessed via real-time PCR, as described in section 2.4.3.3, utilising gene specific primer and probe (Table 2-4, primer pairs 52-54)**.** Statistical significance was assessed on raw ΔCt values and not transformed fold-changes by unpaired Student's t-test. Real-time mRNA analysis confirmed the specific knockdown of PAPSS1 and PAPSS2, 0.34 fold and 0.39 fold, respectively (**Figure 4-16**). Interestingly knockdown of one isoform results in the induction of the alternative isoform (PAPSS1, 1.48 fold; PAPSS2, 1.53 fold).

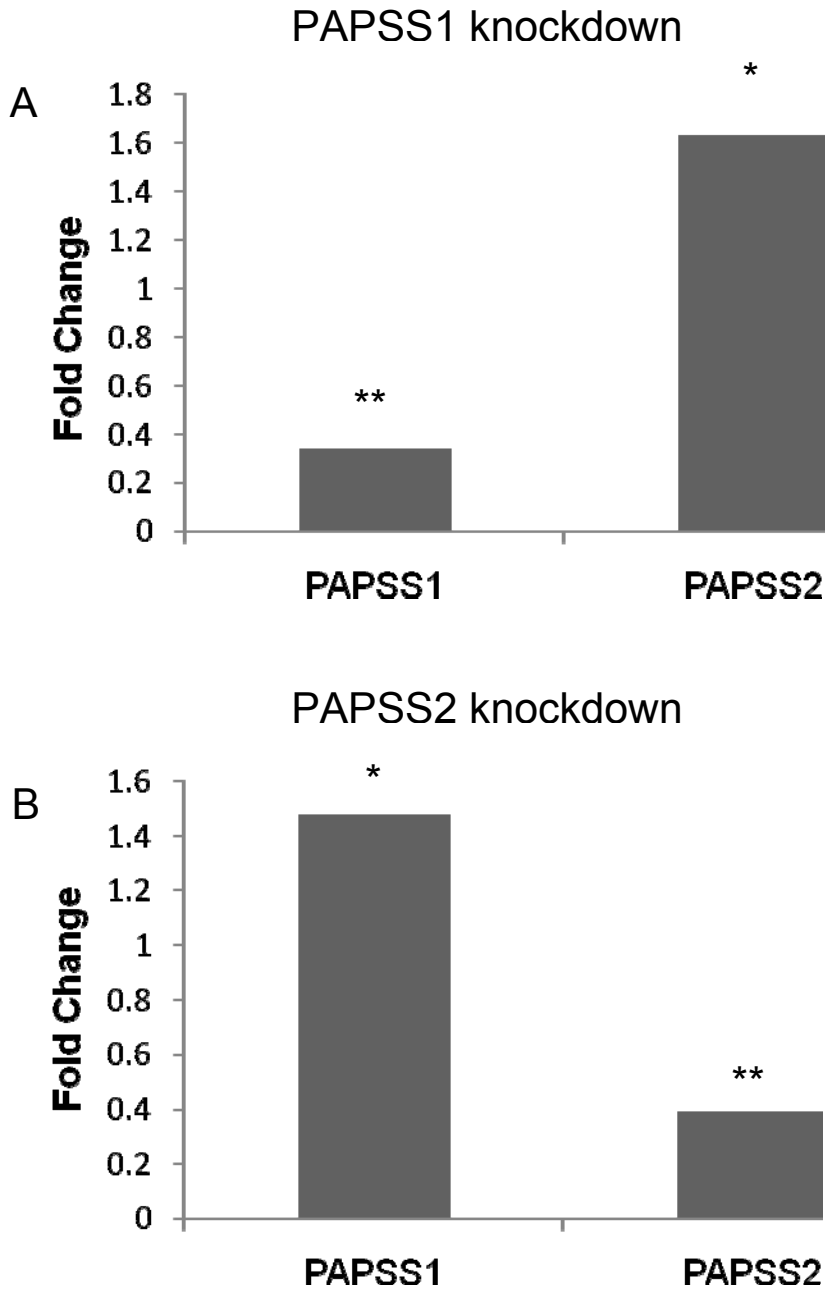

Figure 4-16 siRNA mediated knockdown of PAPSS isoforms. *NCI-H295R cells were transiently transfected with siRNA against PAPSS1 or PAPSS2. Gene expression was analysed 48 hours post transfection.* ***A, Knockdown of PAPSS1****. Real-time mRNA expression analysis confirmed specific knockdown of PAPSS1. Interestingly, knockdown of PAPSS1 resulted in the induction of PAPSS2 expression.* ***B, Knockdown of PAPSS2****. Similarly, mRNA analysis confirmed the knock-down of PAPSS2, which resulted in the induction of PAPSS1. Statistical significance (vs. scramble control) was assessed via Student's t-test. * P < 0.05, ** P < 0.01*

4.5 Discussion

In this chapter I have described our identification of a compound heterozygous mutation in *PAPSS2* as a novel monogenic cause of androgen excess. *PAPSS2* encodes human PAPS synthase 2, an enzyme which generates PAPS, the universal sulfate donor required for all sulfation reactions, including the sulfation of metabolically active DHEA to inactive DHEAS, catalysed by SULT2A1. As only unconjugated DHEA can be directly converted to androgens, our findings highlight the crucial role of DHEA sulfation by SULT2A1 as the regulator of human androgen synthesis, by showing that impaired sulfation increases the DHEA pool available for androgen synthesis. Although it has been speculated for some time, this is the first time it has been demonstrated *in vivo* that a deficiency in activity of SULT2A1 causes increased androgen production. Furthermore, our findings question the common use of elevated DHEAS levels as a determinate of androgen excess of adrenal origin and high androstenedione levels for diagnosing ovarian androgen excess. Using these criteria for our patient would have resulted in the incorrect diagnosis of androgen excess of ovarian origin, although her androgen excess results from a steroidogenic defect of the adrenal.

Our *in vitro* analysis included the heterogeneous mutations identified in our patient, T48R and R329X, and the previously described homozygous mutation, S475X (ul Haque et al., 1998). The previous mutation was identified in a large Pakistani Kindred affected by Spondyloepimetaphyseal dysplasia (SEMD), Pakistani type. In these patients, the homozygous S475X mutation manifests as significant, immediately apparent, short stature associated with short, bowed lower limbs, enlarged knee joints, kyphoscoliosis, and generalized brachydactyly, proposed to be due to a lack of

sulfation of proteoglycans, a key process of extracellular matrix formation (ul Haque et al., 1998) and therefore bone development and growth. Some features of the bone phenotype of our patient resemble those observed in the kindred, although the bone changes were much milder and only evident on follow-up examination. In addition, our patient had no long bone epiphyseal or metaphyseal changes.

I hypothesise that the difference in severity of the bone phenotype between the Pakistani kindred and our patient might be explained by the Pakistani kindred homozygously carrying the completely inactivating S475X mutation, while our patient has compound heterozygous mutations in different domains of the PAPSS2 protein. The maternally inherited mutation, R329X, results in a premature truncation of the ATP sulfurylase domain and thus renders the PAPSS2 protein void of activity as demonstrated by our in vitro functional assay. The paternally inherited mutation, T48R, is located in immediate proximity to the P loop structure within the APS kinase domain, a region previously identified as critical for ATP cleavage and thus for APS kinase activity, although our functional *in vitro* assessment demonstrated that the mutant retains about 5% of residual activity. This residual activity alone might account for the seemingly apparent less severe phenotype observed in our patient compared to the phenotype of the Pakistani kindred with a completely inactivated protein resulting from the homozygous S475X mutation.

In addition, as the mutations our patient possesses are in different domains we hypothesize that the unaffected domain of each allele may be functional, and enable the generation of PAPS by the concerted action of two separate semi-function protein molecules. This would result in a situation analogous to that of lower organisms, where ATP sufurylase and APS kinase are separate proteins encoded for by

separate genes. I am yet to establish if this hypothesis is correct, but hope to investigate this in future experiments, as described in chapter 5.

Our patient presented with androgen excess, premature pubarche, hyperandrogenic anovulation, and serum DHEAS levels below the limit of detection. Unfortunately the previous study was unable to ascertain if the affected females of the Pakistani kindred exhibited an androgen excess phenotype as the affected patients lived in an area difficult to access, the Afghanistan-Pakistani border, and provided only limited access to the female family members (Cohn DH, University of California, Los Angeles: personal communication).

As in humans there are two isoforms of PAPSS, PAPSS1 and PAPSS2 (Xu et al., 2000), it is currently unclear why ubiquitously expressed PAPSS1 cannot compensate for a loss of PAPSS2 activity and abrogate the presentation of a phenotype, despite 80% amino acid identity, identical domain structure and similar tertiary structure (Xu et al., 2000). However, previous *in vitro* expression studies have demonstrated a 10- to 15-fold higher catalytic efficiency for PAPSS2 (Fuda et al., 2002) and it is therefore possible that PAPSS1 alone is not sufficient for PAPS provision in tissues with a high rate of sulfation, such as adrenal and liver, in which I have demonstrated that *PAPSS2* mRNA expression is considerably higher than that of PAPSS1. Interestingly, the opposite was observed to be true in gonads, with ovary and testis expressing relatively high levels of *PAPSS1* mRNA and low levels of *SULT2A1* and *PAPSS2.* The complexity of this situation is further increased when the cellular localization of key enzymes of the DHEA/ DHEAS shuttle are considered. Recently, Besset et al. have demonstrated that in yeast ectopically expressed human PAPSS1 localizes to the nucleus of yeast, mediated by a catalytically dispensable 21

amino acid sequence at the amino terminus. In contrast, ectopically expressed PAPSS2 localises to the cytoplasm, the site of SULT2A1 expression, but translocates to the nucleus when co-expressed with PAPSS1. To date the relative importance of the two isoforms of PAPSS on DHEA sulfation has not been investigated. Furthermore, it is unclear if a PAPS translocase enables influx to the nucleus, as it does from the golgi apparatus (Ozeran et al., 1996a; Ozeran et al., 1996b), or furthermore, if the nucleus is a site of PAPS utilization by sulphotransferases, which is currently only known to occur in the cytoplasm and golgi apparatus (Negishi et al., 2001). However, it is possible that co-localisation is necessary for PAPSS to play a role in SULTA1 activity. I aim to investigate this hypothesis in future experiments.

Our preliminary findings utilising an adrenal cell model demonstrate that siRNA mediated knockdown of one isoform of PAPSS results in a putatively compensatory increase in expression of the alternate isoform. Interestingly, very recently, Fu et al have demonstrated that transient knockdown of PAPSS2 in HepG2 cells results in the induction of SULT2A1 via the nuclear receptor LXR. I aim to establish if this finding is mirrored in an adrenal cell model, and is true for both isoforms. Furthermore, it is currently unclear if a compensatory increase in SULT2A1 and the alternate PAPSS isoform, can maintain SULT2A1 activity. Again, I hope to investigate some of these complexities in future investigations, proposed in chapter 5.

In addition, the relevance of the two splice variants of *PAPSS2* on DHEA sulfation, or normal bone physiology is yet to be determined. mRNA analysis has demonstrated that the major sites of DHEA sulfation, the adrenal and liver, express *SULT2A1* and

PAPSS2b. While the shorter variant, lacking exon 7B, is expressed only in the adrenal. By contrast foetal chondrocytes from three different locations of the skeletal system only expressed *PAPSS2a,* but not *PAPSS2b* and also lacked *SULT2A1* expression. *PAPSS1* was expressed in all tissues examined. Unfortunately the limited difference between the two splice variants (5 amino acids) prohibits the selective knockdown of the varients and hinders their identification by western blot analysis.

Initially I purified PAPSS2 and SULT2A1 for functional analysis with the DHEAS generation assay. However, I was subsequently unable to detect any activity. It is unclear why this is the case as protein quantification and western blot analysis revealed significant concentrations of the purified proteins and no detectable degradation products. However, I was able to overcome this problem by quantifying total protein concentrations, and confirming consistent quantities of the over-expressed protein by western blot analysis. I also had difficulty, cleaving the GST moiety of the fusion protein to result in an untagged protein. However, further analysis with cytosolic cell lysates revealed this not to be necessary for protein function. As the individual GST moiety was detectable I propose this was due to degradation of the protein, possibly due to incorrect protein folding.

In conclusion, in this chapter I have presented our finding of a novel molecular cause of androgen excess- inactivating mutations in the sulfate donor enzyme PAPSS2. These findings highlight the critical role of DHEA sulfation in the regulation of human androgen synthesis. Our patient presented with androgen excess manifesting with premature pubarche and later with hirsutism, acne and secondary amenorrhea, thus fulfilling current diagnostic criteria for polycystic ovary syndrome and supportive of a

previously suggested link between premature pubarche and polycystic ovary syndrome. Future studies are needed to determine the frequency and functional consequences of *PAPSS2* sequence variants in well characterized cohorts of patients with premature pubarche and polycystic ovary syndrome, to further define the role of PAPSS2 in the pathogenesis of these androgen excess disorders.

5 Chapter 5: Final conclusions and future directions

5.1 Final conclusions

This thesis proficiently demonstrates the importance of the regulation of DHEA bioavailability. In humans this is performed in a tissue-specific manner, via the interconversion of DHEA with inactive DHEAS and the downstream metabolism of DHEA to active sex steroids and their precursors. Via the identification of a novel monogenic cause of androgen excess, I have demonstrated that abrogation of DHEA metabolism can result in the manifestation of pathophysiological conditions. This thesis also supports the concept, that in contrast to previous dogma, DHEA and DHEAS have tissue-specific direct effects, further highlighting the importance of the regulation of the circulating and local levels of these hormones.

5.2 Future directions

The work presented in this thesis demonstrates that DHEA has profound effects on the human adipocyte, attenuating adipogenesis, while enhancing glucose uptake, opposing the effects of glucocorticoids. These findings suggest that DHEA may have potent effects on human energy homeostasis *in vivo* and thereby be a promising therapeutic strategy for the treatment of obesity and diabetes. However, prior to future studies *in vivo* it would be of interest to further investigate the effects of DHEA *in vitro* which would provide a greater understanding of the molecular mechanisms of DHEA action and aid a more accurate prediction of the metabolic effects of DHEA. In addition to adipogenesis, adipocyte tissue homeostasis is also dependent on the hypertrophy of pre-existing adipocytes, which involves numerous metabolic processes such as fatty acid influx, lipogenesis (triglyceride accumulation), lipolysis

(triglyceride mobilization) and β-oxidation, all of which are regulated by glucocorticoids to some degree (Berdanier, 1989; Mantha et al., 1999; Samra et al., 1998). I propose that DHEA, via the inhibition of the local amplification of glucocorticoids, will modulate these processes. Therefore, firstly it would be of interest to investigate the effect of DHEA on these pathways, which could be performed using radiolabelled substrates for these reactions, and analysing their incorporation or metabolism. This would elucidate the effect of DHEA on mature adipocytes in addition to preadipocytes and identify the pathway by which glucose DHEA stimulated increased uptake of glucose is metabolised, ultimately establishing the net effect of DHEA on adipose tissue homeostasis, and thus help predict if the beneficial effects of DHEA presented in this thesis are likely to be maintained *in vivo*.

Glucocorticoid excess, androgen excess and the metabolic syndrome are associated with a bias for increased intra-abdominal adipose tissue mass, which itself is associated with increased cardiovascular disease risk factors. Therefore a successful pharmaceutical therapy for these conditions would be required to target the visceral adipose depot exclusively or in addition to the subcutaneous depot. The work in this thesis has been performed utilising Chub-S7 cells, a subcutaneous cell line. It is known that the expression of 11β-HSD1 and GR is greater in omental than subcutaneous adipose tissue depot (Bujalska et al., 2006) and therefore it is likely that DHEA may have an even more potent antiadipogenic effect at this site. Further studies using human primary cultures of subcutaneous and omental adipocytes would identify the depot specific effects of DHEA, confirming if this hypothesis is correct, which would help to establish the effects of DHEA *in vivo,* and if DHEA, or an analogous compound, would be a suitable treatment for these conditions.

Previous *in vivo* murine studies have shown that DHEA has beneficial effects on obesity and insulin sensitivity (Cleary and Zisk, 1986; Coleman, 1988; Coleman et al., 1982; Lea-Currie et al., 1997a; Lea-Currie et al., 1997b; Mohan et al., 1990; Shepherd and Cleary, 1984; Tagliaferro et al., 1986), however it is unclear if these beneficial effects are mediated exclusively via a direct effect on the adipocyte or via effects on other metabolic tissues, namely skeletal muscle and liver, which also contribute to the pathogenesis of these conditions. Furthermore it is unclear if DHEA modulates adipocyte homeostasis *in vivo*, indirectly via an alternate tissue, in addition to the direct effects I have observed *in vitro.* Therefore it would be interesting to evaluate the direct effect of DHEA on these tissues, which would contribute to a metabolic phenotype *in vivo,* and the indirect effect of DHEA on adipose tissue via these tissues. These experiments could be performed using primary cultures of human cells or human cell lines and the indirect effects of DHEA on these tissues could be assessed by co-culturing different cell types. This would provide a greater understanding of the physiological effects of DHEA *in vivo*.

The work in this thesis has shown that the tissue specific metabolism of DHEA is an important regulator of its local effects. It would therefore be interesting to characterise the conversion of DHEA in adipose tissue from different disease states, such as PCOS, obesity and diabetes, to see if the expression or activity of DHEA metabolising enzymes is altered in the affected individuals, as is known to occur in aging (Hammer et al., 2005a). Of particular interest would be PCOS patients, who paradoxical to our findings have elevated circulating levels of DHEA, but display central obesity. This would help identify the molecular pathogenesis of these conditions and potentially identify a novel therapeutic target for their treatment.

The work in this thesis has identified a novel monogenic adrenocortical cause of androgen excess. The phenotype of our patient differs from the previously identified homozygous *PAPSS2* mutation (S475X) which I propose may be due to the patient identified in this thesis having compound heterogeneous mutation in PAPSS2 gene, which are in differing domains. Each unaffected allele may be functional, and enable the generation of PAPS by the concerted action of two separate semi-function protein molecules, in a situation analogous to that of lower organisms, where ATP sufurylase and APS kinase are separate proteins encoded for by separate genes (Lyle et al., 1994b). This could be investigated by performing co-incubation assays of the two mutant proteins, R329X and T48R, and WT SULT2A1 and assessing the effect of the mutants on SULT2A1 activity, as performed in this thesis. This would also provide a greater understanding of PAPSS2 activity and thus androgen synthesis in humans, which will assist the identification of further genetic causes of androgen excess and PCOS, and identify targets for potential therapeutic intervention.

The work in this thesis has identified a mutation in *PAPSS2* gene and shown that a loss of function results in androgen excess. However, it is not fully clear why unaffected PAPSS1 cannot compensate for the loss of PAPSS2. I propose this may be due to the differential importance of the two isoforms on SULT2A1 activity and have begun to investigate this utilising siRNA specific knockdown of the two isoforms, with the preliminary data presented in chapter 4. Our initial findings show that knockdown of the one isoform of PAPSS1 appears to increase the expression of the second isoform. In addition, very recently, Fu et al have demonstrated that siRNA mediated knockdown of PAPSS2 in HepG2 cells results in induction of SULT2A1 via the nuclear receptor LXR (Fu J). Therefore it would be very interesting to identify

firstly, if SULT2A1 expression is also increased in an adrenal cell model by knockdown of PAPSS2, secondly if this putative increase occurs following the knockdown of PAPSS1, and thirdly, if the putative compensatory increase in expression of the opposing isoform and SULT2A1 maintains SULT2A1 activity. However, it is possible that the localisation of the two PAPSS isoforms, in addition to their expression is also important for the provision of PAPS to different sulphotransferases. A recent study investigating the localisation of the two PAPSS isoforms in mammalian cells has reported that PAPSS1 is localised to the nucleus, as is PAPSS2 when co-expressed with PAPSS1 (Besset et al., 2000). However PAPSS2 expression, in the absence of PAPSS1 is localised to the cytoplasm. Therefore, I aim to investigate the localization of the two isoforms of PAPPS in an adrenal cell line. It is currently unclear if the co-localisation of PAPSS and SULT2A1 is necessary for or modulates SULTA1 activity. Therefore, if differing PAPSS expression is detected I aim to investigate how this impacts on SULT2A1 activity via enzymatic activity assays. Again, these studies will help elucidate the molecular mechanisms of human androgen synthesis and therefore may assist the identification of therapeutic targets for the treatment of diseases with altered androgen synthesis.

6 References

Accili, D., and Arden, K. C. (2004). FoxOs at the crossroads of cellular metabolism, differentiation, and transformation. Cell *117*, 421-426.

Adams, J., Polson, D. W., and Franks, S. (1986). Prevalence of polycystic ovaries in women with anovulation and idiopathic hirsutism. Br Med J (Clin Res Ed) *293*, 355-359.

Agarwal, A. K., Monder, C., Eckstein, B., and White, P. C. (1989). Cloning and expression of rat cDNA encoding corticosteroid 11 beta-dehydrogenase. J Biol Chem *264*, 18939-18943.

Agarwal, A. K., Tusie-Luna, M. T., Monder, C., and White, P. C. (1990). Expression of 11 beta-hydroxysteroid dehydrogenase using recombinant vaccinia virus. Mol Endocrinol *4*, 1827-1832.

Aksoy, I. A., Sochorova, V., and Weinshilboum, R. M. (1993). Human liver dehydroepiandrosterone sulfotransferase: nature and extent of individual variation. Clin Pharmacol Ther *54*, 498-506.

Albiston, A. L., Obeyesekere, V. R., Smith, R. E., and Krozowski, Z. S. (1994). Cloning and tissue distribution of the human 11 beta-hydroxysteroid dehydrogenase type 2 enzyme. Mol Cell Endocrinol *105*, R11-17.

Allolio, B., and Arlt, W. (2002). DHEA treatment: myth or reality? Trends Endocrinol Metab *13*, 288-294.

Alperin, E. S., and Shapiro, L. J. (1997). Characterization of point mutations in patients with X-linked ichthyosis. Effects on the structure and function of the steroid sulfatase protein. J Biol Chem *272*, 20756-20763.

Altiok, S., Xu, M., and Spiegelman, B. M. (1997). PPARgamma induces cell cycle withdrawal: inhibition of E2F/DP DNA-binding activity via down-regulation of PP2A. Genes Dev *11*, 1987-1998.

Amato, P., and Simpson, J. L. (2004). The genetics of polycystic ovary syndrome. Best Pract Res Clin Obstet Gynaecol *18*, 707-718.

Amri, E. Z., Dani, C., Doglio, A., Grimaldi, P., and Ailhaud, G. (1986). Coupling of growth arrest and expression of early markers during adipose conversion of preadipocyte cell lines. Biochem Biophys Res Commun *137*, 903-910.

Anderson, L. A., McTernan, P. G., Barnett, A. H., and Kumar, S. (2001). The effects of androgens and estrogens on preadipocyte proliferation in human adipose tissue: influence of gender and site. J Clin Endocrinol Metab *86*, 5045-5051.

Anderson, L. A., McTernan, P. G., Harte, A. L., Barnett, A. H., and Kumar, S. (2002). The regulation of HSL and LPL expression by DHT and flutamide in human subcutaneous adipose tissue. Diabetes Obes Metab *4*, 209-213.

Apostolova, G., Schweizer, R. A., Balazs, Z., Kostadinova, R. M., and Odermatt, A. (2005). Dehydroepiandrosterone inhibits the amplification of glucocorticoid action in adipose tissue. Am J Physiol Endocrinol Metab *288*, E957-964.

Apter, D., Butzow, T., Laughlin, G. A., and Yen, S. S. (1994). Accelerated 24-hour luteinizing hormone pulsatile activity in adolescent girls with ovarian hyperandrogenism: relevance to the developmental phase of polycystic ovarian syndrome. J Clin Endocrinol Metab *79*, 119-125.

Apter, D., and Sipila, I. (1993). Development of children and adolescents: physiological, pathophysiological, and therapeutic aspects. Curr Opin Obstet Gynecol *5*, 764-773.

Arlt, W. (2004a). Dehydroepiandrosterone and ageing. Best Pract Res Clin Endocrinol Metab *18*, 363-380.

Arlt, W. (2004b). Dehydroepiandrosterone replacement therapy. Semin Reprod Med *22*, 379-388.

Arlt, W. (2007). P450 oxidoreductase deficiency and Antley-Bixler syndrome. Rev Endocr Metab Disord *8*, 301-307.

Arlt, W., and Allolio, B. (2003). DHEA replacement in adrenal insufficiency. J Clin Endocrinol Metab *88*, 4001; author reply 4001-4002.

Arlt, W., Callies, F., Koehler, I., van Vlijmen, J. C., Fassnacht, M., Strasburger, C. J., Seibel, M. J., Huebler, D., Ernst, M., Oettel, M.*, et al.* (2001). Dehydroepiandrosterone supplementation in healthy men with an age-related decline of dehydroepiandrosterone secretion. J Clin Endocrinol Metab *86*, 4686-4692.

Arlt, W., Callies, F., van Vlijmen, J. C., Koehler, I., Reincke, M., Bidlingmaier, M., Huebler, D., Oettel, M., Ernst, M., Schulte, H. M., and Allolio, B. (1999). Dehydroepiandrosterone replacement in women with adrenal insufficiency. N Engl J Med *341*, 1013-1020.

Arlt, W., and Stewart, P. M. (2005). Adrenal corticosteroid biosynthesis, metabolism, and action. Endocrinol Metab Clin North Am *34*, 293-313, viii.

Auchus, R. J. (2004). Overview of dehydroepiandrosterone biosynthesis. Semin Reprod Med *22*, 281-288.

Auchus, R. J., Geller, D. H., Lee, T. C., and Miller, W. L. (1998a). The regulation of human p450c17 activity: relationship to premature adrenarche, insulin resistance and the polycystic ovary syndrome. Trends Endocrinol Metab *9*, 47-50.

Auchus, R. J., Lee, T. C., and Miller, W. L. (1998b). Cytochrome b5 augments the 17,20-lyase activity of human P450c17 without direct electron transfer. J Biol Chem *273*, 3158-3165.

Auphan, N., DiDonato, J. A., Rosette, C., Helmberg, A., and Karin, M. (1995). Immunosuppression by glucocorticoids: inhibition of NF-kappa B activity through induction of I kappa B synthesis. Science *270*, 286-290.

Avram, M. M., Avram, A. S., and James, W. D. (2007). Subcutaneous fat in normal and diseased states 3. Adipogenesis: from stem cell to fat cell. J Am Acad Dermatol *56*, 472-492.

Azziz, R., Sanchez, L. A., Knochenhauer, E. S., Moran, C., Lazenby, J., Stephens, K. C., Taylor, K., and Boots, L. R. (2004). Androgen excess in women: experience with over 1000 consecutive patients. J Clin Endocrinol Metab *89*, 453-462.

Bader, T., Zoumakis, E., Friedberg, M., Hiroi, N., Chrousos, G. P., and Hochberg, Z. (2002). Human adipose tissue under in vitro inhibition of 11beta-hydroxysteroid dehydrogenase type 1: differentiation and metabolism changes. Horm Metab Res *34*, 752-757.

Bandurski, R. S., and Lipmann, F. (1956). Studies on an oxalacetic carboxylase from liver mitochondria. J Biol Chem *219*, 741-752.

Barber, T. M., McCarthy, M. I., Wass, J. A., and Franks, S. (2006). Obesity and polycystic ovary syndrome. Clin Endocrinol (Oxf) *65*, 137-145.

Barnes, P. J., and Adcock, I. M. (2003). How do corticosteroids work in asthma? Ann Intern Med *139*, 359-370.

Baulieu, E. E. (1996). Dehydroepiandrosterone (DHEA): a fountain of youth? J Clin Endocrinol Metab *81*, 3147-3151.

Baulieu, E. E., Thomas, G., Legrain, S., Lahlou, N., Roger, M., Debuire, B., Faucounau, V., Girard, L., Hervy, M. P., Latour, F.*, et al.* (2000). Dehydroepiandrosterone (DHEA), DHEA sulfate, and aging: contribution of the DHEAge Study to a sociobiomedical issue. Proc Natl Acad Sci U S A *97*, 4279-4284.

Beishuizen, A., Thijs, L. G., and Vermes, I. (2002). Decreased levels of dehydroepiandrosterone sulphate in severe critical illness: a sign of exhausted adrenal reserve? Crit Care *6*, 434-438.

Belanger, C., Hould, F. S., Lebel, S., Biron, S., Brochu, G., and Tchernof, A. (2006). Omental and subcutaneous adipose tissue steroid levels in obese men. Steroids *71*, 674-682.

Ben-Nathan, D., Padgett, D. A., and Loria, R. M. (1999). Androstenediol and dehydroepiandrosterone protect mice against lethal bacterial infections and lipopolysaccharide toxicity. J Med Microbiol *48*, 425-431.

Berdanier, C. D. (1989). Role of glucocorticoids in the regulation of lipogenesis. Faseb J *3*, 2179-2183.
Besset, S., Vincourt, J. B., Amalric, F., and Girard, J. P. (2000). Nuclear localization of PAPS synthetase 1: a sulfate activation pathway in the nucleus of eukaryotic cells. Faseb J *14*, 345-354.

Bjorntorp, P. (1996). The regulation of adipose tissue distribution in humans. Int J Obes Relat Metab Disord *20*, 291-302.

Blank, S. K., Helm, K. D., McCartney, C. R., and Marshall, J. C. (2008). Polycystic ovary syndrome in adolescence. Ann N Y Acad Sci *1135*, 76-84.

Bloch, M., Schmidt, P. J., Danaceau, M. A., Adams, L. F., and Rubinow, D. R. (1999). Dehydroepiandrosterone treatment of midlife dysthymia. Biol Psychiatry *45*, 1533-1541.

Blouin, K., Richard, C., Belanger, C., Dupont, P., Daris, M., Laberge, P., Luu-The, V., and Tchernof, A. (2003). Local androgen inactivation in abdominal visceral adipose tissue. J Clin Endocrinol Metab *88*, 5944-5950.

Bork, P., Holm, L., Koonin, E. V., and Sander, C. (1995). The cytidylyltransferase superfamily: identification of the nucleotide-binding site and fold prediction. Proteins *22*, 259-266.

Bose, H., Lingappa, V. R., and Miller, W. L. (2002). Rapid regulation of steroidogenesis by mitochondrial protein import. Nature *417*, 87-91.

Boyanov, M. A., Boneva, Z., and Christov, V. G. (2003). Testosterone supplementation in men with type 2 diabetes, visceral obesity and partial androgen deficiency. Aging Male *6*, 1-7.

Bublitz, C., and Steavenson, S. (1988). The pentose phosphate pathway in the endoplasmic reticulum. J Biol Chem *263*, 12849-12853.

Buckingham, J. C. (2006). Glucocorticoids: exemplars of multi-tasking. Br J Pharmacol *147 Suppl 1*, S258-268.

Bujalska, I. J., Draper, N., Michailidou, Z., Tomlinson, J. W., White, P. C., Chapman, K. E., Walker, E. A., and Stewart, P. M. (2005). Hexose-6-phosphate dehydrogenase confers oxo-reductase activity upon 11 beta-hydroxysteroid dehydrogenase type 1. J Mol Endocrinol *34*, 675-684.

Bujalska, I. J., Gathercole, L. L., Tomlinson, J. W., Darimont, C., Ermolieff, J., Fanjul, A. N., Rejto, P. A., and Stewart, P. M. (2008). A novel selective 11beta-hydroxysteroid dehydrogenase type 1 inhibitor prevents human adipogenesis. J Endocrinol *197*, 297-307.

Bujalska, I. J., Kumar, S., Hewison, M., and Stewart, P. M. (1999). Differentiation of adipose stromal cells: the roles of glucocorticoids and 11beta-hydroxysteroid dehydrogenase. Endocrinology *140*, 3188-3196.

Bujalska, I. J., Kumar, S., and Stewart, P. M. (1997). Does central obesity reflect "Cushing's disease of the omentum"? Lancet *349*, 1210-1213.

Bujalska, I. J., Quinkler, M., Tomlinson, J. W., Montague, C. T., Smith, D. M., and Stewart, P. M. (2006). Expression profiling of 11beta-hydroxysteroid dehydrogenase type-1 and glucocorticoid-target genes in subcutaneous and omental human preadipocytes. J Mol Endocrinol *37*, 327-340.

Bureik, M., Lisurek, M., and Bernhardt, R. (2002). The human steroid hydroxylases CYP1B1 and CYP11B2. Biol Chem *383*, 1537-1551.

Butcher, S. K., Killampalli, V., Lascelles, D., Wang, K., Alpar, E. K., and Lord, J. M. (2005). Raised cortisol:DHEAS ratios in the elderly after injury: potential impact upon neutrophil function and immunity. Aging Cell *4*, 319-324.

Callies, F., Fassnacht, M., van Vlijmen, J. C., Koehler, I., Huebler, D., Seibel, M. J., Arlt, W., and Allolio, B. (2001). Dehydroepiandrosterone replacement in women with adrenal insufficiency: effects on body composition, serum leptin, bone turnover, and exercise capacity. J Clin Endocrinol Metab *86*, 1968-1972.

Cao, Z., Umek, R. M., and McKnight, S. L. (1991). Regulated expression of three C/EBP isoforms during adipose conversion of 3T3-L1 cells. Genes Dev *5*, 1538-1552.

Cardounel, A., Regelson, W., and Kalimi, M. (1999). Dehydroepiandrosterone protects hippocampal neurons against neurotoxin-induced cell death: mechanism of action. Proc Soc Exp Biol Med *222*, 145-149.

Carmina, E. (2006). Ovarian and adrenal hyperandrogenism. Ann N Y Acad Sci *1092*, 130-137.

Casson, P. R., Andersen, R. N., Herrod, H. G., Stentz, F. B., Straughn, A. B., Abraham, G. E., and

Buster, J. E. (1993). Oral dehydroepiandrosterone in physiologic doses modulates immune function in postmenopausal women. Am J Obstet Gynecol *169*, 1536-1539.

Catania, R. A., Angele, M. K., Ayala, A., Cioffi, W. G., Bland, K. I., and Chaudry, I. H. (1999). Dehydroepiandrosterone restores immune function following trauma-haemorrhage by a direct effect on T lymphocytes. Cytokine *11*, 443-450.

Chakravarty, K., Cassuto, H., Reshef, L., and Hanson, R. W. (2005). Factors that control the tissue-specific transcription of the gene for phosphoenolpyruvate carboxykinase-C. Crit Rev Biochem Mol Biol *40*, 129-154.

Chandler, V. L., Maler, B. A., and Yamamoto, K. R. (1983). DNA sequences bound specifically by glucocorticoid receptor in vitro render a heterologous promoter hormone responsive in vivo. Cell *33*, 489-499.

Charalampopoulos, I., Alexaki, V. I., Lazaridis, I., Dermitzaki, E., Avlonitis, N., Tsatsanis, C., Calogeropoulou, T., Margioris, A. N., Castanas, E., and Gravanis, A. (2006a). G protein-associated, specific membrane binding sites mediate the neuroprotective effect of dehydroepiandrosterone. Faseb J *20*, 577-579.

Charalampopoulos, I., Alexaki, V. I., Tsatsanis, C., Minas, V., Dermitzaki, E., Lasaridis, I., Vardouli, L., Stournaras, C., Margioris, A. N., Castanas, E., and Gravanis, A. (2006b). Neurosteroids as endogenous inhibitors of neuronal cell apoptosis in aging. Ann N Y Acad Sci *1088*, 139-152.

Christiansen, J. J., Gravholt, C. H., Fisker, S., Svenstrup, B., Bennett, P., Veldhuis, J., Andersen, M., Christiansen, J. S., and Jorgensen, J. O. (2004). Dehydroepiandrosterone supplementation in women

with adrenal failure: impact on twenty-four hour GH secretion and IGF-related parameters. Clin Endocrinol (Oxf) *60*, 461-469.

Chumlea, W. C., Knittle, J. L., Roche, A. F., Siervogel, R. M., and Webb, P. (1981a). Size and number of adipocytes and measures of body fat in boys and girls 10 to 18 years of age. Am J Clin Nutr *34*, 1791-1797.

Chumlea, W. C., Roche, A. F., Siervogel, R. M., Knittle, J. L., and Webb, P. (1981b). Adipocytes and adiposity in adults. Am J Clin Nutr *34*, 1798-1803.

Clarke, S. L., Robinson, C. E., and Gimble, J. M. (1997). CAAT/enhancer binding proteins directly modulate transcription from the peroxisome proliferator-activated receptor gamma 2 promoter. Biochem Biophys Res Commun *240*, 99-103.

Cleary, M. P., Billheimer, J., Finan, A., Sartin, J. L., and Schwartz, A. G. (1984). Metabolic consequences of dehydroepiandrosterone in lean and obese adult Zucker rats. Horm Metab Res *16 Suppl 1*, 43-46.

Cleary, M. P., Zabel, T., and Sartin, J. L. (1988). Effects of short-term dehydroepiandrosterone treatment on serum and pancreatic insulin in Zucker rats. J Nutr *118*, 382-387.

Cleary, M. P., and Zisk, J. F. (1986). Anti-obesity effect of two different levels of dehydroepiandrosterone in lean and obese middle-aged female Zucker rats. Int J Obes *10*, 193-204.

Cole, T. G., Wilcox, H. G., and Heimberg, M. (1982). Effects of adrenalectomy and dexamethasone on hepatic lipid metabolism. J Lipid Res *23*, 81-91.

Coleman, D. L. (1988). Therapeutic effects of dehydroepiandrosterone (DHEA) and its metabolites in obese-hyperglycemic mutant mice. Prog Clin Biol Res *265*, 161-175.

Coleman, D. L., Leiter, E. H., and Schwizer, R. W. (1982). Therapeutic effects of dehydroepiandrosterone (DHEA) in diabetic mice. Diabetes *31*, 830-833.

Coleman, D. L., Schwizer, R. W., and Leiter, E. H. (1984). Effect of genetic background on the therapeutic effects of dehydroepiandrosterone (DHEA) in diabetes-obesity mutants and in aged normal mice. Diabetes *33*, 26-32.

Compagnone, N. A., and Mellon, S. H. (1998). Dehydroepiandrosterone: a potential signalling molecule for neocortical organization during development. Proc Natl Acad Sci U S A *95*, 4678-4683.

Consoli, A. (1992). Role of liver in pathophysiology of NIDDM. Diabetes Care *15*, 430-441.

Cooke, P. S., and Naaz, A. (2004). Role of estrogens in adipocyte development and function. Exp Biol Med (Maywood) *229*, 1127-1135.

Cornelius, P., MacDougald, O. A., and Lane, M. D. (1994). Regulation of adipocyte development. Annu Rev Nutr *14*, 99-129.

Cushing H (1932). Further notes on pituitary basophilism JAMA *99*, 281-284.

Cutler, G. B., Jr., Glenn, M., Bush, M., Hodgen, G. D., Graham, C. E., and Loriaux, D. L. (1978). Adrenarche: a survey of rodents, domestic animals, and primates. Endocrinology *103*, 2112-2118.

Danenberg, H. D., Alpert, G., Lustig, S., and Ben-Nathan, D. (1992). Dehydroepiandrosterone protects mice from endotoxin toxicity and reduces tumor necrosis factor production. Antimicrob Agents Chemother *36*, 2275-2279.

Darimont, C., Zbinden, I., Avanti, O., Leone-Vautravers, P., Giusti, V., Burckhardt, P., Pfeifer, A. M., and Mace, K. (2003). Reconstitution of telomerase activity combined with HPV-E7 expression allow human preadipocytes to preserve their differentiation capacity after immortalization. Cell Death Differ *10*, 1025-1031.

Darlington, G. J., Ross, S. E., and MacDougald, O. A. (1998). The role of C/EBP genes in adipocyte differentiation. J Biol Chem *273*, 30057-30060.

De Pergola, G., Triggiani, V., Giorgino, F., Cospite, M. R., Garruti, G., Cignarelli, M., Guastamacchia, E., and Giorgino, R. (1994). The free testosterone to dehydroepiandrosterone sulphate molar ratio as a marker of visceral fat accumulation in premenopausal obese women. Int J Obes Relat Metab Disord *18*, 659-664.

Demirgoren, S., Majewska, M. D., Spivak, C. E., and London, E. D. (1991). Receptor binding and electrophysiological effects of dehydroepiandrosterone sulfate, an antagonist of the GABAA receptor. Neuroscience *45*, 127-135.

Despres, J. P., and Lemieux, I. (2006). Abdominal obesity and metabolic syndrome. Nature *444*, 881-887.

Deyrup, A. T., Krishnan, S., Cockburn, B. N., and Schwartz, N. B. (1998). Deletion and site-directed mutagenesis of the ATP-binding motif (P-loop) in the bifunctional murine ATP-sulfurylase/adenosine 5'-phosphosulfate kinase enzyme. J Biol Chem *273*, 9450-9456.

Dhatariya, K., Bigelow, M. L., and Nair, K. S. (2005). Effect of dehydroepiandrosterone replacement on insulin sensitivity and lipids in hypoadrenal women. Diabetes *54*, 765-769.

Dhir, V., Ivison, H. E., Krone, N., Shackleton, C. H., Doherty, A. J., Stewart, P. M., and Arlt, W. (2007). Differential inhibition of CYP17A1 and CYP21A2 activities by the P450 oxidoreductase mutant A287P. Mol Endocrinol *21*, 1958-1968.

Diamond, P., Cusan, L., Gomez, J. L., Belanger, A., and Labrie, F. (1996). Metabolic effects of 12-month percutaneous dehydroepiandrosterone replacement therapy in postmenopausal women. J Endocrinol *150 Suppl*, S43-50.

Dieudonne, M. N., Pecquery, R., Leneveu, M. C., and Giudicelli, Y. (2000). Opposite effects of androgens and estrogens on adipogenesis in rat preadipocytes: evidence for sex and site-related specificities and possible involvement of insulin-like growth factor 1 receptor and peroxisome proliferator-activated receptor gamma2. Endocrinology *141*, 649-656.

Diez-Roux, G., and Ballabio, A. (2005). Sulfatases and human disease. Annu Rev Genomics Hum Genet *6*, 355-379.

Dillon, J. S. (2005). Dehydroepiandrosterone, dehydroepiandrosterone sulfate and related steroids: their role in inflammatory, allergic and immunological disorders. Curr Drug Targets Inflamm Allergy *4*, 377-385.

Drake, A. J., Livingstone, D. E., Andrew, R., Seckl, J. R., Morton, N. M., and Walker, B. R. (2005). Reduced adipose glucocorticoid reactivation and increased hepatic glucocorticoid clearance as an early adaptation to high-fat feeding in Wistar rats. Endocrinology *146*, 913-919.

Draper, N., and Stewart, P. M. (2005). 11beta-hydroxysteroid dehydrogenase and the pre-receptor regulation of corticosteroid hormone action. J Endocrinol *186*, 251-271.

Dumesic, D. A., Abbott, D. H., and Padmanabhan, V. (2007). Polycystic ovary syndrome and its developmental origins. Rev Endocr Metab Disord *8*, 127-141.

Dunaif, A. (1997). Insulin resistance and the polycystic ovary syndrome: mechanism and implications for pathogenesis. Endocr Rev *18*, 774-800.

Dunkelman, S. S., Fairhurst, B., Plager, J., and Waterhouse, C. (1964). Cortisol Metabolism in Obesity. J Clin Endocrinol Metab *24*, 832-841.

Edwards, C. R., Stewart, P. M., Burt, D., Brett, L., McIntyre, M. A., Sutanto, W. S., de Kloet, E. R., and Monder, C. (1988). Localisation of 11 beta-hydroxysteroid dehydrogenase--tissue specific protector of the mineralocorticoid receptor. Lancet *2*, 986-989.

Ehrhart-Bornstein, M., and Bornstein, S. R. (2008). Cross-talk between adrenal medulla and adrenal cortex in stress. Ann N Y Acad Sci *1148*, 112-117.

Ekstrand, A., Schalin-Jantti, C., Lofman, M., Parkkonen, M., Widen, E., Franssila-Kallunki, A., Saloranta, C., Koivisto, V., and Groop, L. (1996). The effect of (steroid) immunosuppression on skeletal muscle glycogen metabolism in patients after kidney transplantation. Transplantation *61*, 889-893.

El-Jack, A. K., Hamm, J. K., Pilch, P. F., and Farmer, S. R. (1999). Reconstitution of insulin-sensitive glucose transport in fibroblasts requires expression of both PPARgamma and C/EBPalpha. J Biol Chem *274*, 7946-7951.

Elbers, J. M., Asscheman, H., Seidell, J. C., and Gooren, L. J. (1999a). Effects of sex steroid hormones on regional fat depots as assessed by magnetic resonance imaging in transsexuals. Am J Physiol *276*, E317-325.

Elbers, J. M., de Jong, S., Teerlink, T., Asscheman, H., Seidell, J. C., and Gooren, L. J. (1999b). Changes in fat cell size and in vitro lipolytic activity of abdominal and gluteal adipocytes after a one-year cross-sex hormone administration in transsexuals. Metabolism *48*, 1371-1377.

Entenmann, G., and Hauner, H. (1996). Relationship between replication and differentiation in cultured human adipocyte precursor cells. Am J Physiol *270*, C1011-1016.

Fajas, L., Schoonjans, K., Gelman, L., Kim, J. B., Najib, J., Martin, G., Fruchart, J. C., Briggs, M., Spiegelman, B. M., and Auwerx, J. (1999). Regulation of peroxisome proliferator-activated receptor gamma expression by adipocyte differentiation and determination factor 1/sterol regulatory element binding protein 1: implications for adipocyte differentiation and metabolism. Mol Cell Biol *19*, 5495-5503.

Falany, C. N., Comer, K. A., Dooley, T. P., and Glatt, H. (1995). Human dehydroepiandrosterone sulfotransferase. Purification, molecular cloning, and characterization. Ann N Y Acad Sci *774*, 59-72.
Felig P, F. L. (2001). Endocrinology & metabolism By Philip Felig, Lawrence A. Frohman, 4 edn: Published by McGraw-Hill Professional).

Flood, J. F., and Roberts, E. (1988). Dehydroepiandrosterone sulfate improves memory in aging mice. Brain Res *448*, 178-181.

Flood, J. F., Smith, G. E., and Roberts, E. (1988). Dehydroepiandrosterone and its sulfate enhance memory retention in mice. Brain Res *447*, 269-278.

Floyd, Z. E., and Stephens, J. M. (2003). STAT5A promotes adipogenesis in nonprecursor cells and associates with the glucocorticoid receptor during adipocyte differentiation. Diabetes *52*, 308-314.

Formoso, G., Chen, H., Kim, J. A., Montagnani, M., Consoli, A., and Quon, M. J. (2006). Dehydroepiandrosterone mimics acute actions of insulin to stimulate production of both nitric oxide and endothelin 1 via distinct phosphatidylinositol 3-kinase- and mitogen-activated protein kinase-dependent pathways in vascular endothelium. Mol Endocrinol *20*, 1153-1163.

Foster, P. A., Woo, L. W., Potter, B. V., Reed, M. J., and Purohit, A. (2008). The use of steroid sulfatase inhibitors as a novel therapeutic strategy against hormone-dependent endometrial cancer. Endocrinology *149*, 4035-4042.

Franks, S. (2006). Controversy in clinical endocrinology: diagnosis of polycystic ovarian syndrome: in defense of the Rotterdam criteria. J Clin Endocrinol Metab *91*, 786-789.

Freytag, S. O., Paielli, D. L., and Gilbert, J. D. (1994). Ectopic expression of the CCAAT/enhancer-binding protein alpha promotes the adipogenic program in a variety of mouse fibroblastic cells. Genes Dev *8*, 1654-1663.

Fu J, F. H.-L. a. T. A. Induction of human and murine hepatic hydroxysteroid sulfotransferase gene expression by RNA interference-mediated knock-down of PAPS synthase 2.

Fuda, H., Shimizu, C., Lee, Y. C., Akita, H., and Strott, C. A. (2002). Characterization and expression of human bifunctional 3'-phosphoadenosine 5'-phosphosulphate synthase isoforms. Biochem J *365*, 497-504.

Fung, M. M., Viveros, O. H., and O'Connor, D. T. (2008). Diseases of the adrenal medulla. Acta Physiol (Oxf) *192*, 325-335.

Galluzzo, A., Amato, M. C., and Giordano, C. (2008). Insulin resistance and polycystic ovary syndrome. Nutr Metab Cardiovasc Dis *18*, 511-518.

Garcia de Herreros, A., and Birnbaum, M. J. (1989). The acquisition of increased insulin-responsive hexose transport in 3T3-L1 adipocytes correlates with expression of a novel transporter gene. J Biol Chem *264*, 19994-19999.

Garcia, E., Lacasa, M., Agli, B., Giudicelli, Y., and Lacasa, D. (1999). Modulation of rat preadipocyte adipose conversion by androgenic status: involvement of C/EBPs transcription factors. J Endocrinol *161*, 89-97.

Garside, H., Stevens, A., Farrow, S., Normand, C., Houle, B., Berry, A., Maschera, B., and Ray, D. (2004). Glucocorticoid ligands specify different interactions with NF-kappaB by allosteric effects on the glucocorticoid receptor DNA binding domain. J Biol Chem *279*, 50050-50059.

Geisthovel, F., and Rabe, T. (2007). The ESHRE/ASRM consensus on polycystic ovary syndrome (PCOS)--an extended critical analysis. Reprod Biomed Online *14*, 522-535.

Gerra, G., Monti, D., Panerai, A. E., Sacerdote, P., Anderlini, R., Avanzini, P., Zaimovic, A., Brambilla, F., and Franceschi, C. (2003). Long-term immune-endocrine effects of bereavement: relationships with anxiety levels and mood. Psychiatry Res *121*, 145-158.

Gesta, S., Tseng, Y. H., and Kahn, C. R. (2007). Developmental origin of fat: tracking obesity to its source. Cell *131*, 242-256.

Ghosh, D. (2004). Mutations in X-linked ichthyosis disrupt the active site structure of estrone/DHEA sulfatase. Biochim Biophys Acta *1739*, 1-4.

Ghosh, D. (2007). Human sulfatases: a structural perspective to catalysis. Cell Mol Life Sci *64*, 2013-2022.

Giorgino, F., Almahfouz, A., Goodyear, L. J., and Smith, R. J. (1993). Glucocorticoid regulation of insulin receptor and substrate IRS-1 tyrosine phosphorylation in rat skeletal muscle in vivo. J Clin Invest *91*, 2020-2030.

Glass, A. R., Burman, K. D., Dahms, W. T., and Boehm, T. M. (1981). Endocrine function in human obesity. Metabolism *30*, 89-104.

Glass, I. A., Lam, R. C., Chang, T., Roitman, E., Shapiro, L. J., and Shackleton, C. H. (1998). Steroid sulphatase deficiency is the major cause of extremely low oestriol production at mid-pregnancy: a urinary steroid assay for the discrimination of steroid sulphatase deficiency from other causes. Prenat Diagn *18*, 789-800.

Glatt, H., Bartsch, I., Christoph, S., Coughtrie, M. W., Falany, C. N., Hagen, M., Landsiedel, R., Pabel, U., Phillips, D. H., Seidel, A., and Yamazoe, Y. (1998). Sulfotransferase-mediated activation of mutagens studied using heterologous expression systems. Chem Biol Interact *109*, 195-219.

Glatt, H., Boeing, H., Engelke, C. E., Ma, L., Kuhlow, A., Pabel, U., Pomplun, D., Teubner, W., and Meinl, W. (2001). Human cytosolic sulphotransferases: genetics, characteristics, toxicological aspects. Mutat Res *482*, 27-40.

Glatt, H., and Meinl, W. (2004). Pharmacogenetics of soluble sulfotransferases (SULTs). Naunyn Schmiedebergs Arch Pharmacol *369*, 55-68.

Glatt, H., Pauly, K., Piee-Staffa, A., Seidel, A., Hornhardt, S., and Czich, A. (1994). Activation of promutagens by endogenous and heterologous sulfotransferases expressed in continuous cell cultures. Toxicol Lett *72*, 13-21.

Gordon, G. B., Newitt, J. A., Shantz, L. M., Weng, D. E., and Talalay, P. (1986). Inhibition of the conversion of 3T3 fibroblast clones to adipocytes by dehydroepiandrosterone and related anticarcinogenic steroids. Cancer Res *46*, 3389-3395.

Gordon, G. B., Shantz, L. M., and Talalay, P. (1987). Modulation of growth, differentiation and carcinogenesis by dehydroepiandrosterone. Adv Enzyme Regul *26*, 355-382.

Gregoire, F., Genart, C., Hauser, N., and Remacle, C. (1991). Glucocorticoids induce a drastic inhibition of proliferation and stimulate differentiation of adult rat fat cell precursors. Exp Cell Res *196*, 270-278.

Gregoire, F. M., Smas, C. M., and Sul, H. S. (1998). Understanding adipocyte differentiation. Physiol Rev *78*, 783-809.

Gu, S., Ripp, S. L., Prough, R. A., and Geoghegan, T. E. (2003). Dehydroepiandrosterone affects the expression of multiple genes in rat liver including 11 beta-hydroxysteroid dehydrogenase type 1: a cDNA array analysis. Mol Pharmacol *63*, 722-731.

Gupta, M. K., Geller, D. H., and Auchus, R. J. (2001). Pitfalls in characterizing P450c17 mutations associated with isolated 17,20-lyase deficiency. J Clin Endocrinol Metab *86*, 4416-4423.

Gupta, V., Bhasin, S., Guo, W., Singh, R., Miki, R., Chauhan, P., Choong, K., Tchkonia, T., Lebrasseur, N. K., Flanagan, J. N.*, et al.* (2008). Effects of dihydrotestosterone on differentiation and proliferation of human mesenchymal stem cells and preadipocytes. Mol Cell Endocrinol *296*, 32-40.

Gurnell, E. M., Hunt, P. J., Curran, S. E., Conway, C. L., Pullenayegum, E. M., Huppert, F. A., Compston, J. E., Herbert, J., and Chatterjee, V. K. (2008). Long-term DHEA replacement in primary adrenal insufficiency: a randomized, controlled trial. J Clin Endocrinol Metab *93*, 400-409.

Hammer, F., Drescher, D. G., Schneider, S. B., Quinkler, M., Stewart, P. M., Allolio, B., and Arlt, W. (2005a). Sex steroid metabolism in human peripheral blood mononuclear cells changes with aging. J Clin Endocrinol Metab *90*, 6283-6289.

Hammer, F., Subtil, S., Lux, P., Maser-Gluth, C., Stewart, P. M., Allolio, B., and Arlt, W. (2005b). No evidence for hepatic conversion of dehydroepiandrosterone (DHEA) sulfate to DHEA: in vivo and in vitro studies. J Clin Endocrinol Metab *90*, 3600-3605.

Hansen, F. M., Fahmy, N., and Nielsen, J. H. (1980). The influence of sexual hormones on lipogenesis and lipolysis in rat fat cells. Acta Endocrinol (Copenh) *95*, 566-570.

Hanson, R. W., and Reshef, L. (1997). Regulation of phosphoenolpyruvate carboxykinase (GTP) gene expression. Annu Rev Biochem *66*, 581-611.

Harjes, S., Bayer, P., and Scheidig, A. J. (2005). The crystal structure of human PAPS synthetase 1 reveals asymmetry in substrate binding. J Mol Biol *347*, 623-635.

Hauner, H., Entenmann, G., Wabitsch, M., Gaillard, D., Ailhaud, G., Negrel, R., and Pfeiffer, E. F. (1989). Promoting effect of glucocorticoids on the differentiation of human adipocyte precursor cells cultured in a chemically defined medium. J Clin Invest *84*, 1663-1670.

Hauner, H., Schmid, P., and Pfeiffer, E. F. (1987). Glucocorticoids and insulin promote the differentiation of human adipocyte precursor cells into fat cells. J Clin Endocrinol Metab *64*, 832-835.

Hausman, D. B., DiGirolamo, M., Bartness, T. J., Hausman, G. J., and Martin, R. J. (2001). The biology of white adipocyte proliferation. Obes Rev *2*, 239-254.

Hewitt, K. N., Walker, E. A., and Stewart, P. M. (2005). Minireview: hexose-6-phosphate dehydrogenase and redox control of 11{beta}-hydroxysteroid dehydrogenase type 1 activity. Endocrinology *146*, 2539-2543.

Homburg, R. (2008). Polycystic ovary syndrome. Best Pract Res Clin Obstet Gynaecol *22*, 261-274.
Homma, H., Kurachi, H., Nishio, Y., Takeda, T., Yamamoto, T., Adachi, K., Morishige, K., Ohmichi, M.,

Matsuzawa, Y., and Murata, Y. (2000). Estrogen suppresses transcription of lipoprotein lipase gene. Existence of a unique estrogen response element on the lipoprotein lipase promoter. J Biol Chem *275*, 11404-11411.

Hsiang, B., Zhu, Y., Wang, Z., Wu, Y., Sasseville, V., Yang, W. P., and Kirchgessner, T. G. (1999). A novel human hepatic organic anion transporting polypeptide (OATP2). Identification of a liver-specific human organic anion transporting polypeptide and identification of rat and human hydroxymethylglutaryl-CoA reductase inhibitor transporters. J Biol Chem *274*, 37161-37168.

Hunt, P. J., Gurnell, E. M., Huppert, F. A., Richards, C., Prevost, A. T., Wass, J. A., Herbert, J., and Chatterjee, V. K. (2000). Improvement in mood and fatigue after dehydroepiandrosterone replacement in Addison's disease in a randomized, double blind trial. J Clin Endocrinol Metab *85*, 4650-4656.

Huppert, F. A., Van Niekerk, J. K., and Herbert, J. (2000). Dehydroepiandrosterone (DHEA) supplementation for cognition and well-being. Cochrane Database Syst Rev, CD000304.

Huxtable RJ (1986). Biochemistry of Sulfur. (New York: Plenum Publishing Corp.).

Ibanez, L., de Zegher, F., and Potau, N. (1999). Anovulation after precocious pubarche: early markers and time course in adolescence. J Clin Endocrinol Metab *84*, 2691-2695.

Ibanez, L., Dimartino-Nardi, J., Potau, N., and Saenger, P. (2000). Premature adrenarche--normal variant or forerunner of adult disease? Endocr Rev *21*, 671-696.

Ibanez, L., Potau, N., and Carrascosa, A. (1998a). Insulin Resistance, Premature Adrenarche, and a Risk of the Polycystic Ovary Syndrome (PCOS). Trends Endocrinol Metab *9*, 72-77.

Ibanez, L., Potau, N., Francois, I., and de Zegher, F. (1998b). Precocious pubarche, hyperinsulinism, and ovarian hyperandrogenism in girls: relation to reduced fetal growth. J Clin Endocrinol Metab *83*, 3558-3562.

Ikonen, E. (2006). Mechanisms for cellular cholesterol transport: defects and human disease. Physiol Rev *86*, 1237-1261.

Ishizawa, M., Ishizuka, T., Kajita, K., Miura, A., Kanoh, Y., Kimura, M., and Yasuda, K. (2001). Dehydroepiandrosterone (DHEA) stimulates glucose uptake in rat adipocytes: activation of phospholipase D. Comp Biochem Physiol B Biochem Mol Biol *130*, 359-364.

Ishizuka, T., Kajita, K., Miura, A., Ishizawa, M., Kanoh, Y., Itaya, S., Kimura, M., Muto, N., Mune, T., Morita, H., and Yasuda, K. (1999). DHEA improves glucose uptake via activations of protein kinase C and phosphatidylinositol 3-kinase. Am J Physiol *276*, E196-204.

Ishizuka, T., Miura, A., Kajita, K., Matsumoto, M., Sugiyama, C., Matsubara, K., Ikeda, T., Mori, I., Morita, H., Uno, Y.*, et al.* (2007). Effect of dehydroepiandrosterone on insulin sensitivity in Otsuka Long-Evans Tokushima-fatty rats. Acta Diabetol *44*, 219-226.

Ivandic, A., Prpic-Krizevac, I., Bozic, D., Barbir, A., Peljhan, V., Balog, Z., and Glasnovic, M. (2002). Insulin resistance and androgens in healthy women with different body fat distributions. Wien Klin Wochenschr *114*, 321-326.

Johannsson, G., Burman, P., Wiren, L., Engstrom, B. E., Nilsson, A. G., Ottosson, M., Jonsson, B., Bengtsson, B. A., and Karlsson, F. A. (2002). Low dose dehydroepiandrosterone affects behavior in hypopituitary androgen-deficient women: a placebo-controlled trial. J Clin Endocrinol Metab *87*, 2046-2052.

Jornvall, H., Persson, B., Krook, M., Atrian, S., Gonzalez-Duarte, R., Jeffery, J., and Ghosh, D. (1995). Short-chain dehydrogenases/reductases (SDR). Biochemistry *34*, 6003-6013.

Jullien, D., Crozatier, M., and Kas, E. (1997). cDNA sequence and expression pattern of the Drosophila melanogaster PAPS synthetase gene: a new salivary gland marker. Mech Dev *68*, 179-186.

Kajita, K., Ishizuka, T., Miura, A., Ishizawa, M., Kanoh, Y., and Yasuda, K. (2000). The role of atypical and conventional PKC in dehydroepiandrosterone-induced glucose uptake and dexamethasone-induced insulin resistance. Biochem Biophys Res Commun *277*, 361-367.

Kershaw, E. E., Morton, N. M., Dhillon, H., Ramage, L., Seckl, J. R., and Flier, J. S. (2005). Adipocyte-specific glucocorticoid inactivation protects against diet-induced obesity. Diabetes *54*, 1023-1031.

Khaw, K. T., and Barrett-Connor, E. (1992). Lower endogenous androgens predict central adiposity in men. Ann Epidemiol *2*, 675-682.

Kim, J. B., and Spiegelman, B. M. (1996). ADD1/SREBP1 promotes adipocyte differentiation and gene expression linked to fatty acid metabolism. Genes Dev *10*, 1096-1107.

Kimura, K., Endou, H., Sudo, J., and Sakai, F. (1979). Glucose dehydrogenase (hexose 6-phosphate dehydrogenase) and the microsomal electron transport system. Evidence supporting their possible functional relationship. J Biochem *85*, 319-326.

Klaassen, C. D., and Boles, J. W. (1997). Sulfation and sulfotransferases 5: the importance of 3'-phosphoadenosine 5'-phosphosulfate (PAPS) in the regulation of sulfation. Faseb J *11*, 404-418.

Klemm, D. J., Roesler, W. J., Boras, T., Colton, L. A., Felder, K., and Reusch, J. E. (1998). Insulin stimulates cAMP-response element binding protein activity in HepG2 and 3T3-L1 cell lines. J Biol Chem *273*, 917-923.

Knittle, J. L., Timmers, K., Ginsberg-Fellner, F., Brown, R. E., and Katz, D. P. (1979). The growth of adipose tissue in children and adolescents. Cross-sectional and longitudinal studies of adipose cell number and size. J Clin Invest *63*, 239-246.

Kotelevtsev, Y., Brown, R. W., Fleming, S., Kenyon, C., Edwards, C. R., Seckl, J. R., and Mullins, J. J. (1999). Hypertension in mice lacking 11beta-hydroxysteroid dehydrogenase type 2. J Clin Invest *103*, 683-689.

Kotelevtsev, Y., Holmes, M. C., Burchell, A., Houston, P. M., Schmoll, D., Jamieson, P., Best, R., Brown, R., Edwards, C. R., Seckl, J. R., and Mullins, J. J. (1997). 11beta-hydroxysteroid dehydrogenase type 1 knockout mice show attenuated glucocorticoid-inducible responses and resist hyperglycemia on obesity or stress. Proc Natl Acad Sci U S A *94*, 14924-14929.

Kousta, E. (2006). Premature adrenarche leads to polycystic ovary syndrome? Long-term consequences. Ann N Y Acad Sci *1092*, 148-157.

Koutnikova, H., Cock, T. A., Watanabe, M., Houten, S. M., Champy, M. F., Dierich, A., and Auwerx, J. (2003). Compensation by the muscle limits the metabolic consequences of lipodystrophy in PPAR gamma hypomorphic mice. Proc Natl Acad Sci U S A *100*, 14457-14462.

Kraemer, F. B. (2007). Adrenal cholesterol utilization. Mol Cell Endocrinol *265-266*, 42-45.

Kullak-Ublick, G. A., Fisch, T., Oswald, M., Hagenbuch, B., Meier, P. J., Beuers, U., and Paumgartner, G. (1998). Dehydroepiandrosterone sulfate (DHEAS): identification of a carrier protein in human liver and brain. FEBS Lett *424*, 173-176.

Kumar, A., Woods, K. S., Bartolucci, A. A., and Azziz, R. (2005). Prevalence of adrenal androgen excess in patients with the polycystic ovary syndrome (PCOS). Clin Endocrinol (Oxf) *62*, 644-649.

Kurima, K., Warman, M. L., Krishnan, S., Domowicz, M., Krueger, R. C., Jr., Deyrup, A., and Schwartz, N. B. (1998). A member of a family of sulfate-activating enzymes causes murine brachymorphism. Proc Natl Acad Sci U S A *95*, 8681-8685.

Labrie, F., Luu-The, V., Belanger, A., Lin, S. X., Simard, J., Pelletier, G., and Labrie, C. (2005). Is dehydroepiandrosterone a hormone? J Endocrinol *187*, 169-196.

Labrie, F., Luu-The, V., Labrie, C., Belanger, A., Simard, J., Lin, S. X., and Pelletier, G. (2003). Endocrine and intracrine sources of androgens in women: inhibition of breast cancer and other roles of androgens and their precursor dehydroepiandrosterone. Endocr Rev *24*, 152-182.

Labrie, F., Luu-The, V., Lin, S. X., Simard, J., and Labrie, C. (2000a). Role of 17 beta-hydroxysteroid dehydrogenases in sex steroid formation in peripheral intracrine tissues. Trends Endocrinol Metab *11*, 421-427.

Labrie, F., Luu-The, V., Lin, S. X., Simard, J., Labrie, C., El-Alfy, M., Pelletier, G., and Belanger, A. (2000b). Intracrinology: role of the family of 17 beta-hydroxysteroid dehydrogenases in human physiology and disease. J Mol Endocrinol *25*, 1-16.

Lakshmi, V., and Monder, C. (1988). Purification and characterization of the corticosteroid 11 beta-dehydrogenase component of the rat liver 11 beta-hydroxysteroid dehydrogenase complex. Endocrinology *123*, 2390-2398.

Lavery, G. G., Hauton, D., Hewitt, K. N., Brice, S. M., Sherlock, M., Walker, E. A., and Stewart, P. M. (2007). Hypoglycemia with enhanced hepatic glycogen synthesis in recombinant mice lacking hexose-6-phosphate dehydrogenase. Endocrinology *148*, 6100-6106.

Lavery, G. G., Walker, E. A., Draper, N., Jeyasuria, P., Marcos, J., Shackleton, C. H., Parker, K. L., White, P. C., and Stewart, P. M. (2006). Hexose-6-phosphate dehydrogenase knock-out mice lack 11 beta-hydroxysteroid dehydrogenase type 1-mediated glucocorticoid generation. J Biol Chem *281*, 6546-6551.

Lavery, G. G., Walker, E. A., Tiganescu, A., Ride, J. P., Shackleton, C. H., Tomlinson, J. W., Connell, J. M., Ray, D. W., Biason-Lauber, A., Malunowicz, E. M.*, et al.* (2008a). Steroid biomarkers and genetic studies reveal inactivating mutations in hexose-6-phosphate dehydrogenase in patients with cortisone reductase deficiency. J Clin Endocrinol Metab *93*, 3827-3832.

Lavery, G. G., Walker, E. A., Turan, N., Rogoff, D., Ryder, J. W., Shelton, J. M., Richardson, J. A., Falciani, F., White, P. C., Stewart, P. M.*, et al.* (2008b). Deletion of hexose-6-phosphate dehydrogenase activates the unfolded protein response pathway and induces skeletal myopathy. J Biol Chem *283*, 8453-8461.

Lea-Currie, Y. R., Monroe, D., and McIntosh, M. K. (1999). Dehydroepiandrosterone and related steroids alter 3T3-L1 preadipocyte proliferation and differentiation. Comp Biochem Physiol C Pharmacol Toxicol Endocrinol *123*, 17-25.

Lea-Currie, Y. R., Wen, P., and McIntosh, M. K. (1997a). Dehydroepiandrosterone-sulfate (DHEAS) reduces adipocyte hyperplasia associated with feeding rats a high-fat diet. Int J Obes Relat Metab Disord *21*, 1058-1064.

Lea-Currie, Y. R., Wen, P., and McIntosh, M. K. (1998). Dehydroepiandrosterone reduces proliferation and differentiation of 3T3-L1 preadipocytes. Biochem Biophys Res Commun *248*, 497-504.

Lea-Currie, Y. R., Wu, S. M., and McIntosh, M. K. (1997b). Effects of acute administration of dehydroepiandrosterone-sulfate on adipose tissue mass and cellularity in male rats. Int J Obes Relat Metab Disord *21*, 147-154.

Leiter, E. H., Beamer, W. G., Coleman, D. L., and Longcope, C. (1987). Androgenic and estrogenic metabolites in serum of mice fed dehydroepiandrosterone: relationship to antihyperglycemic effects. Metabolism *36*, 863-869.

Lemieux, S., Despres, J. P., Moorjani, S., Nadeau, A., Theriault, G., Prud'homme, D., Tremblay, A., Bouchard, C., and Lupien, P. J. (1994). Are gender differences in cardiovascular disease risk factors explained by the level of visceral adipose tissue? Diabetologia *37*, 757-764.

Lemieux, S., Prud'homme, D., Bouchard, C., Tremblay, A., and Despres, J. P. (1993). Sex differences in the relation of visceral adipose tissue accumulation to total body fatness. Am J Clin Nutr *58*, 463-467.

Leyh, T. S. (1993). The physical biochemistry and molecular genetics of sulfate activation. Crit Rev Biochem Mol Biol *28*, 515-542.

Li, H., Deyrup, A., Mensch, J. R., Jr., Domowicz, M., Konstantinidis, A. K., and Schwartz, N. B. (1995). The isolation and characterization of cDNA encoding the mouse bifunctional ATP sulfurylase-adenosine 5'-phosphosulfate kinase. J Biol Chem *270*, 29453-29459.

Lin, F. T., and Lane, M. D. (1994). CCAAT/enhancer binding protein alpha is sufficient to initiate the 3T3-L1 adipocyte differentiation program. Proc Natl Acad Sci U S A *91*, 8757-8761.

Lindsay, J., Wang, L. L., Li, Y., and Zhou, S. F. (2008). Structure, function and polymorphism of human cytosolic sulfotransferases. Curr Drug Metab *9*, 99-105.

Lisurek, M., and Bernhardt, R. (2004). Modulation of aldosterone and cortisol synthesis on the molecular level. Mol Cell Endocrinol *215*, 149-159.

Liu, D., and Dillon, J. S. (2002). Dehydroepiandrosterone activates endothelial cell nitric-oxide synthase by a specific plasma membrane receptor coupled to Galpha(i2,3). J Biol Chem *277*, 21379-21388.

Liu, D., and Dillon, J. S. (2004). Dehydroepiandrosterone stimulates nitric oxide release in vascular endothelial cells: evidence for a cell surface receptor. Steroids *69*, 279-289.

Liu, Y., Nakagawa, Y., Wang, Y., Li, R., Li, X., Ohzeki, T., and Friedman, T. C. (2003). Leptin activation of corticosterone production in hepatocytes may contribute to the reversal of obesity and hyperglycemia in leptin-deficient ob/ob mice. Diabetes *52*, 1409-1416.

Livingstone, D. E., Jones, G. C., Smith, K., Jamieson, P. M., Andrew, R., Kenyon, C. J., and Walker, B. R. (2000). Understanding the role of glucocorticoids in obesity: tissue-specific alterations of corticosterone metabolism in obese Zucker rats. Endocrinology *141*, 560-563.

Long, W., Barrett, E. J., Wei, L., and Liu, Z. (2003). Adrenalectomy enhances the insulin sensitivity of muscle protein synthesis. Am J Physiol Endocrinol Metab *284*, E102-109.

Loria, R. M., Padgett, D. A., and Huynh, P. N. (1996). Regulation of the immune response by dehydroepiandrosterone and its metabolites. J Endocrinol *150 Suppl*, S209-220.

Lovas, K., Gebre-Medhin, G., Trovik, T. S., Fougner, K. J., Uhlving, S., Nedrebo, B. G., Myking, O. L., Kampe, O., and Husebye, E. S. (2003). Replacement of dehydroepiandrosterone in adrenal failure: no benefit for subjective health status and sexuality in a 9-month, randomized, parallel group clinical trial. J Clin Endocrinol Metab *88*, 1112-1118.

Lowry, O. H., Rosebrough, N. J., Farr, A. L., and Randall, R. J. (1951). Protein measurement with the Folin phenol reagent. J Biol Chem *193*, 265-275.

Lumbers, E. R. (1999). Angiotensin and aldosterone. Regul Pept *80*, 91-100.

Lyle, S., Ozeran, J. D., Stanczak, J., Westley, J., and Schwartz, N. B. (1994a). Intermediate channeling between ATP sulfurylase and adenosine 5'-phosphosulfate kinase from rat chondrosarcoma. Biochemistry *33*, 6822-6827.

Lyle, S., Stanczak, J., Ng, K., and Schwartz, N. B. (1994b). Rat chondrosarcoma ATP sulfurylase and adenosine 5'-phosphosulfate kinase reside on a single bifunctional protein. Biochemistry *33*, 5920-5925.

MacDougald, O. A., Cornelius, P., Lin, F. T., Chen, S. S., and Lane, M. D. (1994). Glucocorticoids reciprocally regulate expression of the CCAAT/enhancer-binding protein alpha and delta genes in 3T3-L1 adipocytes and white adipose tissue. J Biol Chem *269*, 19041-19047.

MacDougald, O. A., and Lane, M. D. (1995a). Adipocyte differentiation. When precursors are also regulators. Curr Biol *5*, 618-621.

MacDougald, O. A., and Lane, M. D. (1995b). Transcriptional regulation of gene expression during adipocyte differentiation. Annu Rev Biochem *64*, 345-373.

Majewska, M. D., Demirgoren, S., Spivak, C. E., and London, E. D. (1990). The neurosteroid dehydroepiandrosterone sulfate is an allosteric antagonist of the GABAA receptor. Brain Res *526*, 143-146.

Malkoski, S. P., and Dorin, R. I. (1999). Composite glucocorticoid regulation at a functionally defined negative glucocorticoid response element of the human corticotropin-releasing hormone gene. Mol Endocrinol *13*, 1629-1644.

Mantha, L., Palacios, E., and Deshaies, Y. (1999). Modulation of triglyceride metabolism by glucocorticoids in diet-induced obesity. Am J Physiol *277*, R455-464.

Marin, P., Krotkiewski, M., and Bjorntorp, P. (1992). Androgen treatment of middle-aged, obese men: effects on metabolism, muscle and adipose tissues. Eur J Med *1*, 329-336.

Marin, P., Oden, B., and Bjorntorp, P. (1995). Assimilation and mobilization of triglycerides in subcutaneous abdominal and femoral adipose tissue in vivo in men: effects of androgens. J Clin Endocrinol Metab *80*, 239-243.

Marney, A. M., and Brown, N. J. (2007). Aldosterone and end-organ damage. Clin Sci (Lond) *113*, 267-278.

Maroulis, G. B. (1981). Evaluation of hirsutism and hyperandrogenemia. Fertil Steril *36*, 273-305.

Martel, C., Gagne, D., Couet, J., Labrie, Y., Simard, J., and Labrie, F. (1994a). Rapid modulation of ovarian 3 beta-hydroxysteroid dehydrogenase/delta 5-delta 4 isomerase gene expression by prolactin and human chorionic gonadotropin in the hypophysectomized rat. Mol Cell Endocrinol *99*, 63-71.

Martel, C., Melner, M. H., Gagne, D., Simard, J., and Labrie, F. (1994b). Widespread tissue distribution of steroid sulfatase, 3 beta-hydroxysteroid dehydrogenase/delta 5-delta 4 isomerase (3 beta-HSD), 17 beta-HSD 5 alpha-reductase and aromatase activities in the rhesus monkey. Mol Cell Endocrinol *104*, 103-111.

Maser, E., Volker, B., and Friebertshauser, J. (2002). 11 Beta-hydroxysteroid dehydrogenase type 1 from human liver: dimerization and enzyme cooperativity support its postulated role as glucocorticoid reductase. Biochemistry *41*, 2459-2465.

Masuzaki, H., Paterson, J., Shinyama, H., Morton, N. M., Mullins, J. J., Seckl, J. R., and Flier, J. S. (2001). A transgenic model of visceral obesity and the metabolic syndrome. Science *294*, 2166-2170.

Masuzaki, H., Yamamoto, H., Kenyon, C. J., Elmquist, J. K., Morton, N. M., Paterson, J. M., Shinyama, H., Sharp, M. G., Fleming, S., Mullins, J. J.*, et al.* (2003). Transgenic amplification of glucocorticoid action in adipose tissue causes high blood pressure in mice. J Clin Invest *112*, 83-90.

Matthews, L., Berry, A., Ohanian, V., Ohanian, J., Garside, H., and Ray, D. (2008). Caveolin mediates rapid glucocorticoid effects and couples glucocorticoid action to the antiproliferative program. Mol Endocrinol *22*, 1320-1330.

McNicol, A. M. (2008). A diagnostic approach to adrenal cortical lesions. Endocr Pathol *19*, 241-251.

Meikle, A. W., Dorchuck, R. W., Araneo, B. A., Stringham, J. D., Evans, T. G., Spruance, S. L., and Daynes, R. A. (1992). The presence of a dehydroepiandrosterone-specific receptor binding complex in murine T cells. J Steroid Biochem Mol Biol *42*, 293-304.

Meulenberg, E. P., and Hofman, J. A. (1990a). The effect of pretreatment of saliva on steroid hormone concentrations. J Clin Chem Clin Biochem *28*, 923-928.

Meulenberg, P. M., and Hofman, J. A. (1990b). The effect of oral contraceptive use and pregnancy on the daily rhythm of cortisol and cortisone. Clin Chim Acta *190*, 211-221.

Migeon, C. J., Keller, A. R., Lawrence, B., and Shepard, T. H., 2nd (1957). Dehydroepiandrosterone and androsterone levels in human plasma: effect of age and sex; day-to-day and diurnal variations. J Clin Endocrinol Metab *17*, 1051-1062.

Miller, W. H., Jr., Faust, I. M., and Hirsch, J. (1984). Demonstration of de novo production of adipocytes in adult rats by biochemical and radioautographic techniques. J Lipid Res *25*, 336-347.

Miller, W. L. (2002). Androgen biosynthesis from cholesterol to DHEA. Mol Cell Endocrinol *198*, 7-14.

Miller, W. L. (2007). Steroidogenic acute regulatory protein (StAR), a novel mitochondrial cholesterol transporter. Biochim Biophys Acta *1771*, 663-676.

Miller, W. L. (2009). Androgen synthesis in adrenarche. Rev Endocr Metab Disord *10*, 3-17.

Mohan, P. F., and Cleary, M. P. (1988). Effect of short-term DHEA administration on liver metabolism of lean and obese rats. Am J Physiol *255*, E1-8.

Mohan, P. F., Ihnen, J. S., Levin, B. E., and Cleary, M. P. (1990). Effects of dehydroepiandrosterone treatment in rats with diet-induced obesity. J Nutr *120*, 1103-1114.

Morales, A. J., Haubrich, R. H., Hwang, J. Y., Asakura, H., and Yen, S. S. (1998). The effect of six months treatment with a 100 mg daily dose of dehydroepiandrosterone (DHEA) on circulating sex steroids, body composition and muscle strength in age-advanced men and women. Clin Endocrinol (Oxf) *49*, 421-432.

Morales, A. J., Nolan, J. J., Nelson, J. C., and Yen, S. S. (1994). Effects of replacement dose of dehydroepiandrosterone in men and women of advancing age. J Clin Endocrinol Metab *78*, 1360-1367.

Morrison, R. F., and Farmer, S. R. (1999). Insights into the transcriptional control of adipocyte differentiation. J Cell Biochem *Suppl 32-33*, 59-67.

Muller, J. (1995). Aldosterone: the minority hormone of the adrenal cortex. Steroids *60*, 2-9.

Nagata, K. (2008). Mineralocorticoid antagonism and cardiac hypertrophy. Curr Hypertens Rep *10*, 216-221.

Nagata, K., and Yamazoe, Y. (2000). Pharmacogenetics of sulfotransferase. Annu Rev Pharmacol Toxicol *40*, 159-176.

Nechushtan, H., Benvenisty, N., Brandeis, R., and Reshef, L. (1987). Glucocorticoids control phosphoenolpyruvate carboxykinase gene expression in a tissue specific manner. Nucleic Acids Res *15*, 6405-6417.

Negishi, M., Pedersen, L. G., Petrotchenko, E., Shevtsov, S., Gorokhov, A., Kakuta, Y., and Pedersen, L. C. (2001). Structure and function of sulfotransferases. Arch Biochem Biophys *390*, 149-157.

Nestler, J. E., Barlascini, C. O., Clore, J. N., and Blackard, W. G. (1988). Dehydroepiandrosterone reduces serum low density lipoprotein levels and body fat but does not alter insulin sensitivity in normal men. J Clin Endocrinol Metab *66*, 57-61.

Nieuwenhuizen, A. G., and Rutters, F. (2008). The hypothalamic-pituitary-adrenal-axis in the regulation of energy balance. Physiol Behav *94*, 169-177.

Nissen, R. M., and Yamamoto, K. R. (2000). The glucocorticoid receptor inhibits NFkappaB by interfering with serine-2 phosphorylation of the RNA polymerase II carboxy-terminal domain. Genes Dev *14*, 2314-2329.

Norman, R. J., Dewailly, D., Legro, R. S., and Hickey, T. E. (2007). Polycystic ovary syndrome. Lancet *370*, 685-697.

Odermatt, A., Atanasov, A. G., Balazs, Z., Schweizer, R. A., Nashev, L. G., Schuster, D., and Langer, T. (2006). Why is 11beta-hydroxysteroid dehydrogenase type 1 facing the endoplasmic reticulum lumen? Physiological relevance of the membrane topology of 11beta-HSD1. Mol Cell Endocrinol *248*, 15-23.

Okabe, T., Haji, M., Takayanagi, R., Adachi, M., Imasaki, K., Kurimoto, F., Watanabe, T., and Nawata, H. (1995). Up-regulation of high-affinity dehydroepiandrosterone binding activity by dehydroepiandrosterone in activated human T lymphocytes. J Clin Endocrinol Metab *80*, 2993-2996.

Orentreich, N., Brind, J. L., Rizer, R. L., and Vogelman, J. H. (1984). Age changes and sex differences in serum dehydroepiandrosterone sulfate concentrations throughout adulthood. J Clin Endocrinol Metab *59*, 551-555.

Orth, D. N. (1995). Cushing's syndrome. N Engl J Med *332*, 791-803.

Ozeran, J. D., Westley, J., and Schwartz, N. B. (1996a). Identification and partial purification of PAPS translocase. Biochemistry *35*, 3695-3703.

Ozeran, J. D., Westley, J., and Schwartz, N. B. (1996b). Kinetics of PAPS translocase: evidence for an antiport mechanism. Biochemistry *35*, 3685-3694.

Pasquali, R., Casimirri, F., Cantobelli, S., Melchionda, N., Morselli Labate, A. M., Fabbri, R., Capelli, M., and Bortoluzzi, L. (1991). Effect of obesity and body fat distribution on sex hormones and insulin in men. Metabolism *40*, 101-104.

Paterson, J. M., Morton, N. M., Fievet, C., Kenyon, C. J., Holmes, M. C., Staels, B., Seckl, J. R., and Mullins, J. J. (2004). Metabolic syndrome without obesity: Hepatic overexpression of 11beta-hydroxysteroid dehydrogenase type 1 in transgenic mice. Proc Natl Acad Sci U S A *101*, 7088-7093.

Perrini, S., Natalicchio, A., Laviola, L., Belsanti, G., Montrone, C., Cignarelli, A., Minielli, V., Grano, M., De Pergola, G., Giorgino, R., and Giorgino, F. (2004). Dehydroepiandrosterone stimulates glucose uptake in human and murine adipocytes by inducing GLUT1 and GLUT4 translocation to the plasma membrane. Diabetes *53*, 41-52.

Prins, J. B., and O'Rahilly, S. (1997). Regulation of adipose cell number in man. Clin Sci (Lond) *92*, 3-11.

Quinkler, M., Sinha, B., Tomlinson, J. W., Bujalska, I. J., Stewart, P. M., and Arlt, W. (2004). Androgen generation in adipose tissue in women with simple obesity--a site-specific role for 17beta-hydroxysteroid dehydrogenase type 5. J Endocrinol *183*, 331-342.

Quinn, S. J., and Williams, G. H. (1988). Regulation of aldosterone secretion. Annu Rev Physiol *50*, 409-426.

Rabbitt, E. H., Lavery, G. G., Walker, E. A., Cooper, M. S., Stewart, P. M., and Hewison, M. (2002). Prereceptor regulation of glucocorticoid action by 11beta-hydroxysteroid dehydrogenase: a novel determinant of cell proliferation. Faseb J *16*, 36-44.

Rask, E., Olsson, T., Soderberg, S., Andrew, R., Livingstone, D. E., Johnson, O., and Walker, B. R. (2001). Tissue-specific dysregulation of cortisol metabolism in human obesity. J Clin Endocrinol Metab *86*, 1418-1421.

Rask, E., Walker, B. R., Soderberg, S., Livingstone, D. E., Eliasson, M., Johnson, O., Andrew, R., and Olsson, T. (2002). Tissue-specific changes in peripheral cortisol metabolism in obese women: increased adipose 11beta-hydroxysteroid dehydrogenase type 1 activity. J Clin Endocrinol Metab *87*, 3330-3336.

Reed, M. J., Purohit, A., Woo, L. W., Newman, S. P., and Potter, B. V. (2005). Steroid sulfatase: molecular biology, regulation, and inhibition. Endocr Rev *26*, 171-202.

Reichardt, H. M., and Schutz, G. (1998). Glucocorticoid signalling--multiple variations of a common theme. Mol Cell Endocrinol *146*, 1-6.

Rittmaster, R. S., and Loriaux, D. L. (1987). Hirsutism. Ann Intern Med *106*, 95-107.

Robbins, P. W., and Lipmann, F. (1958a). Enzymatic synthesis of adenosine-5'-phosphosulfate. J Biol Chem *233*, 686-690.

Robbins, P. W., and Lipmann, F. (1958b). Separation of the two enzymatic phases in active sulfate synthesis. J Biol Chem *233*, 681-685.

Rogoff, D., Ryder, J. W., Black, K., Yan, Z., Burgess, S. C., McMillan, D. R., and White, P. C. (2007). Abnormalities of glucose homeostasis and the hypothalamic-pituitary-adrenal axis in mice lacking hexose-6-phosphate dehydrogenase. Endocrinology *148*, 5072-5080.

Rosen, E. D., and MacDougald, O. A. (2006). Adipocyte differentiation from the inside out. Nat Rev Mol Cell Biol *7*, 885-896.

Rosen, E. D., and Spiegelman, B. M. (2000). Molecular regulation of adipogenesis. Annu Rev Cell Dev Biol *16*, 145-171.

Rosenthal, E., and Leustek, T. (1995). A multifunctional Urechis caupo protein, PAPS synthetase, has both ATP sulfurylase and APS kinase activities. Gene *165*, 243-248.

Rubin, C. S., Hirsch, A., Fung, C., and Rosen, O. M. (1978). Development of hormone receptors and hormonal responsiveness in vitro. Insulin receptors and insulin sensitivity in the preadipocyte and adipocyte forms of 3T3-L1 cells. J Biol Chem *253*, 7570-7578.

Rumberger, J. M., Wu, T., Hering, M. A., and Marshall, S. (2003). Role of hexosamine biosynthesis in glucose-mediated up-regulation of lipogenic enzyme mRNA levels: effects of glucose, glutamine, and glucosamine on glycerophosphate dehydrogenase, fatty acid synthase, and acetyl-CoA carboxylase mRNA levels. J Biol Chem *278*, 28547-28552.

Saad, M. J., Folli, F., Kahn, J. A., and Kahn, C. R. (1993). Modulation of insulin receptor, insulin receptor substrate-1, and phosphatidylinositol 3-kinase in liver and muscle of dexamethasone-treated rats. J Clin Invest *92*, 2065-2072.

Saltiel, A. R., and Kahn, C. R. (2001). Insulin signalling and the regulation of glucose and lipid metabolism. Nature *414*, 799-806.

Samra, J. S., Clark, M. L., Humphreys, S. M., MacDonald, I. A., Bannister, P. A., and Frayn, K. N. (1998). Effects of physiological hypercortisolemia on the regulation of lipolysis in subcutaneous adipose tissue. J Clin Endocrinol Metab *83*, 626-631.

Sandeep, T. C., Andrew, R., Homer, N. Z., Andrews, R. C., Smith, K., and Walker, B. R. (2005). Increased in vivo regeneration of cortisol in adipose tissue in human obesity and effects of the 11beta-hydroxysteroid dehydrogenase type 1 inhibitor carbenoxolone. Diabetes *54*, 872-879.

Sandri, M., Sandri, C., Gilbert, A., Skurk, C., Calabria, E., Picard, A., Walsh, K., Schiaffino, S., Lecker, S. H., and Goldberg, A. L. (2004). Foxo transcription factors induce the atrophy-related ubiquitin ligase atrogin-1 and cause skeletal muscle atrophy. Cell *117*, 399-412.

Schacke, H., Docke, W. D., and Asadullah, K. (2002). Mechanisms involved in the side effects of glucocorticoids. Pharmacol Ther *96*, 23-43.

Schulz, S., Klann, R. C., Schonfeld, S., and Nyce, J. W. (1992). Mechanisms of cell growth inhibition and cell cycle arrest in human colonic adenocarcinoma cells by dehydroepiandrosterone: role of isoprenoid biosynthesis. Cancer Res *52*, 1372-1376.

Scott, R. E., Florine, D. L., Wille, J. J., Jr., and Yun, K. (1982). Coupling of growth arrest and differentiation at a distinct state in the G1 phase of the cell cycle: GD. Proc Natl Acad Sci U S A *79*, 845-849.

Seckl, J. R., and Meaney, M. J. (2004). Glucocorticoid programming. Ann N Y Acad Sci *1032*, 63-84.
Sekulic, N., Dietrich, K., Paarmann, I., Ort, S., Konrad, M., and Lavie, A. (2007). Elucidation of the active conformation of the APS-kinase domain of human PAPS synthetase 1. J Mol Biol *367*, 488-500.

Seubert, P. A., Renosto, F., Knudson, P., and Segel, I. H. (1985). Adenosinetriphosphate sulfurylase from Penicillium chrysogenum: steady-state kinetics of the forward and reverse reactions, alternative substrate kinetics, and equilibrium binding studies. Arch Biochem Biophys *240*, 509-523.

Shantz, L. M., Talalay, P., and Gordon, G. B. (1989). Mechanism of inhibition of growth of 3T3-L1 fibroblasts and their differentiation to adipocytes by dehydroepiandrosterone and related steroids: role of glucose-6-phosphate dehydrogenase. Proc Natl Acad Sci U S A *86*, 3852-3856.

Shepherd, A., and Cleary, M. P. (1984). Metabolic alterations after dehydroepiandrosterone treatment in Zucker rats. Am J Physiol *246*, E123-128.

Shinzawa, K., Ishibashi, S., Murakoshi, M., Watanabe, K., Kominami, S., Kawahara, A., and Takemori, S. (1988). Relationship between zonal distribution of microsomal cytochrome P-450s (P-450(17)alpha,lyase and P-450C21) and steroidogenic activities in guinea-pig adrenal cortex. J Endocrinol *119*, 191-200.

Sigurjonsdottir, T. J., and Hayles, A. B. (1968). Premature pubarche. Clin Pediatr (Phila) *7*, 29-33.

Silverman, S. H., Migeon, C., Rosemberg, E., and Wilkins, L. (1952). Precocious growth of sexual hair without other secondary sexual development; premature pubarche, a constitutional variation of adolescence. Pediatrics *10*, 426-432.

Simoncini, T., Mannella, P., Fornari, L., Varone, G., Caruso, A., and Genazzani, A. R. (2003). Dehydroepiandrosterone modulates endothelial nitric oxide synthesis via direct genomic and nongenomic mechanisms. Endocrinology *144*, 3449-3455.

Simpson, E. R., and McInnes, K. J. (2005). Sex and fat--can one factor handle both? Cell Metab *2*, 346-347.

Singh, R., Artaza, J. N., Taylor, W. E., Braga, M., Yuan, X., Gonzalez-Cadavid, N. F., and Bhasin, S. (2006). Testosterone inhibits adipogenic differentiation in 3T3-L1 cells: nuclear translocation of androgen receptor complex with beta-catenin and T-cell factor 4 may bypass canonical Wnt signaling to down-regulate adipogenic transcription factors. Endocrinology *147*, 141-154.

Singh, R., Artaza, J. N., Taylor, W. E., Gonzalez-Cadavid, N. F., and Bhasin, S. (2003). Androgens stimulate myogenic differentiation and inhibit adipogenesis in C3H 10T1/2 pluripotent cells through an androgen receptor-mediated pathway. Endocrinology *144*, 5081-5088.

Slavin, B. G., Ong, J. M., and Kern, P. A. (1994). Hormonal regulation of hormone-sensitive lipase activity and mRNA levels in isolated rat adipocytes. J Lipid Res *35*, 1535-1541.

Smas, C. M., Chen, L., Zhao, L., Latasa, M. J., and Sul, H. S. (1999). Transcriptional repression of pref-1 by glucocorticoids promotes 3T3-L1 adipocyte differentiation. J Biol Chem *274*, 12632-12641.

Smas, C. M., and Sul, H. S. (1997). Molecular mechanisms of adipocyte differentiation and inhibitory action of pref-1. Crit Rev Eukaryot Gene Expr *7*, 281-298.

Solerte, S. B., Fioravanti, M., Schifino, N., Cuzzoni, G., Fontana, I., Vignati, G., Govoni, S., and Ferrari, E. (1999a). Dehydroepiandrosterone sulfate decreases the interleukin-2-mediated overactivity of the natural killer cell compartment in senile dementia of the Alzheimer type. Dement Geriatr Cogn Disord *10*, 21-27.

Solerte, S. B., Fioravanti, M., Vignati, G., Giustina, A., Cravello, L., and Ferrari, E. (1999b). Dehydroepiandrosterone sulfate enhances natural killer cell cytotoxicity in humans via locally generated immunoreactive insulin-like growth factor I. J Clin Endocrinol Metab *84*, 3260-3267.

Stanway, S. J., Delavault, P., Purohit, A., Woo, L. W., Thurieau, C., Potter, B. V., and Reed, M. J. (2007). Steroid sulfatase: a new target for the endocrine therapy of breast cancer. Oncologist *12*, 370-374.

Stanway, S. J., Purohit, A., Woo, L. W., Sufi, S., Vigushin, D., Ward, R., Wilson, R. H., Stanczyk, F. Z., Dobbs, N., Kulinskaya, E.*, et al.* (2006). Phase I study of STX 64 (667 Coumate) in breast cancer patients: the first study of a steroid sulfatase inhibitor. Clin Cancer Res *12*, 1585-1592.

Stellato, C. (2004). Post-transcriptional and nongenomic effects of glucocorticoids. Proc Am Thorac Soc *1*, 255-263.

Stelzer, C., Brimmer, A., Hermanns, P., Zabel, B., and Dietz, U. H. (2007). Expression profile of Papss2 (3'-phosphoadenosine 5'-phosphosulfate synthase 2) during cartilage formation and skeletal development in the mouse embryo. Dev Dyn *236*, 1313-1318.

Stewart, P. M. (1996). 11 beta-Hydroxysteroid dehydrogenase: implications for clinical medicine. Clin Endocrinol (Oxf) *44*, 493-499.

Stewart, P. M., Boulton, A., Kumar, S., Clark, P. M., and Shackleton, C. H. (1999). Cortisol metabolism in human obesity: impaired cortisone-->cortisol conversion in subjects with central adiposity. J Clin Endocrinol Metab *84*, 1022-1027.

Stewart, P. M., and Krozowski, Z. S. (1999). 11 beta-Hydroxysteroid dehydrogenase. Vitam Horm *57*, 249-324.

Stewart, P. M., and Tomlinson, J. W. (2009). Selective inhibitors of 11beta-hydroxysteroid dehydrogenase type 1 for patients with metabolic syndrome: is the target liver, fat, or both? Diabetes *58*, 14-15.

Stewart, P. M., Walker, B. R., Holder, G., O'Halloran, D., and Shackleton, C. H. (1995a). 11 beta-Hydroxysteroid dehydrogenase activity in Cushing's syndrome: explaining the mineralocorticoid excess state of the ectopic adrenocorticotropin syndrome. J Clin Endocrinol Metab *80*, 3617-3620.
Stewart, P. M., Whorwood, C. B., and Mason, J. I. (1995b). Type 2 11 beta-hydroxysteroid dehydrogenase in foetal and adult life. J Steroid Biochem Mol Biol *55*, 465-471.
Strott, C. A. (2002). Sulfonation and molecular action. Endocr Rev *23*, 703-732.
Strous, R. D., Maayan, R., Lapidus, R., Goredetsky, L., Zeldich, E., Kotler, M., and Weizman, A. (2004). Increased circulatory dehydroepiandrosterone and dehydroepiandrosterone-sulphate in first-episode schizophrenia: relationship to gender, aggression and symptomatology. Schizophr Res *71*, 427-434.

Suzuki, T., Sasano, H., Takeyama, J., Kaneko, C., Freije, W. A., Carr, B. R., and Rainey, W. E. (2000). Developmental changes in steroidogenic enzymes in human postnatal adrenal cortex: immunohistochemical studies. Clin Endocrinol (Oxf) *53*, 739-747.

Suzuki, T., Suzuki, N., Daynes, R. A., and Engleman, E. G. (1991). Dehydroepiandrosterone enhances IL2 production and cytotoxic effector function of human T cells. Clin Immunol Immunopathol *61*, 202-211.

Suzuki, T., Suzuki, N., Engleman, E. G., Mizushima, Y., and Sakane, T. (1995). Low serum levels of dehydroepiandrosterone may cause deficient IL-2 production by lymphocytes in patients with systemic lupus erythematosus (SLE). Clin Exp Immunol *99*, 251-255.

Tagliaferro, A. R., Davis, J. R., Truchon, S., and Van Hamont, N. (1986). Effects of dehydroepiandrosterone acetate on metabolism, body weight and composition of male and female rats. J Nutr *116*, 1977-1983.

Tanaka, T., Yoshida, N., Kishimoto, T., and Akira, S. (1997). Defective adipocyte differentiation in mice lacking the C/EBPbeta and/or C/EBPdelta gene. Embo J *16*, 7432-7443.

Tang, Q. Q., Otto, T. C., and Lane, M. D. (2003). CCAAT/enhancer-binding protein beta is required for mitotic clonal expansion during adipogenesis. Proc Natl Acad Sci U S A *100*, 850-855.

Tang, Q. Q., Zhang, J. W., and Daniel Lane, M. (2004). Sequential gene promoter interactions of C/EBPbeta, C/EBPalpha, and PPARgamma during adipogenesis. Biochem Biophys Res Commun *319*, 235-239.

Tannin, G. M., Agarwal, A. K., Monder, C., New, M. I., and White, P. C. (1991). The human gene for 11 beta-hydroxysteroid dehydrogenase. Structure, tissue distribution, and chromosomal localization. J Biol Chem *266*, 16653-16658.

Taskinen, M. R., Nikkila, E. A., Pelkonen, R., and Sane, T. (1983). Plasma lipoproteins, lipolytic enzymes, and very low density lipoprotein triglyceride turnover in Cushing's syndrome. J Clin Endocrinol Metab *57*, 619-626.

Teglund, S., McKay, C., Schuetz, E., van Deursen, J. M., Stravopodis, D., Wang, D., Brown, M., Bodner, S., Grosveld, G., and Ihle, J. N. (1998). Stat5a and Stat5b proteins have essential and nonessential, or redundant, roles in cytokine responses. Cell *93*, 841-850.
The Practice Committee of the ASRM (2006). The evaluation and treatment of androgen excess. Fertil Steril *86*, S241-247.

Thomae, B. A., Eckloff, B. W., Freimuth, R. R., Wieben, E. D., and Weinshilboum, R. M. (2002). Human sulfotransferase SULT2A1 pharmacogenetics: genotype-to-phenotype studies. Pharmacogenomics J *2*, 48-56.

Tomlinson, J. W., Finney, J., Gay, C., Hughes, B. A., Hughes, S. V., and Stewart, P. M. (2008). Impaired glucose tolerance and insulin resistance are associated with increased adipose 11beta-hydroxysteroid dehydrogenase type 1 expression and elevated hepatic 5alpha-reductase activity. Diabetes *57*, 2652-2660.

Tomlinson, J. W., Sinha, B., Bujalska, I., Hewison, M., and Stewart, P. M. (2002). Expression of 11beta-hydroxysteroid dehydrogenase type 1 in adipose tissue is not increased in human obesity. J Clin Endocrinol Metab *87*, 5630-5635.

Tomlinson, J. W., and Stewart, P. M. (2002). The functional consequences of 11beta-hydroxysteroid dehydrogenase expression in adipose tissue. Horm Metab Res *34*, 746-751.

Tomlinson, J. W., Walker, E. A., Bujalska, I. J., Draper, N., Lavery, G. G., Cooper, M. S., Hewison, M., and Stewart, P. M. (2004). 11beta-hydroxysteroid dehydrogenase type 1: a tissue-specific regulator of glucocorticoid response. Endocr Rev *25*, 831-866.

Tong, Q., Tsai, J., Tan, G., Dalgin, G., and Hotamisligil, G. S. (2005). Interaction between GATA and the C/EBP family of transcription factors is critical in GATA-mediated suppression of adipocyte differentiation. Mol Cell Biol *25*, 706-715.

Tontonoz, P., Hu, E., and Spiegelman, B. M. (1994). Stimulation of adipogenesis in fibroblasts by PPAR gamma 2, a lipid-activated transcription factor. Cell *79*, 1147-1156.

Tontonoz, P., Kim, J. B., Graves, R. A., and Spiegelman, B. M. (1993). ADD1: a novel helix-loop-helix transcription factor associated with adipocyte determination and differentiation. Mol Cell Biol *13*, 4753-4759.

Trivax, B., and Azziz, R. (2007). Diagnosis of polycystic ovary syndrome. Clin Obstet Gynecol *50*, 168-177.

Ugele, B., St-Pierre, M. V., Pihusch, M., Bahn, A., and Hantschmann, P. (2003). Characterization and identification of steroid sulfate transporters of human placenta. Am J Physiol Endocrinol Metab *284*, E390-398.

ul Haque, M. F., King, L. M., Krakow, D., Cantor, R. M., Rusiniak, M. E., Swank, R. T., Superti-Furga, A., Haque, S., Abbas, H., Ahmad, W.*, et al.* (1998). Mutations in orthologous genes in human spondyloepimetaphyseal dysplasia and the brachymorphic mouse. Nat Genet *20*, 157-162.

Ulick, S., Levine, L. S., Gunczler, P., Zanconato, G., Ramirez, L. C., Rauh, W., Rosler, A., Bradlow, H. L., and New, M. I. (1979). A syndrome of apparent mineralocorticoid excess associated with defects in the peripheral metabolism of cortisol. J Clin Endocrinol Metab *49*, 757-764.

Valsamakis, G., Anwar, A., Tomlinson, J. W., Shackleton, C. H., McTernan, P. G., Chetty, R., Wood, P. J., Banerjee, A. K., Holder, G., Barnett, A. H.*, et al.* (2004). 11beta-hydroxysteroid dehydrogenase type 1 activity in lean and obese males with type 2 diabetes mellitus. J Clin Endocrinol Metab *89*, 4755-4761.

Van Staa TP, L. H., Abenhaim L, Begaud B, Zhang B, Cooper C (2000). Use of oral corticosteroids in the united kingdom. QJM *93*, 105-111.

van Vollenhoven, R. F., Engleman, E. G., and McGuire, J. L. (1995). Dehydroepiandrosterone in systemic lupus erythematosus. Results of a double-blind, placebo-controlled, randomized clinical trial. Arthritis Rheum *38*, 1826-1831.

Venkatachalam, K. V., Akita, H., and Strott, C. A. (1998). Molecular cloning, expression, and characterization of human bifunctional 3'-phosphoadenosine 5'-phosphosulfate synthase and its functional domains. J Biol Chem *273*, 19311-19320.

Venkatachalam, K. V., Fuda, H., Koonin, E. V., and Strott, C. A. (1999). Site-selected mutagenesis of a conserved nucleotide binding HXGH motif located in the ATP sulfurylase domain of human bifunctional 3'-phosphoadenosine 5'-phosphosulfate synthase. J Biol Chem *274*, 2601-2604.

Venturoli, S., Porcu, E., Fabbri, R., Magrini, O., Gammi, L., Paradisi, R., and Flamigni, C. (1992). Longitudinal evaluation of the different gonadotropin pulsatile patterns in anovulatory cycles of young girls. J Clin Endocrinol Metab *74*, 836-841.

Villareal, D. T., and Holloszy, J. O. (2004). Effect of DHEA on abdominal fat and insulin action in elderly women and men: a randomized controlled trial. Jama *292*, 2243-2248.
Wade, G. N., Gray, J. M., and Bartness, T. J. (1985). Gonadal influences on adiposity. Int J Obes *9 Suppl 1*, 83-92.

Wake, D. J., Rask, E., Livingstone, D. E., Soderberg, S., Olsson, T., and Walker, B. R. (2003). Local and systemic impact of transcriptional up-regulation of 11beta-hydroxysteroid dehydrogenase type 1 in adipose tissue in human obesity. J Clin Endocrinol Metab *88*, 3983-3988.

Walker, B. R., Campbell, J. C., Fraser, R., Stewart, P. M., and Edwards, C. R. (1992). Mineralocorticoid excess and inhibition of 11 beta-hydroxysteroid dehydrogenase in patients with ectopic ACTH syndrome. Clin Endocrinol (Oxf) *37*, 483-492.

Walker, J. E., Saraste, M., Runswick, M. J., and Gay, N. J. (1982). Distantly related sequences in the alpha- and beta-subunits of ATP synthase, myosin, kinases and other ATP-requiring enzymes and a common nucleotide binding fold. Embo J *1*, 945-951.

Wang, Y., Jones Voy, B., Urs, S., Kim, S., Soltani-Bejnood, M., Quigley, N., Heo, Y. R., Standridge, M., Andersen, B., Dhar, M.*, et al.* (2004). The human fatty acid synthase gene and de novo lipogenesis are coordinately regulated in human adipose tissue. J Nutr *134*, 1032-1038.

Warnmark, A., Treuter, E., Wright, A. P., and Gustafsson, J. A. (2003). Activation functions 1 and 2 of nuclear receptors: molecular strategies for transcriptional activation. Mol Endocrinol *17*, 1901-1909.

Weinstein, S. P., Paquin, T., Pritsker, A., and Haber, R. S. (1995). Glucocorticoid-induced insulin resistance: dexamethasone inhibits the activation of glucose transport in rat skeletal muscle by both insulin- and non-insulin-related stimuli. Diabetes *44*, 441-445.

Weiss, E. P., Shah, K., Fontana, L., Lambert, C. P., Holloszy, J. O., and Villareal, D. T. (2009). Dehydroepiandrosterone replacement therapy in older adults: 1- and 2-y effects on bone. Am J Clin Nutr *89*, 1459-1467.

White, P. C., Mune, T., Rogerson, F. M., Kayes, K. M., and Agarwal, A. K. (1997). Molecular analysis of 11 beta-hydroxysteroid dehydrogenase and its role in the syndrome of apparent mineralocorticoid excess. Steroids *62*, 83-88.

Wolf, G. (1999). The molecular mechanism of the stimulation of adipocyte differentiation by a glucocorticoid. Nutr Rev *57*, 324-326.

Wolkowitz, O. M., Reus, V. I., Keebler, A., Nelson, N., Friedland, M., Brizendine, L., and Roberts, E. (1999). Double-blind treatment of major depression with dehydroepiandrosterone. Am J Psychiatry *156*, 646-649.

Wong, K. P., Khoo, B. Y., and Sit, K. H. (1991). Biosynthesis of PAPS in vitro by human liver. Measurement by two independent assay procedures. Biochem Pharmacol *41*, 63-69.

Wood, T. C., Her, C., Aksoy, I., Otterness, D. M., and Weinshilboum, R. M. (1996). Human dehydroepiandrosterone sulfotransferase pharmacogenetics: quantitative Western analysis and gene sequence polymorphisms. J Steroid Biochem Mol Biol *59*, 467-478.

Wu, Z., Bucher, N. L., and Farmer, S. R. (1996). Induction of peroxisome proliferator-activated receptor gamma during the conversion of 3T3 fibroblasts into adipocytes is mediated by C/EBPbeta, C/EBPdelta, and glucocorticoids. Mol Cell Biol *16*, 4128-4136.

Wu, Z., Rosen, E. D., Brun, R., Hauser, S., Adelmant, G., Troy, A. E., McKeon, C., Darlington, G. J., and Spiegelman, B. M. (1999). Cross-regulation of C/EBP alpha and PPAR gamma controls the transcriptional pathway of adipogenesis and insulin sensitivity. Mol Cell *3*, 151-158.

Wu, Z., Xie, Y., Bucher, N. L., and Farmer, S. R. (1995). Conditional ectopic expression of C/EBP beta in NIH-3T3 cells induces PPAR gamma and stimulates adipogenesis. Genes Dev *9*, 2350-2363.

Xu, X., De Pergola, G., and Bjorntorp, P. (1990). The effects of androgens on the regulation of lipolysis in adipose precursor cells. Endocrinology *126*, 1229-1234.

Xu, X., De Pergola, G., Eriksson, P. S., Fu, L., Carlsson, B., Yang, S., Eden, S., and Bjorntorp, P. (1993). Postreceptor events involved in the up-regulation of beta-adrenergic receptor mediated lipolysis by testosterone in rat white adipocytes. Endocrinology *132*, 1651-1657.

Xu, X. F., De Pergola, G., and Bjorntorp, P. (1991). Testosterone increases lipolysis and the number of beta-adrenoceptors in male rat adipocytes. Endocrinology *128*, 379-382.

Xu, Z. H., Freimuth, R. R., Eckloff, B., Wieben, E., and Weinshilboum, R. M. (2002). Human 3'-phosphoadenosine 5'-phosphosulfate synthetase 2 (PAPSS2) pharmacogenetics: gene resequencing, genetic polymorphisms and functional characterization of variant allozymes. Pharmacogenetics *12*, 11-21.

Xu, Z. H., Otterness, D. M., Freimuth, R. R., Carlini, E. J., Wood, T. C., Mitchell, S., Moon, E., Kim, U. J., Xu, J. P., Siciliano, M. J., and Weinshilboum, R. M. (2000). Human 3'-phosphoadenosine 5'-phosphosulfate synthetase 1 (PAPSS1) and PAPSS2: gene cloning, characterization and chromosomal localization. Biochem Biophys Res Commun *268*, 437-444.

Xu, Z. H., Thomae, B. A., Eckloff, B. W., Wieben, E. D., and Weinshilboum, R. M. (2003). Pharmacogenetics of human 3'-phosphoadenosine 5'-phosphosulfate synthetase 1 (PAPSS1): gene resequencing, sequence variation, and functional genomics. Biochem Pharmacol *65*, 1787-1796.

Yamada, K., Duong, D. T., Scott, D. K., Wang, J. C., and Granner, D. K. (1999). CCAAT/enhancer-binding protein beta is an accessory factor for the glucocorticoid response from the cAMP response element in the rat phosphoenolpyruvate carboxykinase gene promoter. J Biol Chem *274*, 5880-5887.

Yamazoe, Y., Nagata, K., Ozawa, S., and Kato, R. (1994). Structural similarity and diversity of sulfotransferases. Chem Biol Interact *92*, 107-117.

Yanase, T., Fan, W., Kyoya, K., Min, L., Takayanagi, R., Kato, S., and Nawata, H. (2008). Androgens and metabolic syndrome: lessons from androgen receptor knock out (ARKO) mice. J Steroid Biochem Mol Biol *109*, 254-257.

Yanase, T., Sasano, H., Yubisui, T., Sakai, Y., Takayanagi, R., and Nawata, H. (1998). Immunohistochemical study of cytochrome b5 in human adrenal gland and in adrenocortical adenomas from patients with Cushing's syndrome. Endocr J *45*, 89-95.

Yen, P. H., Allen, E., Marsh, B., Mohandas, T., Wang, N., Taggart, R. T., and Shapiro, L. J. (1987). Cloning and expression of steroid sulfatase cDNA and the frequent occurrence of deletions in STS deficiency: implications for X-Y interchange. Cell *49*, 443-454.

Yen, P. H., Ellison, J., Salido, E. C., Mohandas, T., and Shapiro, L. (1992). Isolation of a new gene from the distal short arm of the human X chromosome that escapes X-inactivation. Hum Mol Genet *1*, 47-52.

Yen, S. S., Morales, A. J., and Khorram, O. (1995). Replacement of DHEA in aging men and women. Potential remedial effects. Ann N Y Acad Sci *774*, 128-142.

Yusuf, S., Hawken, S., Ounpuu, S., Dans, T., Avezum, A., Lanas, F., McQueen, M., Budaj, A., Pais, P., Varigos, J., and Lisheng, L. (2004). Effect of potentially modifiable risk factors associated with myocardial infarction in 52 countries (the INTERHEART study): case-control study. Lancet *364*, 937-952.

Zeng, G., Dave, J. R., and Chiang, P. K. (1997). Induction of proto-oncogenes during 3-deazaadenosine-stimulated differentiation of 3T3-L1 fibroblasts to adipocytes: mimicry of insulin action. Oncol Res *9*, 205-211.

Zuk, P. A., Zhu, M., Mizuno, H., Huang, J., Futrell, J. W., Katz, A. J., Benhaim, P., Lorenz, H. P., and Hedrick, M. H. (2001). Multilineage cells from human adipose tissue: implications for cell-based therapies. Tissue Eng *7*, 211-228.